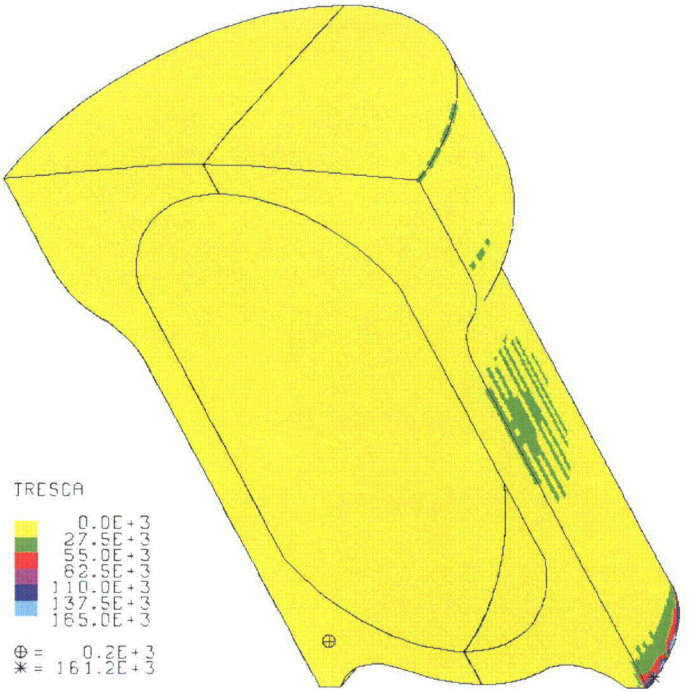

Figure 2-495. Tresca Stress in the TB-1 for 30-ft Drop Run 1 – SC-2 with Support Structure Rotated 45 Degrees and Side Impact

2.12.5.7.2 831g Plutonium Metal Hollow Cylinder Angled with End Impact

The 831g plutonium metal hollow cylinder contents was used for the 30-ft drop with end impact since this case produced one of the most severe loadings of the aircraft end impacts. Pre-impact model geometry shown in Figure 2-496, and the final displacement shown in Figure 2-497. The kinetic energy history is shown in Figure 2-498 to verify that the analysis ran through the time of rebound. The T-Ampoule equivalent plastic strain was zero, and there were no T-Ampoule elements exceeding the experimental strain locus. The negligible 0.255% equivalent plastic strain in the localized outer surface of the TB-1 (due to a minor contact modeling artifact) is shown in Figure 2-499. Tresca stress in the TB-1 is shown in Figure 2-500, with through-thickness values below even the NCT allowables from Table 2-4.

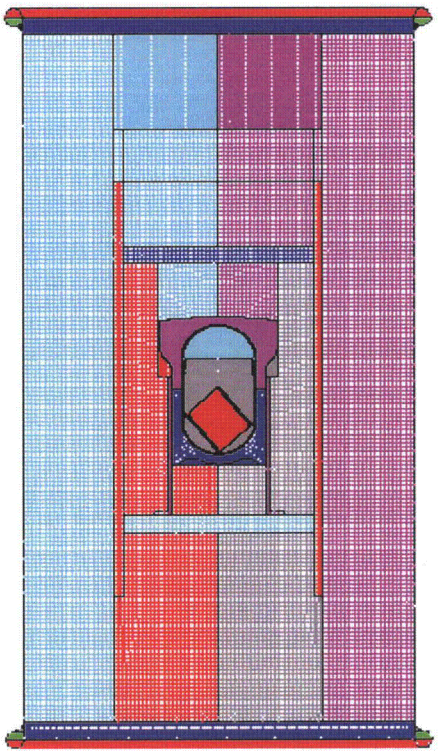

Figure 2-496. Finite Element Mesh for 30-ft Drop Run 2 – Angled 831 g Plutonium Metal Hollow Cylinder with End Impact

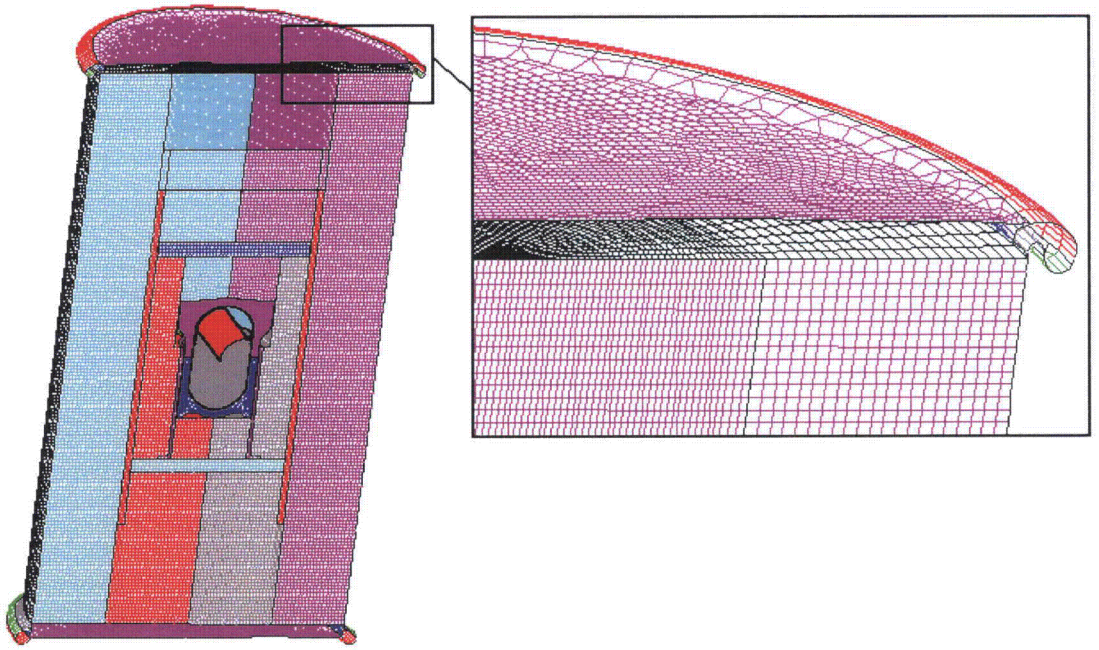

Figure 2-497. Final Displacement for 30-ft Drop Run 2 – Angled 831 g Plutonium Metal Hollow Cylinder with End Impact

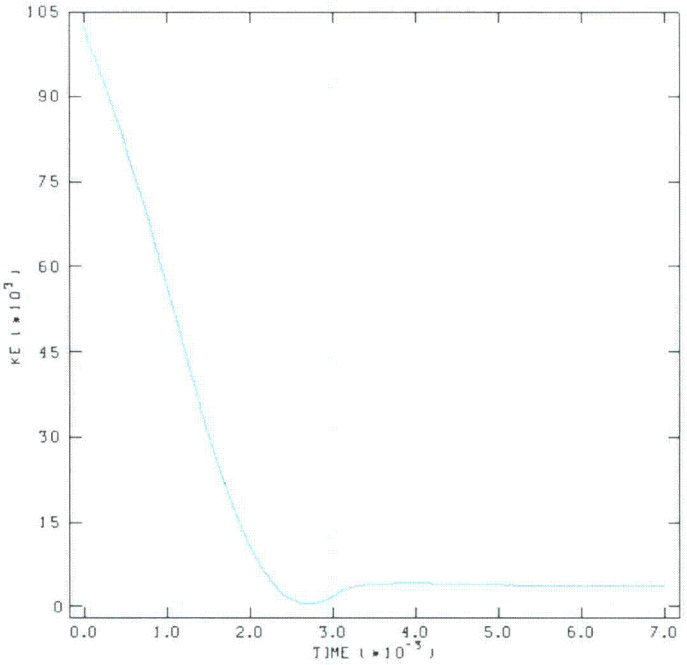

Figure 2-498. Kinetic Energy for 30-ft Drop Run 2 – Angled 831 g Plutonium Metal Hollow Cylinder with End Impact

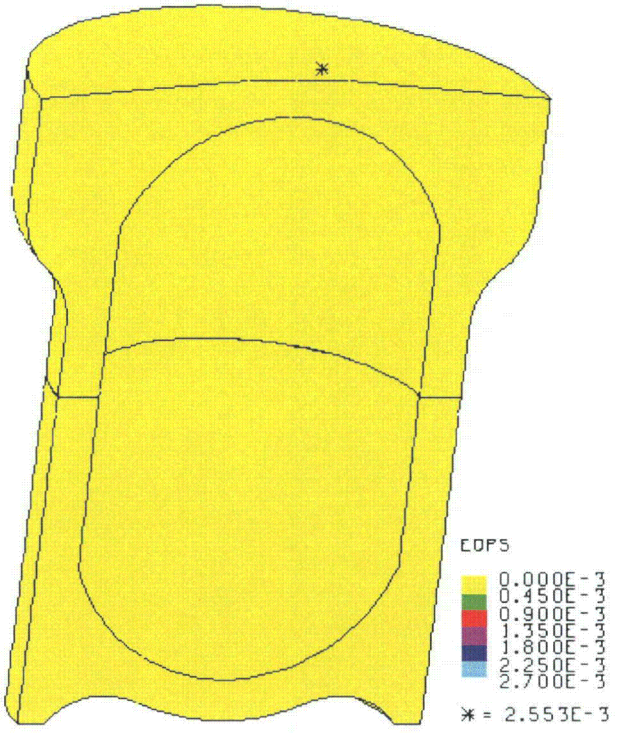

Figure 2-499. EQPS in TB-1 for 30-ft Drop Run 2 – Angled 831 g Plutonium Metal Hollow Cylinder with End Impact

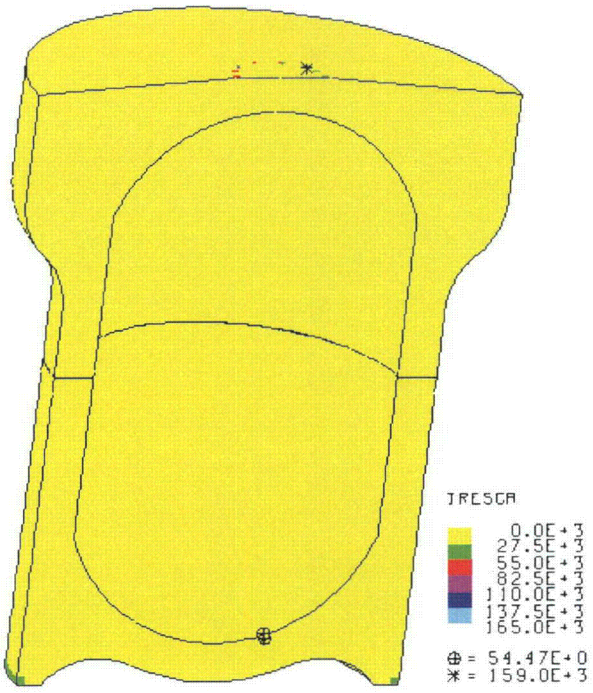

Figure 2-500. Tresca Stress in the TB-1 for 30-ft Drop Run 2 – Angled 831 g Plutonium Metal Hollow Cylinder with End Impact

2.12.5.7.3 831g Plutonium Metal Hollow Cylinder Angled with CGOC Impact

The angled 831g plutonium metal hollow cylinder contents was used for the 30-ft drop with corner impact since this case produced one of the most severe loadings of the aircraft CGOC impacts. Pre-impact model geometry is shown in Figure 2-501, and the final displacement shown in Figure 2-502. The kinetic energy history is shown in Figure 2-503 to verify that the analysis ran through the time of rebound. The T-Ampoule equivalent plastic strain was zero, and there were no T-Ampoule elements exceeding the experimental strain locus. There was zero equivalent plastic strain in the TB-1. Tresca stress in the TB-1 is shown in Figure 2-504, with through-thickness values below even the NCT allowables from Table 2-4.

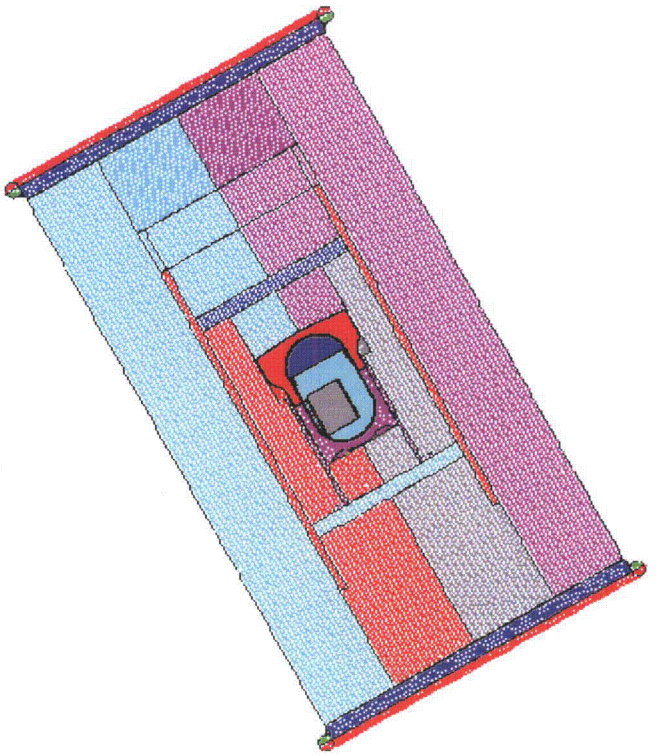

Figure 2-501. Finite Element Mesh for 30-ft Drop Run 3 – Angled 831 g Plutonium Metal Hollow Cylinder with CGOC Impact

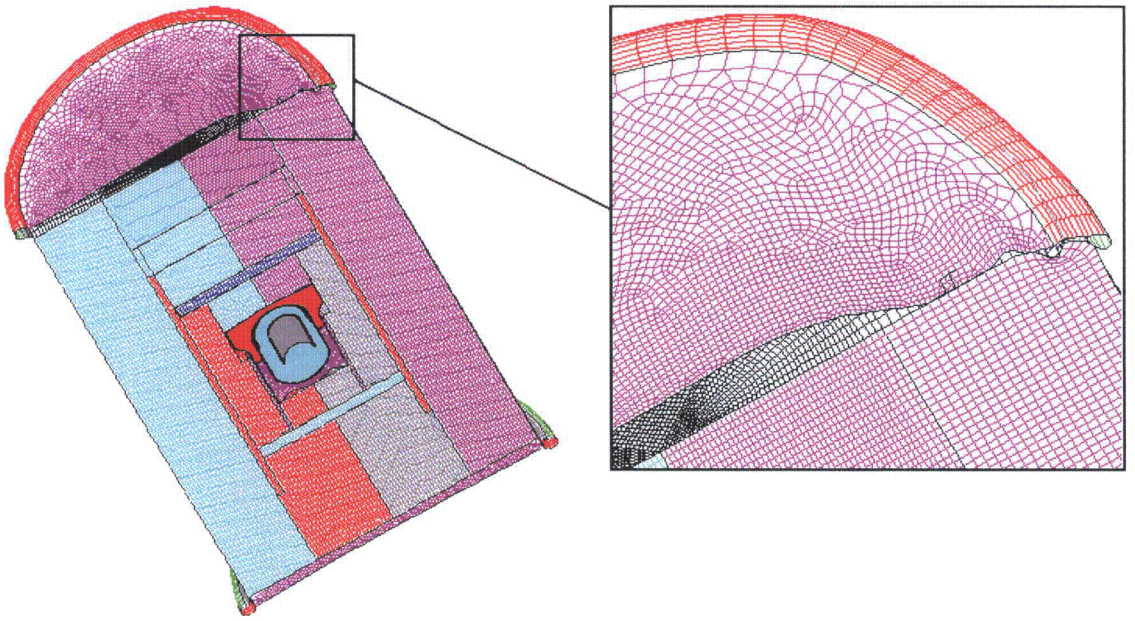

Figure 2-502. Final Displacement for 30-ft Drop Run 3 – Angled 831 g Plutonium Metal Hollow Cylinder with CGOC Impact

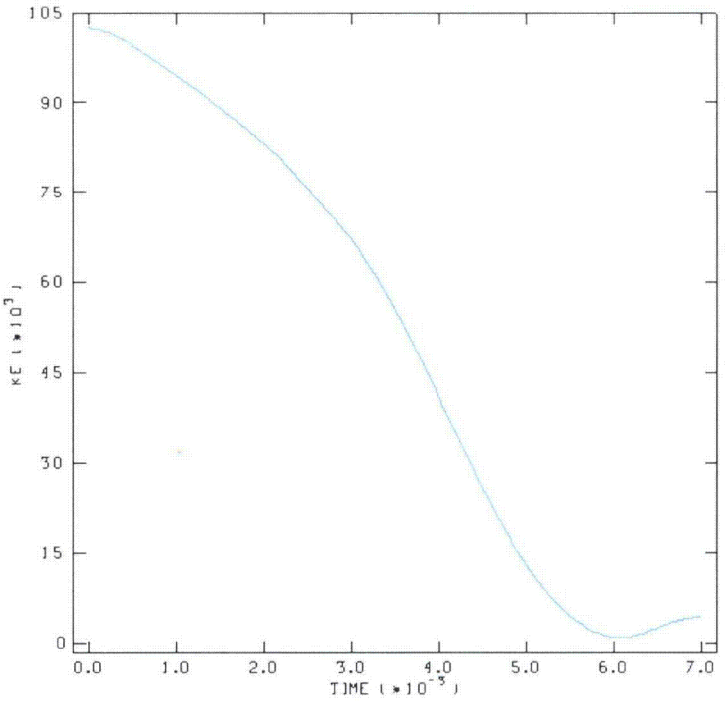

Figure 2-503. Kinetic Energy for 30-ft Drop Run 3 – Angled 831 g Plutonium Metal Hollow Cylinder with CGOC Impact

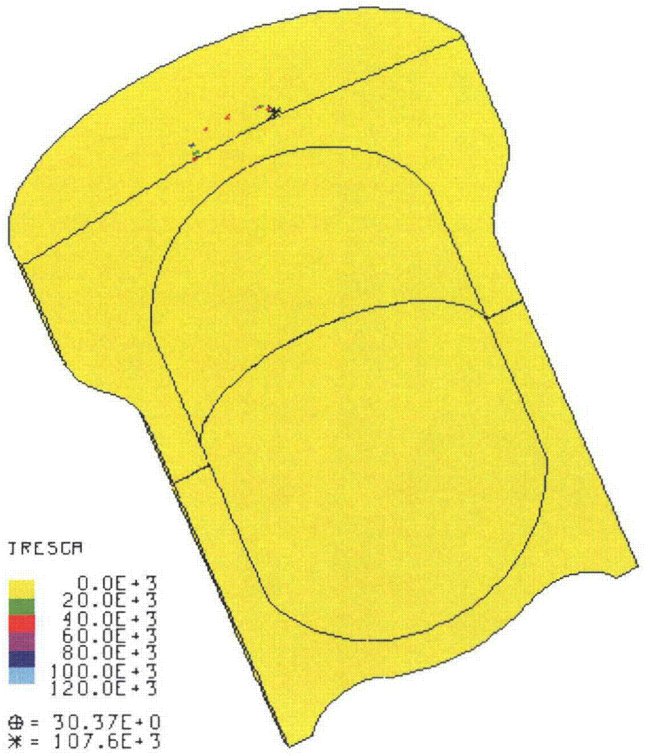

Figure 2-504. Tresca Stress in the TB-1 for 30-ft Drop Run 3 – Angled 831 g Plutonium Metal Hollow Cylinder with CGOC Impact

2.12.5.8 References

1. USNRC, NUREG-0361. Safety Analysis Report for the Plutonium Air Transportable Package, Model PAT-1. Washington, D.C. 1978.

2. Reference deleted.

3. Hecker, Siegfried S. and Michael F. Stevens. "Mechanical Behavior of Plutonium and Its Alloys." *Los Alamos Science* Number 26 (2000).

4. Wellman, G.W., Diegert, K.V., and Saizbrenner, R. "Two-Dimensional Quasistatic Modeling of Exclusion Region Barriers in Support of Design Guide Development." SAND93-0905. Sandia National Laboratories. Albuquerque, NM. 1993.

5. Bao, Y., and T. Wierzbicki. "On the Cut-Off Value of Negative Triaxiality for Fracture." Engineering Fracture Mechanics, 72, pp. 1049-1069, 2005..

6. Johnson, G.R., and Cook, W.H., "Fracture Characteristics of Three Metals Subjected to Various Strains, Strain Rates, Temperature and Pressures." *Engineering Fracture Mechanics* 21 (1985):31-48.

7. Bao, Y. "Prediction of Ductile Crack Formation in Uncracked Bodies," Report 100. Impact & Crash Worthiness Laboratory, Massachusetts Institute of Technology. Cambridge, MA. 2003.

8. Am*erican Society of Mechanical Eng*ineers (ASME). "Boiler and Pressure Vessel Code," 2008a, Section II, Part D, Table 2A: Design Stress Intensity Values S_m for Ferrous Materials. pp. 298. 2008.

9. American Society of Mechanical Engineers (ASME). "Boiler and Pressure Vessel Code," Section III, Division 1--Appendices, Nonmandatory Appendix F: Article F-1000, Rules for Evaluation of Service Loadings with Level D Service Limits. pp. 232. 2007.

2.12.6 Bolt Analysis

The following section is an analysis of the bolts that secure the TB-1 lid when subjected to the loads applied during the high-speed aircraft accident test condition (10 CFR 71.74). The impulse loads are obtained from the component analyses (see Section 2.12.5).

The TB-1 lid is secured by (12) ½ -20 UNJF-3A bolts. The following calculation shows that the total bolt preload is approximately 108,000 lbs.

$$\text{Bolt torque}: T = 75 \text{ ft - lbs}$$

$$\text{Nominal bolt diameter } d = 0.5 \text{ in}$$

$$\text{Friction coefficien t}: K = 0.2$$

$$\text{Shigley}^{[1]}\text{ Boltforce}: F_i = \frac{T}{Kd}$$

$$Fi = \frac{900}{(0.2)(0.5)} = 9000 \text{ lbf}$$

$$(12 \text{ bolts}) \times 9000 = 108{,}000 \text{ lbf}$$

The contact force of the redwood pushing on the top of the TB-1 to decelerate it is shown as the dashed curve in Figure 2-505. The bolt preload is also shown along with the sum of the contact force and the total bolt preload. These are the forces holding the lid in place during the end impact event.

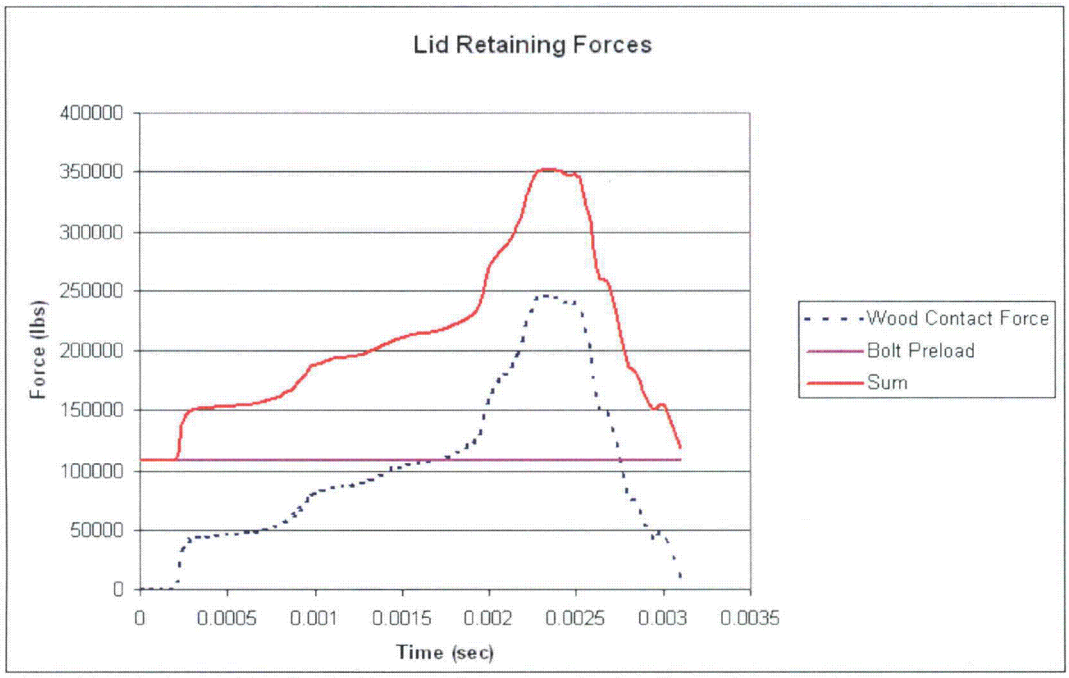

Figure 2-505. Contact Forces on the Top Surface of the TB-1 Lid

The force generated by the impacting components calculated in Section 2.12.5 along with the redwood contact force and bolt preload are shown in Figure 2-506. As shown in the figure, the forces from the components are only a fraction of the bolt preload. The peak impulse load is a factor of 2.1 less than the bolt preload and a factor of 6 less than the total of the sum of the wood retaining force and the bolt preload. Therefore, the lid of the TB-1 will remain tight and torqued during the aircraft impact accident.

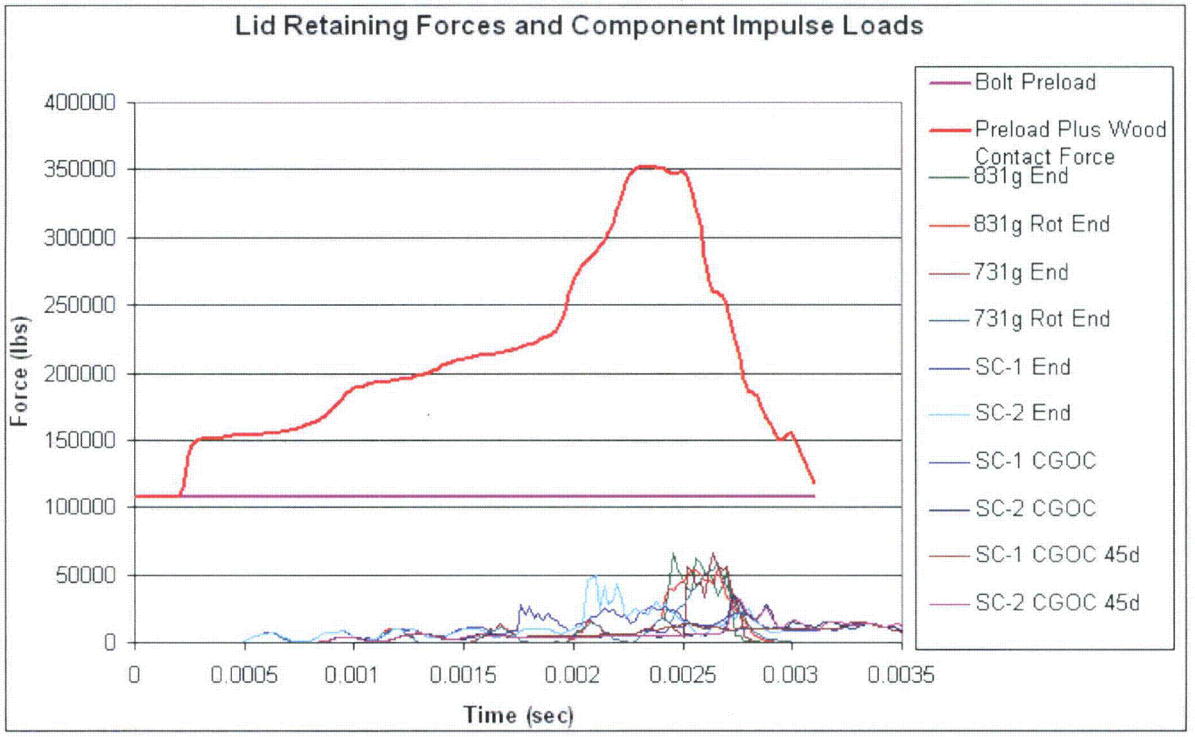

Figure 2-506. Contact Forces on the Top Surface of the TB-1 Lid Along with Impulse Loads from Various Contents

2.12.6.1 References

1. Shigley, J. E. *Mechanical Engineering Design*. McGraw-Hill, 1977.

2.12.7 Sample Input

The PRONTO3D input file for Run 3 of the high speed aircraft impact analysis (831 gram angled cylinder with CGOC impact) which resulted in the highest tearing parameter in the T-Ampoule is included below. Dollar signs designate comment lines.

```
TITLE
Full Overpack with TB1 with 831g cylinder top rot CGOC impact
$
TERM TIME,0.006
PLOT TIME,0.00003
PLOT NODAL,DISPLACEMENT, VELOCITY, ACCELERATION,reactions,force
PLOT ELEMENT, STRESS, VONMISES,DOPT, EPS
PLOT STATE, EQPS
SUM NODAL_MOMENTUMY MATERIAL 5
```

```
SUM CONTACT_FORCEY NODESET 500
SUM CONTACT_FORCEX NODESET 500
SUM CONTACT_FORCEZ NODESET 500
write restart .0005
$
$ symmetry boundary condition
$
$  no displ, y, 100
$  no displ, x, 100
  no displ, z, 100
  no displ, z, 101
$
$ hourglass control
$
$   assumed strain hourglass
    hourglass stiffening .08 .09
$
$ set up initial velocity
$
  initial velocity material 1   0.0  5064.0  0.0    $ cantop
  initial velocity material 2   0.0  5064.0  0.0    $ canbot
  initial velocity material 4   0.0  5064.0  0.0    $ TB-1 top
  initial velocity material 5   0.0  5064.0  0.0    $ PU cylinder (1)
  initial velocity material 6   0.0  5064.0  0.0    $ TB-1 bot
  initial velocity material 20  0.0  5064.0  0.0    $ spreader
  initial velocity material 21  0.0  5064.0  0.0    $ copper
  initial velocity material 22  0.0  5064.0  0.0    $ top plate 7075
  initial velocity material 23  0.0  5064.0  0.0    $ lower plate 7075
  initial velocity material 10  0.0  5064.0  0.0    $ shell
  initial velocity material 24  0.0  5064.0  0.0    $ wood 1 X
  initial velocity material 25  0.0  5064.0  0.0    $ wood 1 Z
  initial velocity material 26  0.0  5064.0  0.0    $ wood 1 X
  initial velocity material 27  0.0  5064.0  0.0    $ wood 2 X
  initial velocity material 28  0.0  5064.0  0.0    $ wood 2 Z
  initial velocity material 29  0.0  5064.0  0.0    $ wood 2 X
  initial velocity material 30  0.0  5064.0  0.0    $ wood 3 X
  initial velocity material 31  0.0  5064.0  0.0    $ wood 3 Z
  initial velocity material 32  0.0  5064.0  0.0    $ wood 3 X
  initial velocity material 33  0.0  5064.0  0.0    $ wood 4 X
  initial velocity material 34  0.0  5064.0  0.0    $ wood 4 Z
  initial velocity material 35  0.0  5064.0  0.0    $ wood 4 X
  initial velocity material 36  0.0  5064.0  0.0    $ wood 5 X
  initial velocity material 37  0.0  5064.0  0.0    $ wood 5 Z
  initial velocity material 38  0.0  5064.0  0.0    $ wood 5 X
  initial velocity material 39  0.0  5064.0  0.0    $ wood 6 X
  initial velocity material 40  0.0  5064.0  0.0    $ wood 6 Z
  initial velocity material 41  0.0  5064.0  0.0    $ wood 6 X
$
$ Death
$
$
$ set up contact by region for  model
$
  contact material 1
  contact material 2
  contact material 4
  contact material 5
```

```
  contact material 6
  contact material 20
  contact material 21
  contact material 22
  contact material 23
  contact material 24
  contact material 25
  contact material 26
  contact material 27
  contact material 28
  contact material 29
  contact material 30
  contact material 31
  contact material 32
  contact material 33
  contact material 34
  contact material 35
  contact material 36
  contact material 37
  contact material 38
  contact material 39
  contact material 40
  contact material 41
$ contact surfaces
  contact surface 30  $ mid tbl
  contact surface 31  $ mid tbl
  contact surface 800  $ top wood by pipe
  contact surface 801  $ top of pipe
$
$ define surface pairs
$
  contact data surface 800 surface 801 $
  kinematic partition 1.0
  friction static -1.0
  capture tolerance 0.005
  end
  contact data surface 30 surface 31 $
  kinematic partition 0.5
  friction static -1.0
  capture tolerance 0.005
  end
$
$ define friction
$
$ Top of Tamp and Cylinder
  contact data material 1 material 5
   kinematic partition 0.1
   friction static 0.36
   friction dynamic 0.3
  end
$ Bottom of Tamp and Cylinder
  contact data material 2 material 5
   kinematic partition 0.1
   friction static 0.36
   friction dynamic 0.3
  end
$
```

```
$ Rigid surface
$
 rigid surface 700 0.0 23.45 0.0 0.0 -1.0 0.0  $ top impact
$
$ define the shell thickness
$
  scale shell thickness 10 0.0625  $ can shell
$
$
$
$ define material properties
$
$
 MATERIAL, 1, ep power hardening, 0.000414, $  titanium
   YOUNGS MODULUS,        15.5E06
   POISSONS RATIO,         0.3
   YIELD STRESS,          141.7E03
   HARDENING constant,     12.6E04
   hardening exponent     0.6554
   luders strain          0.0
  END
 MATERIAL, 2, ep power hardening, 0.000414, $  titanium
   YOUNGS MODULUS,        15.5E06
   POISSONS RATIO,         0.3
   YIELD STRESS,          141.7E03
   HARDENING constant,     12.6E04
   hardening exponent     0.6554
   luders strain          0.0
  END
 Material, 4, ep power hardening, 0.00074, $  TB1 Top
   YOUNGS MODULUS,        30.E06
   POISSONS RATIO,         0.30
   YIELD STRESS,          141E03
   HARDENING constant,     30e4
   hardening exponent     1
   luders strain          0.0
  END
 MATERIAL, 5, ep power hardening, 0.001853, $  PU alpha phase 1
   YOUNGS MODULUS,        14.1E06
   POISSONS RATIO,         0.3
   YIELD STRESS,          36.0E03
   HARDENING constant,     85000
   hardening exponent     0.4
   luders strain          0.0
  END
 Material, 6, ep power hardening, 0.00074, $  TB1 Left
   YOUNGS MODULUS,        30.E06
   POISSONS RATIO,         0.30
   YIELD STRESS,          141E03
   HARDENING constant,     30e4
   hardening exponent     1
   luders strain          0.0
  END
 MATERIAL, 10, ep power hardening, 0.00074, $  304 stainless shell
   YOUNGS MODULUS,        28.E6
   POISSONS RATIO,         0.27
   YIELD STRESS,          40.E3
```

```
   HARDENING constant,    192746.
   hardening exponent    0.748190
   luders strain         0.0
  END
 MATERIAL, 20, ep power hardening, 0.0002536, $  6061
   YOUNGS MODULUS,       9.9E06
   POISSONS RATIO,        0.3
   YIELD STRESS,         45.0E03
   HARDENING constant,    37852
   hardening exponent    0.55
   luders strain         0.0
  END
 MATERIAL, 21, ep power hardening, 0.000414, $  copper
   YOUNGS MODULUS,       17.2E06
   POISSONS RATIO,        0.33
   YIELD STRESS,         45.0E03
   HARDENING constant,    38000
   hardening exponent    0.55
   luders strain         0.0
  END
 MATERIAL, 22, ep power hardening, 0.000264, $  7075
   YOUNGS MODULUS,       10.4E06
   POISSONS RATIO,        0.33
   YIELD STRESS,         73.0E03
   HARDENING constant,    37852
   hardening exponent    0.55
   luders strain         0.0
  END
 MATERIAL, 23, ep power hardening, 0.000264, $  7075
   YOUNGS MODULUS,       10.4E06
   POISSONS RATIO,        0.33
   YIELD STRESS,         73.0E03
   HARDENING constant,    37852
   hardening exponent    0.55
   luders strain         0.0
  END
MATERIAL 24 = ORTHOTROPIC CRUSH, 5.682e-5
        Compacted YOUNGS MODULUS = 1.5e6
        Compacted POISSONS RATIO = 0.3
        Compacted YIELD STRESS  = 20000.
        X ID = 1   Y ID = 1
        Z ID = 2   XY ID = 4
        YZ ID = 5   ZX ID = 4
        Full Compaction = 0.9 $ 0 = no compaction, 1 = very flat
        Modulus x = 1.5e6
        Modulus y = 0.3e6
        Modulus z = 0.3e6
        Modulus xy = 0.2e6
        Modulus yz = 0.25e6
        Modulus zx = 0.2e6
End
Function 1  $ x-direction ( T-Direction)
        0.       2000.
        0.14     4200.
        0.28     5100.
        0.42     5430.
        0.57     6100.
```

```
        0.71     10100.
        0.80     15000.
        0.90     20000.
End
Function 2    $  y-direction (L-Direction) z-direction approx the same
        0.       400.
        0.14     986.
        0.28     1200.
        0.42     1275.
        0.57     1432.
        0.71     2371.
        0.80     3521.
        0.90     4690.
End
Function 4   $ sigxy or sigxz vs volume
        0.0      1000.
        0.60     1000.
        0.70     10000.
        0.90     10000.
End
Function 5   $ sigyz vs volume
        0.0      1000.
        0.60     1000.
        0.70     10000.
        0.90     10000.
End
MATERIAL 25 = ORTHOTROPIC CRUSH, 5.682e-5
        Compacted YOUNGS MODULUS = 1.5e6
        Compacted POISSONS RATIO = 0.3
        Compacted YIELD STRESS  = 20000.
        X ID = 2   Y ID = 1
        Z ID = 1   XY ID = 4
        YZ ID = 5   ZX ID = 4
        Full Compaction = 0.9 $ 0 = no compaction, 1 = very flat
        Modulus x = 1.5e6
        Modulus y = 0.3e6
        Modulus z = 0.3e6
        Modulus xy = 0.2e6
        Modulus yz = 0.25e6
        Modulus zx = 0.2e6
End
Function 1  $ x-direction ( T-Direction)
        0.       2000.
        0.14     4200.
        0.28     5100.
        0.42     5430.
        0.57     6100.
        0.71     10100.
        0.80     15000.
        0.90     20000.
End
Function 2    $  y-direction (L-Direction) z-direction approx the same
        0.       400.
        0.14     986.
        0.28     1200.
        0.42     1275.
        0.57     1432.
```

```
        0.71     2371.
        0.80     3521.
        0.90     4690.
End
Function 4   $ sigxy or sigxz vs volume
        0.0     1000.
        0.60    1000.
        0.70    10000.
        0.90    10000.
End
Function 5   $ sigyz vs volume
        0.0     1000.
        0.60    1000.
        0.70    10000.
        0.90    10000.
End
MATERIAL 26 = ORTHOTROPIC CRUSH, 5.682e-5
        Compacted YOUNGS MODULUS = 1.5e6
        Compacted POISSONS RATIO = 0.3
        Compacted YIELD STRESS  = 20000.
        X ID = 1   Y ID = 1
        Z ID = 2   XY ID = 4
        YZ ID = 5   ZX ID = 4
        Full Compaction = 0.9 $ 0 = no compaction, 1 = very flat
        Modulus x = 1.5e6
        Modulus y = 0.3e6
        Modulus z = 0.3e6
        Modulus xy = 0.2e6
        Modulus yz = 0.25e6
        Modulus zx = 0.2e6
End
Function 1  $ x-direction ( T-Direction)
        0.       2000.
        0.14     4200.
        0.28     5100.
        0.42     5430.
        0.57     6100.
        0.71     10100.
        0.80     15000.
        0.90     20000.
End
Function 2    $  y-direction (L-Direction) z-direction approx the same
        0.       400.
        0.14     986.
        0.28     1200.
        0.42     1275.
        0.57     1432.
        0.71     2371.
        0.80     3521.
        0.90     4690.
End
Function 4   $ sigxy or sigxz vs volume
        0.0     1000.
        0.60    1000.
        0.70    10000.
        0.90    10000.
End
```

```
Function 5   $ sigyz vs volume
        0.0     1000.
        0.60    1000.
        0.70    10000.
        0.90    10000.
End
MATERIAL 27 = ORTHOTROPIC CRUSH, 5.682e-5
        Compacted YOUNGS MODULUS = 1.5e6
        Compacted POISSONS RATIO = 0.3
        Compacted YIELD STRESS  = 20000.
        X ID = 1   Y ID = 1
        Z ID = 2   XY ID = 4
        YZ ID = 5   ZX ID = 4
        Full Compaction = 0.9 $ 0 = no compaction, 1 = very flat
        Modulus x = 1.5e6
        Modulus y = 0.3e6
        Modulus z = 0.3e6
        Modulus xy = 0.2e6
        Modulus yz = 0.25e6
        Modulus zx = 0.2e6
End
Function 1  $ x-direction ( T-Direction)
        0.      2000.
        0.14    4200.
        0.28    5100.
        0.42    5430.
        0.57    6100.
        0.71    10100.
        0.80    15000.
        0.90    20000.
End
Function 2    $  y-direction (L-Direction) z-direction approx the same
        0.      400.
        0.14    986.
        0.28    1200.
        0.42    1275.
        0.57    1432.
        0.71    2371.
        0.80    3521.
        0.90    4690.
End
Function 4   $ sigxy or sigxz vs volume
        0.0     1000.
        0.60    1000.
        0.70    10000.
        0.90    10000.
End
Function 5   $ sigyz vs volume
        0.0     1000.
        0.60    1000.
        0.70    10000.
        0.90    10000.
End
MATERIAL 28 = ORTHOTROPIC CRUSH, 5.682e-5
        Compacted YOUNGS MODULUS = 1.5e6
        Compacted POISSONS RATIO = 0.3
        Compacted YIELD STRESS  = 20000.
```

```
        X ID = 2   Y ID = 1
        Z ID = 1   XY ID = 4
        YZ ID = 5   ZX ID = 4
        Full Compaction = 0.9 $ 0 = no compaction, 1 = very flat
        Modulus x = 1.5e6
        Modulus y = 0.3e6
        Modulus z = 0.3e6
        Modulus xy = 0.2e6
        Modulus yz = 0.25e6
        Modulus zx = 0.2e6
End
Function 1  $ x-direction ( T-Direction)
        0.       2000.
        0.14     4200.
        0.28     5100.
        0.42     5430.
        0.57     6100.
        0.71     10100.
        0.80     15000.
        0.90     20000.
End
Function 2    $  y-direction (L-Direction) z-direction approx the same
        0.       400.
        0.14     986.
        0.28     1200.
        0.42     1275.
        0.57     1432.
        0.71     2371.
        0.80     3521.
        0.90     4690.
End
Function 4   $ sigxy or sigxz vs volume
        0.0     1000.
        0.60    1000.
        0.70    10000.
        0.90    10000.
End
Function 5   $ sigyz vs volume
        0.0     1000.
        0.60    1000.
        0.70    10000.
        0.90    10000.
End
MATERIAL 29 = ORTHOTROPIC CRUSH, 5.682e-5
        Compacted YOUNGS MODULUS = 1.5e6
        Compacted POISSONS RATIO = 0.3
        Compacted YIELD STRESS  = 20000.
        X ID = 1   Y ID = 1
        Z ID = 2   XY ID = 4
        YZ ID = 5   ZX ID = 4
        Full Compaction = 0.9 $ 0 = no compaction, 1 = very flat
        Modulus x = 1.5e6
        Modulus y = 0.3e6
        Modulus z = 0.3e6
        Modulus xy = 0.2e6
        Modulus yz = 0.25e6
        Modulus zx = 0.2e6
```

```
End
Function 1  $ x-direction ( T-Direction)
        0.       2000.
        0.14     4200.
        0.28     5100.
        0.42     5430.
        0.57     6100.
        0.71     10100.
        0.80     15000.
        0.90     20000.
End
Function 2    $  y-direction (L-Direction) z-direction approx the same
        0.       400.
        0.14     986.
        0.28     1200.
        0.42     1275.
        0.57     1432.
        0.71     2371.
        0.80     3521.
        0.90     4690.
End
Function 4   $ sigxy or sigxz vs volume
        0.0     1000.
        0.60    1000.
        0.70    10000.
        0.90    10000.
End
Function 5   $ sigyz vs volume
        0.0     1000.
        0.60    1000.
        0.70    10000.
        0.90    10000.
End
MATERIAL 30 = ORTHOTROPIC CRUSH, 5.682e-5
        Compacted YOUNGS MODULUS = 1.5e6
        Compacted POISSONS RATIO = 0.3
        Compacted YIELD STRESS  = 20000.
        X ID = 1   Y ID = 1
        Z ID = 2   XY ID = 4
        YZ ID = 5   ZX ID = 4
        Full Compaction = 0.9 $ 0 = no compaction, 1 = very flat
        Modulus x = 1.5e6
        Modulus y = 0.3e6
        Modulus z = 0.3e6
        Modulus xy = 0.2e6
        Modulus yz = 0.25e6
        Modulus zx = 0.2e6
End
Function 1  $ x-direction ( T-Direction)
        0.       2000.
        0.14     4200.
        0.28     5100.
        0.42     5430.
        0.57     6100.
        0.71     10100.
        0.80     15000.
        0.90     20000.
```

```
End
Function 2    $  y-direction (L-Direction) z-direction approx the same
        0.       400.
        0.14     986.
        0.28     1200.
        0.42     1275.
        0.57     1432.
        0.71     2371.
        0.80     3521.
        0.90     4690.
End
Function 4   $ sigxy or sigxz vs volume
        0.0     1000.
        0.60    1000.
        0.70    10000.
        0.90    10000.
End
Function 5   $ sigyz vs volume
        0.0     1000.
        0.60    1000.
        0.70    10000.
        0.90    10000.
End
MATERIAL 31 = ORTHOTROPIC CRUSH, 5.682e-5
        Compacted YOUNGS MODULUS = 1.5e6
        Compacted POISSONS RATIO = 0.3
        Compacted YIELD STRESS  = 20000.
        X ID = 2   Y ID = 1
        Z ID = 1   XY ID = 4
        YZ ID = 5   ZX ID = 4
        Full Compaction = 0.9 $ 0 = no compaction, 1 = very flat
        Modulus x = 1.5e6
        Modulus y = 0.3e6
        Modulus z = 0.3e6
        Modulus xy = 0.2e6
        Modulus yz = 0.25e6
        Modulus zx = 0.2e6
End
Function 1  $ x-direction ( T-Direction)
        0.       2000.
        0.14     4200.
        0.28     5100.
        0.42     5430.
        0.57     6100.
        0.71     10100.
        0.80     15000.
        0.90     20000.
End
Function 2    $  y-direction (L-Direction) z-direction approx the same
        0.       400.
        0.14     986.
        0.28     1200.
        0.42     1275.
        0.57     1432.
        0.71     2371.
        0.80     3521.
        0.90     4690.
```

```
End
Function 4    $ sigxy or sigxz vs volume
        0.0      1000.
        0.60     1000.
        0.70     10000.
        0.90     10000.
End
Function 5    $ sigyz vs volume
        0.0      1000.
        0.60     1000.
        0.70     10000.
        0.90     10000.
End
MATERIAL 32 = ORTHOTROPIC CRUSH, 5.682e-5
        Compacted YOUNGS MODULUS = 1.5e6
        Compacted POISSONS RATIO = 0.3
        Compacted YIELD STRESS  = 20000.
        X ID = 1    Y ID = 1
        Z ID = 2    XY ID = 4
        YZ ID = 5    ZX ID = 4
        Full Compaction = 0.9 $ 0 = no compaction, 1 = very flat
        Modulus x = 1.5e6
        Modulus y = 0.3e6
        Modulus z = 0.3e6
        Modulus xy = 0.2e6
        Modulus yz = 0.25e6
        Modulus zx = 0.2e6
End
Function 1   $ x-direction ( T-Direction)
        0.       2000.
        0.14     4200.
        0.28     5100.
        0.42     5430.
        0.57     6100.
        0.71     10100.
        0.80     15000.
        0.90     20000.
End
Function 2     $  y-direction (L-Direction) z-direction approx the same
        0.       400.
        0.14     986.
        0.28     1200.
        0.42     1275.
        0.57     1432.
        0.71     2371.
        0.80     3521.
        0.90     4690.
End
Function 4    $ sigxy or sigxz vs volume
        0.0      1000.
        0.60     1000.
        0.70     10000.
        0.90     10000.
End
Function 5    $ sigyz vs volume
        0.0      1000.
        0.60     1000.
```

```
        0.70    10000.
        0.90    10000.
End
MATERIAL 33 = ORTHOTROPIC CRUSH, 5.682e-5
        Compacted YOUNGS MODULUS = 1.5e6
        Compacted POISSONS RATIO = 0.3
        Compacted YIELD STRESS  = 20000.
        X ID = 1   Y ID = 1
        Z ID = 2   XY ID = 4
        YZ ID = 5   ZX ID = 4
        Full Compaction = 0.9 $ 0 = no compaction, 1 = very flat
        Modulus x = 1.5e6
        Modulus y = 0.3e6
        Modulus z = 0.3e6
        Modulus xy = 0.2e6
        Modulus yz = 0.25e6
        Modulus zx = 0.2e6
End
Function 1  $ x-direction ( T-Direction)
        0.       2000.
        0.14     4200.
        0.28     5100.
        0.42     5430.
        0.57     6100.
        0.71     10100.
        0.80     15000.
        0.90     20000.
End
Function 2    $  y-direction (L-Direction) z-direction approx the same
        0.       400.
        0.14     986.
        0.28     1200.
        0.42     1275.
        0.57     1432.
        0.71     2371.
        0.80     3521.
        0.90     4690.
End
Function 4   $ sigxy or sigxz vs volume
        0.0     1000.
        0.60    1000.
        0.70    10000.
        0.90    10000.
End
Function 5   $ sigyz vs volume
        0.0     1000.
        0.60    1000.
        0.70    10000.
        0.90    10000.
End
MATERIAL 34 = ORTHOTROPIC CRUSH, 5.682e-5
        Compacted YOUNGS MODULUS = 1.5e6
        Compacted POISSONS RATIO = 0.3
        Compacted YIELD STRESS  = 20000.
        X ID = 2   Y ID = 1
        Z ID = 1   XY ID = 4
        YZ ID = 5   ZX ID = 4
```

```
        Full Compaction = 0.9 $ 0 = no compaction, 1 = very flat
        Modulus x = 1.5e6
        Modulus y = 0.3e6
        Modulus z = 0.3e6
        Modulus xy = 0.2e6
        Modulus yz = 0.25e6
        Modulus zx = 0.2e6
End
Function 1  $ x-direction ( T-Direction)
        0.       2000.
        0.14     4200.
        0.28     5100.
        0.42     5430.
        0.57     6100.
        0.71     10100.
        0.80     15000.
        0.90     20000.
End
Function 2    $  y-direction (L-Direction) z-direction approx the same
        0.       400.
        0.14     986.
        0.28     1200.
        0.42     1275.
        0.57     1432.
        0.71     2371.
        0.80     3521.
        0.90     4690.
End
Function 4   $ sigxy or sigxz vs volume
        0.0     1000.
        0.60    1000.
        0.70    10000.
        0.90    10000.
End
Function 5   $ sigyz vs volume
        0.0     1000.
        0.60    1000.
        0.70    10000.
        0.90    10000.
End
MATERIAL 35 = ORTHOTROPIC CRUSH, 5.682e-5
        Compacted YOUNGS MODULUS = 1.5e6
        Compacted POISSONS RATIO = 0.3
        Compacted YIELD STRESS  = 20000.
        X ID = 1   Y ID = 1
        Z ID = 2   XY ID = 4
        YZ ID = 5   ZX ID = 4
        Full Compaction = 0.9 $ 0 = no compaction, 1 = very flat
        Modulus x = 1.5e6
        Modulus y = 0.3e6
        Modulus z = 0.3e6
        Modulus xy = 0.2e6
        Modulus yz = 0.25e6
        Modulus zx = 0.2e6
End
Function 1  $ x-direction ( T-Direction)
        0.       2000.
```

```
        0.14     4200.
        0.28     5100.
        0.42     5430.
        0.57     6100.
        0.71     10100.
        0.80     15000.
        0.90     20000.
End
Function 2    $  y-direction (L-Direction) z-direction approx the same
        0.       400.
        0.14     986.
        0.28     1200.
        0.42     1275.
        0.57     1432.
        0.71     2371.
        0.80     3521.
        0.90     4690.
End
Function 4   $ sigxy or sigxz vs volume
        0.0     1000.
        0.60    1000.
        0.70    10000.
        0.90    10000.
End
Function 5   $ sigyz vs volume
        0.0     1000.
        0.60    1000.
        0.70    10000.
        0.90    10000.
End
MATERIAL 36 = ORTHOTROPIC CRUSH, 5.682e-5
        Compacted YOUNGS MODULUS = 1.5e6
        Compacted POISSONS RATIO = 0.3
        Compacted YIELD STRESS  = 20000.
        X ID = 1   Y ID = 1
        Z ID = 2   XY ID = 4
        YZ ID = 5   ZX ID = 4
        Full Compaction = 0.9 $ 0 = no compaction, 1 = very flat
        Modulus x = 1.5e6
        Modulus y = 0.3e6
        Modulus z = 0.3e6
        Modulus xy = 0.2e6
        Modulus yz = 0.25e6
        Modulus zx = 0.2e6
End
Function 1  $ x-direction ( T-Direction)
        0.       2000.
        0.14     4200.
        0.28     5100.
        0.42     5430.
        0.57     6100.
        0.71     10100.
        0.80     15000.
        0.90     20000.
End
Function 2    $  y-direction (L-Direction) z-direction approx the same
        0.       400.
```

```
        0.14     986.
        0.28     1200.
        0.42     1275.
        0.57     1432.
        0.71     2371.
        0.80     3521.
        0.90     4690.
End
Function 4   $ sigxy or sigxz vs volume
        0.0      1000.
        0.60     1000.
        0.70     10000.
        0.90     10000.
End
Function 5   $ sigyz vs volume
        0.0      1000.
        0.60     1000.
        0.70     10000.
        0.90     10000.
End
MATERIAL 37 = ORTHOTROPIC CRUSH, 5.682e-5
        Compacted YOUNGS MODULUS = 1.5e6
        Compacted POISSONS RATIO = 0.3
        Compacted YIELD STRESS  = 20000.
        X ID = 2   Y ID = 1
        Z ID = 1   XY ID = 4
        YZ ID = 5   ZX ID = 4
        Full Compaction = 0.9 $ 0 = no compaction, 1 = very flat
        Modulus x = 1.5e6
        Modulus y = 0.3e6
        Modulus z = 0.3e6
        Modulus xy = 0.2e6
        Modulus yz = 0.25e6
        Modulus zx = 0.2e6
End
Function 1  $ x-direction ( T-Direction)
        0.       2000.
        0.14     4200.
        0.28     5100.
        0.42     5430.
        0.57     6100.
        0.71     10100.
        0.80     15000.
        0.90     20000.
End
Function 2    $  y-direction (L-Direction) z-direction approx the same
        0.       400.
        0.14     986.
        0.28     1200.
        0.42     1275.
        0.57     1432.
        0.71     2371.
        0.80     3521.
        0.90     4690.
End
Function 4   $ sigxy or sigxz vs volume
        0.0      1000.
```

```
        0.60    1000.
        0.70    10000.
        0.90    10000.
End
Function 5   $ sigyz vs volume
        0.0     1000.
        0.60    1000.
        0.70    10000.
        0.90    10000.
End
MATERIAL 38 = ORTHOTROPIC CRUSH, 5.682e-5
        Compacted YOUNGS MODULUS = 1.5e6
        Compacted POISSONS RATIO = 0.3
        Compacted YIELD STRESS  = 20000.
        X ID = 1   Y ID = 1
        Z ID = 2   XY ID = 4
        YZ ID = 5   ZX ID = 4
        Full Compaction = 0.9 $ 0 = no compaction, 1 = very flat
        Modulus x = 1.5e6
        Modulus y = 0.3e6
        Modulus z = 0.3e6
        Modulus xy = 0.2e6
        Modulus yz = 0.25e6
        Modulus zx = 0.2e6
End
Function 1  $ x-direction ( T-Direction)
        0.       2000.
        0.14     4200.
        0.28     5100.
        0.42     5430.
        0.57     6100.
        0.71     10100.
        0.80     15000.
        0.90     20000.
End
Function 2    $  y-direction (L-Direction) z-direction approx the same
        0.       400.
        0.14     986.
        0.28     1200.
        0.42     1275.
        0.57     1432.
        0.71     2371.
        0.80     3521.
        0.90     4690.
End
Function 4   $ sigxy or sigxz vs volume
        0.0     1000.
        0.60    1000.
        0.70    10000.
        0.90    10000.
End
Function 5   $ sigyz vs volume
        0.0     1000.
        0.60    1000.
        0.70    10000.
        0.90    10000.
End
```

```
MATERIAL 39 = ORTHOTROPIC CRUSH, 5.682e-5
        Compacted YOUNGS MODULUS = 1.5e6
        Compacted POISSONS RATIO = 0.3
        Compacted YIELD STRESS  = 20000.
        X ID = 1   Y ID = 1
        Z ID = 2   XY ID = 4
        YZ ID = 5   ZX ID = 4
        Full Compaction = 0.9 $ 0 = no compaction, 1 = very flat
        Modulus x = 1.5e6
        Modulus y = 0.3e6
        Modulus z = 0.3e6
        Modulus xy = 0.2e6
        Modulus yz = 0.25e6
        Modulus zx = 0.2e6
End
Function 1  $ x-direction ( T-Direction)
        0.       2000.
        0.14     4200.
        0.28     5100.
        0.42     5430.
        0.57     6100.
        0.71     10100.
        0.80     15000.
        0.90     20000.
End
Function 2    $  y-direction (L-Direction) z-direction approx the same
        0.       400.
        0.14     986.
        0.28     1200.
        0.42     1275.
        0.57     1432.
        0.71     2371.
        0.80     3521.
        0.90     4690.
End
Function 4   $ sigxy or sigxz vs volume
        0.0     1000.
        0.60    1000.
        0.70    10000.
        0.90    10000.
End
Function 5   $ sigyz vs volume
        0.0     1000.
        0.60    1000.
        0.70    10000.
        0.90    10000.
End
MATERIAL 40 = ORTHOTROPIC CRUSH, 5.682e-5
        Compacted YOUNGS MODULUS = 1.5e6
        Compacted POISSONS RATIO = 0.3
        Compacted YIELD STRESS  = 20000.
        X ID = 2   Y ID = 1
        Z ID = 1   XY ID = 4
        YZ ID = 5   ZX ID = 4
        Full Compaction = 0.9 $ 0 = no compaction, 1 = very flat
        Modulus x = 1.5e6
        Modulus y = 0.3e6
```

```
        Modulus z = 0.3e6
        Modulus xy = 0.2e6
        Modulus yz = 0.25e6
        Modulus zx = 0.2e6
End
Function 1  $ x-direction ( T-Direction)
        0.       2000.
        0.14     4200.
        0.28     5100.
        0.42     5430.
        0.57     6100.
        0.71     10100.
        0.80     15000.
        0.90     20000.
End
Function 2    $  y-direction (L-Direction) z-direction approx the same
        0.       400.
        0.14     986.
        0.28     1200.
        0.42     1275.
        0.57     1432.
        0.71     2371.
        0.80     3521.
        0.90     4690.
End
Function 4   $ sigxy or sigxz vs volume
        0.0     1000.
        0.60    1000.
        0.70    10000.
        0.90    10000.
End
Function 5   $ sigyz vs volume
        0.0     1000.
        0.60    1000.
        0.70    10000.
        0.90    10000.
End
MATERIAL 41 = ORTHOTROPIC CRUSH, 5.682e-5
        Compacted YOUNGS MODULUS = 1.5e6
        Compacted POISSONS RATIO = 0.3
        Compacted YIELD STRESS  = 20000.
        X ID = 1   Y ID = 1
        Z ID = 2   XY ID = 4
        YZ ID = 5   ZX ID = 4
        Full Compaction = 0.9 $ 0 = no compaction, 1 = very flat
        Modulus x = 1.5e6
        Modulus y = 0.3e6
        Modulus z = 0.3e6
        Modulus xy = 0.2e6
        Modulus yz = 0.25e6
        Modulus zx = 0.2e6
End
Function 1  $ x-direction ( T-Direction)
        0.       2000.
        0.14     4200.
        0.28     5100.
        0.42     5430.
```

```
        0.57     6100.
        0.71     10100.
        0.80     15000.
        0.90     20000.
End
Function 2    $  y-direction (L-Direction) z-direction approx the same
        0.       400.
        0.14     986.
        0.28     1200.
        0.42     1275.
        0.57     1432.
        0.71     2371.
        0.80     3521.
        0.90     4690.
End
Function 4   $ sigxy or sigxz vs volume
        0.0     1000.
        0.60    1000.
        0.70    10000.
        0.90    10000.
End
Function 5   $ sigyz vs volume
        0.0     1000.
        0.60    1000.
        0.70    10000.
        0.90    10000.
End
 exit
```

2.12.8 Design Pressure Calculations for the T-Ampoule (in Accordance with Section VIII Division 1 of the ASME Boiler and Pressure Vessel Code

See stand-alone document that follows.

This page intentionally left blank

Design Pressure Calculations for the T-Ampoule in Accordance with Section VIII Division 1 of the ASME Boiler and Pressure Vessel Code

The objective of the T-Ampoule (Drawing 2A0261) is to provide a eutectic prevention barrier between the plutonium it contains and the PH13-8Mo stainless steel of the TB-1 containment vessel. The barrier will minimize any formation of a Pu/Fe eutectic under the elevated temperature of 1080°F during a fire accident. In forming the barrier, the T-Ampoule becomes a pressure vessel requiring analysis.

Section 1 describes the preparation of the pressure-temperature map which is necessary for a full pressure vessel analysis. This includes not only the interaction between the TB-1 pressure vessel and the T-Ampoule, but also the impact of pyrolysis of both O-ring material and of any ancillary plastic used for tagging and bagging within the T-Ampoule.

Section 2 presents an analysis performed to validate the maximum pressure specification of TB-1 taken from the original Safety Analysis Report (SAR).

The third section, Section 3, describes the actual pressure analysis for the T-Ampoule. The criteria selected for the analysis of T-Ampoule pressure containing capability is the ASME Boiler and Pressure Vessel Code (BPVC), Section VIII, Division 1.[1][2] The T-Ampoule's unusual design has some aspects, e.g., its small size or the use of O-ring seals, that require

exceptions to Section VIII. This section enumerates these exceptions. It also identifies specific paragraphs of the ASME Code that do apply to the T-Ampoule design.

Section 4 addresses the O-ring seal, a device not covered by Section VIII.

Throughout this report, individual sections identify and discuss instances of conservatism and uncertainty in the analyses. Chapter 5 accumulates all of these discussions into a single location to help the reader grasp the total level of conservatism and the risk associated with uncertainty involved in the analysis.

Finally, Section 6 recaps the whole paper into a single discussion of the results.

1 Pressure Temperature Map

A previous analysis described in LA-UR-10-05846, [3] addresses increased pressure inside the TB-1 pressure vessel in an aircraft accident scenario. This report treats the TB-1 interior as a single volume subjected to a uniform temperature of 1080°F. A uniform internal pressure is determined by analysis. This is in fact a good description of the final state of the package. However, the assembly starts out as two pressure envelopes. The T-Ampoule is a pressure vessel itself. Subdividing the TB-1 into two zones, the T-Ampoule forms the first zone; the second zone consists of the extremely small annulus between the T-Ampoule and the TB-1 wall, referred to herein as the Annulus. These two zones exist as separate pressure envelopes until the O-rings inside the vessels decompose and/or the O-ring seal in the T-Ampoule fails and pressures equilibrate. Before equilibration these two zones respond differently to temperature changes. After equilibration, the whole assembly acts as the single pressure containing device described by LA-UR-10-05846.

This analysis uses LA-UR-10-05846's conclusion that packing configuration #3, shown in Figure 1, is the worst case. It also adopts LA-UR-10-05846's assumption that sufficient oxygen somehow enters the vessels to oxidize all char and heavy hydrocarbons resulting from pyrolysis. It is, however, possible to provide a more realistic estimate of the pyrolysis impact. This less conservative calculation is included to provide a measure of the degree of conservatism in this analysis.

1.1 Package Volumes

Consider the assembly drawing in Figure 1: TB-1 Assembly for Packing Configuration #3. Three sample plutonium containers reside within the T-Ampoule. These three containers are designed to carry plutonium and are not pressure vessels. The T-Ampoule with the three containers fits snuggly within the TB-1 containment vessel. This leaves a small annulus volume between the TB-1 wall and the external surface of the T-Ampoule. More detailed inspection of Figure 1 illustrates just how small the annulus volume is. The TB-1 vessel's inner diameter is 4.250 inches. The T-Ampoule's outer diameter is 4.220 inches. Both numbers are average values. Assuming they are somehow perfectly centered, these dimensions leave a 0.015 inch radial gap between the two vessels. This gap integrated around the whole surface of the T-Ampoule creates an annulus volume of just 37.7 cubic centimeters (2.30 cubic inches). This analysis uses SI units to maintain consistency with the LA-UR-10-05846 report.

The T-Ampoule uses an O-ring seal to contain pressure. The three SC-1 containers also use O-rings. However, they are not considered pressure vessels. The T-Ampoule may also contain some PVC labels or polyethylene bags (referred to as ancillary plastic). As temperature increases during a design fire accident, the O-rings and ancillary plastic will decompose, or pyrolyze, increasing the mass of vapor in each pressure envelope. The amount of new vapor

differs between the T-Ampoule and the annulus. These differences plus the volumetric differences cause different pressure responses to temperature increase.

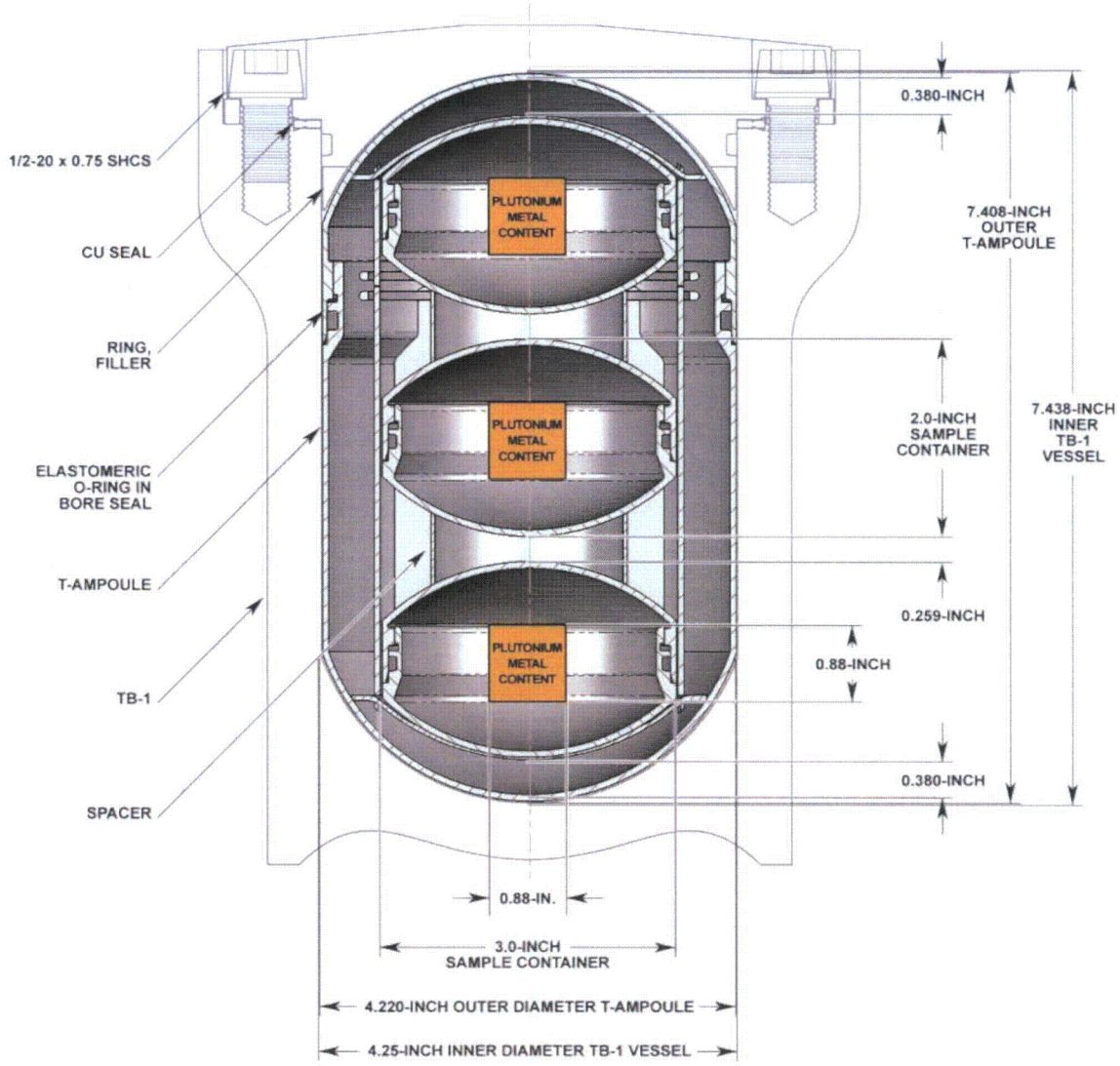

Figure 1: TB-1 Assembly for Packing Configuration #3

The following analysis tracks the response of three individual pressure envelopes:

- The annulus zone is the space between the TB-1 containment vessel and the T-Ampoule.
- The T-Ampoule zone consists of the volume within the T-Ampoule less the volume of solids contained there.
- The third zone is TB-1 volume. It is the sum of the first two volumes.

As will be discussed in detail below, the TB-1 becomes meaningful only after the T-Ampoule's seal fails and pressure equilibrates between the first two zones.

The volumes for each zone are listed in Table 1. They were taken from the LA-UR-10-05846 paper. In addition, the empty internal T-Ampoule volume of 1280 cm^3 was estimated specifically for this analysis. The vapor volume of the TB-1 container remains 1103 cm^3. The T-Ampoule, designed to nestle within the TB-1 container, is only slightly smaller with an internal volume of 1065 cm^3. The difference between these two volumes is the volume of the annulus at 37.7 cm^3.

Table 1: Summary of Pressure Envelope Volumes

Description	TB-1	T-Ampoule	Annulus	Units
Empty Volume	1460	1280		cm^3
Metal Volume		128		cm^3
Occupied Volume		1410		cm^3
Filler Ring	14.75			cm^3
T-Amp Contents Volume		214		cm^3
Vapor Volume (cm^3)	1103	1065	37.7	cm^3
Vapor Volume (m^3)	0.001103	0.001065	0.000038	m^3

The TB-1 device is fabricated from PH13-8Mo, equivalent to 13Cr-8Ni-2Mo, stainless steel while the T-Ampoule is fabricated of Ti-6Al-4V titanium alloy. These two materials have different thermal expansion coefficients with the stainless steel expanding slightly faster with temperature. The relative volume change with temperature between the two materials would be proportional to the cube of the thermal expansion coefficients integrated over the temperature range. These cubes of the thermal expansion coefficients are plotted in Figure 2. The values for thermal expansion coefficients for the two metals were taken from the BPVC, Section II Part D [2]. The volumes are expected to equilibrate pressures at approximately 800°F when O-ring seals fail. At that temperature, the value for the cube of thermal expansion factor for stainless steel is 1.015 in^3/in^3. For the titanium alloy of the T-Ampoule, the value at the same temperature was 1.011 in^3/in^3. Roughly estimated, the annulus volume would grow by the difference between these two values or by about 0.4% when the assembly is heated from 70°F to 800°F. Since the stainless always expands more than the titanium, the annulus volume change with temperature is always positive.

Subsequent analyses assume zero thermal growth. The above discussion demonstrates that the relative volume change with temperature is small but positive. Trying to quantify this volume change further would require significant analysis given the complex shapes involved. Further, since the annulus volume change with temperature is always positive, pressures calculated ignoring this change will slightly exceed actual pressures. Hence the assumption of no growth is conservative.

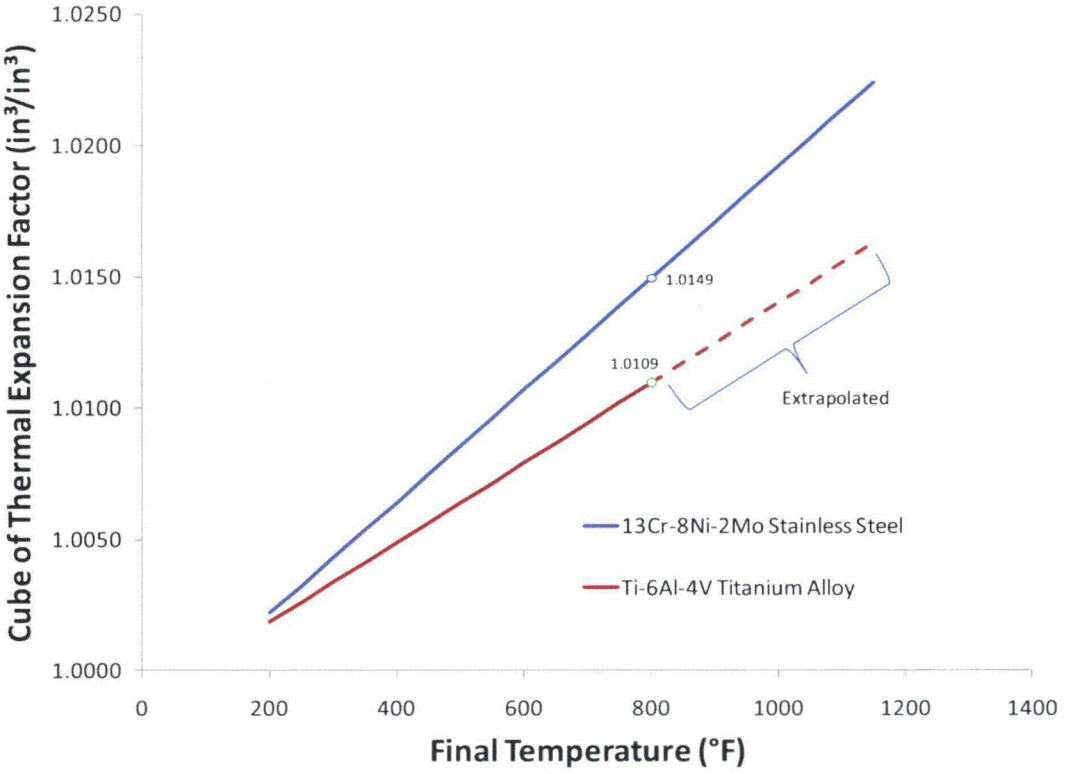

Figure 2: Plot of the Cube of the Thermal Expansion for Selected Materials as a Function of Temperature

1.2 O-ring Decomposition

Table 2 provides a summary of O-ring volumes and masses with the initial volumes extracted from LA-UR-10-05846. The T-Ampoule contains three O-rings, one for each sample container seal. In addition, this analysis allocates one half of the O-ring volume used to seal the T-Ampoule to the T-Ampoule zone's volume. The remaining one half of the T-Ampoule O-ring seal is allocated to the annulus zone volume. The TB-1 column in Table 2 contains the sum of the T-Ampoule and the annulus columns. The masses listed on the last line of Table 2 are based on an O–ring density of 1.8 g/cm^3.

Table 2: O-ring Volumes and Weights

Description	Annulus	TB-1	T-Ampoule	Units
T-Ampoule Seal	1.56	3.12	1.56	cm^2
SC-1 Seals (3 times)	0.00	3.58	3.58	cm^3
Total Volume	1.56	6.70	5.14	cm^3
Total O-ring mass	2.81	12. 1	9.24	g

According to LA-UR-10-05846, a fluoro-elastomeric O-ring decomposes per equation 1

$$0.147CF_2CH_2(s)+0.0178C_3F_6(s)\rightarrow 0.320C(s)+.294HF(g)+.0265CF_4(g) \qquad 1$$

This equation differs slightly from LA-UR-10-05846 in the coefficients of the products. This difference is due to rounding. LA-UR-10-05846 asserts, based on references, that the O-ring initially contains 78% by mass CF_2HC_2 and 22% by mass C_3F_6. The report also assumes complete O-ring decomposition by 1080°F. For the purposes of the pressure temperature map, this report assumes pyrolysis based on a simplified version Figure 3 that assumes complete pyrolysis by 1080°F.

In fact, fluorocarbon decomposition, or pyrolysis, is a function of temperature as shown in Figure 3. This figure was constructed from data for Viton® A also known as poly (vinylidene fluoride-co-hexafluoro-propylene) CAS # 9011-17-0. The first steep loss of mass on this curve between 700 and 900°F marks the transition of O-ring material to hydrogen fluoride (*HF*). The remaining slow decline traces the conversion of the remaining material to CF_4. At 1080°F, approximately 78% of the O-ring material has pyrolized. The above notwithstanding, subsequent analyses assume the O-ring pyrolizes completely at the first step (800°F). The figure was included to illustrate the degree of conservatism involved.[4]

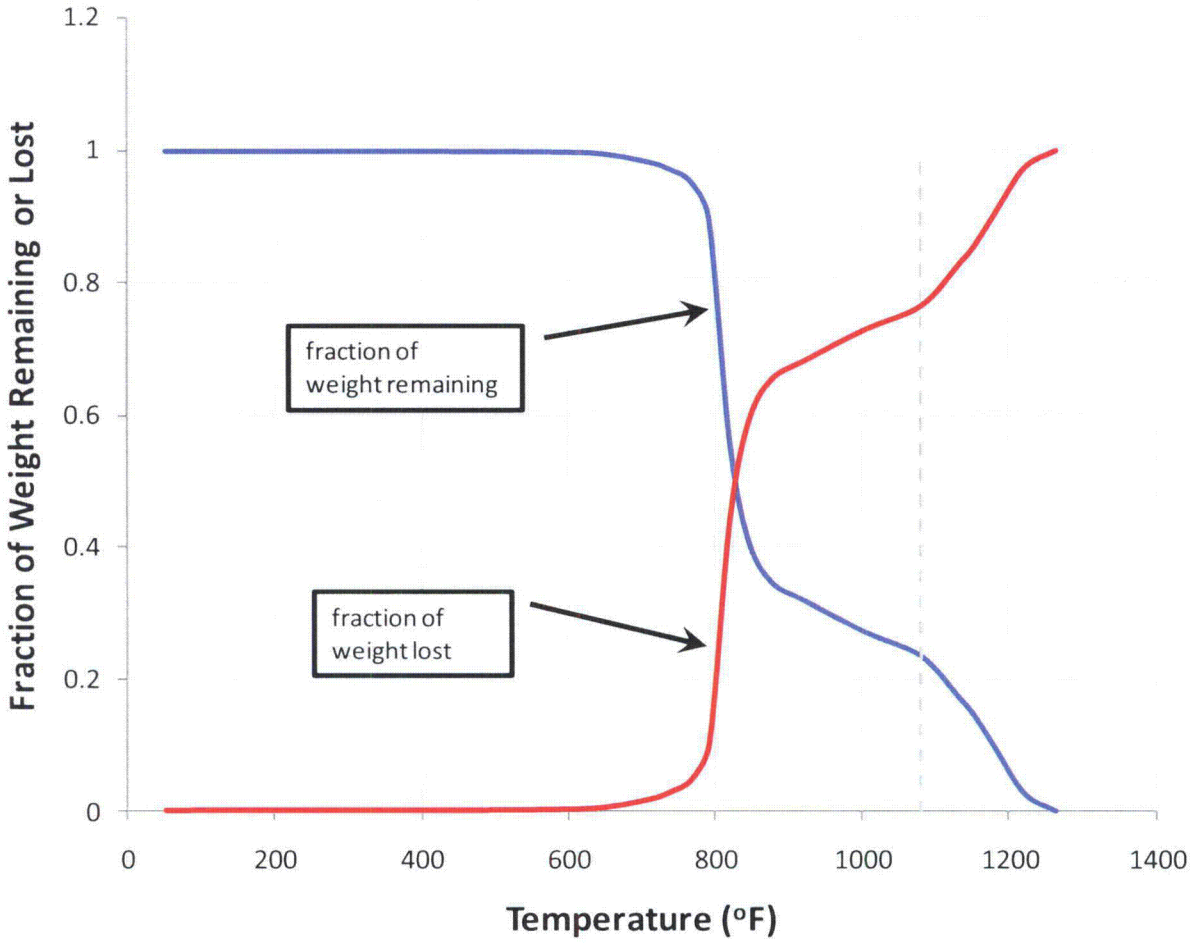

Figure 3: Pyrolysis of vinylidene fluoride-co-hexafluoro-propylene with Temperature [4, Figure 6.3.11]

An additional conservative assumption involves the sequence assumed for pressure release. This analysis assumes that the O-ring contains all pressure until the device reaches full design temperature of 1080°F. Only then does the pressure barrier fail. In fact, failure of the O-ring as a pressure containing device would occur gradually between 700°F when pyrolysis starts and the final temperature of 1300°F.

The LA-UR-10-05846 analysis assumes only two materials evolve during pyrolysis, carbon tetrafluoride (MW = 88 g/mol) and hydrofluoric acid (MW = 20 g/mol). These materials combine for an average molecular mass ratio on the order of 25 to 30 g/mol. On the other hand, Moldoveanu suggests that these reactions are more complex but fails to adequately quantify this assertion. His analysis did, however, say that the resulting products of pyrolysis would have higher molecular mass ratios than were used by LA-UR-10-05846. Compounds with molecular mass ratios exceeding 154 g/mol were seen but were not identified.[4] Higher molecular mass ratios would result in fewer moles released per gram of material generating lower pressures. Use of the LA-UR-10-05846 analysis is therefore conservative.

This analysis assumes, as does LA-UR-10-05846, that the solid carbon, or char, generated in equation 1 is subsequently oxidized into carbon dioxide.

$$0.320C(s)+0.320O_2(g)\rightarrow 0.320CO_2(g) \qquad 2$$

While LA-UR-10-05846 assumes carbon converts to carbon monoxide, at temperatures less than 3000°F (1920 K) the carbon monoxide/carbon dioxide equilibrium strongly favors carbon dioxide. In either case the reaction forms the same number of moles of vapor. No attempt is made to identify the source of the oxygen.

The moles of reactants in Equation 1 are based on the calculation summarized in Table 3. The first line, total O-ring mass for the three cases under consideration is a repetition of the last line of Table 2. For the purposes of this table, the molar mass ratio of CF_2CH_2 is 64.0 g/mol and the molar mass ratio of C_3F_6 is 150.0 g/mol.

Table 3: O-ring Decomposition Results -- Reactants

Description	T-Ampoule	Annulus	TB-1	Units
Total O-ring mass	9.25	2.81	12. 06	g
Mass of CF_2CH_2	7.21	2.19	9.41	g
Mass of C_3F_6	2.04	0.62	2.65	g
Moles of CF_2CH_2	0.113	0.0342	0.147	mol
Moles of C_3F_6	0.0136	0.00412	0.0177	mol

Note that LA-UR-10-05846 has adjusted the coefficients in Equation 1 to match the moles of reactants for the TB-1 column. This means the moles products for TB-1 will also match the coefficients of the products in Equation 2 also. The moles of reactants and products for the T-Ampoule and the Annulus will vary as the ratio of the O-ring mass for that volume to the O-ring mass for TB-1. The O-ring mass reported in the TB-1 column is the total of the masses from other two volumes. This results only after equilibration. This carries through to the products also, as shown in Table 4.

Table 4: O-ring Complete Oxidation -- Products

Description	T-Ampoule	Annulus	TB-1	Units
Moles of HF	0.225	0.0685	0.294	mol
Moles of CF_4	0.0203	0.00618	0.02650	mol
Moles of CO_2	0.246	0.0747	0.320	mol
Total Moles from O-rings	**0.491**	**0.149**	**0.640**	mol

These molar quantities are constant and contribute a specific amount to the pressure calculation of Section 1.5.

1.3 Ancillary Plastic Pyrolysis/Oxidation

T-Ampoule assembly procedures allow the inclusion of labels and bags inside the T-Ampoule. Labels are typically metalized Poly(Ethylene Terephthalate) or metalized PET. Mylar™ is an example of this material. No specification exists regarding the exact composition and quantity of this packaging material. Nonetheless, this plastic will degrade with temperature in a manner similar to the O-ring pyrolysis discussed in the previous section. The four most likely candidates for inclusion in a PAT-1 package are:

1. Metalized PET, Poly(Ethylene terephthalate), of which only the polyester (Polyethylene terephthalate) is active.
2. Poly(Ethylene) (all densities)
3. PVC, Poly(Vinyl Chloride)
4. PTFE, Poly(TetraFluoroEthylene). An example of PTFE is Teflon™.

For any plastic composed of hydrocarbons and other chemicals, the products of a complete oxidation to carbon dioxide reaction depends on the chemical composition of the plastic's monomer. Each plastic consists of chains built by repeating the same monomer. What happens to that monomer happens to the whole chain. The complete oxidation reaction equations for the four plastics monomers listed above are listed in Table 5.

Table 5: Monomer Complete Oxidation Reactions

Plastic	Monomer	Reaction
PET	Ethylene Terephthalate	$C_{10}H_8O_4 + 10O_2 \rightarrow 10CO_2 + 4H_2O$
PE	Ethylene	$CH_2 + 1.5O_2 \rightarrow CO_2 + H_2O$
PVC	Vinyl Chloride	$C_2H_3Cl + 2.75O_2 \rightarrow 2CO_2 + 1.5H_2O + .5Cl_2$
PTFE	TetraFluoro Ethylene	$C_2F_4 + 2O_2 \rightarrow 2CO_2 + 2F_2$

Table 6 extends the information in Table 5 to include some statistics of the reactions including the number of moles of vapor formed per mole of monomer, the number of moles of oxygen consumed per mole of monomer consumed and the molecular mass ratio of the monomer.

Table 6: Complete Oxidation Reaction Statistics

Plastic	Monomer Molecular Mass (g/mol)	Moles of Vapor per Mole of Monomer	Mols O_2 per mol monomer
PET	192	14	10
PE	14.0	2	1.5
PVC	98.0	4	2.75
PTFE	100	4	2

This information will be used in pressure calculations in Section 1.5. The total number of moles of vapor from ancillary plastic will be adjusted to achieve the final maximum allowable pressure. The number of moles will be the same for any plastic. However, the mass in grams of ancillary plastic allowed depends on the plastic.

1.4 Helium Generation from Alpha Decay

Based on the discussion in Section 4.5.3 of this addendum, alpha decay of plutonium generates an insignificant molar quantity, n_{he}, of helium equal to a rate, r_{he}, of 1.42E-07 mol of helium per gram of plutonium per year. Design mass of plutonium is 821 grams. The value used here is 1300 grams of ^{241}Pu, a bounding condition for the analysis. For the purposes of this study, it was assumed that the T-Ampoule was assembled one year prior to the accident and that no helium leaked from the container via molecular diffusion. With this assumption, the total of helium generated is 4.62E-05 moles. This quantity is assumed constant for this report. It contributes a specific amount to the pressure calculation of Section 1.5.

1.5 Pressure Calculation

Table 7 contains a summary of the pressure calculation to be completed for this report. The first calculation estimates the molar mass of argon initially trapped in the PAT-1 package during loading in the glove box. The second calculation uses the specified final temperature and pressure to estimate the limiting amount of ancillary plastic allowed in the package. This information then contributes to the final calculation of the pressures in the two initial volumes, annulus and T-Ampoule, prior to and after equilibration.

Table 7: Pressure Cases

Description	Pressure (*psia*)	Temperature (°*F*)	Mass Involved (*mol*)	Zones Involved
Initial	14.7	75	to be calculated	Annulus, T-Ampoule
Just before equilibration	to be calculated	800	Initial, Ancillary Plastic, O-Rings, He from alpha decay	Annulus, T-Ampoule
Final	1110	1080	to be calculated	TB-1

Pressure in a pressure envelope is driven by the quantity and properties of the vapor phase constituents in that volume. There will be no liquids in the package; and solids' impact on pressure is so small that its impact is lost in rounding. For a vapor, the relationship between mass, temperature and pressure is

$$P = z\left(\frac{n}{V}\right)R_u T \qquad 3$$

In SI units, the universal gas constant R_u is 8.314 N-m/mol-K, temperature, T, is in Kelvin, volume, V, is in cubic meters and vapor mass, n, is in mols. This analysis will assumes ideal conditions (z = 1) in order to maintain consistency with LA-UR-10-05846 analysis.

As Figure 4 illustrates, ideal gas is a reasonable assumption. This figure contains a standard corresponding states plot over which estimated compressibility factors for the gases involved are plotted for the three cases listed in Table 7. Most points cluster around the z = 1 line. The two outliers are Cl_2 and F_2, which only show up in rare choices of ancillary plastic.

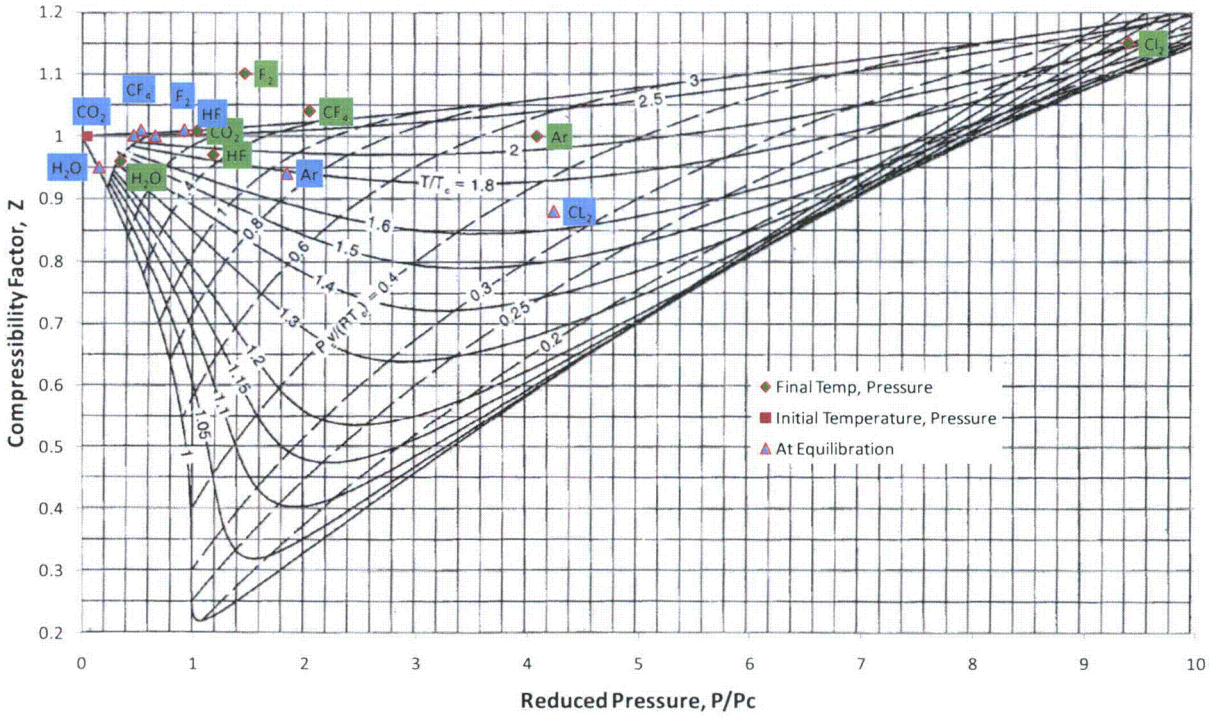

Figure 4: Compressibility Factors for TB-1 Molecules at 1110 psia and 1080 °F[4]

1.5.1 Initial Charge of Argon

The PAT-1 package will be assembled in a glove box. It is assumed here that the glove box contains argon. Since pressure depends only on the moles of vapor present any other inert gas would require the same mass. This report also assumes that the glove box assembly occurs at 14.7 psia (1 atmosphere) and 75 °F. The amount of argon can be estimated via a manipulation of equation 3.

$$n = \frac{PV}{R_u T} \qquad 4$$

Note the omission of the compressibility factor (assumed = 1.0). Table 8: displays the results.

Table 8: Initial Molar Contents

Parameter	T-Ampoule	Annulus	TB-1	Units
Temperature, T	297.	297.	297.	K
Pressure P	101,325	101,325	101,325	N/m^2
Gas Constant, R_u	8.314	8.314	8.314	$N\text{-}m/mol\text{-}K$
Volume, V	0.001065	3.77E-05	0.00110	m^3
moles, n	0.0437	0.00155	0.0453	mol

These moles of initial argon are constant and contribute a specific amount to the pressure calculation.

1.5.2 Final State – Estimate of Ancillary Plastic Content

As Table 7 indicates, the final pressure and temperature are known. The only unknown is the mass of ancillary plastic that can be allowed. With known pressure, temperature and volume, the total moles can be calculated from Equation 3 after minor algebraic manipulation. The calculation returns a total molar mass equaling 1.19 mol. The breakdown by source is shown in Table 9. The molar quantities from argon, helium generated from alpha decay of plutonium, O-ring decomposition, and char oxidation are known. The molar quantity from oxidation of ancillary plastic is back-calculated by subtracting the sum of the above sources from the total moles calculated using equation 3.

Table 9: Final Conditions Molar Estimate

Source	Contribution (mol)	Mol Fraction	Pressure Contribution (psia)
Argon (Original Atmosphere)	0.0453	0.0381	42.3
He (from Alpha Decay)	0.000185	0.00016	0.173
HF (from O-Ring decomposition)	0.294	0.248	275
CF_4 (from O-Ring decomposition)	0.027	0.0227	25.2
CO_2 (from oxidation of char)	0.32	0.27	299
Ancillary Plastic Oxidation	0.501	0.422	468
Total mols Vapor	**1.19**	**1.00**	**1110**

Table 9 provides the allowable contribution to pressure (468 psi) from ancillary plastics based on an allowable amount (0.501 mol). The question to be answered is how much initial plastic in grams should be allowed. Table 10 answers that question.

The first five lines of Table 10 (excluding the titles) contain information repeated from Table 5 and Table 6. Below these lines, the allowable quantity of vapor from plastic (0.501 moles) comes from Table 9. The quantity of moles of monomer derives from the number of moles of vapor per mole of monomer, 14 in the case of metalized PET. The allowable mass is calculated by multiplying the allowable moles of monomer by the molecular mass of the monomer, 6.87 grams of plastic in the case of metalized PET. Note that this is only plastic. Metalized PET will have some additional mass from the metal layered with the plastic.

For the purposes of discussion only, this mass was equated to an equivalent square sheet of 0.001 inch thick material assuming an average density for plastics of 1.4 g/cm^3. For metalized PET, for example, 6.87 grams of plastic can be rolled out to a sheet 0.001in. thick and 17.3 in. x 17.3 in.

on each side. For reference, a typical kitchen sandwich bag is 0.001 in. thick and a plastic tarp is 0.005 in. thick.

Table 10: Conversion of Vapor Mass to Grams of Ancillary Plastic

Common Name	Metalized PET	Poly ethylene	PVC	PTFE	Units
Chemical name of monomer	ethylene terephthalate	ethylene	vinyl chloride	tetrafluoro ethylene	
Monomer formula	$C_{10}H_8O_4$	CH_2	C_2H_4Cl	C_2F_4	
Monomer mol/mass ratio	192	14	98	100	g/mol
mol vapor/ mol monomer	14	2	4	4	
mol O_2/mol monomer	10	1.5	2.75	2	
Allowable mols from plastic vapor	0.501	0.501	0.501	0.501	mol
Allowable mols monomer	0.0358	0.251	0.125	0.125	mol
Allowable mass (plastic only)	**6.87**	**3.51**	**12.2**	**12.5**	g
Size of 0.001 in thick square (for illustration only)	17.3	12.4	23.2	23.3	in

As Table 5 demonstrates, the products of oxidation of ancillary plastic differ with monomer. Table 11 lists the pressure contribution of these different products.

Table 11: Pressure Results Showing All Components

Common Name	Metalized PET		Polyethylene		PVC		PTFE	
	mol	psia	mol	psia	mol	psia	mol	psia
Original Atmosphere	0.0452	42.3	0.0452	42.3	0.0452	42.3	0.0452	42.3
Helium generated from alpha decay	0.0002	0.173	0.0002	0.173	0.0002	0.173	0.0002	0.173
O-ring Thermal Decomposition								
HF	0.2940	275	0.2940	275	0.2940	275	0.2940	275
CF_4	0.0270	25.2	0.0270	25.2	0.0270	25.2	0.0270	25.2
CO_2 from char oxidation	0.3200	299	0.3200	299	0.3200	299	0.3200	299
Subtotal of all above sources	**0.6864**	**642**	**0.6864**	**642**	**0.6864**	**642**	**0.6864**	**642**
Ancillary Plastic -- thermal pyrolysis with oxidation								
CO_2	0.3577	334	0.2504	234.1	0.2504	234.1	0.2504	234.1
H_2O	0.1431	134	0.2504	234.1	0.1878	175.6		
Cl_2					0.0626	58.53		
F_2							0.2504	234.1
Total Pressure	**1.1872**	**1110**	**1.1872**	**1110**	**1.1872**	**1110**	**1.1872**	**1110**

It is important to remember that these quantities are mutually exclusive. It is allowable to include 6.88 g of metalized PET or 3.51 grams of grams polyethylene or 12.3 grams of PVC or 12.5 grams of PTFE.

All that remains is to estimate the amount of oxygen required to support all the reactions discussed above. Table 12 provides that answer.

Table 12: Oxygen Required for Oxidation

Description	Metalized PET	Poly ethylene	PVC	PTFE	Units
Moles to oxidize O-ring char	0.320	0.320	0.320	0.320	mol
Moles to oxidize Ancillary Plastic	0.358	0.377	0.344	0.250	mol
Total moles of oxygen (O_2) required	0.678	0.697	0.664	0.570	mol
Equivalent Pressure at 75 °F	220	226	216	185	psia

The moles of O_2 required to oxidize O-ring char is constant because O-ring char mass is constant. The moles of O_2 required to oxidize ancillary plastic varies with the plastic. The calculated amount is the product of line 6 (mol O_2/mol monomer) and line 8 (Allowable moles monomer) of Table 10. The last line of Table 12 contains the result of a simple calculation using equation 3 for the full volume of the TB-1 vessel. In order to enable all of the oxidation assumed in this section, a package assembly containing 12.3 grams PVC (the allowable limit from Table 10) must contain O_2 at 216 psi over and above its original charge of argon. This is impossible and its assumption represents an extreme degree of conservatism. To illustrate the degree of conservatism, Section 1.7 presents an alternative but still conservative calculation of allowable ancillary plastic.

1.6 Pressure before and after Equilibration

Figure 5 contains a plot of the pressure/temperature map for the package. The upper (green) line represents pressure in the small annular space between the TB-1 wall and the T-Ampoule. The solid line denotes pressure before equilibration. The dashed line is what the pressure would be without equilibration. The bottom (red) line represents pressure in the large volume of the T-Ampoule. Again, the dotted line extends the pressure curve to what could be without equilibration. The solid (blue) line denotes the pressure in the combined volumes, called the TB-1 volume in previous sections.

Pressures prior to about 600°F are equal in both the annulus and the T-Ampoule. At these low temperatures, mass and volume are both constant. After 600°F, the O-rings and plastic begin

pyrolysis. The changing mass affects the pressure in the low volume Annulus more severely than it affects the T-Ampoule pressure.

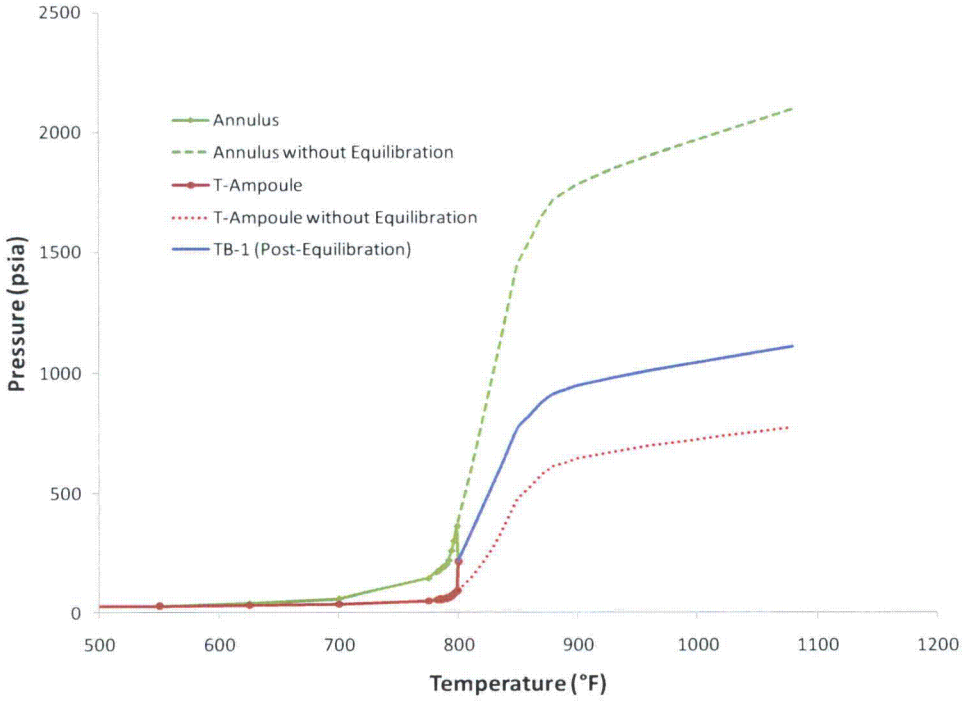

Figure 5: Pressure Temperature Map for Package

At approximately 800°F, the pressure difference between the two pressure envelopes has reached a point such that the O-ring seal fails by design (See Chapter 4). Pressure in the Annulus is higher than is pressure in the T-Ampoule. At this point, the pressure in the two volumes equilibrates and the two pressure envelopes merge into the single TB-1 pressure. The Annulus pressure drops and the T-Ampoule pressure rises. Pressure continues to rise with increasing temperature in the single volume until it reaches 1110 psia at 1080°F.

An issue arises in Chapter 4 regarding the repeatability of the O-ring failure point. This section is intended to provide information for the discussion there. Assume the O-ring seal does not fail. The Annulus pressure will continue to rise, as will the T-Ampoule pressure, as temperature continues to go up. What happens to the differential pressure? It goes up following the rapidly rising Annulus pressure. Figure 6 contains a plot of the annulus pressure as a function of pressure differential.

The O-ring seal is intended to fail when pressure differential reaches 160 psi. At that point, Annulus pressure will be 368 psia, well below the maximum allowable pressure (MAP) for the TB-1 pressure vessel. Pressure against the TB-1 wall stays below the MAP of 1110 psia until the differential pressure reaches 515 psi.

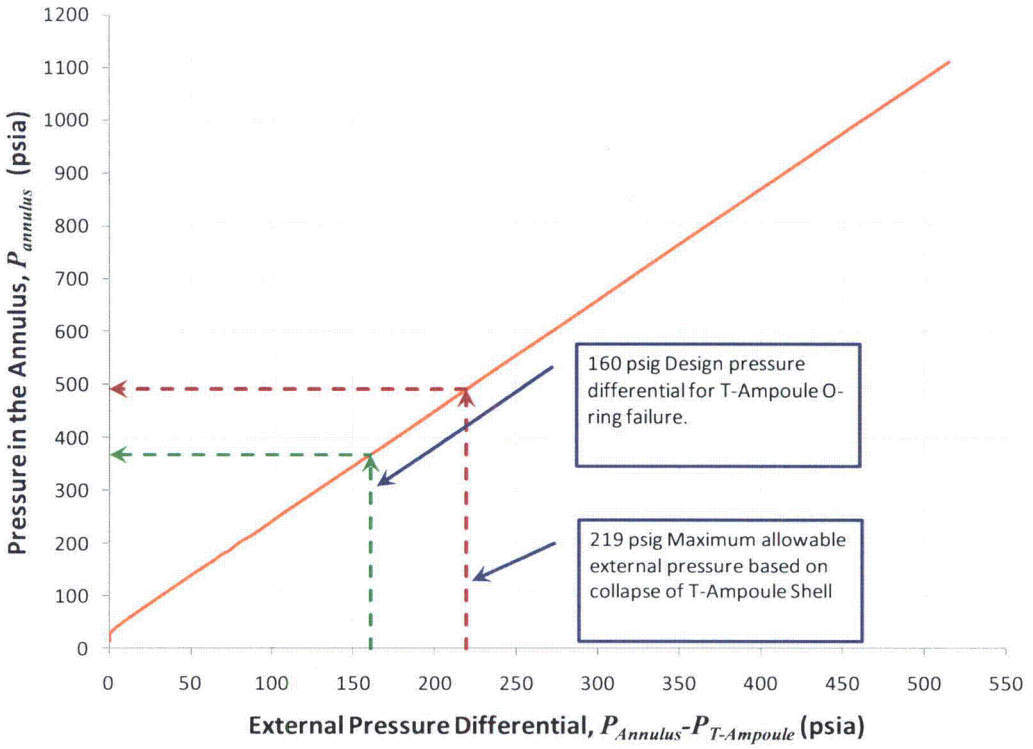

Figure 6: Relationship Between Annulus Pressure and Pressure Difference

In other words, the O-ring seal failure point can be high by a factor of safety of 3.2 (515/160) before its failure to equilibrate affects pressure on the TB-1 vessel wall.

Contingency against buckling failure of the T-Ampoule shell due to excessive external pressure is tighter. The nominal maximum external pressure difference is 219 psi. This is a factor of 1.33 above the nominal failure point of the O-ring.

1.7 Alternative Ancillary Plastic Calculation

As discussed in Section 1.6, the allowable ancillary plastic limit is based on an assumption that oxygen is always available for reaction with the products of pyrolysis. Analysis there assumes the oxygen appears without speculating as to its source. Table 12 demonstrates that the one feasible source, accidental inclusion during assembly is in fact impossible. The initial assembly would have to include between 150 and 350 psi of pure oxygen depending on the monomer involved. Since assembly is in a glove box these levels of pressure are impossible.

A more feasible, but still conservative, scenario assumes package assembly on an open workbench at 75°F and one atmosphere of air. While more feasible, it is still highly unlikely. Both engineering and administrative controls exist to ensure an inert glove box atmosphere during assembly. Nonetheless, this section stipulates that this scenario exists. The package

would be assembled at 14.7 psia and it would contain 79% nitrogen (N_2) and 21% oxygen (O_2) as its initial charge. Only 0.00950 mol of oxygen as O_2, 0.21 x 0.0453 (see Table 8), is available to burn char. Limited O_2 limits CO_2 formation to only 0.00950 moles. The resulting final vapor phase mixture is summarized in Table 13. Compare this to Table 9. Original argon is now original N_2 and is 21% lower. CO_2 has dropped from 0.320 mol contributing 299 psi to final pressure to 0.00950 mol contributing only 8.89 psi to final pressure. Most important, ancillary plastic oxidation has changed to ancillary plastic pyrolysis and has gone numerically from 0.501 mol contributing 468 psi to 0.821 mol contributing 767 psi to the final pressure.

Table 13: Less Conservative Calculation of Ancillary Plastic Contribution

Source	Contribution (mol)	Mol Fraction	Pressure
Original N_2	0.0357	0.0301	33.4
He (from Alpha Decay)	0.00019	0.00016	0.173
HF O-Ring decay	0.294	0.248	275
CF_4 O-Ring decay	0.027	0.0227	25.2
CO_2	0.0095	0.008	8.89
Ancillary Plastic Pyrolysis	0.821	0.691	767
Total mols Vapor	1.19	1.00	1110

How does this increased molar mass impact allowable plastic? Using PET as an example, Figure 7 shows the results of pyrolysis in an inert atmosphere for PET. The analysis was done at 1112°F, sufficiently close to the final PAT-1 temperature of 1080 °F. The figure shows selected mol-mass ratios to illustrate the distribution. In fact the mol fraction weighted average for all 31 compounds is 108 g/mol. Similar analyses were done for all four plastics. The results are tabulated on the third line of Table 14. The table also lists the calculated allowable mass. For PET, allowable ancillary plastic has gone up from 6.87 g (Table 10) to 89.0 g (Table 14) an increase of an order of magnitude. For the purposes of illustration only, and assuming an average plastic density of 1.4 g/cm^3, the PET plastic, if rolled out to a 0.001 in. thickness, has gone from a square 17.3 in. on edge to square 62.3 in. on edge.

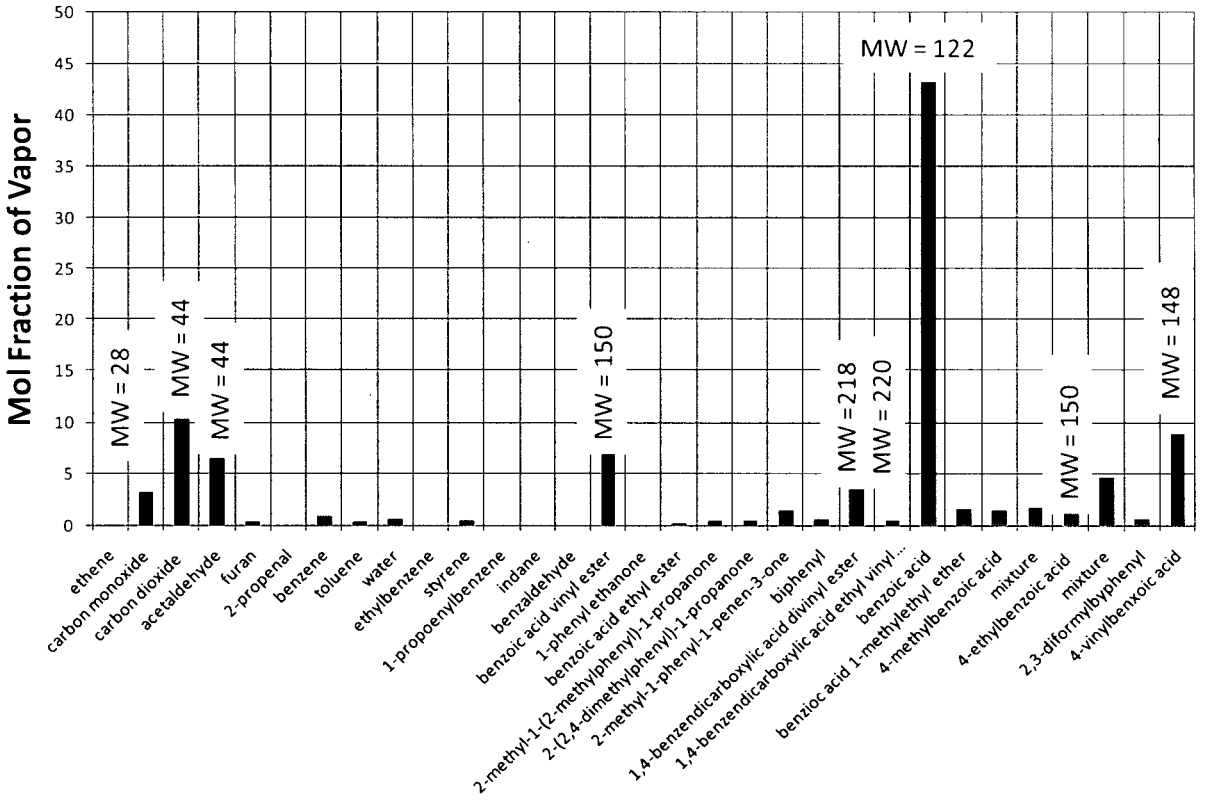

Figure 7: Pyrolysis of PET at 600 °C (1112 °F)[4]

Other plastics have similar increases. Polyethylene increases from 3.52 to 200 g. PVC jumps from 12.2 to 71 g. PTFE goes from 8.35 to 82.4 grams. In conclusion, the more conservative scenario used in this report reduces allowable ancillary plastic mass by as much as an order of magnitude.

Table 14: Pyrolysis Example

Common Name	Metalized PET	Polyethylene	PVC	PTFE	Units
Chemical name of monomer	ethylene terephthalate	ethylene	vinyl chloride	tetrafluoro-ethylene	
Pyrolized Vapor Mole Mass Ratio	108	243	86.1	100	g/mol
Allowable Total mols Vapor	1.19	1.19	1.19	1.19	mol
Moles from all other sources	0.366	0.366	0.366	0.366	mol
Allowable mols monomer	0.824	0.824	0.824	0.824	mol
Allowable mass (plastic only)	89	200	70.9	82.4	g
Size of 0.001 in thick square (for illustration only)	62.3	93.4	55.6	59.9	in

2 Verification of TB-1 Maximum Allowable Pressure

The calculations in this chapter verify the use of 1110 psia (1095.7 psig) as maximum allowable pressure (MAP) at a temperature of 1080 °F. This value for MAP was taken from the original Safety Analysis Report (SAR) for the PAT-1 package.[8]

It is important emphasize that the SAR's MAP will remain the specified maximum pressure for the TB-1. The value of this analysis is in the demonstration of the safety inherent in using the SAR value.

2.1 Results

The analysis of this section demonstrates that the MAP specified by the SAR is safe. Its value of 1110 psia at 1080°F is used elsewhere in this report where a maximum allowable pressure is needed.

Based on an ASME Boiler and Pressure Vessel Code (BPVC) Section VIII, Division 1 analysis, the maximum allowable operating pressure (MAOP) at 1080°F for the TB-1 pressure vessel is 2200 psia. This MAOP exceeds the SAR MAP (1110 psia @ 1080°F) with a factor of safety of 1.98. [1]

The allowable pressure based on vessel wall strength is 5386 psig (5400 psia). The allowable pressure based on closure is 2185 psig (2200 psia). The minimum of the two, 2200 psia, is the MAOP for the TB-1 vessel based on the analysis documented below.

2.2 Method

The following analysis looks first at the vessel wall's strength and then at the ability of its closure to contain pressure. It calculates first the maximum pressure allowed by the shell. It then calculates the maximum pressure allowed by the closure. The MAOP is the minimum of the two. This number is then compared to the SAR's MAP.

The TB-1 vessel is sufficiently thick-walled with sufficient structural reinforcement that a concern arose that a standard BPVC analysis based on a thin-wall model would not provide reasonable or conservative results.[1] Consequently, a simplified Finite Element Method (FEM) model was run first. These results were then compared with a more traditional BPVC type analysis. This comparison will demonstrate that a thin wall assumption is valid. This conclusion clears the way for an allowable pressure calculation using the thin wall model dictated by the BPVC.

The closure analysis concentrates on bolting. The FEM analysis will demonstrate that the stresses in the head are sufficiently low to be accepted without further analysis. The bolting analysis follows standard BPVC methods. It calculates the loading on the bolts needed to offset the pressure on the head and to ensure pressure containment of the gasket material. Pressure is adjusted until this load, converted to a stress per bolt, equals the allowable stress for the given bolting material. This pressure is the allowable pressure based on closure.

The minimum of the two allowable pressures calculated above is the MAOP for the system.

2.3 Allowable Pressure based on Vessel Wall

2.3.1 Numerical Analysis

The FEM model used the same grid generated for impact analysis in Section 2 of the Addendum to the SAR. This grid was imported into the Abaqus FEM program for analysis. This analysis used the MAP (1110 psia) as a boundary condition to the numerical model. This numerical model was simplified in that it ignored the gasket seal. The model was run as a steady state calculation at 1080°F.

Figure 8 shows the calculated hoop stress in the vessel wall. Based on the FEM analysis, maximum hoop stress is 4367 psi (tension). As would be expected in a pressure vessel hoop stress reaches a maximum on the shell wall away from reinforced ends. Again as expected maximum hoop stress occurs on the inner surface of the vessel. In a thin wall analysis, this hoop stress is assumed constant across the vessel. Figure 8 also demonstrates that the variation of stress through the wall is small.

2.3.2 Thin Wall Vessel Analysis

The BPVC uses the following formula from paragraph UG-26 to estimate the maximum allowable pressure, P, in a thin-walled shell as a function of hoop stress, S.

$$P = \frac{SE_J t}{R_i + 0.6t} \qquad 5$$

Refer to Table 15 for a description of variables, their value and their units. Manipulation of the above allows the estimation of hoop stress as a function of internal pressure:

$$S = \frac{P(R_i + 0.6t)}{E_J t} \qquad 6$$

Table 15: Summary of Parameters Used in Equation 6

Parameter	Description	Value	Units
P	Internal Pressure	1095.3	psig
R_i	Radius to inside surface of vessel	2.125	in
t	Wall thickness	0.55	in
E_J	Longitudinal Joint Efficiency	1.00	

The longitudinal joint efficiency, E_J, equals 1.0 because the TB-1 vessel is machined from a solid material and has no longitudinal joint.

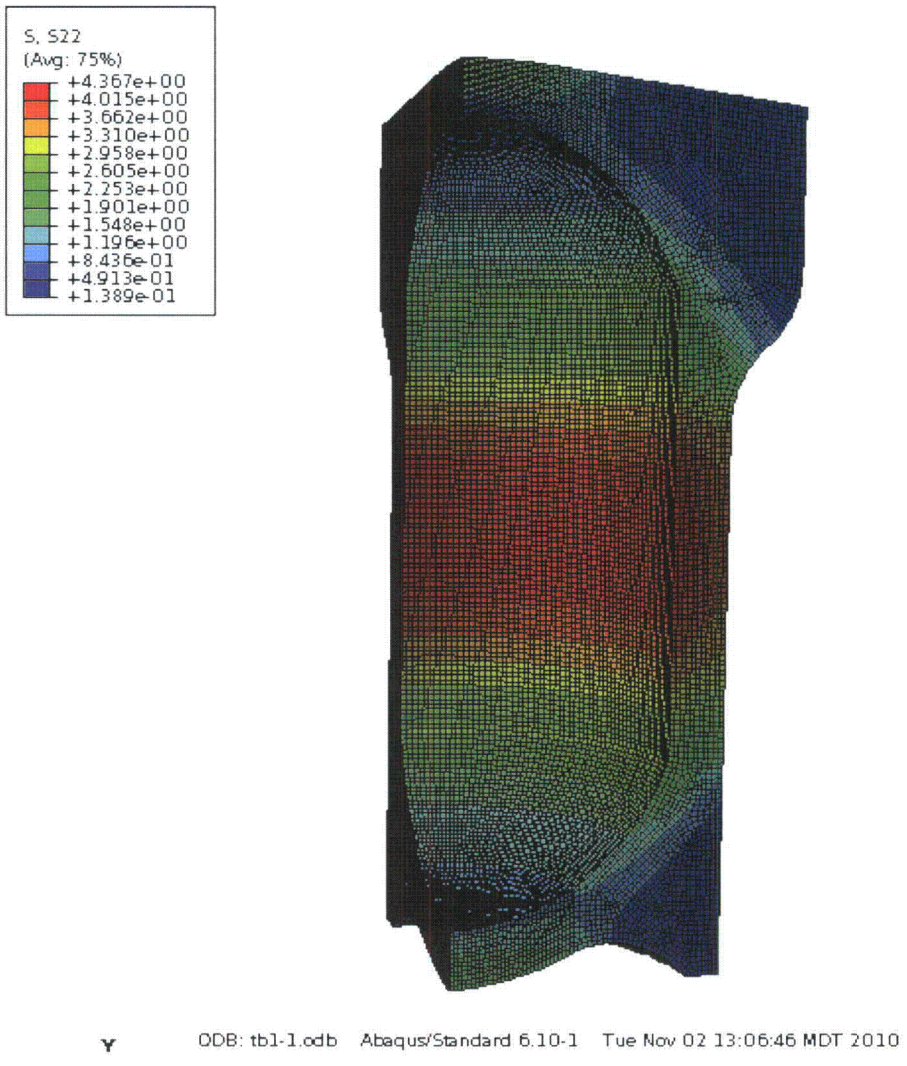

Figure 8: Hoop Stress Experienced by TB-1 with 1110 psia Internal Pressure

Using the values listed in Table 15, equation 6 returns a thin wall hoop stress of 4890 psi. This number compares well with the FEM result of 4367 psi, demonstrating the validity of the BPVC style of thin wall vessel analysis. Since it generates the higher and therefore more conservative stress, the thin wall result will be used for ongoing discussion.

2.3.3 TB-1 Material Strength Criteria

There still remains the issue of comparing this stress to a strength parameter for the material. The BPVC compares hoop stress directly to a strength value called the allowable stress, S_A, which is in turn related to the ultimate tensile strength of the material. This ultimate tensile strength used must be at operating temperature. In this case, operating temperature would be 1080°F.

Per the SAR Addendum, material for the TB-1 is stainless steel with a UNS number 13800 with heat treatment at 1075°F (H1075). This UNS number is equivalent to the designation PH13-8Mo used in the handbook MIL-HDBK-5J from which TB-1 material properties were extracted. Figure 9 contains a curve from that source showing the impact of temperature on tensile ultimate and the tensile yield strength of this material.[7]

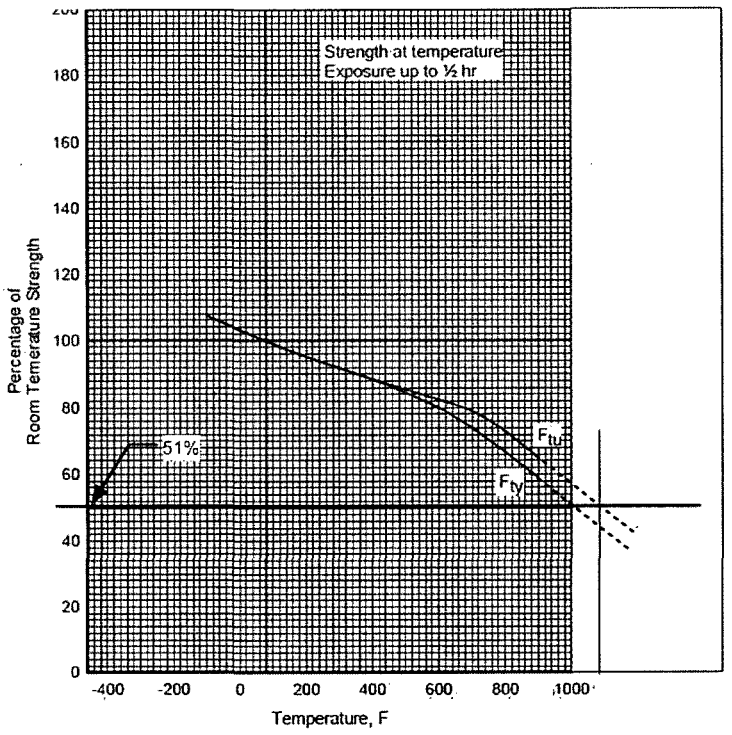

Figure 9: Figure 2.6.6.1.1. Effect of temperature on the tensile ultimate strength (F_{tu}) and the tensile yield strength (F_{ty}) of PH13-8Mo (H950 and H1000) stainless steel bar [7]

For the purposes of the BPVC analysis, ultimate tensile strength is the important parameter. Hence the curve labeled F_{tu} will be used. The curve stops at 900°F making a 180°F extrapolation necessary. Based on this extrapolation, ultimate tensile strength at operating temperature will be 51% of room temperature ultimate tensile strength, S_T. Note that S_T is the same thing as F_{tu} at room temperature.

The same reference provides room temperature tensile strength for two bracketing heat treatment temperatures, 1050°F (175,000 psi) and 1100°F (150,000 psi). The lower of these two values will be used. Thus S_T = 150,000 psi.

Within the BPVC, Section VIII references Section II part D (Section II) for allowable stress values. However, Section II does not tabulate allowable stress properties for this material. In the event allowable stresses are not published in Tables 1A or 1B of that document, Section II refers the user to an internal appendix, *Mandatory Appendix 1 Basis for Establishing Stress Values in Tables 1A and 1B*. The following criteria were extracted from TABLE 1-100 of that appendix:[2]

$$S_A = \begin{cases} \dfrac{S_T}{3.5} & temperature \le 77\,°F \\ \dfrac{1.1 S_T R_T}{3.5} & temperature > 77\,°F \end{cases} \qquad 7$$

In this case, the value for parameter R_T would be 0.51 based on Figure 9. As a result, the allowable stress, S_A, for this high temperature scenario would be 24,000 psi.

2.3.4 Vessel Wall Results

Based on a FEM analysis of the TB-1 vessel, a thin-wall pressure vessel analysis will be valid. Using a thin wall model as outlined in the BPVC with an allowable stress, S_A, of 24,000 and the values for system geometry contained in Table 15, the maximum allowable operating pressure, P calculated using equation 6 would be 5390 psig.

2.4 Allowable Pressure based on Vessel Closure

Based on Figure 8, the stress in the material at the top of the vessel, in the vicinity of the closure, would be on the order of 1,000 psi. This is low enough to assure that material stress will not limit operating pressure. However, bolting needs further review.

The analysis uses the process set forward in BPVC Section VIII Mandatory Appendix 2 Rules for Bolted Flange Connections with Ring Type Gaskets for calculating the load on a set of bolts.

2.4.1 BPVC Closure Analysis

Bolts on a closure generally perform two functions. They contain the pressure in the vessel and they impose sufficient load on the closure gasket to ensure no leakage. In terms of forces on the closure, they can be characterized as follows:

$$W_{m1} = H + H_p \begin{cases} H = Total\ hydrostatic\ end\ force, lb_f & \frac{\pi G^2}{4} P \\ H_p = Total\ gasket\ compression\ load, lb_v & 2\pi bGmP \end{cases} \qquad 8$$

The first force, H, is the force the bolts must exert to counteract the force the internal pressure exerts on the closure. It is equivalent to the pressure, P, times the area over which the pressure exerts itself. In this case the area is a circle with diameter, G, to the midpoint of the gasket.

The second force, H_p, is the force the bolts must exert to effect a seal on the gasket. The sealing pressure is modeled as a constant factor, m, times the external pressure. For soft smooth copper, $m = 4.75$. [1 Table 2-5.1,2]. From the same reference the effective sealing width, b, is half the width, N, of the gasket. With the geometry of the TB-1 copper gasket (Figure 10) the above equation reduces to.

$$W_{m1} = \left(\frac{\pi G^2}{4} + 2\pi bGm \right) P \qquad 9$$

The TB-1 design actually assumes a single knife edge cutting into the gasket. Hence using smooth copper m factor is conservative.

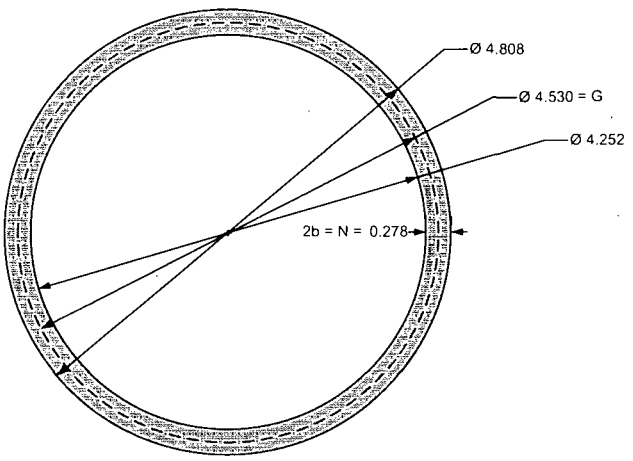

Figure 10: Geometry of TB-1 Gasket

The force, W_{m2}, necessary to initially seat the gasket is the seating stress, y, (13000 psi for soft copper) times the area of the gasket

$$W_{m2} = \pi b G y \tag{10}$$

This equation assumes the TB-1 is assembled with equal pressure internal and external, which is reasonable for this package. The bolts must exert the maximum of either W_{m1} or W_{m2}. The value for W_{m2} is 25,700 lb_f/bolt. Subsequent discussion will demonstrate that W_{m1} is much larger than this. For 12 bolts of diameter, D_b, equal to 0.5 in, the stress, S, in each of the bolts will be

$$S = \frac{\frac{\pi G^2}{4} + 2\pi b G m}{12\pi\left(\frac{D_b}{2}\right)^2} P \tag{11}$$

Using this equation, the maximum allowable operating pressure (MAOP) to be allowed in the vessel can be given in terms of the bolt material's allowable stress:

$$MAOP = \frac{12\pi\left(\frac{D_b}{2}\right)^2}{\frac{\pi G^2}{4} + 2\pi b G m} S_a = 0.0675 S_a \tag{12}$$

2.4.2 Vessel Closure Material Strength

Bolt allowable stress, S_a, is set per BPVC Section VIII, Paragraph UG-23.[1] The bolts are to be fabricated of A-286 stainless steel heat treated per AMS 5731 (Solution treated at 1800°F). Figure 11 contains a curve showing the response to this material to temperature. The vertical axis returns the R_T factor used in equation 7, which applies here in the form:

$$S_a = \begin{cases} \frac{S_T}{3.5} & temperature \le 77\,°F \\ \frac{1.1 S_T R_T}{3.5} & temperature > 77\,°F \end{cases} \tag{13}$$

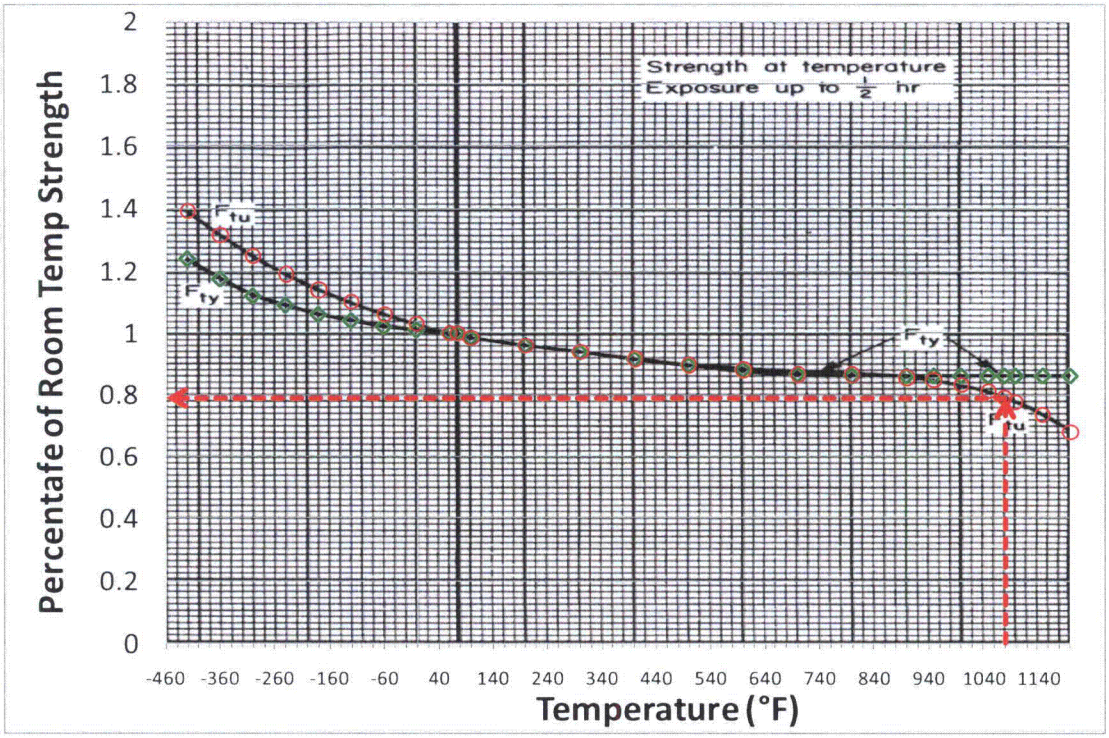

Figure 11: Figure 6.2.1.1.1. Effect of temperature on the tensile yield strength (F_{ty}) and tensile ultimate strength (F_{tu}) of A-286 alloy (1800°F solution treatment temperature).[7]

The ultimate tensile strength at room temperature, S_T, for this material per the reference is 130,000 psi. Note that drawings for these bolts specify a minimum tensile strength of 180,000 psi. The lower value will be used here.

Using equation 13, the allowable stress, S_a, in the bolts is 32,300 psi at 1080 °F. The stress ratio, R_T, is 0.79 from Figure 11. The ultimate tensile strength at room temperature is 130,000 psi.

2.4.3 Vessel Closure Results

Using the bolt allowable stress, S_a, of 32,300 equation 12 returns a maximum pressure safely containable by the closure of 2181 psig (2196 psia). This is a factor of safety of 1.98 over the MAP of 1110 psia specified by the SAR.

At this pressure, the load per bolt, W_{m2}, is 76,100 lb_f, significantly greater than the value for W_{m2} of 25,700 lbf. As initially assumed, W_{m1} dominates the calculation.

3 Application of the Boiler and Pressure Vessel Code (Section VIII)

3.1 Exceptions to the ASME Boiler and Pressure Vessel Code

With the exception of the elastomeric (O-ring) seal, the T-Ampoule (Drawing 2A0261) was designed, and will be fabricated and inspected to meet the requirements of the ASME Boiler and Pressure Vessel Code (Section VIII) [1]. However, the following exceptions or explanations apply:

1) The T-Ampoule was designed to Section VIII as modified by this document:
   a) The size requirements in section *U-1(c)(2)(i)* of Section VIII, do not apply.
   b) The marking requirements of parts UG 115-119 do not apply. T-Ampoules will be marked with part and serial numbers as specified in fabrication specification PAT-1040 [7].
2) Given the dry inert gaseous initial atmosphere and the general non-reactivity of titanium with the vessel contents, the design requires a no corrosion allowance.
3) T-Ampoule MAWP will be established with calculations as set forth in this document. Allowable pressure calculations will be performed based on the following paragraphs of Section VIII:
   a) Torispherical Head allowable pressure was calculated based on the requirements of Section VIII's Mandatory Appendix 1, Supplementary Design Formulas, paragraph 1-4(d).
   b) Allowable pressure, based on membrane stress in the hemispherical head, was estimated based on the criteria set forth in paragraph UG-32.
   c) Allowable pressures in the both the longitudinal and circumferential direction of the shell and lid are estimated based on the criteria set forth in paragraph UG-27 of Section VIII.
   d) T-Ampoule is exempt from the requirements of paragraph UG-32, *Thickness of Shells and Tubes Under External Pressure*. As the T-Ampoule will be subject to impact loading and a separate impact analysis will be conducted as described in Chapter 2 of the PAT-1 Safety Analysis Report Addendum Docket No. 71-0361, Rev. 0, August 2009.
4) T-Ampoule design specifies no welded joints. Consequently joint efficiency, E, in all subsequent Section VIII equations will be applied as 1.0.
5) The requirements of paragraph UG-125 regarding pressure relief devices do not apply. Over pressure response will be discussed in detail in the body of this paper
6) T-Ampoule will be fabricated from Ti-6Al-4V titanium alloy produced to material specification ASTM 348 except, as modified below:
   a) Titanium alloy will have procurement specified values of 150,000 psi ultimate strength and 140,000 psi yield strength, both at 77°F (room temperature).
   b) Temperature dependant allowable stress criteria will be determined using the procedures outlined in the ASME Boiler and Pressure Vessel Code, Section IID, Mandatory Appendix 1 Basis for Establishing Stress Values in Tables 1A and 1B.

c) In either case, titanium maintains ductility at low temperatures and is therefore, exempt from the requirements of Sections UCS 66 through 68 pertaining to derating allowable stress for low temperature operation.

7) In the case of analysis of the torispherical heads, and in accordance with Section UG-32(e), allowable stress will be limited to 20,000 psi for temperatures below 77°F, and will be reduced proportional to the curves developed in 2.b above for temperatures above 77°F.
8) The T-Ampoule quality program will meet the requirements of Section VIII with the following exceptions:
   a) The standard hydrostatic test of paragraph UG-99 or the pneumatic test from paragraph UG-100, are not required.
   b) The requirements of paragraph UF-55 regarding ultrasonic examination do not apply. Inspection will consist of visual inspection and physical measurement of specified dimensions.
   c) As the T-Ampoule components are either formed or spun without welding, the requirements of part UW and part UB do not apply.
9) In lieu of the requirements of paragraph UG-91, the inspector will meet the requirements listed below:
   a) Inspector will demonstrate experience with spinning and fabrication processes, and
   b) Inspector will demonstrate experience with Section VIII.

The elastomeric (O-ring) seal and the associated threaded joint were analyzed using accepted engineering practices and manufacturers' recommendations.

3.2 Pressure Envelope Analysis

Within this section:

- Sections 3.2.1 and 3.2.2 summarize the results used for subsequent analyses. Section 3.2.1 provides a summary of results for internal pressure while Section 3.2.2 does the same for external pressure calculations.
- Section 3.2.3 describes calculations done to provide metal properties for subsequent calculations. The T-Ampoule will be built using an alloy of titanium not addressed, in detail within Section II.
- Sections 3.2.4 through 3.2.7 summarize individual analyses for areas 1 through 4 identified in Figure 12.

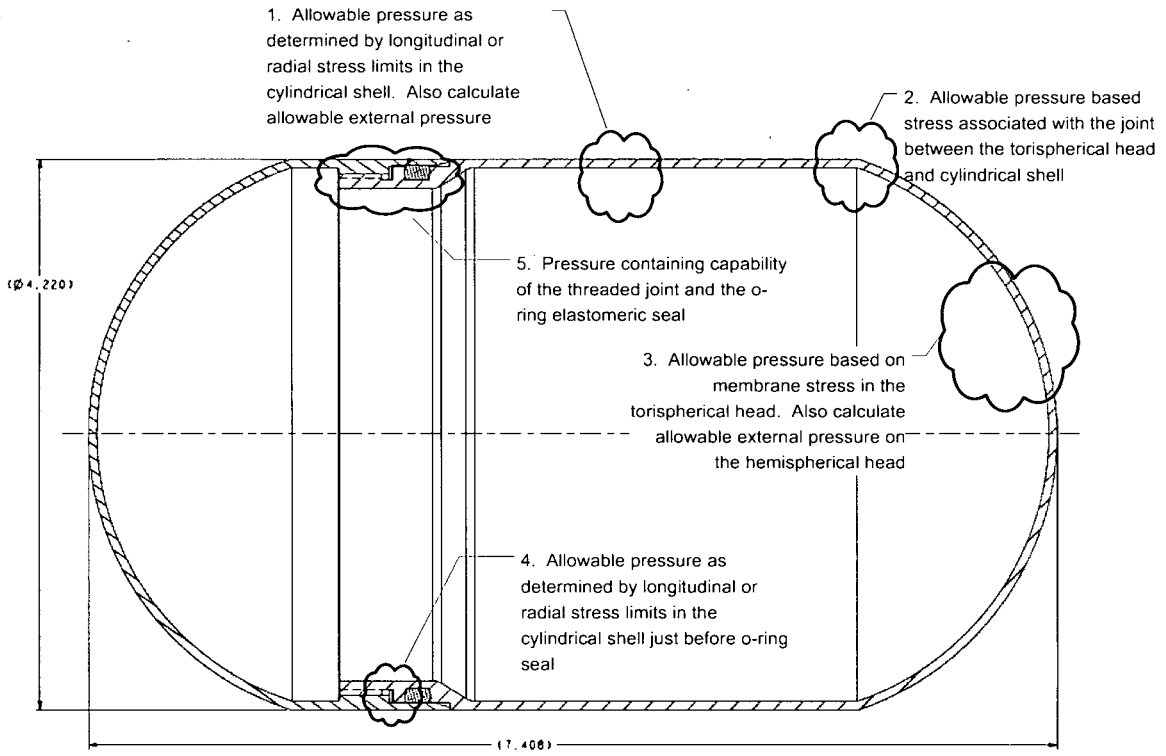

Figure 12: Five Analyses Performed for MAWP Determination

The O-ring seal identified as Area 5 in the figure will be addressed in Chapter 4.

3.2.1 Maximum Allowable Working Pressure (Internal Pressure Limits)

Figure 13 contains a plot of maximum allowable working pressure (MAWP) as a function of temperature for the T-Ampoule. The MAWP declines with temperature from 617 psig at room temperature (77°F) to 263 psig at 1080°F. At temperatures exceeding 1080°F, the T-Ampoule's O-ring seal has failed and pressure has equilibrated with the external environment resulting in zero pressure stress on the T-Ampoule.

It is important to later recall that MAWP is presented as gauge pressure, the difference between external and internal pressures.

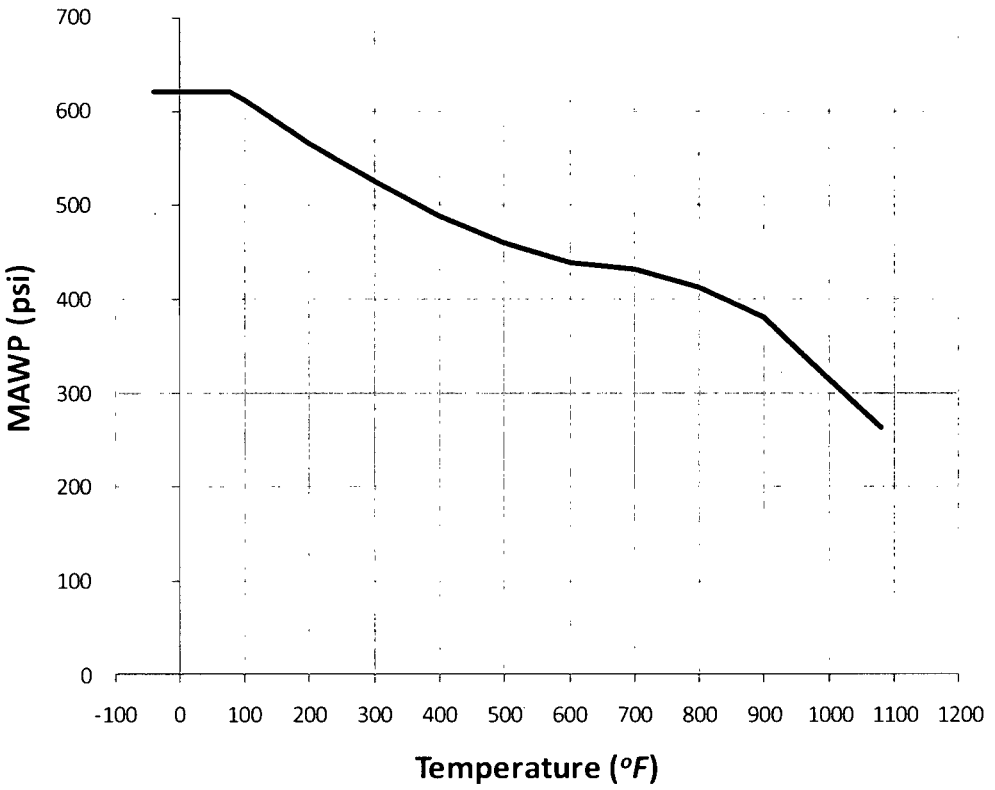

Figure 13: Maximum Allowable Working Pressure (MAWP) for T-Ampoule

Table 16 contains a summary of the results.

Table 16: Summary of Allowable Internal Pressure by Analysis Area

Analysis Area	Description	Allowable Pressure (psig) @ 77°F	Allowable Pressure (psig) @ 1080°F
1	Cylindrical Shell Longitudinal Stress	2790	1180
1	Cylindrical Shell Circumferential Stress	1360	576
2	**Joint, Torispherical Head to Shell**	**624**	**263**
3	Torispherical head, membrane stress	2600	1100
4	Seal Area Longitudinal Stress	1910	809
4	Seal Area Circumferential Stress	935	396
5	O-Ring Seal	900	n/a

The MAWP is set to the lowest allowable pressure for the analysis areas. For this design, the joint between the torispherical head and the cylindrical shell, determined MAWP. The five analyses are summarized below, preceded by a review of the methodology used to determine temperature dependant allowable stresses.

3.2.2 External Pressure Limits

Figure 14 contains a plot of maximum allowable, external pressure as a function of temperature for the cylindrical shell and the hemispherical head. Allowable pressure for the cylindrical head is the lower of the two and would provide the limiting criteria for the T-Ampoule as a pressure vessel. As is discussed in the applicable sections, this is a conservative calculation.

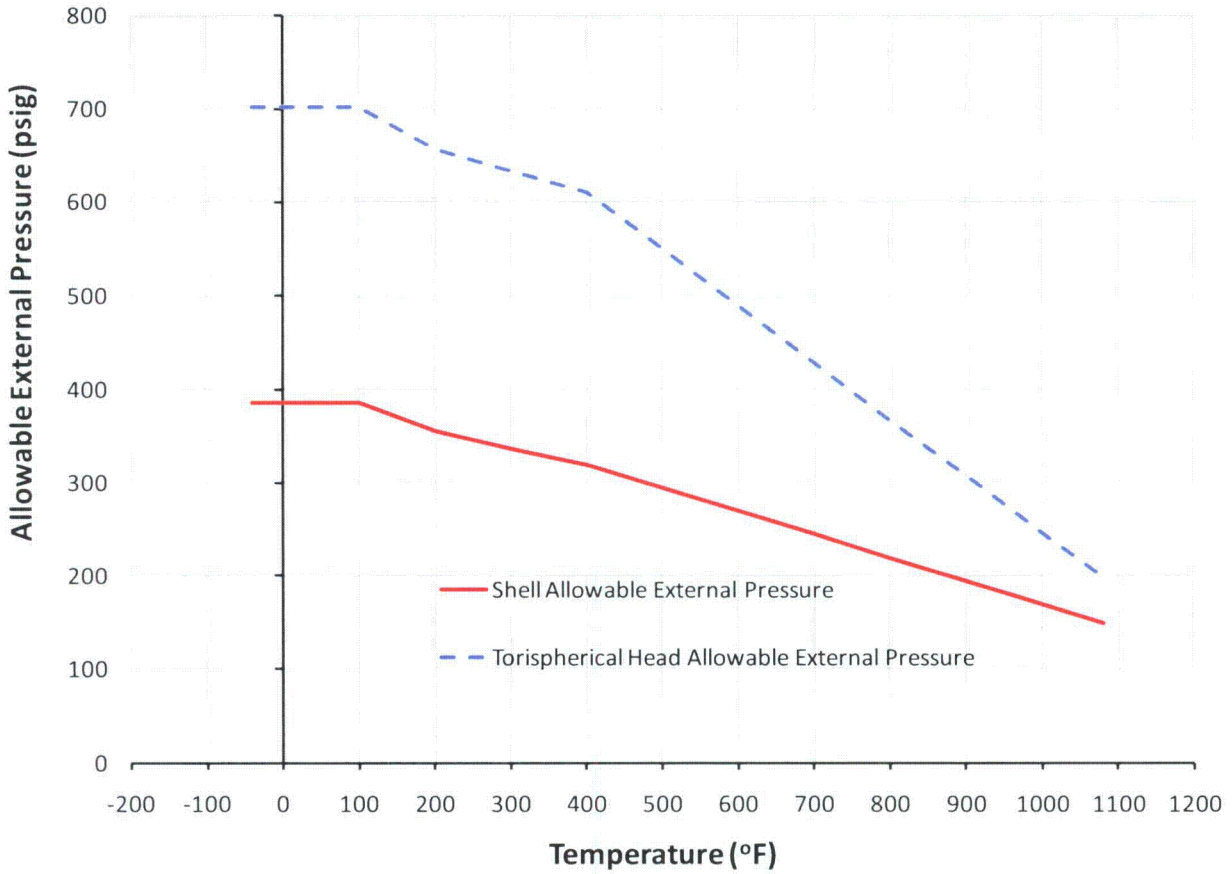

Figure 14: Allowable External Pressure

Table 17 contains a summary of allowable external pressures. This table lists values for room temperature (71°F) and for 700°F, the temperature at which the T-Ampoule's O-ring seal is expected to fail.

Table 17: Summary of Allowable External Pressure by Analysis Area

Analysis Area	Description	Allowable Pressure (psig) @ 71°F	Allowable Pressure (psig) @ 800°F
1	Cylindrical Shell	386	219
3	Torispherical head	687	368
5	O-ring Seal	180	160

3.2.3 Titanium Properties

The document controlling design and fabrication of the T-Ampoule [Reference 6, paragraph 3.1.1] specifies that the titanium alloy Ti-6Al-4V will be procured with a minimum tensile (ultimate) strength, S_T, of 150,000 psi and minimum yield strength, S_Y, of 140,000 psi at room temperature (77°F). The analyses below require allowable stress, S_A, values at temperatures, both below and well above room temperature. Allowable stress values should be for a wrought non-ferrous metal.

Section VIII references Section II part D (Section II) for allowable stress values. However, Section II does not tabulate properties for this material. In the event allowable stresses are not published in Tables 1A or 1B of that document, Section II refers the user to an internal appendix, *Mandatory Appendix 1 Basis for Establishing Stress Values in Tables 1A and 1B*. The following criteria were extracted from TABLE 1-100 of that appendix:

$$S_A = \begin{cases} \dfrac{S_T}{3.5} & temperature \le 77\,°F \\ \dfrac{1.1 S_T R_T}{3.5} & temperature > 77\,°F \end{cases} \qquad 14$$

The Parameter R_T is defined as the ratio of the average temperature dependent, trend curve value of tensile strength to the room temperature tensile strength, the value of which was extracted from the curve F_{tu} in Figure 11.

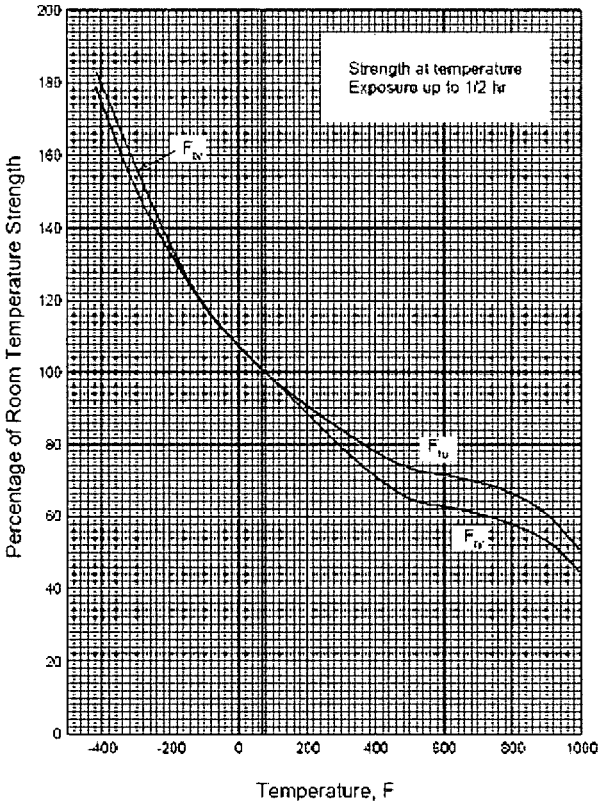

Figure 15: The Effect of Temperature on the Tensile Ultimate Strength of Annealed Ti-6Al-4V Alloy [7, Figure 5.4.1.1.1]

For Titanium, the useful temperature range is from -320 to 750°F [Reference 7, p 5-51]. Unlike ferritic steels, titanium maintains ductility throughout its operating range, as shown in Figure 16. For these reasons, allowable stresses for temperatures below room temperature were extended down to -40°F.

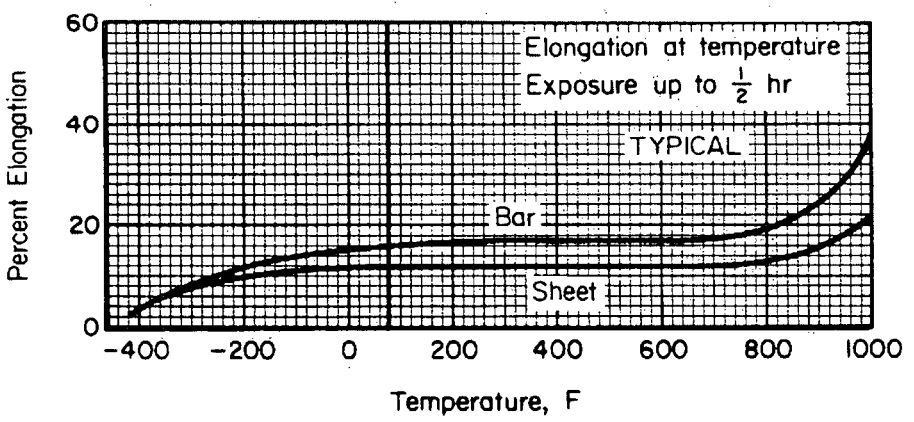

Figure 16: The Effect of Temperature on the Elongation of Annealed Ti-6Al-4V [7, Figure Fig 5.4.1.1.5]

The temperature factor for this analysis was extrapolated to 1080°F, 80°F beyond the data presented in Figure 15 and Figure 16 in order to estimate the response of the T-Ampoule at the theoretical accident temperature (1080°F).

The torispherical head analysis, per Section VIII, paragraph UG-32(e), mandates lower allowable stresses. In this single case, the following applies:

Torispherical Head $$S_A = \begin{cases} 20,000 & temperature \le 77\,°F \\ 20,000 R_T & temperature > 77\,°F \end{cases} \quad (15)$$

Figure 11 contains plots of the allowable stress values that result from the above equations.

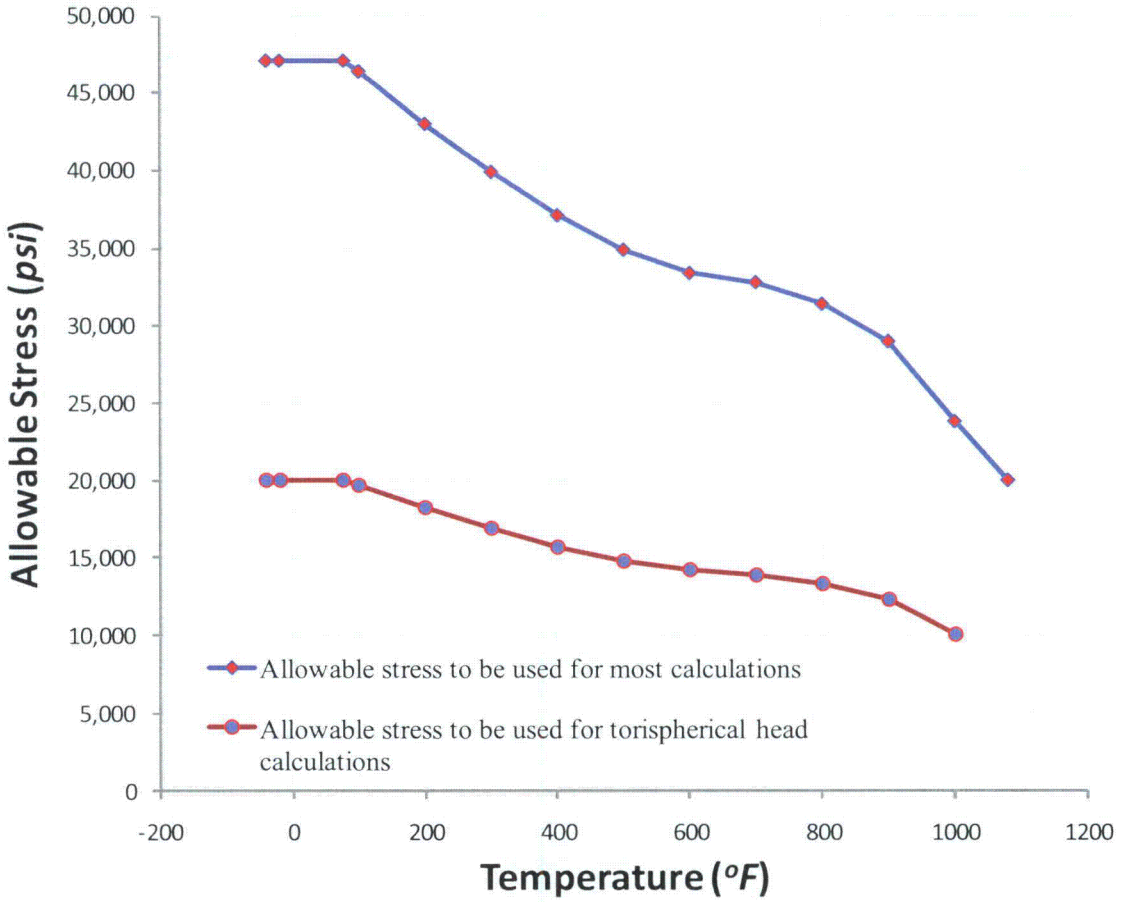

Figure 17: Allowable Stress Values for Ti-6Al-4

Section VIII references Section II part D for computation of yield stress values. In the event yield stresses are not published in Tables 1A or 1B of that document, Section II refers the user to an internal appendix, *Mandatory Appendix 1 Basis for Establishing Stress Values in Tables 1A and 1B*. The following criteria were extracted from TABLE 1-100 of that appendix:

$$Y = \begin{cases} \frac{2}{3} S_Y & temperature \leq 77\,^{\circ}F \\ \frac{2}{3} S_Y R_Y & temperature > 77\,^{\circ}F \end{cases} \qquad 16$$

The Parameter R_Y is defined as the ratio of the average temperature dependent value of yield strength to the room temperature yield strength, the value of which was extracted from the curve F_{ty} in Figure 15. The results of equation 16 are plotted in Figure 18.

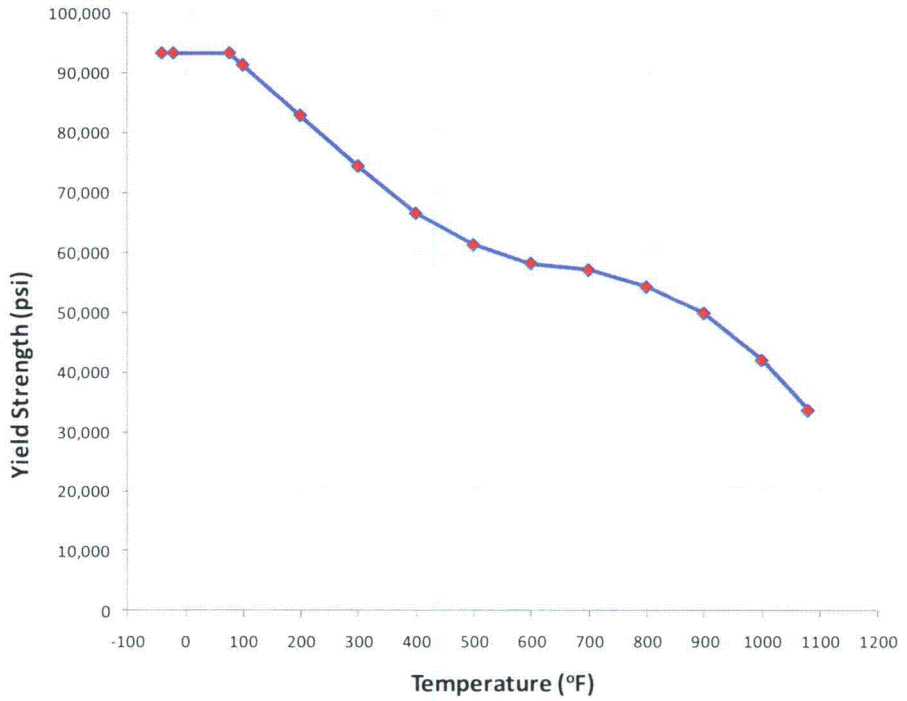

Figure 18: Yield Strength for Ti-6Al-4V

As with tensile strength, the curve is extended to -40°F based on low temperature ductility arguments.

External pressure calculations incorporate the modulus of elasticity at temperature. Figure 19 contains a plot for the T-Ampoule's material based data from a metals handbook published by the U.S. Department of Transportation [7].

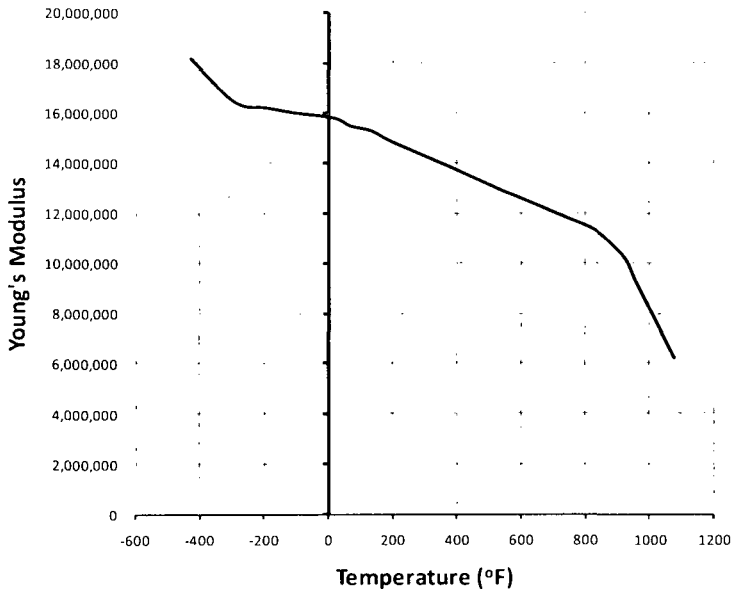

Figure 19: Effect of Temperature on the Young's Modulus of AnnealedTi-6Al-4V [Ref. 7, Figure 5.4.1.1.4]

Figure 20 contains the chart extracted from Section II, from which Factor B was extracted for external pressure calculations. This chart is in fact for an alloy of titanium with similar elastic moduli, but of yield strength half that of Ti-6Al-4V.

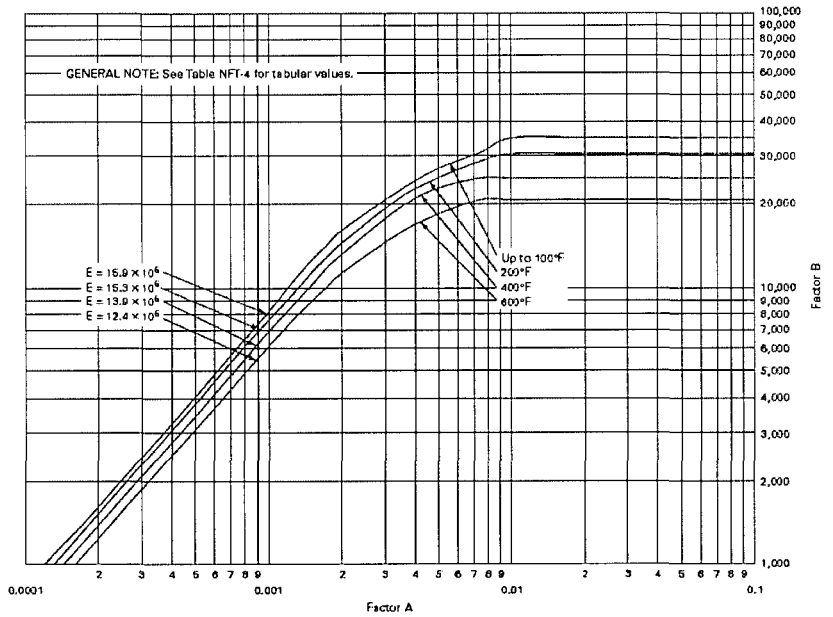

Figure 20: Fig. NFT-4 Chart for Determining Shell Thickness of Components Under External Pressure Developed For Titanium Grade 9 Alloy (Uns R56320) [2]

3.2.4 Analysis 1, Cylindrical Shell

Internal Pressure – This section summarizes the analysis performed on the cylindrical shell, the area designated as analysis area 1 in Figure 12. Allowable pressures in the both the longitudinal and circumferential direction of the shell are based on the criteria set forth in Section UG-27 of Section VIII.

Longitudinal Limit, shell $$P_L = \frac{2S_A Et}{R_i - 0.4t} \quad (17)$$

Circumferential Limit, shell $$P_\phi = \frac{S_A Et}{R_i + 0.6t} \quad (18)$$

The analyst should use data from the upper curve of Figure 17 for allowable stress, S_A because the device in question has a formed joint efficiency, E, of 1.0. The internal radius, R_i, is based on dimensions taken from Figure 21, and uses specified minimum/maximum values that result in the smallest radius value. Wall thickness, t, is derived from the same dimensions. It is based on the difference between outer and inner diameters using tolerances to obtain the largest value.

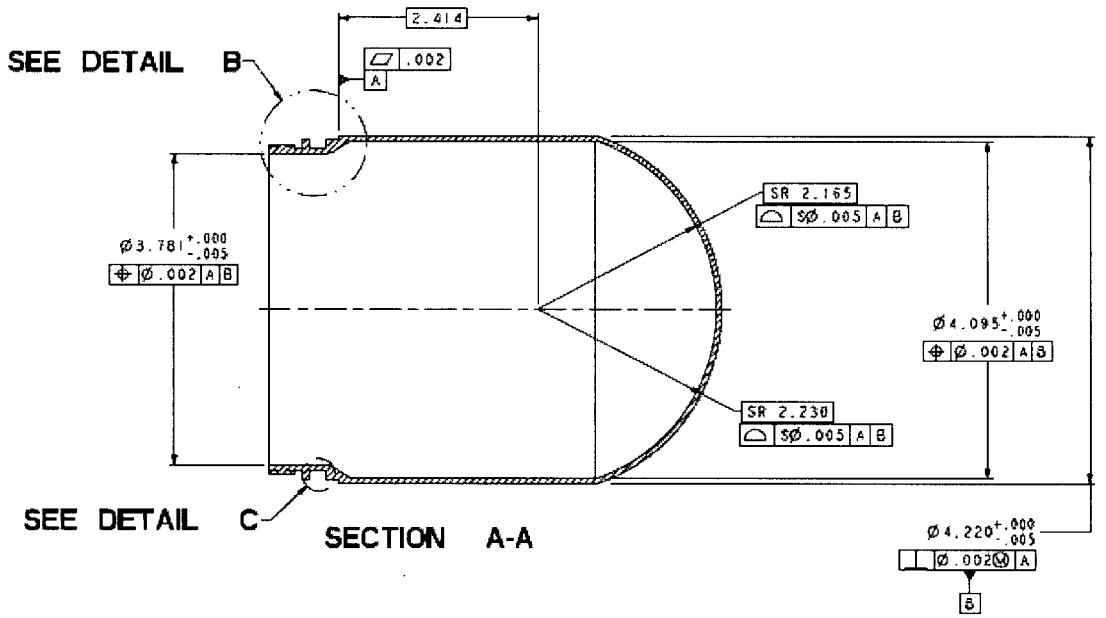

Figure 21: Dimensional Sketch of T-Ampoule Body

Table 18 contains both the input parameters to equations 17 and 18 as well as the final results. The allowable pressure for this analysis area is the pressure determined based on allowable circumferential stress with a value of 1356 psig at room temperature.

Table 18: Parameters and Calculated Values Analysis Area 1

Parameter	Value	Units
d_i	4.095	in
d_o	4.215	in
R_i	2.0475	in
R_o	2.1075	in
t	0.06	in
E	1	n/a
S_A	47100	psi
P_L	**2790**	**psi**
P_ϕ	**1360**	**psi**

Values for allowable stress and therefore, pressure are at room temperature.

External Pressure - This external pressure calculation is conservative. Given the snug fit between the T-Ampoule and the TB-1 containment vessel, it is unlikely that the T-Ampoule will be allowed to flex enough to buckle elastically. The Section VIII external pressure analysis ignores this type of external support and the analysis assumes no support exists. In addition, B factor charts for the Ti-6Al-4V material used for the T-Ampoule do not exist. The curve for a titanium alloy with UNS designation R56320 will be assumed instead. This substitute alloy has a room temperature yield strength of 70,000, a factor of 2 lower than the alloy actually in use. These two assumptions combine to under-predict allowable external pressure. Since the predicted pressures are still sufficiently high that failure is not predicted, no attempt was made to refine the analysis.

Rules for calculating allowable external pressure are presented in Section VIII, paragraph UG-33(d). The methodology is graphic oriented. The first important parameter, A, is obtained from the graph in Section II, Figure G, which correlates A to geometric parameters derived from external diameter, D_o, shell length, SL, and wall thickness, t. Using this value, one can determine the allowable stress, B, from Figure 20. This value of B for room temperature is 18,800 psi.

A B-factor feeds into the following equation:

$$P_{ex} = \frac{4B}{3\left(\frac{L_o}{t}\right)} \qquad 19$$

Table 19 summarizes the results of the above calculations. Allowable external pressure is 481 psig. At 700°F when the T-Ampoule equilibrates with the annulus pressure, the allowable

external pressure difference will be 244 psig, providing a reasonable margin above the estimated equilibration threshold of 150 psig difference.

Table 19: Allowable External Pressure of Hemispherical Head

Parameter	Value	Units
D_o	4.22	In.
t	0.06	In.
SL	4.426	length
SL/D_o	2.098	
D_o/t	64.9	
A	0.00250	
B	18,800	psi
P_{ex}	386	psi

3.2.5 Analysis Area 2, Torispherical Head Joint

Criteria for analysis area 2 are based on paragraph UG-32 *Formed Heads, and Sections, Pressure on the Concave Side* of Section VIII. This paragraph refers in turn to Section VIII's Mandatory Appendix 1, Supplementary Design Formulas, paragraph 1-4(d) which applies the following criteria:

Torispherical Head Joint

$$P_T = \frac{2S_A E t_s}{LM + 0.2t_s} \qquad 20$$

Where

$$M = \frac{1}{4}\left(3 + \sqrt{\frac{L}{r}}\right) \qquad 21$$

In this case the analyst should employ the lower curve of Figure 17 for allowable stress. Dimensions were obtained from Figure 21. The crown radius, L, or the radius of the head, must be the minimum value possible when considering tolerances. The head wall thickness, t_s, should also be the minimum possible value. The parameter M is based on the ratio of crown radius, L, to knuckle radius, r. Knuckle radius is the radius of curvature of the titanium at the joint between the head and the cylindrical shell. This value is specified to be 0.125 inch. As above, the joint efficiency, E, is 1.0 since no joint exists.

In addition to the above, the following criteria apply:

$$\frac{t_s}{L} \geq 0.002,$$
$$L \leq d_o \qquad 22$$

Table 20 contains input parameters and results for the torispherical head joint. The value for t_s is based on the difference between outer and inner crown radii with tolerances chosen to minimize thickness. The allowable stress at room temperature is limited to a maximum of 20,000 psi at room temperature. The two criteria of equation 19 are met. The ratio of head thickness to crown radius is 0.0277, an order of magnitude above the criterion. The crown radius itself, at 2.225 inches is less than the outer diameter of the shell which equals 4.095 inches. All of this results in an allowable pressure of 624 psig. This is, in fact, the lowest allowable pressure of all calculated for the five analysis areas, and as such provides the criteria for MAWP.

Table 20: Parameters and Calculated Values Analysis Area 2

Parameter	Value	Units
d_i	4.095	in
d_o	4.215	in
R_i	2.0475	in
R_o	2.1075	in
L	2.225	in
t_s	0.06	in
E	1	n/a
t_s/L	**0.0277**	nd
S_A	**20,000**	psi
M	**1.790**	nd
P_T	**624**	psi

3.2.6 Analysis Area 3, Head Membrane

Internal Pressure - Stress in the hemispherical head away from the joint is uniform in all directions normal to the radius and is governed by the criteria of paragraph UG-32 of Section VIII, Formed Heads and Sections.

Hemispherical Head Membrane $$P_H = \frac{2S_A E t_s}{L + 0.2t_s} \qquad 23$$

The following additional constraints apply:

$$\frac{t_s}{L} < 0.356$$
$$\frac{P_H}{SE} < 0.665 \qquad 24$$

Values and definitions are as defined in the previous section.

Table 21 contains input parameters and results for the hemispherical head membrane. The two supplemental criteria of equation 24 are satisfied. The calculated value for allowable pressure of 2600 psig is well above the previously calculated allowable pressure for the torispherical joint.

Table 21: Parameters and Calculated Values Analysis Area 3

Parameter	Value	Units
d_i	4.095	*in*
d_o	4.215	*in*
R_i	2.048	*in*
R_o	2.108	*in*
L	2.225	*in*
t_s	0.060	*in*
E	1	*n/a*
S_A	47100	*psi*
t_s/L	0.0277	*nd*
P_H/SE	0.0551	*nd*
P_H	2600	*psi*

External Pressure - This external pressure calculation is conservative. Given the snug fit between the T-Ampoule and the TB-1 containment vessel, it is unlikely that the T-Ampoule will be allowed to flex enough to buckle elastically. The Section VIII external pressure analysis ignores this type of external support and the analysis assumes no support exists. In addition, B factor charts for the Ti-6Al-4V material used for the T-Ampoule do not exist. The curve for a titanium alloy with UNS designation R56320 will be assumed instead. This substitute alloy has a room temperature yield strength of 70,000, a factor of 2 lower than the alloy actually in use. These two assumptions combine to under-predict allowable external pressure. Since the predicted pressures are still sufficiently high that failure is not predicted, no attempt was made to refine the analysis.

Rules for calculating allowable external pressure are presented in Section VIII, paragraph UG-33(e). Methods are graphic oriented. First important parameter, A, is calculated as:

$$A = 0.125\left(\frac{t}{L_o}\right) \qquad 25$$

Note: This equation uses the external crown radius, L_o. Using this value, allowable stress, B from Figure 20 can be determined. This value at room temperature is 23,400 psi. The B factor feeds into the following equation:

$$P_{ex} = \frac{B}{\left(\frac{L_o}{t}\right)} \qquad 26$$

Table 22 summarizes the results of the above calculations. Allowable external pressure is 687 psig. At 700°F when the T-Ampoule equilibrates with the annulus pressure, the allowable external pressure difference will be 419 psig, providing a reasonable margin above the estimated equilibration threshold of 150 psig, difference between the annulus and the T-Ampoule.

Table 22: Allowable External Pressure of Hemispherical Head

Parameter	Value	Units
L_o	2.22	In.
t	0.065	In.
L	4.43	
L_o/t	34.1	
A	0.00367	psi
B	23,400	psi
P_{ext}	687	

3.2.7 Analysis Area 4, Seal Area

This section summarizes the analysis performed on the cylindrical shell in the area designated as area 5. Figure 22 shows the area in extreme close-up. The thin cap section just after the threads, but before the O-ring is of concern. This section still experiences internal pressure and yet, is substantially thinner than the T-Ampoule body. This analysis ignores possible rib reinforcement from the threaded area.

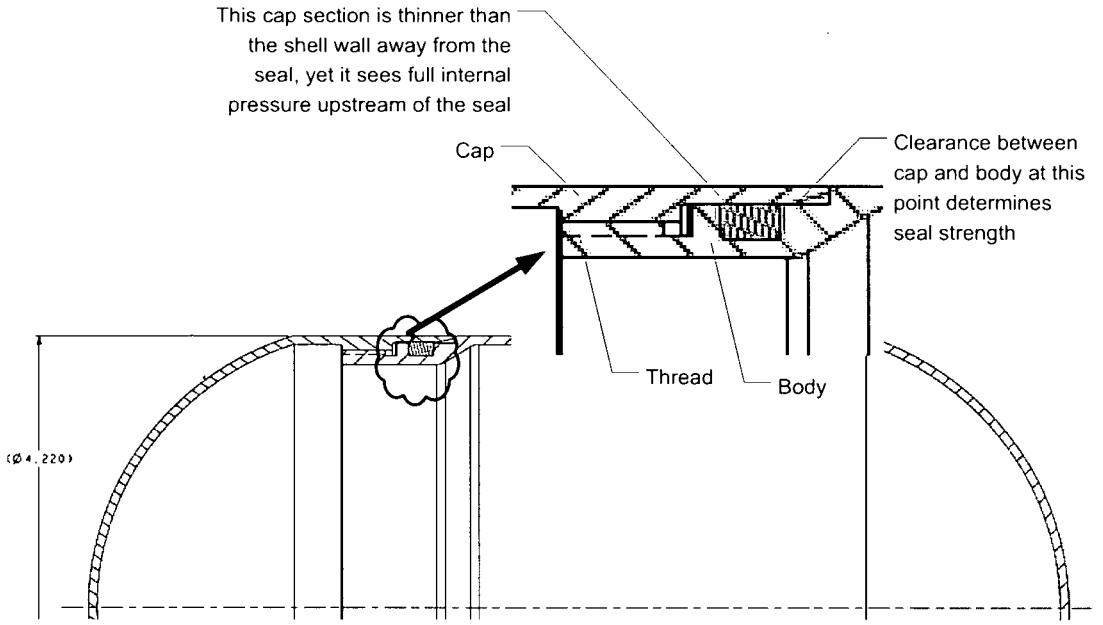

Figure 22: Blowup of Seal Area

The analysis is similar to that already completed for analysis area 1 with the dimensions, however, as specified in Figure 17. Allowable pressures in both the longitudinal and circumferential direction of the shell are based on the criteria set forth in Section UG-27 of Section VIII, and are summarized in equations 17 and 18.

The analyst should use data from the upper curve of Figure 17 for allowable stress, SA. Since the device in question is formed, joint efficiency, E, is 1.0.

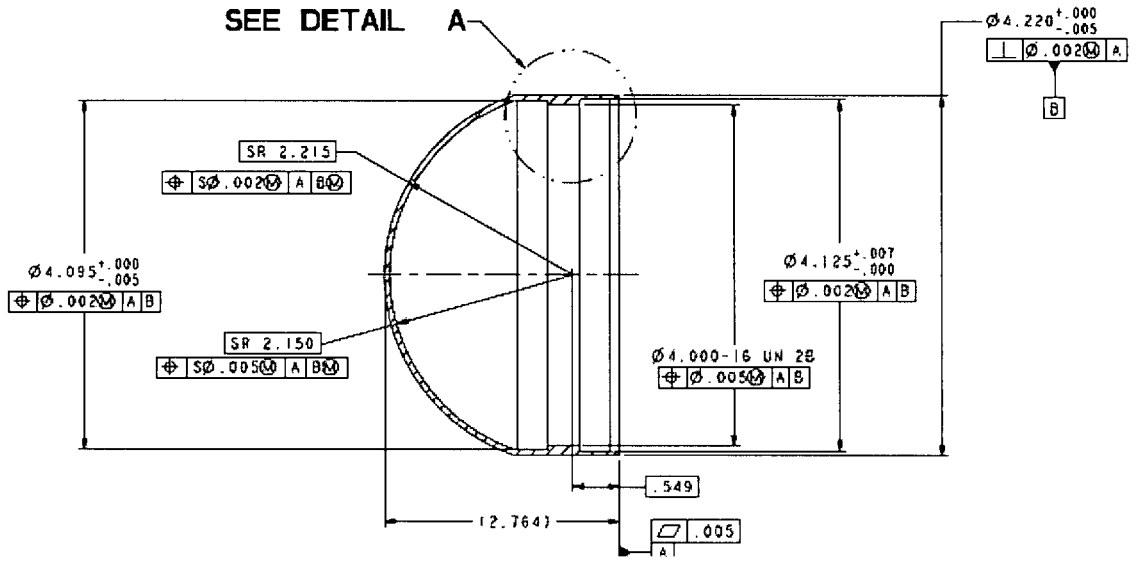

Figure 17: Dimensioned Sketch of T-Ampoule Lid

Table 23 contains both the input parameters to equations 14 and 15, as well as the final results. The allowable pressure for this analysis area is the pressure determined based on allowable circumferential stress with a value of 935 psig at room temperature.

Table 23: Parameters and Calculated Values Analysis Area 4

Parameter	Value	Units
d_i	4.132	in
d_o	4.22	in
R_i	2.066	in
R_o	2.11	in
t	0.0415	in
E	1	n/a
S_A	47100	psi
P_L	1910	psi
$P\phi$	935	psi

4 O-ring Seal Design

While O-ring static seals are ubiquitous in industry and are well respected, their analysis is not part of the Boiler and Pressure Vessel Code. Neither does their analysis possess the rigor found in the Boiler and Pressure Vessel Code. This analysis that follows relies, instead on the vendor's recommendations and good engineering practice.

A static O-ring seal designed to the dimensional specifications of SAE standard AS5857 will hold pressure to 1500 psig [11]. The T-Ampoule design follows this standard with two exceptions. Per the standard, the specified radial clearance in both directions, between the body and the cap should be 0.0015 to 0.003 inches. T-Ampoule clearances for both directions are relaxed for different reasons. Referring to Figure 18, the downstream clearance has been relaxed slightly to facilitate assembly in a glove box. The upstream clearance has relaxed even further to guard against excessive, external pressure. Sustainable pressures therefore require some adjustment.

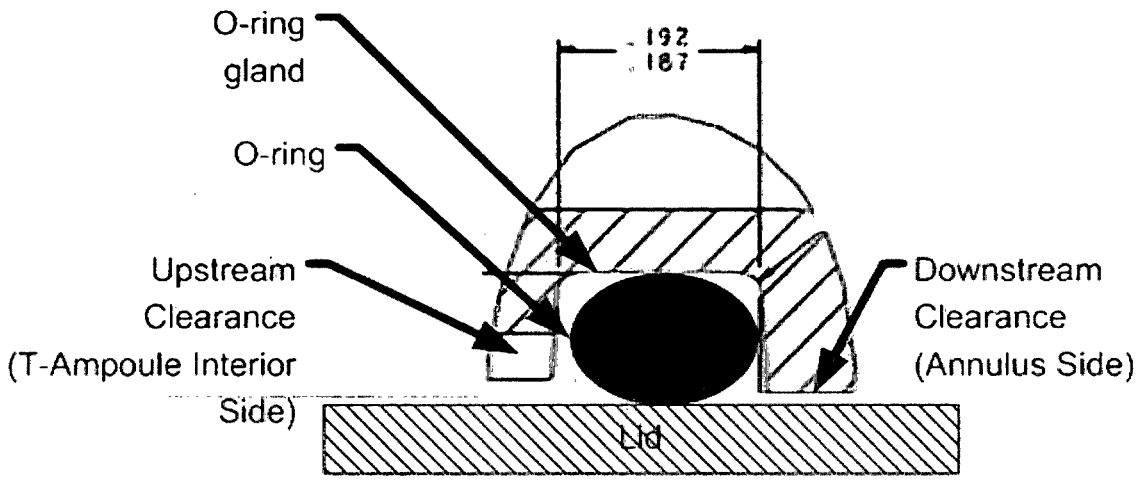

Figure 18: Pressure Containment for O-Ring Seals-[10, 11]

O-rings seal when pressure forces the relatively flexible elastomeric O-ring against the clearance between the cap and the body of the T-Ampoule. The downstream clearance supports the O-ring against internal pressure. The upstream O-ring supports the O-ring against external pressure.

Seal failure occurs when the O-ring extrudes into the clearance. As this clearance becomes tighter (smaller), the seal can sustain more pressure. Loosening (opening) the clearance causes

the seal to hold less pressure. In addition, a seal's ability to withstand pressure depends on O-ring hardness, typically measured on the "Shore A" scale. Figure 19 contains a plot of information taken from an O-ring design manual illustrating the relationship of an O-ring meeting the T-Ampoule seal's hardness specification.

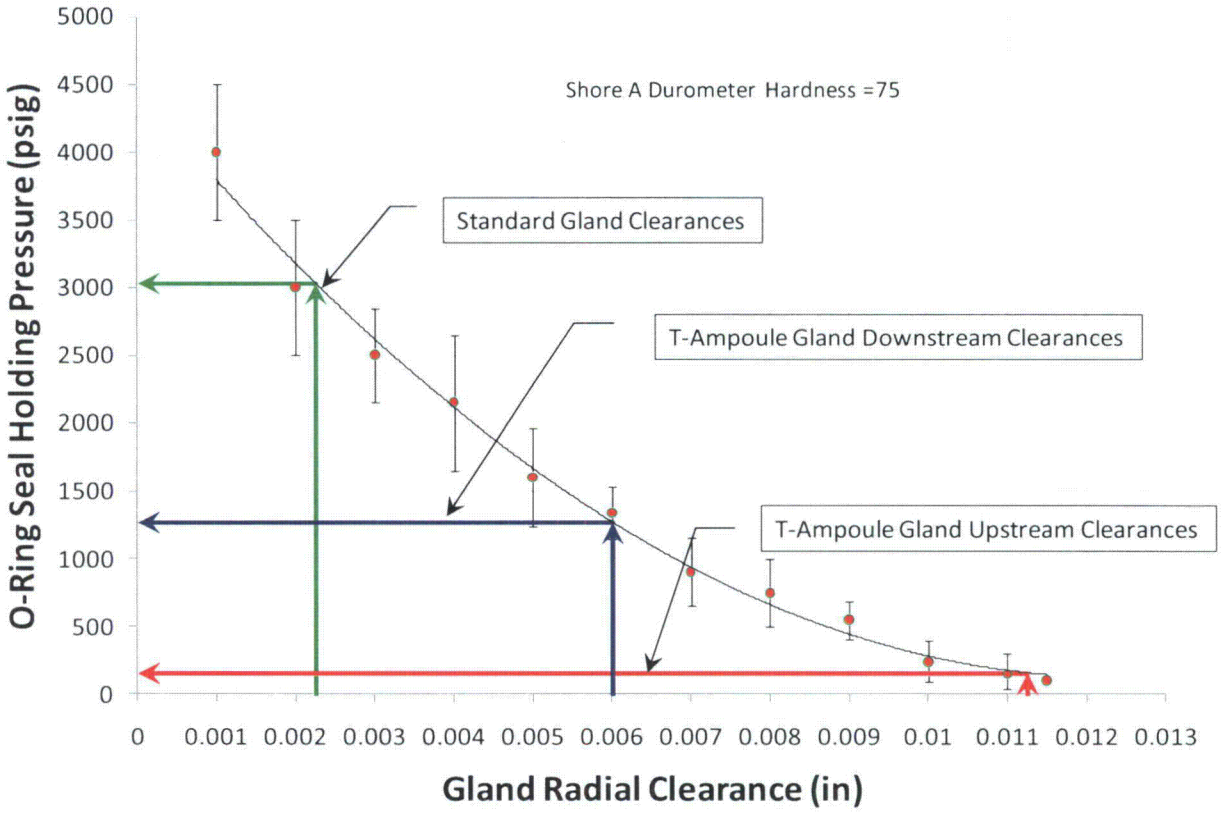

Figure 19: Internal Pressure Containment for O-Ring Seals [source:10]

T-Ampoule design specifies an O-ring with a Shore A hardness of 75 over its useful temperature range (-15°F to 400°F). A standard O-ring gland specification would call for a radial clearance between 0.0015 and 0.003 inches. From Figure 19, sustainable pressure is 3000 psig. The difference between this value and the value of 1500 psig quoted by the manufacturer represents factor of safety of 2.0 for a standard gland design.

The downstream clearance (radial) has been increased to 0.006. From the figure, this level of clearance can sustain a pressure of 1270 psig. With the same factor of safety, the seal should be rated for internal pressure at 635 psig.

The upstream clearance (radial) has been relaxed at selected locations to an average radial value of 0.01125 inches. From Figure 19, the seal can sustain a pressure of 160 psig. With the same factor of safety used above, the seal will be rated for a backpressure of 80 psig.

5 Conservatism and Uncertainty

This analysis is conservative. This section is intended to document this conservatism on a section by section basis.

Section 1.1. Analysis ignores the impact of thermal expansion on the annulus volume. Since stainless steel expands faster than titanium, the volume will grow slightly with temperature. As a consequence, real pressures will be slightly lower than predicted by this analysis.

Section 1.2. O-ring decomposition analysis assumes O-rings decompose to relatively low molecular mass ratio materials. This results in a relatively large the molecular population of the vapor. In fact molecules generated could be more than 5 times as large, reducing the contribution of O-ring pyrolysis to final pressure by as much as 80% of predicted.

Section 1.2. The analysis assumes that O-rings decompose completely. As documented, other sources indicate that only 76% of O-rings will decompose at 1080°F. Hence, predicted pressures could be as much as 33% higher than real values.

Section 1.2. The analysis assumes that O-ring failure due to pyrolysis occurs at 1080°F, and after all material has already vaporized. In reality, O-rings will decompose starting as early as 700°F. This earlier decomposition could shift pressure rise to earlier temperatures with vessel strength is greater, thus improving safety margin.

Section 1.3 Analysis assumes sufficient oxygen exists inside TB-1 to completely oxidize ancillary plastic to a vapor. This reduces the allowable ancillary plastic by an order of magnitude.

Section 1.4 Helium generation model assumes helium accumulates without diffusion for one year. The length of time the T-Ampoule exists as an assembly seems excessive. The assumption that no molecular diffusion of helium occurs during that period is conservative.

Section 1.5 O-ring seal is set to relieve with back pressure a factor of 1.33 below allowable back pressure.

Section 2. The ASME BPVC Section VIII, D1 MAOP method is inherently conservative in order to accommodate the wide range of boundary and initial conditions covered by the code. The code's criteria call for a vessel to last for an unspecified long time under extreme conditions in close proximity to humans.

Section 2 The ASME BPVC Section II material properties are inherently conservative. For example, allowable stresses include a safety factor of 3.5 on tensile strength. These tensile strengths are the minimum predicted by the alloy chemistry allowed within a material's specification.

Section 2.1 The MAP has a safety factor of 1.98 when compared to the MAOP calculated using ASME BPVC.

Section 2.3 Thin wall analysis is the most conservative of the two methods used.

Section 2.3 Allowable stress is based on a heat treatment (H1050) lower than that actually specified (H1075). This results in a lower ultimate tensile strength for the material.

Section 2.4 Bolt material strength is conservatively low. SAR specification calls for an ultimate strength of 180,000 psi. Value used in analysis was 130,000 psi because this is the strength defined by the material reference.

Section 3.2 Failure case for the T-Ampoule is via buckling collapse under external pressure. Estimated resistance to buckling pressure is understated. Like all buckling, collapse occurs at the eigenmodes composed of sinusoids with progressively increasing frequencies. Per ASME BPVC Section VIII D1, collapse occurs at the first eigenmode of pressure. Such a collapse requires that the vessel distort to look like a figure eight -- the sides of the vessel displace outwards. Since the TB-1 vessel constrains the T-Ampoule against such flexure, collapse at the first eigenvalue cannot happen. In reality, collapse will occur at a higher pressure where the displacement associated with the eigenmode is small enough to accommodate the physical constraints of the containing vessel.

Section 3.2.3 The theoretical cylinder external collapse critical pressure is based on a material with tensile strength at room temperature of 70,000 psi. The titanium actually used has a tensile strength at room temperature exceeding 100,000. This strength will translate to increased strength at design temperature and increased resistance to buckling.

Uncertainties:

Section 1.2 Analysis assumes one half of the products of O-ring pyrolysis enters the annulus and one half enters T-Ampoule. While both paths are symmetric, nothing exists to force this even distribution. As such, it is conceivable in the extreme that the split could be 10% into one side and 90% into the other. Should this occur, the

only consequence is that the T-Ampoule O-ring seal fails and relieves pressure sooner.

Section 1.2 Uncertainty exists regarding the relationship between the degree of O-ring decomposition and O-ring sealing ability. This analysis assumes the O-ring holds pressure completely until the last of its material has vaporized. In reality, the pressure will equalize much sooner.

Section 1.4 Actual gauge pressure at which the T-Ampoule's O-ring seal fails could be as high as 360 psig (double the design failure point) rather than the 180 psig design pressure. As above, the TB-1 maximum pressure is significantly lower than the design point. Increasing maximum pressure from 600 to 780 still leaves a significant margin for error. Consider this margin for error in the context of the extremely conservative ASME Boiler and Pressure Vessel Code and potential for failure becomes vanishingly small.

6 Conclusions

The objective of the T-Ampoule is to provide a eutectic prevention barrier between the plutonium it contains and the PH13-8Mo stainless steel of the TB-1 containment vessel The barrier will minimize any formation of a Pu/Fe eutectic under the elevated temperature of 1080°F during a fire accident. In forming the barrier, the T-Ampoule becomes a pressure vessel requiring analysis. A pressure vessel analysis demonstrates that the design is sound and will withstand the environment predicted for it. The analysis is conservative. These conservatisms were included to address a list of uncertainties, all of which are addressed in the analysis.

The TB-1/T-Ampoule system can generate a more complex than normal pressure environment. The assembly involves a titanium T-Ampoule designed to fit snugly inside the stainless steel TB-1 vessel. Both are pressure containing devices. They combine to create a very small annular volume between the inside diameter of the TB-1 and the outside diameter of the T-Ampoule. This arrangement results in a complex pressure/temperature environment. At the high temperatures, the small annular space between the two vessels fills with products of O-ring decomposition and can develop pressures there significantly greater than the interior pressure. This negative pressure difference creates forces potentially capable of buckling the T-Ampoule. At lower temperatures, the T-Ampoule's greater internal pressure creates tensile stresses in the shell, threatening failure via bursting. This analysis demonstrates that the T-Ampoule design is sufficiently robust that neither of these possibilities poses a threat.

Analysis included both the creation of the complex pressure/temperature map for the T-Ampoule vessel. This map is reflected in the graph contained in Figure 5. This map serves as input to a pressure vessel analysis based on the ASME Boiler and Pressure Vessel Code, Section VIII, Division 1 (BPVC). The pressure analysis provided temperature dependent limits for both internal (burst) pressure loading at low temperatures and external (collapse) pressure loading at high temperatures. The parameters of the pressure/temperature map were adjusted to ensure the predicted pressure stayed within these parameters.

The parameter adjustment resulted in two important constraints on T-Ampoule design. First, any ancillary plastic (bags, labels, tape, etc.) is limited to the values listed in Table 10 for four plastics. Second, the O-ring seal must be designed to ensure it will fail inward under high external pressure difference. Thus at a specific point in the accident scenario the TB-1/annulus volume equilibrates with the T-Ampoule interior. These constraints also combine to ensure the maximum TB-1 pressure, either before equilibration or after, never exceeds the 1110 psia (1095 psig) limit imposed by its design.

The special nature of the T-Ampoule design mandated some exceptions to a standard BPVC analysis, which are identified in this report.

7 References

1. American Society of Mechanical Engineers (ASME); Boiler and Pressure Vessel Code, Section VIII Division 1, Rules for Construction of Pressure Vessels. 2007.
2. American Society of Mechanical Engineers (ASME); Boiler and Pressure Vessel Code, Section II Part D, Properties (Customary) Materials; 2007.
3. Rubin, J.B. "Thermal Decomposition of Viton® O-rings for the PAT-1 Packaging Accident Scenario." LA-UR-10-05846. Los Alamos National Laboratory. Los Alamos, NM.
4. Serban Moldoveanu: Analytical Pyrolysis of Synthetic Organic Polymers, Volume 25 (Techniques and Instrumentation in Analytical Chemistry) (Elsevier Science, 2005).
5. W.C. Reynolds; Thermodynamic Properties in SI; Stanford Department of Mechanical Engineering; 1979; ISBN 0-917606-05-1.
6. PAT-1040. Titanium and O-Ring Materials and Component Fabrication Specification.
7. DOT/FAA/AR-MMPDS-01 Metallic Materials Properties Development and Standardization: January 2003.
8. United States. Nuclear Regulatory Commission. NUREG-0361. "Safety Analysis Report for the Plutonium Air Transportable Package, Model PAT-1." Washington, D.C. 1978.
9. Society of Automotive Engineers; Standard AS5857; Gland Design, O-Ring and Other Elastomeric Seals, Static Applications; March 2005.
10. Parker Hannifin Corp document. "Parker O-Ring Handbook." ORD 5700.
11. Minnesota Rubber/Quadion Corporation, Elastomers and Thermoplastics Engineering Design Guide: copyright 2007.

This page intentionally left blank

3. THERMAL EVALUATION

The thermal evaluation in this addendum examines the incorporation of plutonium metal as a new payload for the PAT-1 package. The Pu metal is packed in an inner container (*T-Ampoule Assembly*,[A] Drawing 2A0261, designated the T-Ampoule) that replaces the PC-1 inner container. The T-Ampoule and associated Pu metal contents packing configurations are described in Section 1.2.1 and Section 1.2.2 of this addendum, respectively.

The thermal evaluations documented in Chapter 3 of the Safety Analysis Report (SAR)[1] for the Plutonium Air Transportation Package, Model PAT-1, NUREG-0361[1] (SAR[1]) apply to this PAT-1 Safety Analysis Report Addendum for the T-Ampoule and its contents. The thermal evaluation of the T-Ampoule contents addressed in this addendum assumes a bounding internal heating scenario where three plutonium metal samples (25 watts total) from a three-nested *Sample Container-1 (SC-1) Assembly* configuration, (Drawing 2A0268, designated SC-1) are collocated along the seal area of the T-Ampoule to present a concentrated heat source. The other configurations described in Section 1 of this addendum, which are the 831 g (1.83 lbm) Pu hollow cylinder, wrapped in tantalum foil or not wrapped based on operational determination, supported with crushed tantalum foil, and the two-nested sample container configuration (*Sample Container-2 [SC-2] Assembly*, Drawing 2A0265, designed SC-2) supported by a titanium *Inner Cradle* (Drawing 2A0385, designated Inner Cradle) present a less concentrated heat source against the seal area. Although the quantity of plutonium metal assumed for the bounding case has a lower decay heat energy (see Section 4 of this addendum) than the 25 watts (85.3 Btu/hr) the PAT-1 package is certified for, the 25-watt decay heat limit is conservatively used for this analysis. The heat absorbed by the components within the T-Ampoule is neglected also for conservatism. Results from thermal analyses presented in this section demonstrate that the thermal performance of the PAT-1 with the proposed metal payload will be acceptable under normal conditions of transport (NCT) as defined in 10 CFR 71.71,[2] under hypothetical accident conditions (HAC) as defined in 10 CFR 71.73,[2] and under the accident conditions for air transport of plutonium as defined in 10 CFR 71.74.[2] The results also demonstrate that the T-Ampoule will provide a eutectic barrier for the proposed metal payload under the accident conditions for air transport of plutonium, as defined in 10 CFR 71.74.[2] The components of the PAT–1 packaging not modified by this addendum perform as documented in the SAR.[1]

3.1 Description of Thermal Design

The thermal design description provided in the SAR[1] remains valid for this addendum, as there are no alterations to the AQ-1 protective overpack (*Overpack AQ*, Drawing 1002, designated AQ-1) or the TB-1 stainless steel containment vessel (*Containment Vessel*, Drawing 1017, designated TB-1). The thermal effects of replacing the PC-1 inner container and aluminum spacer with the T-Ampoule inner container inside the TB-1, with the same 25 watts (85.3 Btu/hr) maximum heat generation, were conservatively bounded in the computer analyses, as explained in the next sections. Changing the content form inside the TB-1 has no negative effects on the thermal performance of the AQ-1 overpack thermal design features or the TB-1 containment vessel. The thermal performance of the PAT-1 package is adequate and will safely contain its

[A] The drawing titles are in italics and are used interchangeably with the designated names in this addendum. See Section 1.3.2 in this addendum and Chapter 9 in the SAR[1] for drawing number, title, and revision.

contents as described in this Addendum under the test conditions specified in 10 CFR 71.71, 71.73, and 71.74.[2]

3.1.1 Design Features

The design features of the PAT-1, TB-1 stainless steel containment vessel, and the AQ-1 protective overpack assembly are unchanged and are described in Chapter 3 of the SAR[1]. The *Ring, Filler* (Drawing 2A0262, designated Ring Filler) and the T-Ampoule inner container in the configurations depicted in Figures 1-3 through 1-5 of this addendum replace the PC–1 inner container and aluminum spacer documented in the SAR.[1] The effect of this change was captured in the thermal computer models described later in this section.

There are three basic configurations for plutonium metal contents within the T-Ampoule. One configuration consists of two titanium SC-2 sample containers supported and held in position inside the T-Ampoule by a titanium Inner Cradle (see Figure 1-3 in Section 1 of this addendum). The plutonium metal content within the SC-2 is a solid plutonium (Pu) cylinder of a diameter and length of 1.1 inches (0.0279 m). A second configuration consists of three SC-1 sample containers supported and held in position inside the T-Ampoule by a titanium Inner Cradle (see Figure 1-4). This configuration is similar to the two SC-2 configuration except it consists of three SC-1s and the plutonium metal sample packed in an SC-1 is a solid cylinder 0.88 inches (0.0224 m) in diameter and length. A third configuration consists of a single Pu hollow cylinder weighing from 731 to 831 grams (1.61 to 1.83 lbm) supported by crushed tantalum foil surrounding the cylinder (see Figure 1-5). The T-Ampoule, Ring Filler, SC-1, SC-2, Inner Cradle, and plutonium metal content all have melting temperatures above the 582°C (1080°F) temperature observed in the TB-1 during the plutonium air transport fire test described in SAR,[1] Section 3.6.1.2. Since the maximum total heat generation allowed in the TB-1 is limited to 25 watts (85.3 Btu/hr), a very conservative and bounding case for the application of the internal heating was used in the evaluation discussed in this section.

3.1.2 Decay Heat of the Contents

The PAT-1 package was assessed for a total decay heat load of its radioactive contents of 25 watts (85.3 Btu/hr). Sections 3.3 and 3.4 of this addendum demonstrate that with the 25 watt (85.3 Btu/hr) decay heat, the overall thermal performance of the PAT-1 package with the T-Ampoule and its plutonium metal payload is essentially the same as demonstrated in the SAR.[1] For the purpose of the analysis of the PAT–1 with the T-Ampoule and its plutonium metal content configurations addressed in this evaluation, the decay heat is conservatively assumed to be 25 watts. A bounding internal heating scenario was assumed in the analyses presented in this addendum. All 25 watts (85.3 Btu/hr) were assumed to be concentrated in a small region directly applying heat to the T-Ampoule elastomeric O-ring, as if all the solid plutonium metal cylinders were to group and transfer all their thermal energy to a small seal region. From the three basic configurations of plutonium metal contents discussed in Section 3.1.1 of this addendum, the hypothetical configuration that yields the smallest projected area for heat to flow through and therefore, provides maximum heat flux into the seal region is one where three plutonium metal cylinders are close together and aligned along the seal region as illustrated in Figure 3-1. Assuming the total 25 watts (85.3 Btu/hr) from these three plutonium cylinders are transferred to the seal region through the small projected area illustrated in Figure 3-2, the total concentrated heat flux q'' is:

$$q'' = \frac{25W}{(2.64")(0.88")} = \frac{25W}{(0.067056m)(0.022352m)} \cong 16{,}680\frac{W}{m^2} \quad \underline{or} \quad 5{,}288\frac{Btu}{hr - ft^2}. \qquad (3\text{-}1)$$

Note that this scenario is extremely unlikely because the Pu cylinders will not come out of the sample containers during NCT or HAC, as documented in Section 2 of this addendum. In addition, if the three Pu cylinders were to align as described, a portion of the assumed 25 watts (85.3 Btu/hr) will be transferred by convection and radiation to other regions (and components) inside the T-Ampoule, and thereby reduce the actual quantity of energy available to be transferred by conduction through the hypothetical localized heating region described herein. Since this highly concentrated heat flux is understood to bound all plutonium metal loading configurations discussed in Section 3.1.1 of this addendum, only this heat flux was used to very conservatively represent the decay heat inside the T-Ampoule during the NCT and HAC evaluations.

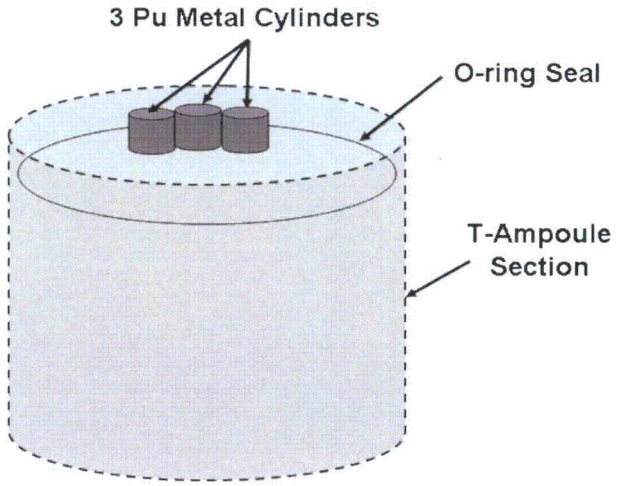

Figure 3-1. Schematic of Assumed Worst-Case Heating-to-the-Seal Scenario

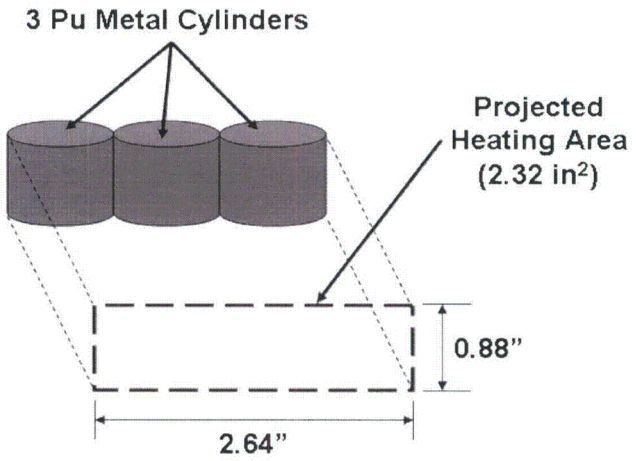

Figure 3-2. Schematic of Approximated Projected Heating Area [m=0.0254*in.; m^2=6.45x10^{-4}*$in.^2$]

3.1.3 Summary Tables of Temperatures

The SAR[1] describes how design features in the PAT-1 adequately contain the material inside the TB-1 even after the PAT–1 is exposed to the regulatory conditions specified in 10 CFR 71.71, 71.73, and 71.74.[2] The results from the thermal evaluation of the AQ-1, TB-1, and the T-Ampoule assuming the bounding concentrated internal heat described in Section 3.1.2 of this addendum are summarized in Table 3-1 of this addendum. These results show that the PAT-1 also protects the new components inside the TB-1 described in this addendum and adequately contains the material inside the TB-1, as the T-Ampoule seal temperatures are within the manufacturer's specifications and the T-Ampoule can withstand the pressure buildup during and after the regulatory specified heating.

Table 3-1. Summary of Temperatures Under NCT and HAC

Component	NCT		HAC
	Maximum	Minimum	Maximum
T-Ampoule (Seal)	122°C (251°F)	-40°C (-40°F)	153°C (308°F) @ 260 minutes after the fire
TB-1 (and TB-1 seal)*	114°C (238°F)	-40°C (-40°F)	147°C (296°F) @ 260 minutes after the 30-minute fire
Center of Redwood Between TB-1 and Load Spreader	99°C (211°F)	-40°C (-40°F)	132°C (270°F) @ 240 minutes after the 30-minute fire
Aluminum Load Spreader	98°C (208°F)	-40°C (-40°F)	131°C (267°F) @ 190 minutes after the 30-minute fire
Center of Redwood Between Load Spreader and Outer Skin	95°C (203°F)	-40°C (-40°F)	164°C (328°F) @ 30 minutes after the 30-minute fire
Stainless Steel Outer Drum	93°C (200°F)	-40°C (-40°F)	1003°C (1837°F) @ end of fire

*Maximum seal temperature was conservatively taken as the TB-1 maximum temperature.

3.1.4 Summary Table of Maximum Pressures

Table 3-2 of this addendum summarizes the maximum pressures inside the T-Ampoule for the NCT, HAC and plutonium air transport accident conditions specified in 10 CFR 71.71,[2] 71.73,[2] and 71.74,[2] respectively. As demonstrated in Sections 2, 3.3.2, 3.4.3, 3.4.5, and 4 of this addendum, the pressures that arise in the container during NCT, HAC, and plutonium air transport accident conditions do not result in a loss of containment.

Table 3-2. Summary of Maximum Pressures inside the T-Ampoule for NCT and HAC

Regulatory Condition	Maximum Pressure
NCT (or MNOP)	29 kPa (4.2 psig)
HAC	40 kPa (5.8 psig)
Plutonium Air Transport	7.55 MPa (1095 psig)

3.2 Material Properties and Component Specifications

3.2.1 Material Properties

A summary of the thermophysical properties of the materials used in PAT-1 is provided in the SAR,[1] Section 3.2, Table 3.2. To be consistent with the SAR[1] the same material properties for aluminum, ETC copper, stainless steel, and redwood (up to a certain temperature as described below) were used for the analyses presented in this addendum.

The following was considered for modeling the thermal response of redwood. Slow degradation (slow pyrolysis) of wood occurs in the temperature range of 200°C to 280°C (392°F to 536°F), until active pyrolysis begins in the 280°C to 500°C (536°F to 932°F) range. A temperature of 288°C (550°F) is used to locate the base of the char layer. Reference 3 (*Application of CMA Program to Wood Charring*) and the references cited therein contain additional information about temperature-dependent wood properties and wood charring. The thermal conductivity and specific heat provided in the SAR[1] are given in expressions that are a function of temperature. While these expressions are valid for the temperature range used for their determination, which was approximately 93°C (200°F) (see Section 3.2 and Appendix 3-A of the SAR[1]), the same equations were used to determine properties up to the temperature at which wood starts to decompose (i.e., 200°C [392°F]). Given that the properties of redwood provided in the SAR[1] do not take degradation of wood into account, property values and mathematical expressions from Reference 3 were used at temperatures greater than 200°C (392°F). For thermal conductivity at temperatures above pyrolysis, a fixed value within the range in Reference 3 for charcoal was used. Therefore, the temperature-dependent thermal properties presented in Table 3-3 of this addendum were specified in the P/Thermal model to adequately represent the state and response of the redwood. In cases were wood reached pyrolysis temperatures, it was assumed that the properties would remain those of charred wood throughout the cool-down process. To corroborate the validity of these modeling assumptions, thermal models discussed in Sections 3.3 and 3.4 of this addendum were completed and results compared with tests of the PAT-1 under transient NCT and HAC documented in the SAR.[1] These comparisons showed acceptable agreement as demonstrated by the data presented in those sections. Thus, a computer model that was calibrated with the test and analysis data presented in the SAR[1] was developed and used.

Table 3-3. Thermophysical Properties Used to Represent Redwood

Wood State	Temperature °C [°F]	Density kg/m^3 [lb/ft^3]	Specific Heat J/kg-K [Btu/lb-F]	Thermal Conductivity W/m-K [Btu/hr-ft-°F]	
				Parallel to Grain	Perpendicular to Grain
Before Pyrolysis	16 [60]	352 [22]	1273 [0.30]	0.330 [0.19]	0.117 [0.07]
	38 [100]	352 [22]	1591 [0.38]	0.390 [0.22]	0.136 [0.08]
	93 [200]	352 [22]	2386 [0.57]	0.533 [0.31]	0.190 [0.11]
	199 [390]	352 [22]	3898 [0.93]	0.810 [0.47]	0.290 [0.17]
During Slow and Active Pyrolysis	200 [392]	214 [13]	1151 [0.28]	0.073 [0.04]	0.026 [0.02]
	280 [536]	214 [13]	1314 [0.34]	0.073 [0.04]	0.026 [0.02]
	500 [932]	214 [13]	1657 [0.44]	0.073 [0.04]	0.026 [0.02]
	800 [1472]	214 [13]	1876 [0.45]	0.073 [0.04]	0.026 [0.02]
	1000 [1832]	214 [13]	1861 [0.45]	0.073 [0.04]	0.026 [0.02]

In addition to the material properties listed in the SAR[1] and in Table 3-3 of this addendum, the thermal properties for Ti-6Al-4V used in the computer analysis are presented in Table 3-4 of this addendum. These values were obtained from the MSC PATRAN Thermal (P/Thermal) computer code materials database,[4] which lists References 5, 6, and 7 as the source. Reference 8 supports the temperature-dependent trend of the data presented in Table 3-4. Materials inside the T-Ampoule were conservatively neglected for the thermal analysis (no credit was taken for heat absorbed by components inside the T-Ampoule); therefore, the thermal properties of those materials are not presented in this section.

Table 3-4. Thermophysical Properties of the Titanium Ampoule (Ti 6Al-4V)

Temperature °C [°F]	Thermal Conductivity W/m-K [Btu/hr-ft-°F]	Specific Heat J/kg-K [Btu/lbm-°F]	Density Kg/m^3 [lbm/ft^3]
-50 [-58]	–	502 [0.120]	4450 [277.8]
0 [32]	6.9 [3.99]	–	
100 [212]	–	561 [0.134]	
200 [392]	9.0 [5.20]	–	
300 [572]	–	615 [0.147]	
400 [752]	11.9 [6.89]	-	

3.2.2 Component Specifications

The service temperature range for package components inside the TB-1 are presented in Table 3-5 of this addendum.

Table 3-5. Service Temperatures of Packaging Components and Content inside the TB-1

Component	Service Temperature Range °C [°F]	Reference
T-Ampoule O-ring	-17°C to 204°C [1.4°F to 400°F]	Appendix 3.5.2[i]
TB-1 Copper Gasket	-40°C to >582°C [-40°F to >1080°F]	PAT-1 SAR[ii]
T-Ampoule (as eutectic barrier)[iii]	-40°C to 625°C [-40°F to 1157°F]	[9]
Titanium Inner Cradle[iii]	-40°C to 625°C [-40°F to 1157°F]	[9]
Ring, Filler[iv]	-40°C to >593°C [-40°F to >1100°F]	[10]
Pu/Be Content[vi]	-40°C to 595°C [-40°F to 1103°F]	[9]
Tantalum Foil[vii]	-40°C to 640°C [-40°F to 1184°F]	[9]

[i] Appendix 3.5.2 of this addendum provides the manufacturer's specifications for the O-ring material used in the T-Ampoule and in the SC-1 and SC-2 sample containers.

[ii] Based on thermal tests performed and documented in the PAT-1 SAR,[1] the TB-1 maintained containment after experiencing temperatures as high as 582°C (1080°F). Therefore, the copper gasket in the TB-1 can maintain seal at temperatures above these observed maximums.

[iii] The melting point of the eutectic that may form when titanium is in contact with gallium is 625°C (1157°F).

iv. Ti-6A1-4V has a yield strength of about 331 MPa (48 ksi) at 593°C (1100°F), which is approximately 40% of the nominal room temperature value of 827 MPa (120 ksi)[9] and there are no forces other than gravitational acting on these components during and after the fire accident condition.

v Copper-Plutonium eutectic melting point.

vi The plutonium/beryllium eutectic represents the lowest melting point eutectic at 595°C (1103°F) in the system. The Pu/Be is a content, not a component within the TB-1.

vii Upper temperature assumed to be the Plutonium-Tantalum eutectic melting point. From page 11 of Reference 9, there is insufficient gallium in the entire mass of plutonium metal for Tantalum-Gallium eutectic formation and melting to have a negative effect on the system.

3.3 Thermal Evaluation under NCT

The commercially available MSC Patran Thermal (P/Thermal) finite element (FE) computer code[4] was used for the thermal evaluation of the PAT-1 package under NCT. P/Thermal is a well-respected FE code widely used to analyze a variety of thermal issues, including those related to nuclear transport packages. P/Thermal can solve one-, two-, and three-dimensional conduction, convection, and radiation heat transfer issues.

A three-dimensional model of the PAT-1 package was built using P/Thermal to demonstrate that containment is maintained by the TB-1 and that the temperature of the O-ring in the T-Ampoule does not exceed the manufacturer's recommended temperature range. The computational mesh of the PAT-1 model built using P/Thermal is shown in Figure 3-3. The model consists of 31,180 hexahedral finite elements and 34,697 nodes. Package features such as the different wood grain orientations and the respective anisotropic thermal properties of the redwood, the aluminum Load Spreader, the copper heat transfer tube, the stainless steel TB-1, and the titanium T-Ampoule where included in the model. The thin-walled outer drum was conservatively neglected. As mentioned in Section 3.1.2 of this addendum, the presence of components inside the T-Ampoule such as the sample containers (SC-1 and SC-2) and the titanium Inner Cradle were also conservatively neglected, and no other mass was assumed to absorb heat inside the T-Ampoule. Additionally, the 25-watt (85.3 Btu/hr) power from the Pu was conservatively applied to a small region on the inner surface of the T-Ampoule to maximize the thermal affect to the T-Ampoule seal, as explained in Section 3.1.2 of this addendum. The regions of the T-Ampoule, internal wall that did not receive this localized heat were conservatively assumed to be perfectly insulated (i.e., no heat transfer was allowed within the T-Ampoule, preventing the localized heated region from losing heat through convection or radiation to cooler T-Ampoule surface regions). Therefore, the small heated region was only allowed to transfer heat to the unheated (solid) regions through conduction.

The simplified temperature- and diameter-dependent correlation for a horizontal cylinder with laminar flow as employed in the TOPAZ heat transfer code 10 was used for the determination of the natural convection coefficient during NCT. That is:

$$h_{natural} = 1.32*[(T_{surface} - T_{ambient})/Diameter_{cylinder}]^{0.25} \text{ W/m}^2\text{-K} \quad (3\text{-}2)$$

Assuming

$T_{surface}$ = 176°F (80°C) (value obtained from NCT solution in the SAR[1])
$T_{ambient}$ = 100°F (38°C) (ambient temperature in 10 CFR 71.71[2])
$Diameter_{cylinder}$ = 20 in. (0.5588 m) (PAT-1 approximate external diameter)

$$h_{natural} = 1.32*[(80°C - 38°C)/0.5588\ m]^{0.25}\ W/m^2\text{-}K \quad (3\text{-}3)$$

$$h_{natural} = 3.9\ W/m^2\text{-}K \text{ or } 0.69\ Btu/hr\text{-}ft^2\text{-}°F \quad (3\text{-}4)$$

This value of $h_{natural}$ is on the low end of typical natural convection heat transfer coefficients for gases[11]. Ultimately, a more conservative value of **$h_{natural}$ = 3.5 W/m^2-K (0.62 Btu/hr-ft^2-°F)** was used for the NCT calculation in this addendum.

The PAT-1 package model was subjected to the thermal conditions specified in 10 CFR 71.71[2] to evaluate if the TB-1 can maintain containment during NCT. It was assumed that the package will be transported horizontally as specified in Section 1 of this addendum. The boundary conditions used in the model to simulate the "heat" conditions specified in 10 CFR 71.71(c)(1)[2] are summarized in Table 3-6 of this addendum. Note that the temperature of the environment was increased to 54.4 °C (130°F) as in the SAR.[1] Also note that the insolation data presented in this table represents a 24-hour average of the values as specified in 10 CFR 71.71,[2] as is typically assumed when a steady-state simulation is used to evaluate packages under the prescribed environment. For example, for curved surfaces, 10 CFR 71[2] specifies a 12-hour–period, total insolation energy of 400 g-cal/cm^2 (16,747 kJ/m^2 or 1,475 Btu/ft^2). In order to more adequately model the NCT in a computer code running in steady-state mode, the total energy per unit area is spread over 24 hours:

$$Insolation_{Curved\_Srurfaces} = \frac{400\ \text{g-cal/cm}^2}{(24hr)(3600\text{sec}/hr)} \cong 4.63E^{-3}\frac{g-cal}{cm^2-s} \cong 193.8\frac{W}{m^2}\ \ or\ \ 61.4\frac{Btu}{hr-ft^2} \quad (3\text{-}5)$$

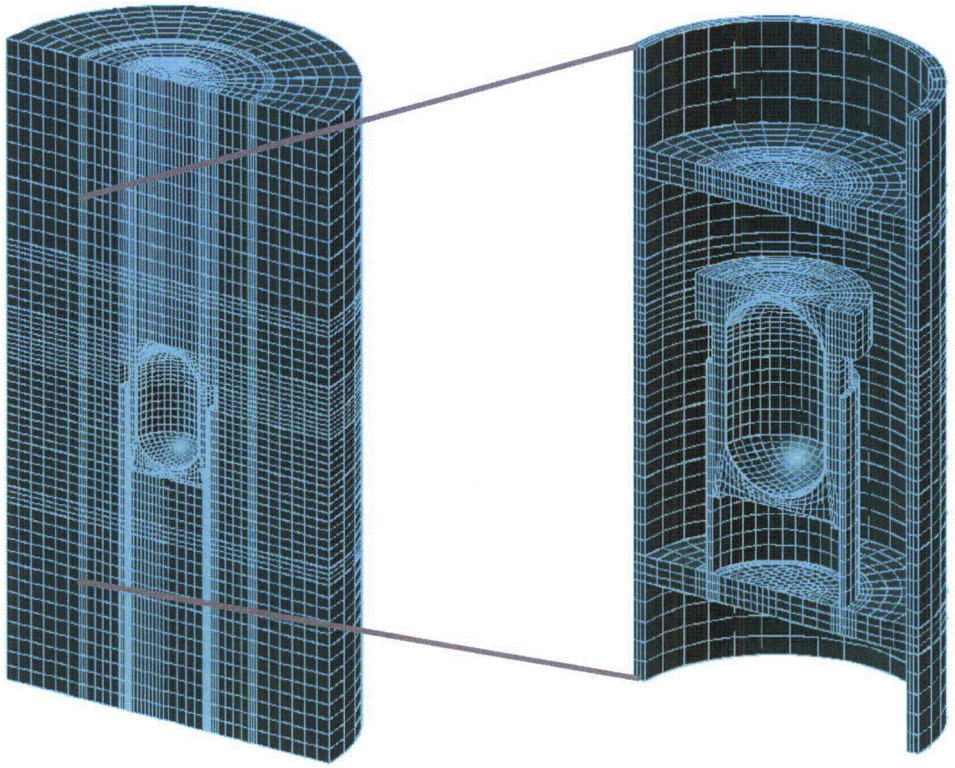

Figure 3-3. Finite Element Mesh of the PAT-1 Half-Symmetry Thermal Model and Enlarged Load Spreader, Copper Cylinder, TB-1, and T-Ampoule

Table 3-6. Boundary Conditions Used for the "Heat" NCT Thermal Evaluation

Boundary Condition	Application Region	Value Used
Environment Temperature	External node representing environment	54.4 °C (130°F)
Convection	Entire outer surface of the package	3.5 W/m^2-K (0.62 Btu/hr-ft^2-°F)
Radiation	Entire outer surface of the package	Package surface emissivity of 0.2,* Environment emissivity of 1
Insolation (Solar Flux averaged over 24 hours)	Curved surfaces	193.83 W/m^2 (61.44 Btu/hr-ft^2)
	Flat surfaces transported vertically (package ends)	96.92 W/m^2 (30.72 Btu/hr-ft^2)
Internal heat Flux (Decay heat)	Small region described in Section 3.1.2 of this addendum	16,680 W/m^2 (5287.5 Btu/hr-ft^2)

* From Table 3.2 in the SAR[1]

In addition to the "heat" NCT analysis, the package has to be able to maintain containment when exposed to an ambient temperature of -40°C (-40°F) in still air and shade as specified in 10 CFR 71.71(c)(2).[2] The results of exposing PAT-1 to these conditions are discussed in Section 3.3.1 of this addendum.

3.3.1 Heat and Cold

The finite element model described above was used for the NCT analysis. First, the model was verified by simulating both the steady-state test and the transient NCT analysis described in the SAR[1]. These models evenly distributed the 25W (85.3 Btu/hr) internal heat load and applied it to the inside wall of the TB-1. The results from this validation exercise are presented in Section 3.3.1.1 of this addendum. Once the model was verified against the results in the SAR,[1] the concentrated internal heat load described in Section 3.1.2 of this addendum was applied to the inner wall of the T-Ampoule. These results are presented in Section 3.3.1.2. of this addendum

3.3.1.1 Model Verification

The FE model described in Section 3.3 of this addendum was verified by simulating both the steady-state test and the transient NCT analysis described in the SAR.[1] The intent of this exercise was to verify the computer model against the data available in the SAR.[1] The validated model was then used to analyze the thermal response of the package with the plutonium metal content. These models evenly distributed the 25W (85.3 Btu/hr) internal heat load and applied it to the inside wall of the TB-1, as was the case for the models in the SAR.[1]

First, the computer model was verified against a low-temperature thermal test that was performed and presented in the SAR.[1] This test was performed to empirically determine the effective thermal resistance values for PAT-1 components. While boundary conditions are not well known, it is understood that a PAT-1 package was placed in a temperature-controlled chamber maintained at approximately 93°C (200°F). An internal heater was maintained at 25 watts (85.3 Btu/hr) using a variable resistance power supply. Transient response was measured with thermocouples placed at key locations within and outside the package. These data are documented in Sections 3.4.1.2 and Appendix 3-A of the SAR.[1] The results of the verification analysis are presented in Figure 3-4. Temperature results after 50 hours favorably compare with those reported in Table 3-A.1 of Appendix 3-A in the SAR,[1] as illustrated in Table 3-7 of this addendum. Figure 3-4 also favorably compares with Figure 3.4 in the SAR.[1] The results from this validation exercise demonstrate that the geometry representation, material properties, and finite element representation are adequate to predict the performance of the PAT-1 package when exposed to similar thermal loads.

Second, the computer model was verified against the transient NCT analysis results presented in the SAR.[1] This included variable insolation heating (over time and position) as described in Section 3.4.1.2 in the SAR.[1] All boundary conditions were applied as described in that section of the SAR.[1] In order to model those conditions adequately, the half-symmetry model was mirror-copied to make a full three-dimensional model of the package. The results from this verification exercise, presented in Figures 3-5 and 3-6, compare favorably with the results presented in the SAR.[1] The data documented in Figure 3-6 is in agreement with the data shown in Figure 3.5 of the SAR.[1] This indicates proper three-dimensional modeling of the package. The three-dimensional temperature distribution of the package at the time just before sundown (the most severe case) is shown in Figure 3-7. This temperature distribution shows a peak outer skin temperature of 116°C (241°F), which is approximately 9°C (17°F) hotter than the maximum surface temperature reported in SAR,[1] Section 3.4.1.2.

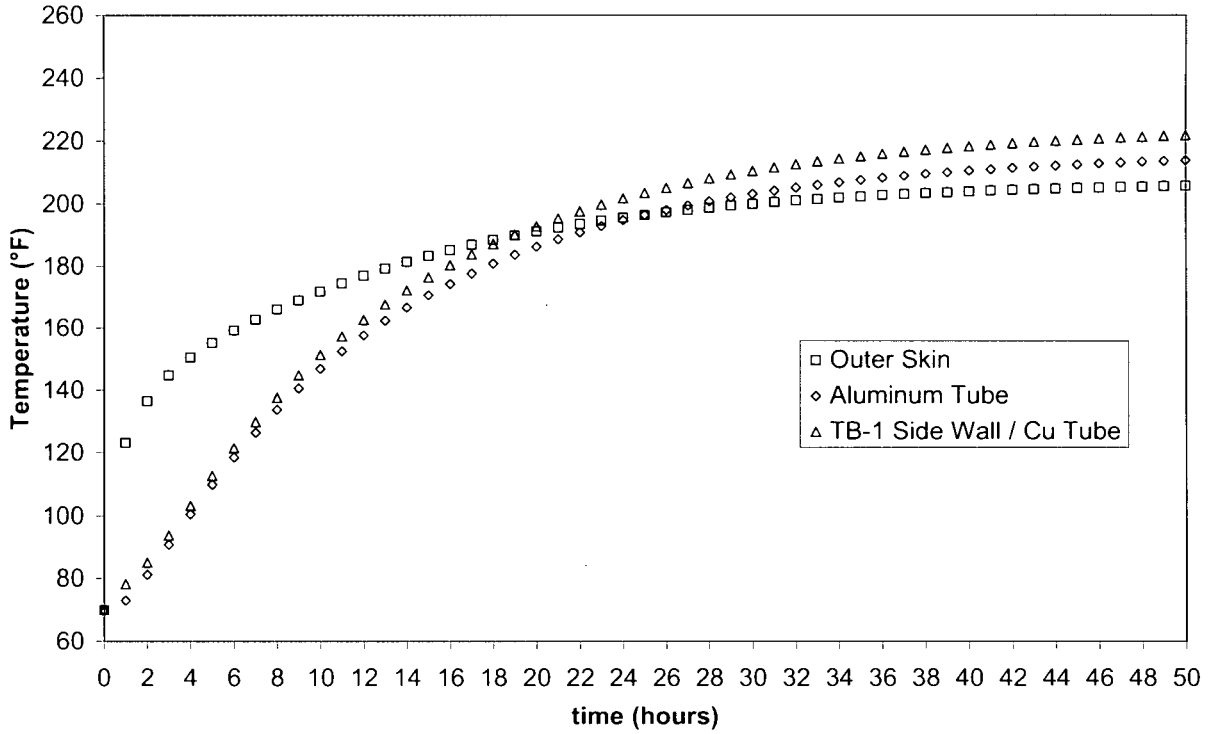

Figure 3-4. Low-Temperature Thermal Test Simulation Results. (°C=[°F-32]/1.8)

Table 3-7. Comparison of Test and Analysis Temperatures – Low Temperature Test

Location	Steady-State Temperature – Test Data	Steady-State Temperature – Analysis Data at Package Mid-Height
Cu Tube	105°C (221°F)	105.6°C (222°F)
Al Tube	100°C (212°F)	101°C (214°F)
Outer Skin	93°C (200°F)	96.6°C (206°F)

Third, the boundary conditions in the computer model were changed to reflect those specified in 10 CFR 71.71[2] in a steady-state simulation and to verify how the package response under these conditions compares to the transient method used in the SAR.[1] The intent of this exercise was to determine if the new analysis for this addendum is still bounding when using the steady-state method. The results from this exercise are presented in Figures 3-7 and 3-8. A comparison of the results in these two figures with those obtained from the transient simulation described above indicate that while the outer temperatures (maximums and distributions) are different, the steady-state analysis thoroughly envelops the transient response of the TB-1 and its surrounding regions. Therefore, it was decided to run a steady-state NCT analysis of the PAT-1 with the new contents configuration. The results from the steady-state analysis for this addendum are presented in Section 3.3.1.2.

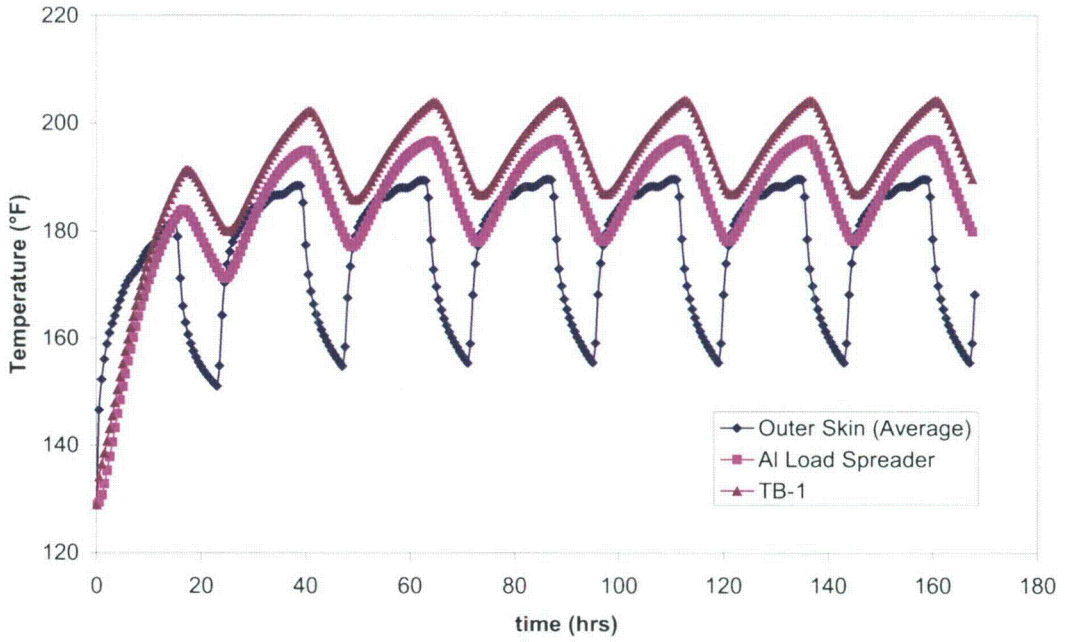

Figure 3-5. Seven-day Thermal Cycling for Quasi-Steady-State Analysis – Package Mid-Height Response (°C=[°F-32]/1.8)

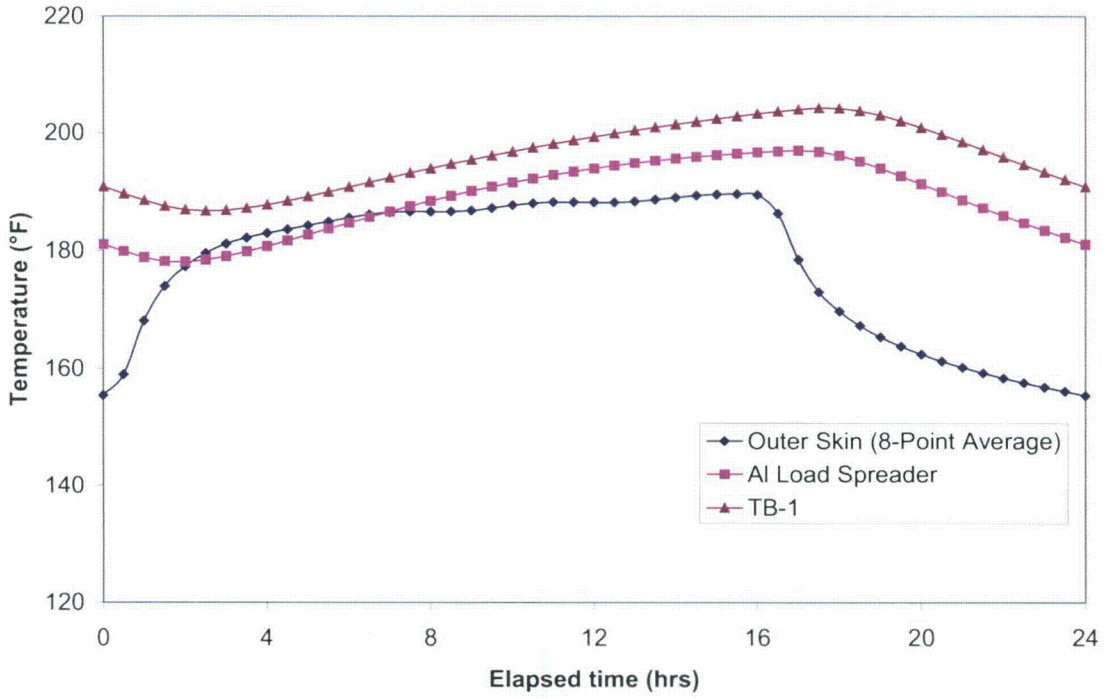

Figure 3-6. NCT Daily Thermal Cycle (Quasi-Steady-State NCT Solution) – Package Mid-Height Response (°C=[°F-32]/1.8)

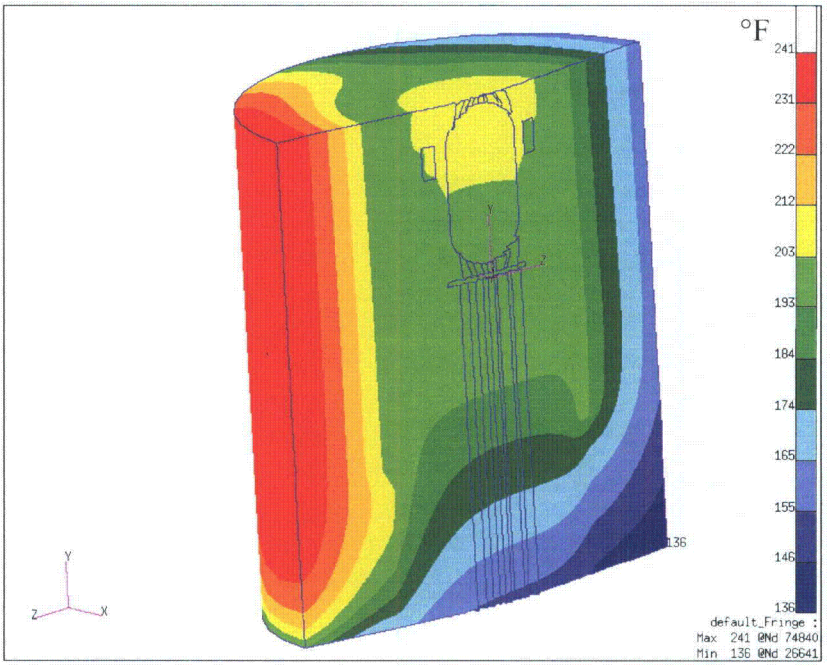

Figure 3-7. Temperature Distribution of PAT-1 Just Before Sundown – Most Severe Case of Transient NCT SAR[1] Analysis (Plot of ¼ of Package, °C=[°F-32]/1.8)

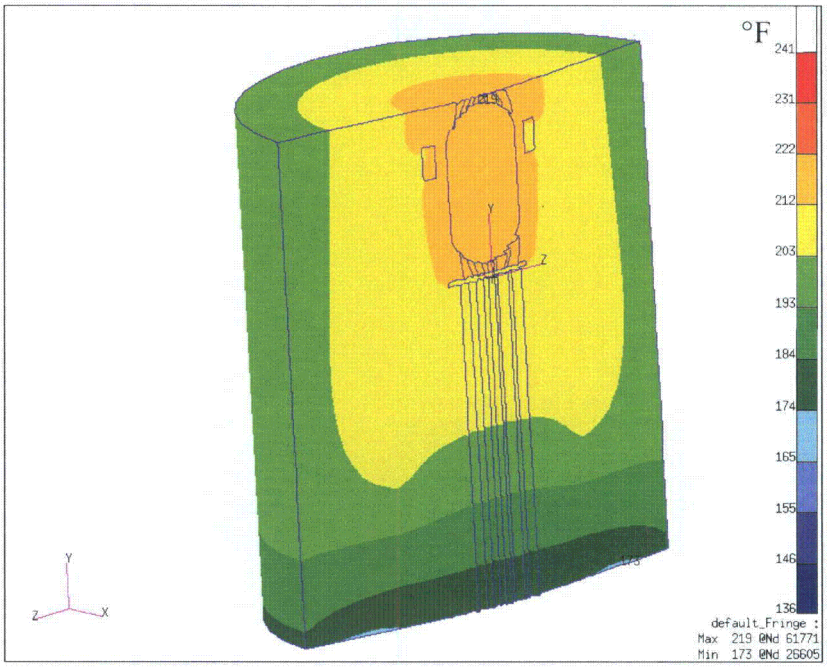

Figure 3-8. Temperature Distribution of PAT-1 – Steady-State NCT SAR[1] Analysis (Plot of ¼ of Package, °C=[°F-32]/1.8)

3.3.1.2 Addendum Analysis

The results from the NCT steady-state analysis of the package with the conservative internal heat load configuration of the new plutonium metal contents are presented in Figure 3-9. Note that the scale of the temperature distribution for this figure (and others in this section) is different from those previously shown. The temperature distribution shown in Figure 3-9 clearly illustrates the effect of the very concentrated heat applied to the seal region as described in Section 3.1.2 of this addendum. The T-Ampoule seal temperature was conservatively assumed to be the inside wall temperature of the T-Ampoule. This is conservative because the T-Ampoule closure was not explicitly modeled; instead the wall thickness of the T-Ampoule was assumed to be constant everywhere and therefore, that seal region had less thermal mass. This allows for more direct heating of the T-Ampoule seal, as energy that would be absorbed by the additional titanium in the vicinity of the seal is neglected and the heat path from the heated surface to the seal is shorter. The maximum T-Ampoule "seal" temperature is approximately 122°C (251°F) even in the very conservative internal heat load scenario. Therefore, the performance of the elastomeric O-ring in the T-Ampoule is not degraded and maintains product quality, as this temperature is within the operating range specified by the manufacturer. The maximum seal region temperature of the TB-1 was 114°C (238°F). This temperature is within the operating temperature range of the metallic seal. Therefore, the TB-1 is able to maintain containment.

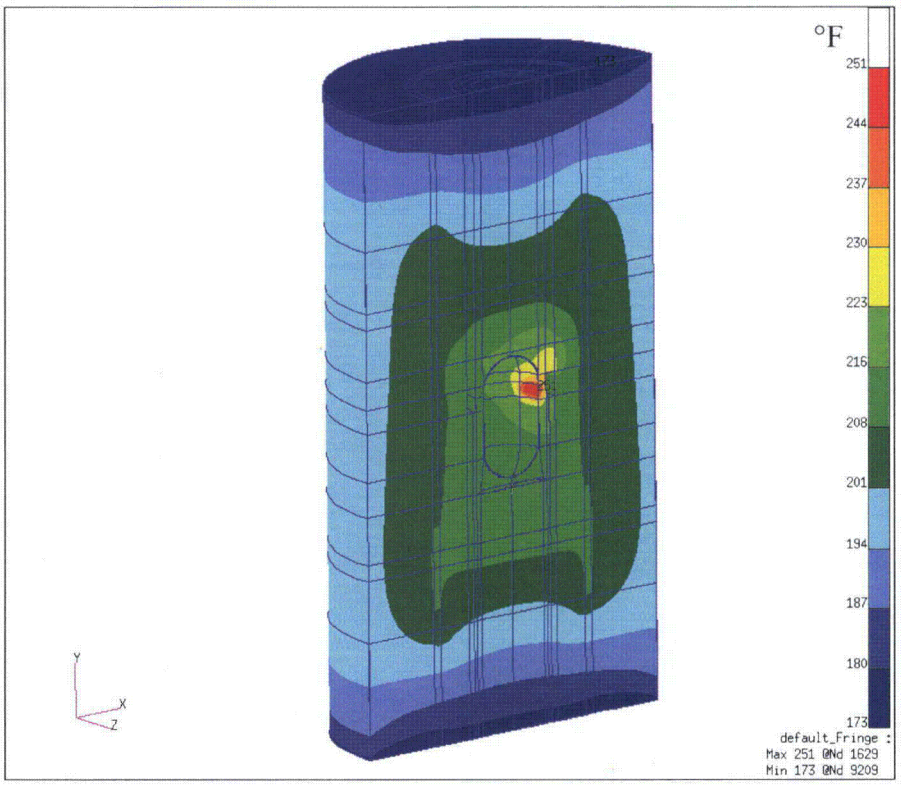

Figure 3-9. NCT Steady-State Temperature Distribution (°C=[°F-32]/1.8)

Regulatory requirements in 10 CFR 71.71(c)(2)[2] specify that the package must be capable of maintaining containment when it is exposed to an ambient temperature of -40°C (-40°F) in still air and shade. If one assumes no internal heating, the minimum temperature any PAT-1 package

component could reach is -40°C (-40°F). As discussed in Section 3.4.6 of the SAR,[1] the copper seal used in the TB-1 is unaffected at this low temperature. Therefore, the PAT-1 can maintain containment at this low temperature extreme even without taking credit for any decay heat of the contents, which will definitely heat the seal region of the TB-1 to above -40°C (-40°F).

Since the results in Figure 3-9 show parts of the outer surface at temperatures above 85°C (185°F), an additional analysis was performed assuming the package is in the shade (no insolation), still air, and exposed to the conservative ambient temperature of 55°C (130°F). This was done to demonstrate compliance with 10 CFR 71.43(g),[2] which specifies that any accessible surface of a package must not exceed 85°C (185°F) in an exclusive use shipment. The results from this analysis are presented in Figure 3-10. Compliance with 10 CFR 71.43(g) is demonstrated, since the maximum outer surface temperature of the package is less than 58°C (137°F). The somewhat "skewed" temperature distribution seen in Figure 3-10(b) is the result of the concentrated internal heating of the package.

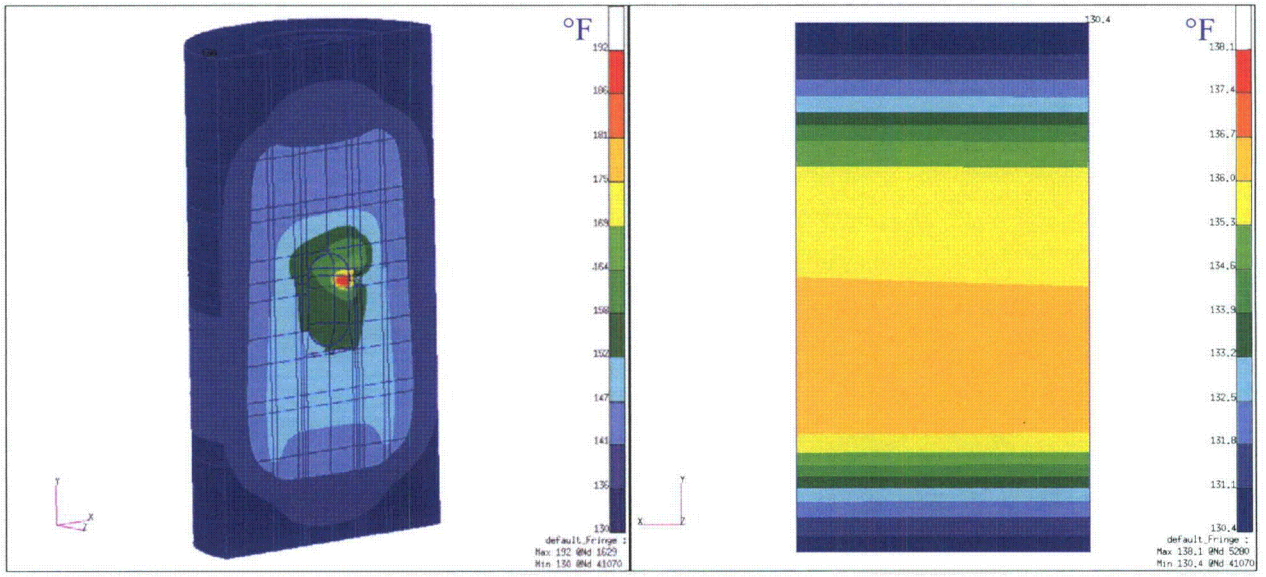

(a) Internal Temperatures **(b) Outer Surface Temperatures**

Figure 3-10. Steady-State Analysis in the Shade – 10 CFR 71.43(g) (°C=[°F-32]/1.8)

3.3.2 Maximum Normal Operating Pressure

The maximum normal operating pressure (MNOP) that may occur within the TB-1 is estimated to be 29 kPa (4.2 psig) (see Section 4 of this addendum). This was calculated using the average internal surface temperature of the T-Ampoule as the average temperature of the gas inside the TB-1, which is 103.3°C (218°F) and the contribution to the internal pressure over time due to alpha decay. The MNOP was then estimated as $P_{gauge} = (P_{initial} + P_{alpha\_decay})*(T_2/T_1)$ - 1atm = [(1 atm + 0.005 atm) * (678°R / 530°R) -1 atm] = 0.286 atm or ~ 29 kPa (4.2 psig), assuming initial fill of the TB-1 is done with gas at a room temperature of 21°C (70°F) and in an environment with an atmospheric pressure of one.

3.4 Thermal Evaluation under HAC

The P/Thermal FE model that was used for the NCT analysis was also used for the HAC analysis. Since the deformations shown in the SAR[1] after the package was dropped from 30 feet are minimal, the computer model used for the HAC thermal evaluation represents an undamaged package. Boundary conditions were modified to meet those specified in 10 CFR 71.73(c)(4).[2] In addition, the same model was used in a model verification exercise to simulate the 52-minute fire test documented in the SAR.[1]

In the SAR,[1] a description of a longer-than-regulatory fire test and results are presented. The PAT-1 package used for the test did not have internal heating. The SAR[1] does not indicate the temperature distribution or overall temperature of the package prior to the test. For the purpose of model verification, an initial uniform temperature of 27°C (80°F) was assumed within the PAT-1 package and no internal heating was applied. The boundary conditions used are summarized in Table 3-8 of this addendum. The estimation for the convection heat transfer coefficients in this table is presented following the table. Note that for the purpose of this model verification exercise, the average temperature of 982°C (1800°F) on the thin-walled AQ-1 drum reported in Table 3.4 in the SAR[1] was used as the effective fire temperature.

Table 3-8. Boundary Conditions Used for the Transient Model Verification Exercise

Boundary Condition	Application Region	Value Used During 52-Minute Fire	Value Used After Fire (Cool-down)
Environment Temperature	External node representing environment	982°C (1800°F)*	27°C (80°F)**
Convection	Entire outer surface of the package	11.5 W/m^2-K (2.03 Btu/hr-ft^2-°F)	3.5 W/m^2-K (0.62 Btu/hr-ft^2-°F)
Radiation	Entire outer surface of the package (exchange with environment node)	Package surface emissivity of 0.8, Fire emissivity of 1	Package surface emissivity of 0.2,*** Environment emissivity of 1
Internal Heat Flux (Decay Heat)	N/A	0	0

*From Table 3.4 in the SAR[1]
**Assumed ambient temperature
***From Table 3.2 in the SAR[1]

Values for convection heat transfer coefficients were estimated using correlations and verified with typically used values. For the convection heat transfer coefficient applied to the package surface during the fire (h_{fire}), a simplified temperature-only dependent correlation for a horizontal cylinder with turbulent flow as employed in the TOPAZ heat transfer code[10] was used. That is,

$$h_{fire} = 1.24*(T_{ambient} - T_{surface})^{1/3} \text{ W/m}^2\text{-K}$$

where $T_{ambient}$ is the temperature of the environment around the package and $T_{surface}$ is the outer surface temperature of PAT-1, with both temperatures in °C or Kelvin.

Assuming
$T_{ambient}$ = 1475°F (800°C) (fire temperature in 10 CFR 71.73)
$T_{surface}$ = 176°F (80°C) (value obtained from NCT solution in the SAR[1])

$$h_{fire} = 1.24*(800°C - 80°C)^{1/3} \text{ W/m}^2\text{-K}$$

$$h_{fire} = 11.11 \text{ W/m}^2\text{-K or } 1.96 \text{ Btu/hr-ft}^2\text{-°F}$$

This value of forced convection coefficient was corroborated using a more complex correlation proposed by Churchill and Bernstein[12] and experimental open-pool fire velocity measurements in Reference 13. In calm wind conditions for open-pool fires, vertical gas velocities are typically in the range of 5-10 m/s (16.4-32.8 ft/s) approximately 2 meters (6.56 ft) above the pool, but decrease to about 1 m/s (3.28 ft/s) near the surface of the pool.[13] Table 3-9 of this addendum presents typical values of the Grashof number (Gr_D) and the Reynolds number (Re_D) using a 5 m/s (16.4 ft/s) vertical gas velocity. To obtain these values, the temperature of the fire was assumed to be 800°C (1475°F) and air properties were used.

When $Gr_D/(Re_D)^2$ is less than 1, forced convection dominates. Therefore, the correlation suggested by Churchill and Bernstein for forced convection applies and was used to obtain an average convection coefficient:

$$\overline{Nu}_D = 0.3 + \frac{0.62\,\mathrm{Re}_D^{1/2}\,\mathrm{Pr}^{1/3}}{\left[1+(0.4/\mathrm{Pr})^{2/3}\right]^{1/4}}\left[1+\left(\frac{\mathrm{Re}_D}{282{,}000}\right)^{5/8}\right]^{4/5} \qquad (3\text{-}6)$$

where $\overline{Nu}_D$ is the Nusselt number and Pr is the Prandtl number. The convective coefficient, h, is equal to $\overline{Nu}_D k/D$, where k is the thermal conductivity of air and D is the diameter of the package. As demonstrated in Table 3-9 of this addendum the convection heat transfer coefficient is highest at the beginning of the fire when the temperature difference between the flame and the external wall of the cylinder is highest.

Table 3-9. Grashof, Reynolds, Nusselt Numbers for Calm Wind, Open-Pool Fire Conditions

Surface Temperature, Ts	Gr_D	Re_D	Gr_D/Re_D^2	Nu_D (Pr=0.7 for Air)	Convection Coefficient, h W/m²-K [Btu/hr-ft²-°F]
80°C [176°F]	2.39E+08	32870	0.22	106.1	10.0 [1.76]
527°C [981°F]	2.39E+07	21166	0.06	81.8	9.5 [1.67]
800°C [1472°F]	0	15102	0	67.4	8.7 [1.53]

Given that the value of h_{fire} using the correlation suggested by Churchill and Bernstein is between 8.7 and 10 and the simplified correlation from Shapiro and Edwards[10] is 11.11, a conservative heat transfer coefficient of **h_{fire} = 11.5 W/m²-K (2.03 Btu/hr-ft²-°F)** was used in the model.

The same simplified temperature- and diameter-dependent correlation for a horizontal cylinder with laminar flow that was used to calculate the natural convection coefficient for NCT in Section 3.3 of this addendum was used to estimate the natural convection coefficient for the modeling of the cool-down process after the fire. That is:

$$h_{natural} = 1.32*[(T_{surface} - T_{ambient})/Diameter_{cylinder}]^{0.25} \text{ W/m}^2\text{-K} \quad (3\text{-}7)$$

Assuming
$T_{surface}$ = 1475°F (800°C) (assuming outer surface at prescribed regulatory fire temperature for bounding, maximum value calculation)
$T_{ambient}$ = 100°F (38°C) (ambient temperature in 10 CFR 71.71[2])
$Diameter_{cylinder}$ = 20 in. (0.5588 m) (PAT-1 approximate external diameter)

$$h_{natural} = 1.32*[(800°C - 38°C)/0.5588 \text{ m}]^{0.25} \text{ W/m}^2\text{-K} \quad (3\text{-}8)$$

$$h_{natural} = 8 \text{ W/m}^2\text{-K or } 1.4 \text{ Btu/hr-ft}^2\text{-°F} \quad (3\text{-}9)$$

This estimated maximum value of $h_{natural}$ is in the mid range of typical natural convection heat transfer coefficients for gases.[11] However, a more conservative value of **$h_{natural}$ = 3.5 W/m^2-K (0.62 Btu/hr-ft^2-°F)** (the same value used in the evaluation of NCT) was assumed for the cool-down calculation.

The results from the verification model are presented in Figures 3-11 through 3-15. Figures 3-11 and 3-12 show the temperature distribution of the overall package and the internal components at the end of the 52-minute fire. Figures 3-13 and 3-14 are similar to the previous two, but show the temperature distribution at the time when the internal temperature of the TB-1 peaked (300 minutes after the fire). The plot in Figure 3-15 illustrates the temperature history of the package at selected locations.

When the simulated temperature response was compared to the results of the 52-minute fire test discussed in the SAR,[1] it was found that the computer prediction overestimated the thermal response of the package. The spatial average temperature of the TB-1 at the time the peak temperature occurred was 100°C (212°F). This is 7°C (12°F) hotter than the average TB-1 temperature reported in the SAR.[1] Since the model in this verification exercise overestimated the TB-1 average temperature, the simulation of the package response to the HAC with the concentrated heat is also overestimated. Therefore, it is conservative to use this model to estimate the thermal response of the package configuration for this addendum. The results are presented in the following sections.

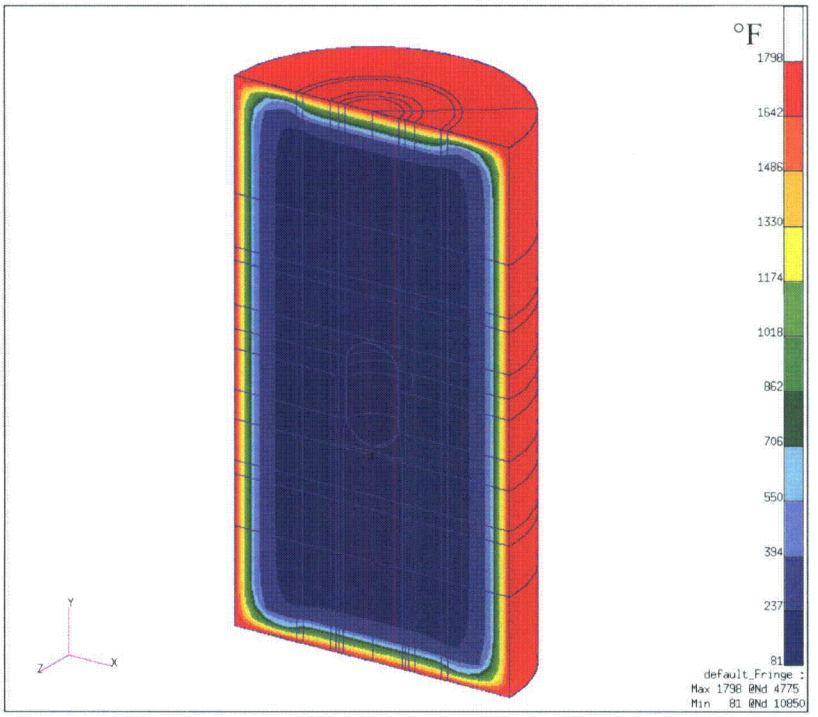

Figure 3-11. Temperature Distribution of the Verification Model at the End of the 52 Minute Fire — Complete Model (°C=[°F-32]/1.8)

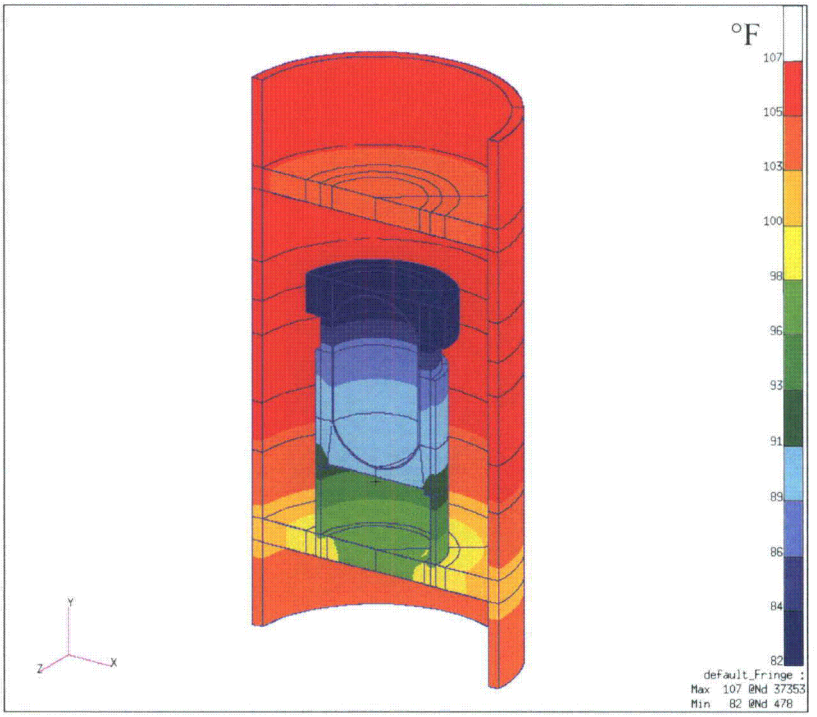

Figure 3-12. Temperature Distribution of the Verification Model at the End of the 52 Minute Fire — T-Ampoule, TB-1, Heat Transfer Cu Cylinder, and Aluminum Load Spreader (°C=[°F-32]/1.8)

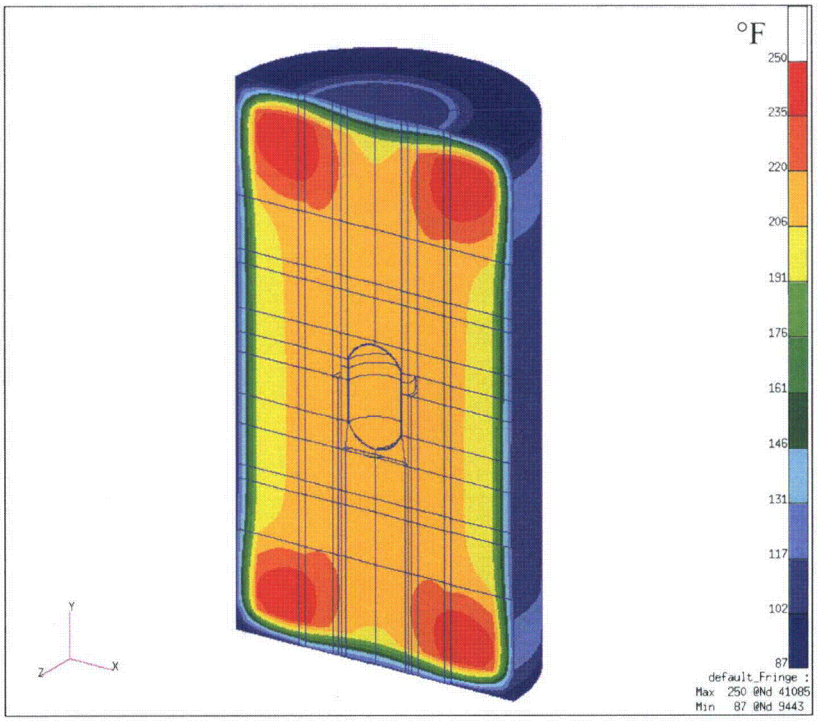

Figure 3-13. Temperature Distribution of the Verification Model at t=352 Minutes (300 Minutes after the 52 Minute Fire) — Complete Model (°C=[°F-32]/1.8)

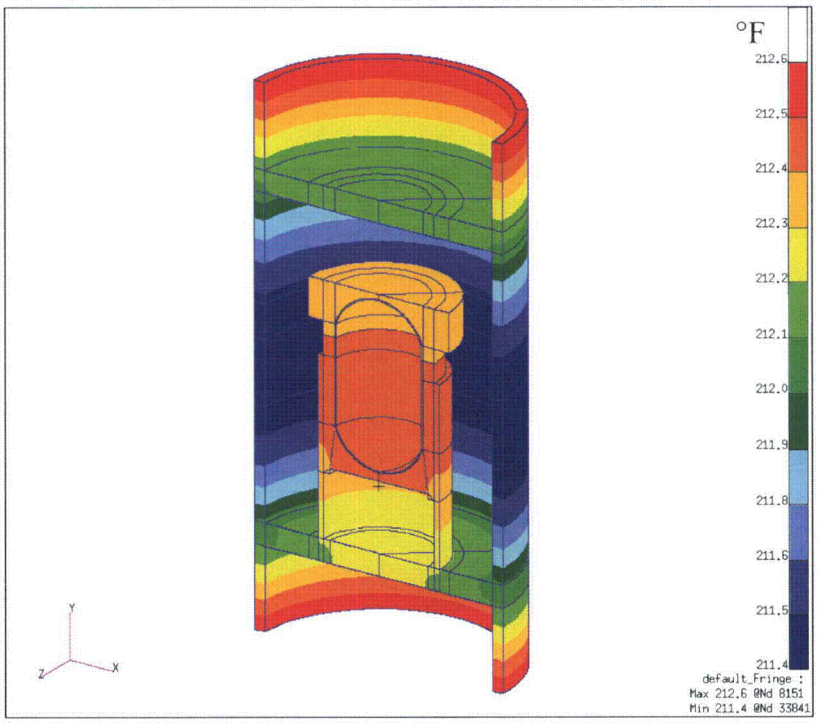

Figure 3-14. Temperature Distribution of the Verification Model at t=352 Minutes (300 Minutes after the 52 Minute Fire) — T-Ampoule, TB-1, Heat Transfer Cu Cylinder, and Aluminum Load Spreader (°C=[°F-32]/1.8)

3.4.1 Initial Conditions

The initial condition for the transient thermal analysis described in 10 CFR 71.73[2] is the temperature distribution calculated for the NCT. This initial temperature distribution is shown in Figure 3-9.

3.4.2 Hypothetical Accident Conditions (HAC)

The PAT-1 package model was subjected to the thermal transient conditions specified in 10 CFR 71.73[2] to evaluate whether the TB-1 can maintain containment and the T-Ampoule maintain seal (for product quality, not regulatory purpose) during and after a HAC fire event. The boundary conditions that were used in the model are summarized in Table 3-10 of this addendum. Note that only two boundary conditions were changed between this model and the one that was run for the 52-minute fire test verification exercise. That is, the fire duration was set to 30 minutes, and the same concentrated internal heat load applied to the NCT model was also used. As in the SAR,[1] the fire temperature was conservatively assumed to be 1010°C (1850°F) and the environment temperature for the cool-down period was conservatively assumed to be 54.4°C (130°F).

For the simulation of the HAC, the effect of a vertical and a horizontal package orientation in the fire were considered to determine the most damaging configuration. The calculations presented in Section 3.5.4 show that the package would receive more heat during HAC if it is positioned horizontally in the fire. Thus that conservative configuration was assumed for the fire analysis summarized in this section of the Addendum. Section 3.5.4 also shows that the value used for the cool-down is bounding.

The results from the simulation of the 10 CFR 71.73(c)(4)[2] environment are presented in Figures 3-16 through 3-20. Figures 3-16 and 3-17 show the temperature distribution of the overall package and the internal components at the end of the 30-minute regulatory fire. Figures 3-18 and 3-19 are similar to the previous two but show the temperature distribution at the time when the internal temperature of the TB-1 peaked (260 minutes after the fire). The plot in Figure 3-20 illustrates the temperature history of the package at selected locations.

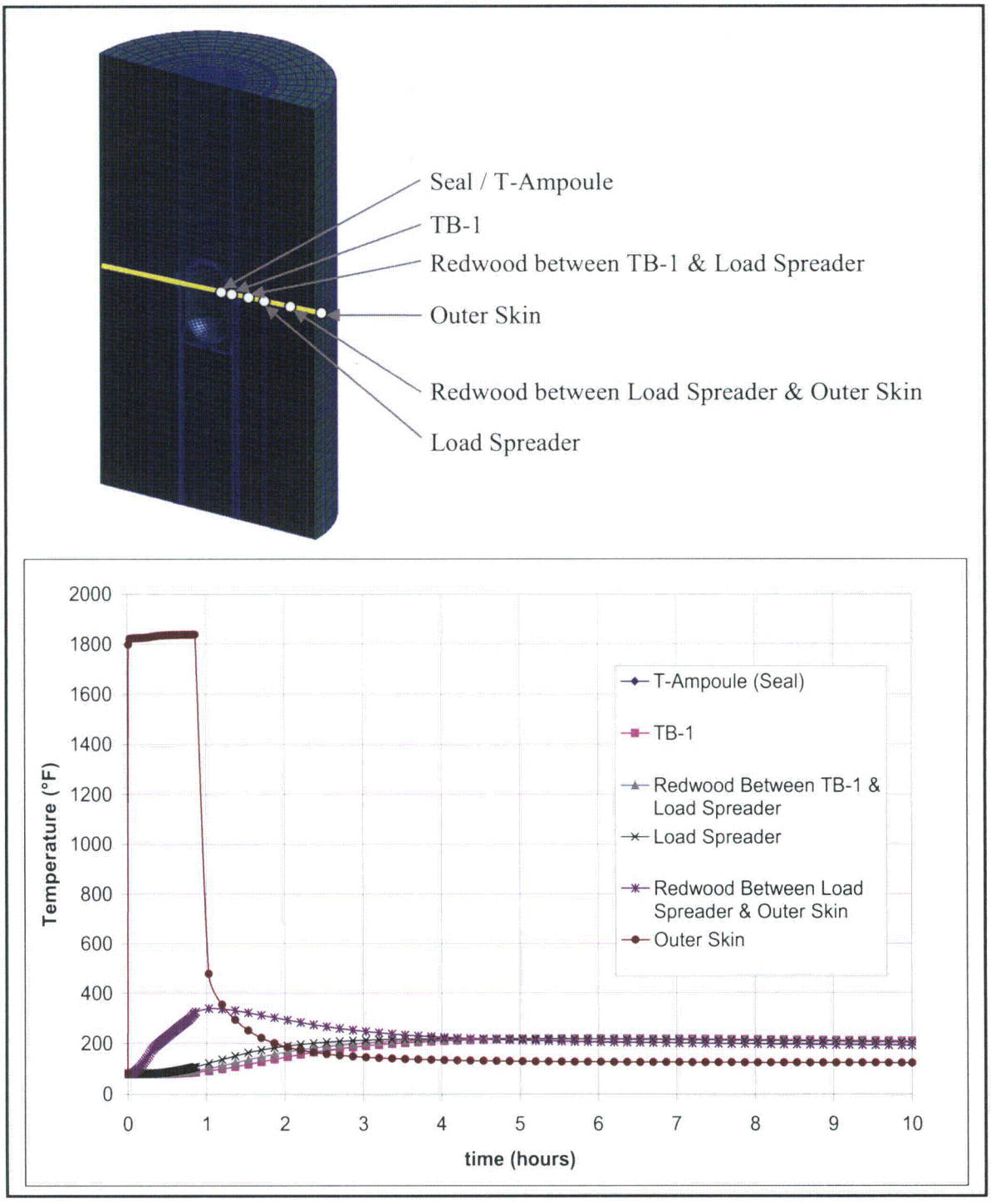

Figure 3-15. Temperature History at T-Ampoule Seal Height for the 52-Minute Fire Model Verification Exercise (°C=[°F-32]/1.8). Note: In the schematic above the plot, the reference yellow line crosses the cask at the T-Ampoule-seal height and the white dots are the approximate locations of the temperature history lines in the plot. The "T-Ampoule (Seal)" curve is completely covered by the "TB-1" curve.

Table 3-10. Boundary Conditions Used for the HAC Thermal Evaluation

Boundary Condition	Application Region	Value Used During 30-minute Fire	Value Used After Fire (Cool-down)
Environment Temperature	External node representing environment	1010°C (1850°F)	54°C (130°F)
Convection	Entire outer surface of the package	11.5 W/m^2-K (2.03 Btu/hr-ft^2-°F)	3.5 W/m^2-K (0.62 Btu/hr-ft^2-°F)
Radiation	Entire outer surface of the package	Package surface emissivity of 0.8, Fire emissivity of 1	Package surface emissivity of 0.2,* Environment emissivity of 1
Internal Heat Flux (Decay Heat)	Small region described in Section 3.1.2 of this addendum	16,680 W/m^2 (5287.5 Btu/hr-ft^2)	16,680 W/m^2 (5287.5 Btu/hr-ft^2)

* From Table 3.2 in the SAR[1]

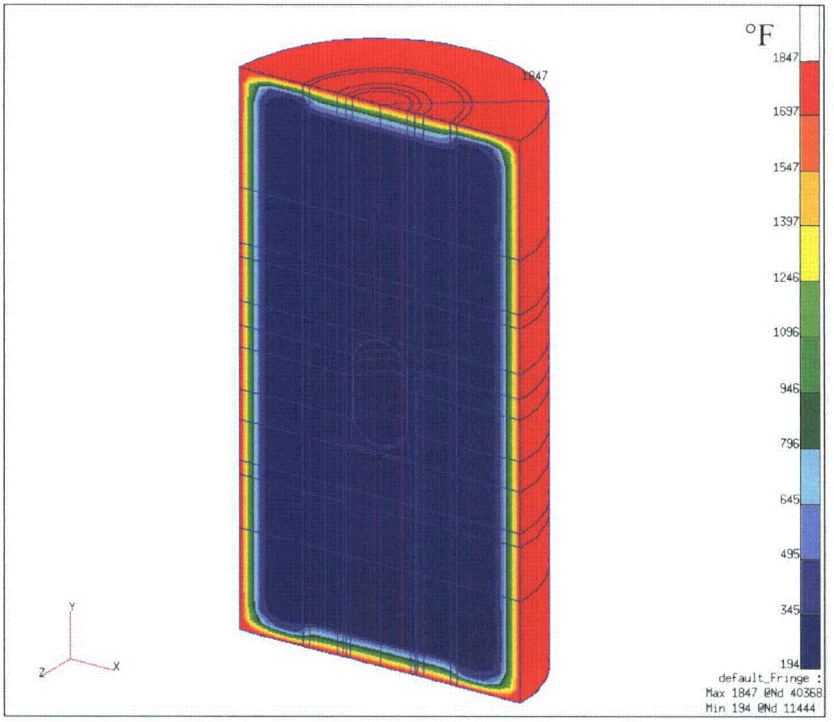

Figure 3-16. Temperature Distribution at the End of the 30-Minute Regulatory Fire — Complete Model (°C=[°F-32]/1.8)

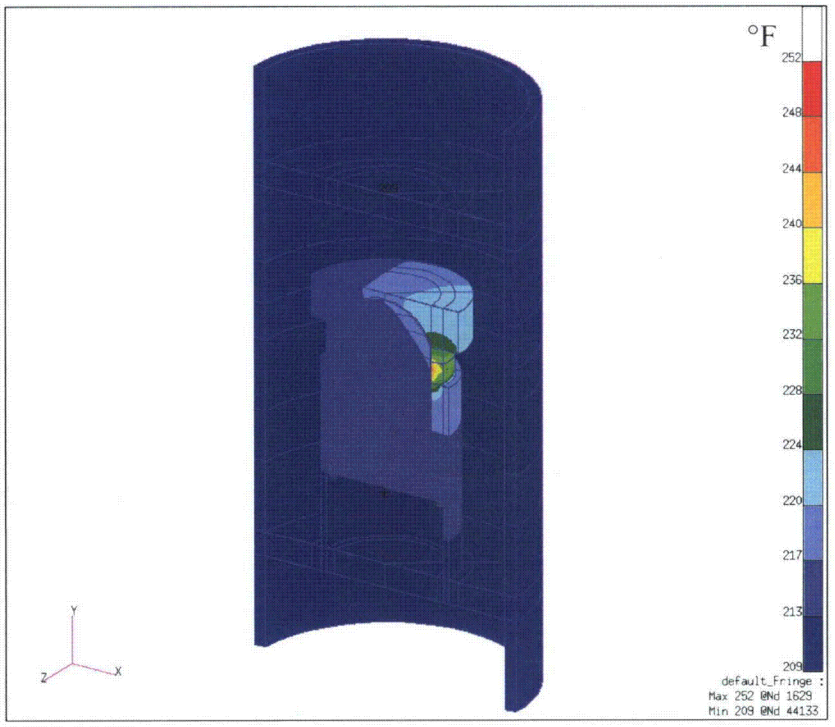

Figure 3-17. Temperature Distribution at the End of the 30-Minute Regulatory Fire — T-Ampoule, TB-1, Heat Transfer Cu Cylinder, and Aluminum Load Spreader (°C=[°F-32]/1.8)

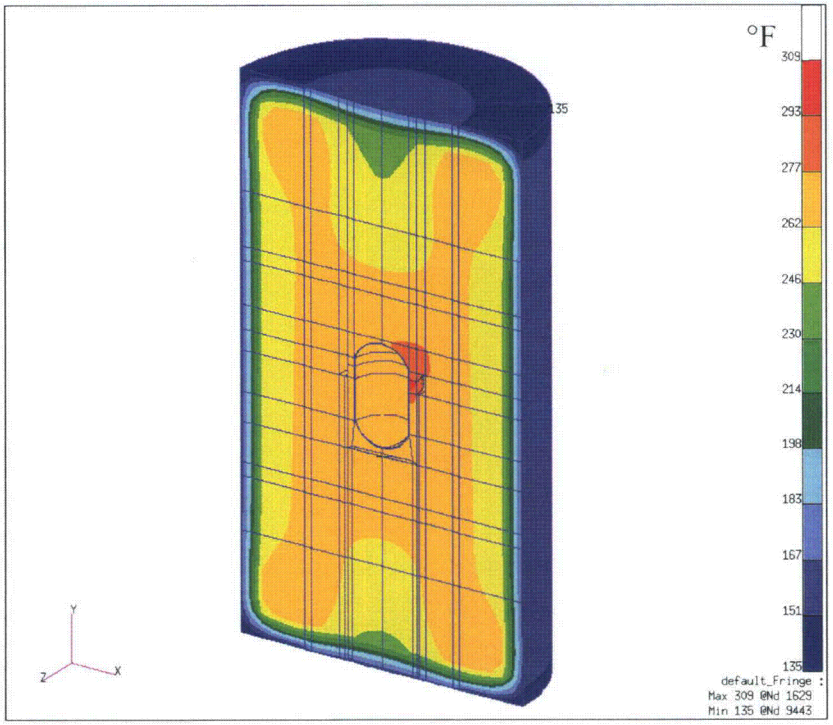

Figure 3-18. Temperature Distribution at t=290 Minutes (260 Minutes after the 30-Minute Fire) — Complete Model (°C=[°F-32]/1.8)

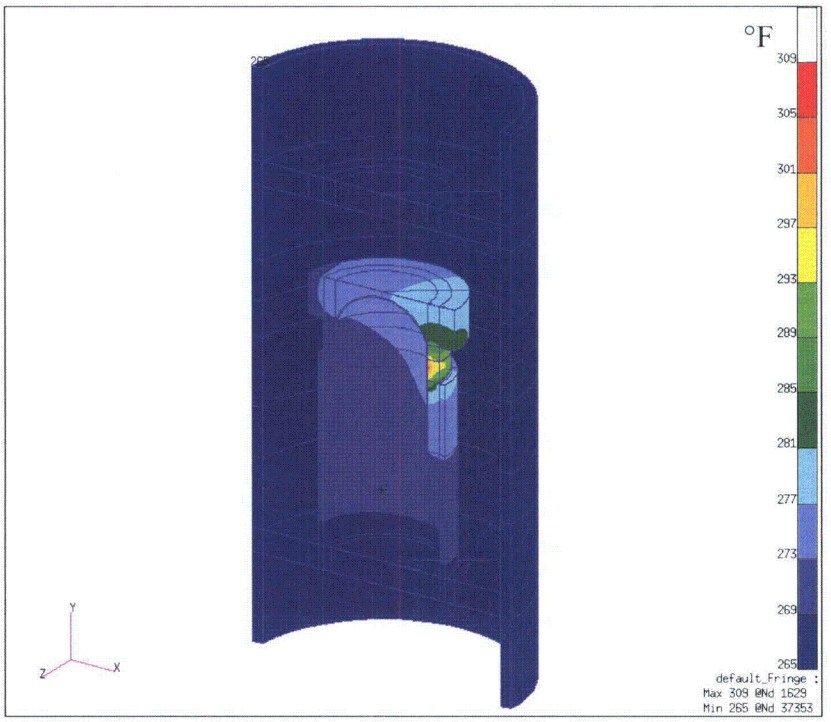

Figure 3-19. Temperature Distribution at t=290 Minutes (260 Minutes after the 30-Minute Fire) — T-Ampoule, TB-1, Heat Transfer Cu Cylinder, and Aluminum Load Spreader (°C=[°F-32]/1.8)

3.4.3 Maximum Temperatures and Pressure

Results from the hypothetical accident conditions evaluation of the AQ–1, TB-1, and the T-Ampoule, assuming the bounding concentrated internal heat described in Section 3.1.2 of this addendum and using the conservative transient computer model described in Section 3.4 of this addendum, are summarized in Table 3-11 of this addendum.

The components listed in this table did not reach temperatures of concern. Only the redwood regions closer to the outer skin of the package are expected to degrade (see Section 3.2.1 of the Addendum). Nevertheless, PAT-1 protects the package contents during and after the exposure to a severe fire environment, as required by 10 CFR 71.73.

The HAC evaluation indicated a peak T-Ampoule seal temperature of 153°C (308°F) and a peak TB-1 (and seal) temperature of 147°C (296°F). This TB-1 seal temperature is 38°C (69°F) higher than that reported as the TB-1 temperature in Section 3.5.1.1 of the PAT-1 SAR[1] and is, once again, considered to be overestimated (or conservative) due to the concentrated heat loading assumption. Nevertheless, this temperature does not exceed the limit temperature of the copper seal. Therefore, the TB-1 is able to maintain containment. In addition, the T-Ampoule is also able to maintain a seal for product quality.

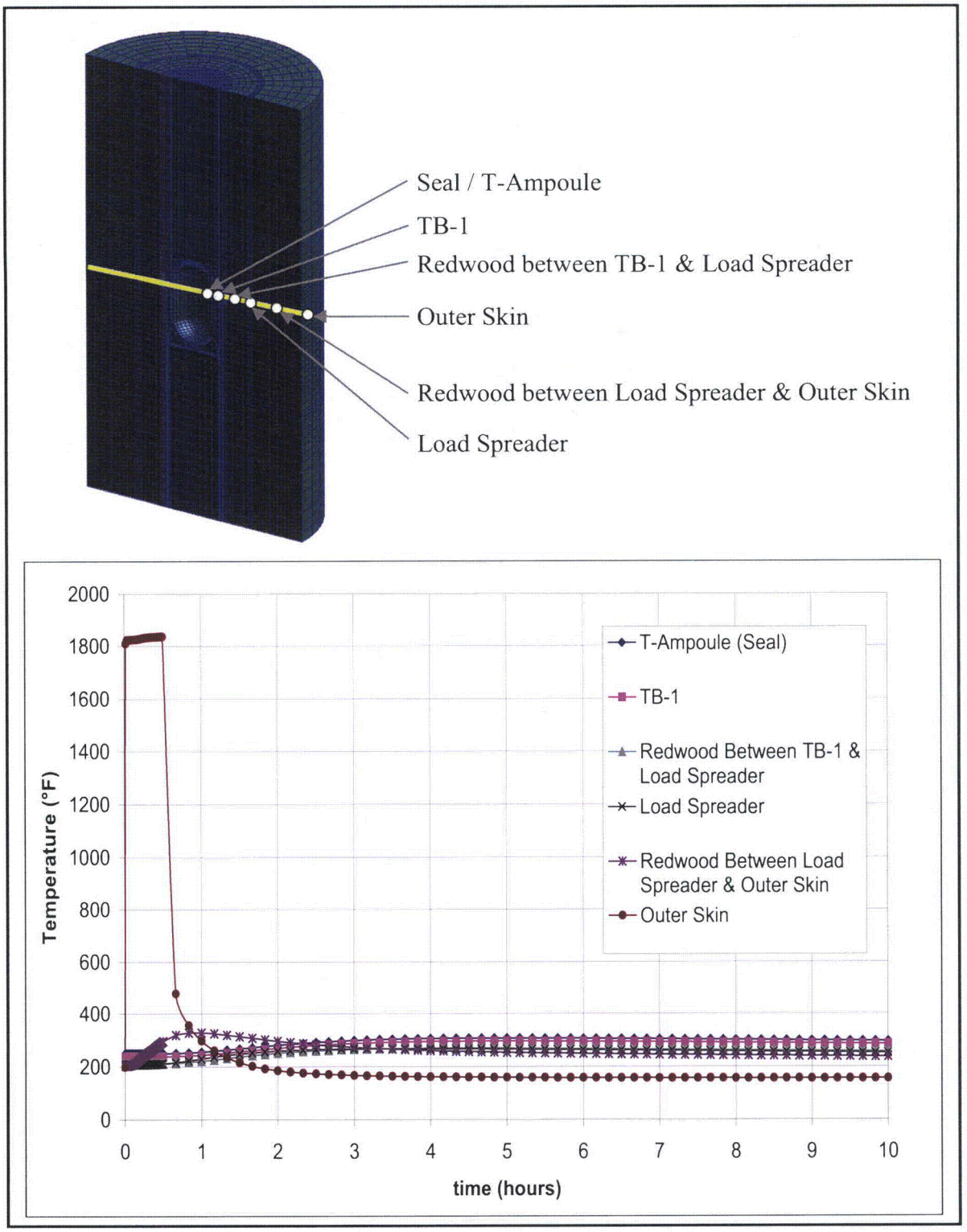

Figure 3-20. Temperature History at T-Ampoule Seal Height for the 30-Minute Regulatory Fire (°C=[°F-32]/1.8). Note: In the schematic above the plot, the reference yellow line crosses the cask at T-Ampoule-seal height and the white dots are the approximate locations of the temperature history lines in the plot.

Table 3-11. Summary of Maximum Temperatures and Times for the HAC

Component	HAC Maximum Temperature and Time to Reach Temperature
T-Ampoule (Seal)	153°C (308°F) @ 260 minutes after the fire
TB-1 (and TB-1 seal)*	147°C (296°F) @ 260 minutes after the 30-minute fire
Center of Redwood between TB-1 and Load Spreader	132°C (270°F) @ 240 minutes after the 30-minute fire
Aluminum Load Spreader	131°C (267°F) @ 190 minutes after the 30-minute fire
Center of Redwood between Load Spreader and Outer Skin	164°C (328°F) @ 30 minutes after the 30-minute fire
Stainless Steel Outer Drum	1003°C (1837°F) @ end of fire

*Maximum seal temperature was conservatively taken as the TB-1 maximum temperature.

The average T-Ampoule internal surface temperature was 136°C (276°F). Assuming the gas inside the TB-1 is at this average temperature, the maximum internal pressure that the TB-1 could experience under HAC can be estimated. When calculating this pressure, it was also assumed that the TB-1 was initially loaded at a room temperature of 21°C (70°F) and in a pressure environment of 1 atmosphere. Additionally, pressure generation due to alpha decay as calculated in Section 4 of this addendum was included in the total pressure calculation. Thus:

$$P_{TB\text{-}1@276°F\text{-}gauge} = (P_{initial} + P_{alpha\_decay})*(T_2/T_1) - 1atm$$

$$= (1\ atm + 0.005\ atm) * (736°R/530°R) - 1atm$$

$$= 0.4\ atm \text{ or } \sim 40\ kPa\ (5.8\ psig) \qquad (3\text{-}10)$$

In summary, these results show that the PAT–1 provides containment for the proposed new payload inside the TB-1 and adequately contains the material inside the T-Ampoule, as maximum seal temperatures are within the service temperature range specified in Table 3-5 and the TB-1 can withstand the pressure that would arise during and after the HAC fire event. Additionally, the eutectic prevention barrier is retained because the T-Ampoule is constructed of titanium 6Al-4V alloy and can withstand the temperatures and pressures observed under the 10 CFR 71[2] HAC, as documented in Section 2 of this addendum.

3.4.4 Maximum Thermal Stresses

The maximum thermal stresses are determined from results of the differential thermal expansion analysis conducted and documented in Section 2.7.4.2 of this addendum. Since the American Society of Mechanical Engineers (ASME) Boiler and Pressure Vessel (B&PV) code does not provide the coefficient of thermal expansion (α) for Ti-6Al-4V, the value listed in the MIL-HDBK-5E[14] (9.18×10^{-6} m/m/°C [5.1×10^{-6} in/in/°F]) was used in this analysis.

A conservative estimate of the T-Ampoule maximum expansion can be calculated by assuming the T-Ampoule is a 0.2 m (7.418 in.) long cylinder (the actual T-Ampoule is capped) with a diameter of 0.11 m (4.22 in). Assuming a temperature increase of (153°C – 21.1°C) = 132°C

([308°F – 70°F] = 238°F), the expansion produced equals $\alpha\Delta TL$, or 0.23 mm (0.009 in.) in the longitudinal direction and 0.41 mm (0.0161 in.) in circumference (or 0.13 mm [0.0051 in.] in diameter). Since the gap between the T-Ampoule and the TB-1 is 0.381 mm (0.015 in.) around the entire perimeter, the T-Ampoule will not expand enough to induce any stress on the TB-1, even if thermal expansion of the TB-1 is ignored.

3.4.5 Hypothetical Accident Conditions for Fissile Material Packages for Air Transport

Thermal tests that meet the specifications in 10 CFR 71.64[2] were conducted on the PAT-1 and are documented in Chapter 3 of the SAR[1]. Physical tests were the primary means used to demonstrate that the PAT-1 package met the requirements of the NRC Qualification Criteria (10 CFR 71.74[2]). The purpose of the assessment documented in Section 3.6 of the SAR[1] was to demonstrate that the maximum TB-1 temperature (reported in Section 3.6.3 of the SAR[1]) used in Section 4.4.2 of the SAR[1] was a reasonable upper limit for bounding the results.

The package temperatures cited in Section 3.6.3 of the SAR[1] stated the following: "Based on the analysis and test results in Sections 3.6.1.1 and 3.6.1.2, the TB-1 is estimated to have attained a maximum temperature of approximately 582°C (1080°F) during the thermal test specified in the NRC Qualification Criteria." This maximum temperature is not affected by any of the packing or content modifications presented in this addendum. That is, the maximum internal heat generation of the content remains the same (25 watts [85.3 Btu/hr]) and the design of the TB-1 and the rest of the packaging outward of the TB-1 is the same as evaluated in the SAR.[1] Therefore, the maximum temperature of the TB-1 used for this addendum, for the calculation of loads due to internal pressure and thermal expansion during the plutonium aircraft fire environment is 582°C (1080°F).

At the maximum temperature of the TB-1 after the plutonium aircraft accident fire, there is a potential for plutonium metal to form eutectics with certain metals such as iron in the TB-1. The materials that were selected for the components within the TB-1 were based on the resistance to eutectic formation with plutonium. The melting temperatures for different material combinations are presented in Section 3.5.3 of this addendum. Given that the melting point of the plutonium-iron eutectic is lower than the maximum TB-1 temperature in the plutonium air transport thermal evaluation, the titanium T-Ampoule is used as a barrier between the plutonium metal and the PH13-8Mo material in the TB-1. The structural analysis documented in Section 2 of this addendum demonstrates that the T-Ampoule wall will not be breached as a result of NCT, HAC, or the accident conditions for air transport of plutonium. Thus, the formation of a Pu-Fe eutectic as a result of the thermal conditions resulting from a 10 CFR 71.74 specified fire is not possible because of the separation between the Pu content and the Fe in the TB-1 provided by the T-Ampoule wall. The service temperatures of all components (T-Ampoule and its packing within the TB-1) shown in Table 3-5 in this addendum, which were derived in part from the eutectic evaluation in Section 3.5.3 in this addendum, are all above 582°C (1080°F).

In addition to the Pu-Fe eutectic potential discussed above, a plutonium-beryllium eutectic may also form. The melting point of this Pu-Be eutectic is 595°C (1103°F) (see Section 3.5.3 in this addendum). This is 13°C (23°F) higher than the highest temperature excursion that occurs in the system.

The maximum internal pressure that may occur within the TB-1 during the air transport thermal evaluation is 7.55 MPa (1095 psig) (see Section 4 and 2.12.8 of this addendum). This was calculated by adding the pressure generated from the decomposition of the O-rings in the SC-1 configuration, which includes the elastomeric seal of the T-Ampoule and three SC-1s (highest amount of elastomeric material), which yielded a pressure of 599.2 psi (from Section 2.12.8 of this addendum), the pressure generated from the decomposition of the ancillary plastic (468 psi from Table 11 in Section 2.12.8), the pressure generated due to the change in temperature of the initial fill gas (42.3 psi), and the pressure from gas generation from alpha decay of plutonium [0.173 psi (from Table 11 in 2.12.8)]. This maximum pressure of 1110 psia is equal to the maximum TB-1 pressure stipulated in the PAT-1 SAR[1] (1095.3 psig, see Section 4.3.1 and 2.12.8 of this addendum). Therefore, the TB-1 is capable of sustaining this maximum pressure observed during the plutonium air transport fire accident condition without rupturing. Note that the T-Ampoule will not retain any pressure because its elastomeric O-ring can extrude out of the O-ring groove and no longer maintain a seal at temperatures above its service temperature of 204°C (400°F).

The thermal expansion calculation in Section 2.8.6 of this addendum demonstrates that no stresses will be induced in the TB-1 by differential thermal expansion resulting from the air transport fire accident.

The analysis in this section demonstrates that the replacement of the PC-1 inner container (with its packing and contents) with the T-Ampoule inner container (with its packing and contents) does not alter the thermal performance of the PAT-1. Therefore, the discussion in Section 3.6 of the SAR[1] regarding the ability of the package to meet the requirements in the plutonium air transport regulations due to thermal loads remains valid. That is, the performance of the PAT-1 with the T-Ampoule (with its packing and contents) inside the TB-1 is bounded by the tests presented in the SAR[1] and therefore the TB-1 maintains containment.

3.5 Appendix

3.5.1 References

1. United States. Nuclear Regulatory Commission. NUREG-0361. "Safety Analysis Report for the Plutonium Air Transportable Package, Model PAT-1." Washington, D.C. 1978.

2. United States. Nuclear Regulatory Commission. Code of Federal Regulations, 10 CFR 64, 71, 73, and 74. January 1, 2009.

3. White, R.H., and E.L. Schaffer. "Application of CMA Program to Wood Charring," *Fire Technology*. Volume 14, Number 4 (1978): 279-290.

4. MSC Patran Thermal 2005 r2. MSC Software Corporation. <www.mscsoftware.com.>

5. Touloukian, Y.S., "Thermophysical Properties of High-Temperature Solid Materials." (1967).

6. Schorsch, R.H., "Engineering Properties of Selected Materials." (1966).

7. Hodge, A.W. and D.J. Maykuth. "Properties of New High-Temperature Titanium Alloys," DMIC Memo 230, Defense Metals Information Center, Battelle Memorial Institute, Columbus Ohio. February 1968.

8. Boivineau, M., C. Cagran, D. Doytier, V. Eyraud, M.-H. Nadal, B. Wilthan, and G. Pottlacher, "Thermophysical Properties of Solid and Liquid Ti-6Al-4V (TA6V) Alloy," International Journal of Thermophysics, Vol. 27, No. 2, March 2006.

9. Mason, R.E. and S.P. Willson, "Eutectic Analysis of Ti-6Al-4V with Plutonium and Copper," LA-UR-08-07663. Los Alamos National Laboratory. Los Alamos, NM. 2008. (Presented in Appendix 3.5.3).

10. Shapiro, A.B. and A.L. Edwards. "TOPAZ2D Heat Transfer Code Users Manual and Property Data Base," UCRL-ID--104558. Lawrence Livermore National Laboratory. Livermore, CA. 1990.

11. Incropera, F.P. and D.P. DeWitt. "Fundamentals of Heat and Mass Transfer, 4th ed.," New Jersey: Wiley & Sons, Inc., 1996.

12. Churchill, S.W. and J. M. Bernstein. *Heat Transfer*. 99, 300. (1977).

13. Nakos, J.T., "Uncertainty Analysis of Steady-State Incident Heat Flux Measurements in Hydrocarbon Fuel Fires," SAND2005-7144. Sandia National Laboratories. Albuquerque, NM. December 2004.

14. Department of Defense. *Military Standardization Handbook: Metallic Materials and Elements for Aerospace Vehicle Structures.* MIL-HDBK-5E: May 1988.

3.5.2 Viton® O-Ring Technical Information

Technical Information

Rev. 6, November 2005

Viton® fluoroelastomer

From DuPont Performance Elastomers

Selection Guide

Introduction

Viton® fluoroelastomer was introduced in 1957 to meet the needs of the aerospace industry for a high-performance seal elastomer. Since then, the use of Viton® fluoroelastomer has expanded to many other industries, especially in the automotive, fluid power, appliance, and chemical fields. With over 40 years of proven performance, Viton® fluoroelastomer has developed a reputation for outstanding performance in high temperature and extremely corrosive environments.

Valuable Properties of Viton® Fluoroelastomer

Vulcanizates based on Viton® provide an exceptional balance of physical property characteristics, including the following features:

- Resistance to temperature extremes:

Heat—Compared to most other elastomers, Viton® is better able to withstands high temperature, while simultaneously retaining its good mechanical properties. Oil and chemical resistance are also essentially unaffected by elevated temperatures. Compounds of Viton® remain substantially elastic substantially indefinitely when exposed to laboratory air oven aging up to 204°C or to intermittent exposures up to 316°C. High temperature service limits are generally considered to be:

3,000 hr at 232°C
1,000 hr at 260°C
240 hr at 288°C
48 hr at 316°C

Cold—Viton® is generally serviceable in dynamic applications to temperatures of –18 to –23°C. Special formulations permit its use in static applications down to –54°C. Also, Viton® has proven to be satisfactory for static seals used under conditions approaching absolute zero. Viton® is characterized by its;

- Resistance to degradation by a greater variety of fluids and chemicals than any nonfluorinated elastomer. Excellent resistance to oils, fuels, lubricants, and most mineral acids.
- Extremely low permeability to a broad range of substances, including particularly good performance in oxygenated automotive fuels.
- Resistance to aliphatic, aromatic hydrocarbons that dissolve other rubbers.
- Exceptionally good resistance to compression set, even at high temperatures.
- Exceptionally good resistance to atmospheric oxidation, sun, and weather. Excellent resistance to fungus and mold.
- Good electrical properties in low voltage, low frequency applications.
- Low burning characteristics; inherently more resistant to burning than other, non-fluorinated hydrocarbon rubbers.

Safety and Handling

As with many polymers, minute quantities of potentially irritating or harmful gases may diffuse from uncured Viton® even at room temperature. Therefore, all containers should be opened and used only in well-ventilated areas. In case of eye contact, immediately flush the eyes for at least 15 min with water. Always wash contacted skin with soap and water after handling Viton®.

Potential hazards, including the evolution of toxic vapors, may arise during compounding, processing, and curing of the raw polymers into finished products or under high-temperature service conditions. Therefore, before handling or processing Viton®, make sure that you read and follow the recommendations in the DuPont Performance Elastomers bulletin "Handling Precautions for Viton® and Related Chemicals."

Compounding ingredients and solvents that are used with Viton® to prepare finished products may present hazards in handling and use. Before proceeding with any compounding or processing work, consult and follow label directions and handling precautions from suppliers of all ingredients.

The Various Families and Types of Viton® Fluoroelastomer

Standard types of Viton® fluoroelastomer products are designated as A, B, or F according to their relative resistance to attack by fluids and chemicals. The differences in fluid resistance are the result of different levels of fluorine in the polymer, which is determined by the types and relative amounts of copolymerized monomers that comprise the polymer.

In general, Viton® exhibits outstanding resistance to attack from a wide variety of fluids, including mineral acids and aliphatic and aromatic hydrocarbons. The higher the fluorine content of the polymer, the less will be the effect, as measured by volume increase, for example. The most significant differences between A, B and F types of Viton®, in terms of resistance to volume change or retention of physical properties, are exhibited in low molecular weight, oxygenated solvents (such as methanol and methyl t-butyl ether).

As mentioned above, the fluid resistance of Viton® A, B, and F types improves with increasing fluorine levels. This is shown in Table 1 (note the volume increase after aging in methanol at 23°C). As the fluorine content increases, however, the low temperature flexibility of the polymer decreases, and a compromise must be made between fluid resistance and low temperature flexibility of the final vulcanizate.

For those applications that require the best performance in both fluid resistance and low temperature flexibility a number of specialty types of Viton® were developed that contain a copolymerized fluorinated vinyl ether monomer. Polymers that contain this monomer exhibit significantly improved low temperature flexibility, compared to standard types of fluoroelastomer.

Viton® GLT introduced in 1976, was the first commercial fluoroelastomer to incorporate this fluorinated vinyl ether monomer. This polymer provides the same excellent resistance to heat and fluids that is typical of the A types of Viton® fluoroelastomer. Viton® GFLT, like Viton® GLT, exhibits significantly improved low temperature flex characteristics compared to standard types of fluoroelastomer. In addition, Viton® GFLT provides the same superior resistance to fluids that is typical of the F types of Viton® fluoroelastomer.

Types of Viton® Extreme™

Fluoroelastomers that contain copolymerized vinylidene fluoride(VF2) are subject to attack by high pH materials, including caustics and amines. In addition, standard fluoroelastomers are not resistant to low molecular weight carbonyl compounds, such as methyl ethyl ketone, acetone, or methyl tertiarybutyl ether.

Viton® Extreme™ ETP-600S is a copolymer of ethylene, tetrafluoroethylene (TFE), and perfluoromethylvinyl ether (PMVE). This unique combination of monomers provides outstanding resistance to fluids and is an example of an ETP polymer. The ETP types of Viton® exhibit the same excellent resistance to acids and hydrocarbons typical of A, B and F types of Viton®. Unlike conventional fluoroelastomers, however, ETP types of Viton® also provide excellent resistance to low molecular weight esters, ketones, and aldehydes. In addition, these unique polymers are inherently resistant to attack by base, and thus provide excellent resistance to volume swell and property loss in highly caustic solutions and amines.

Additional information regarding performance differences between the various families and types of Viton® fluoroelastomer is presented in Tables 3–6 to assist in selecting the particular grade of

Viton® that is best suited for both a given end-use application and for a specific manufacturing process.

Table 1
Polymer Fluorine Content versus Fluid Resistance and Low Temperature Flexibility

	Standard Types			Specialty Types		
	A	B	F	GLT-S	GFLT-S	ETP-S
Nominal Polymer Fluorine Content, wt%	66	68	70	64	67	67
Percent Volume Change in Fuel C, 168 hr at 23°C*	4	3	2	5	2	4
Percent Volume Change in Methanol, 168 hr at 23°C*	90	40	5	90	5	5
Percent Volume Change in Methyl ethyl Ketone, 168 hr at 23°C*	>200	>200	>200	>200	>200	19
Percent Volume Change in 30% Potassium Hydroxide, 168 hr at 70°C*	(Samples too swollen and degraded to test)					14
Low Temperature Flexibility, TR-10, °C*	-17	-13	-6	-30	-24	-12

*Nominal values, based on results typical of those obtained from testing a standard, 30 phr MT (N990) carbon black-filled, 75 durometer vulcanizate. These are not intended to serve as specifications.

Curing Systems for Viton® Fluoroelastomer

In addition to inherent differences between the various types and families of Viton® fluoroelastomer, a number of compounding variables have major effects on the physical property characteristics of the final vulcanizates. One very important variable is the crosslinking or curing system that is used to vulcanize the elastomer.

Diamine curatives were introduced in 1957 for crosslinking Viton® A. While these diamine curatives are relatively slow curing, and do not provide the best possible resistance to compression set, they do offer unique advantages. For example, compounds cured with diamines exhibit excellent adhesion to metal inserts and high hot tensile strength.

Most fluoroelastomers are crosslinked with Bisphenol AF, a curative introduced in 1970, in the first commercial curative-containing precompound, Viton® E-60C. Compounds of Viton® that use this curative exhibit fast rates of cure and excellent scorch safety and resistance to compression set.

In 1987, an improved bisphenol curative was introduced, which was made available in several different precompounds. The modified system provides faster cure rates, improved mold release, and slightly better resistance to compression set, compared to the original bisphenol cure system used in Viton® E-60C and E-430. Additional precompounds of Viton®, incorporating this modified curative, were introduced in 1993, including Viton® A-331C, A-361C, B-601C, and B-651C. A brief description of all these products can be found in Table 6.

In 1976, efficient peroxide curing of fluoroelastomers was made possible for the first time with the introduction of Viton® GLT. The peroxide cure system provides fast cure rates and excellent physical properties in polymers such as GLT and GFLT which cannot be readily cured with either diamine or bisphenol crosslinking systems. In the case of polymers such as Viton® GF, GBL-200, and GBL-900, the peroxide cure provides enhanced resistance to aggressive automotive lubricating oils and steam and acids. Generally, vulcanizates of Viton® fluoroelastomers cured with peroxide do not show any significant difference in resistance to other fluids and chemicals compared to the same polymer cured with bisphenol.

In 2003, a series of peroxide-cure types of Viton® made with Advanced Polymer Architecture was introduced. These polymers, designated as APA polymers by having an "S" suffix on the product name, incorporate a significantly improved cure site. As a result, they provide substantially better processing and physical properties, compared to the original, non-APA peroxide-cure types of Viton®. A comparison of the various processing and physical property characteristics of compounds using the various cure systems is shown in Table 2.

4

Table 2
A Comparison of Cure Systems Used in Crosslinking Viton®

Property, Processing Characteristic	Type of Cure System		
	Diamine	Bisphenol	Peroxide*
Processing Safety (Scorch)	P-F	E	E
Fast Cure Rate	P-F	E	E
Mold Release/Mold Fouling	P	G-E	G-E
Adhesion to Metal Inserts	E	G	G
Compression Set Resistance	P	E	E
Steam, Water, Acid Resistance	F	G	E
Flex Fatigue Resistance	G	G	G

Rating: E=Excellent G=Good F=Fair P=Poor
*Luperco 101-XL (trademark of Pennwalt Corporation) and Varox Powder (trademark of R.T. Vanderbilt Co., Inc.) are commonly used.

Selecting a Specific Type of Viton® Fluoroelastomer
Inherent Physical Property Differences Between Types/Families of Viton® Products

The physical properties of vulcanizates based on Viton® fluoroelastomers are determined to a large extent by the type and amount of the filler(s) and curative(s) used in the formulation, and by the temperature and duration of the curing cycle used in their manufacture.

In terms of resistance to compression set, low temperature flexibility, and resistance to certain classes of fluids, however, some inherent differences exist among the various families of Viton® fluoroelastomers. These are the result of differences in the relative amount and type of monomers used in the manufacture of the various types of Viton® fluoroelastomers.

The differences in physical property characteristics which exist between various types and families of Viton® fluoroelastomer products are outlined in general terms in Table 3.

As an example, resistance to compression set is an important property for seals and if this property were considered to be the most important feature for a particular part, then one of the A-types of Viton® might be the best choice for the application. However, if resistance to the widest possible range of fluids is a more important consideration then an F-type Viton® fluoroelastomer might well be a better choice for that particular end-use application. Further, if both fluid resistance and low temperature flexibility are equally important requirements for maximizing the end-use suitability of a given part GFLT-types of Viton® would represent the best overall choice.

Table 3
Physical Property Differences Between Types/Families of Viton® Products

Type of Viton® Fluoroelastomer	Resistance to Compression Set	General Fluids/ Chemical Resistance*	Low Temperature Flexibility**
A	1	3	3
B, GBL-S	2	3	3
F, GF-S	3	2	3
GLT-S	2	3	1
GFLT-S	2	2	2
ETP-S	3	1	3

1=Excellent—Best performance capability of all types; 2=Very Good; 3=Good—Sufficient for all typical fluoroelastomer applications
*See *Table 4* for a detailed guide to choosing the best type of Viton® fluoroelastomer, relative to specific classes of fluids and chemicals.
**Flexibility, as measured by Temperature of Retraction (TR-10), Gehman Torsional Modulus, Glass Transition (Tg), or Clash-Berg Temperature. Brittle-Point tests are a measure of impact resistance only and do not correlate at all with the low temperature sealing capability of a vulcanizate.

Selecting a Specific Type of Viton® Fluoroelastomer
Differences in Fluid Resistance Between Types of Viton® Products

As in the case of physical properties, different polymer compositions will result in inherent differences with regard to fluid resistance.

Table 4 outlines the differences that exist between types of Viton® products, in terms of their resistance to various classes of fluids and chemicals.

Because as certain types of Viton® products may exhibit performance that is superior to other types in one regard, but not quite as good in some other aspect, it is important to consider the requirements of the part to be manufactured, in terms of both physical property requirements and fluid or chemical resistance needs.

Using Tables 3 and 4, the compounder can select the best type of Viton® product for a given end-use application, based on the best combination of physical property and fluid resistance characteristics.

Table 4
Differences in Fluid Resistance Between Types of Viton® Fluoroelastomer

	Type of Viton® Fluoroelastomer							
	A	B	F	GBL-S	GF-S	GLT-S	GFLT-S	ETP-S
	Cure System							
	Bisphenol			Peroxide				
Hydrocarbon Automotive, Aviation Fuels	1	1	1	1	1	1	1	1
Oxygenated Automotive Fuels (containing MeOH, EtOH, MTBE, etc.)	NR	2	1	2	1	NR	1	1
Reciprocating Engine Lubricating Oils (SE-SF Grades)	2	1	1	1	1	1	1	1
Reciprocating Engine Lubricating Oils (SG-SH Grades)	3	2	2	1	1	1	1	1
Aliphatic Hydrocarbon Process Fluids, Chemicals	1	1	1	1	1	2	1	1
Aromatic Hydrocarbon Process Fluids, Chemicals	2	2	1	1	1	2	1	1
Aqueous Fluids: Water, Steam, Mineral Acids (H_2SO_4, HNO_3, HCl, etc.)	3	2	2	1	1	1	1	1
Amines, High pH Caustics (KOH, NaOH, etc.)	NR	NR	NR	3	3	3	3	1
Low Molecular Weight Carbonyls (MTBE, MEK, MIBK, etc.)	NR	NR	NR	NR	NR	NR	NR	1

1=Excellent—Best choice of Viton® type(s) for service in this class of fluid/chemical; minimal volume increase, change in physical properties.
2=Very Good—Good serviceability in this class of fluid/chemical; small amounts of volume increase and/or changes in physical properties.
3=Good—Suitable for use in this class of fluid/chemical; acceptable amounts of volume increase and/or changes in physical properties.
NR=Not Recommended—Excessive volume increase or change in physical properties.

6

Viton® Product Naming System

With the introduction of six improved processing precompounds in 1993, a new nomenclature system was adopted for Viton® fluoroelastomer products. The new system incorporates the following information in a product name:

- Nominal Mooney Viscosity
- Family type (relative fluid resistance)
- Relative state of cure (relative level of crosslinking agent present in curative-containing precompounds)
- An indication of whether the product can be crosslinked using a peroxide cure system
- An indication of whether the product is a gum polymer or a precompound, which contains a preset, carefully controlled amount of bisphenol crosslinking system.

Each character in the product name indicates a specific characteristic as outlined below:

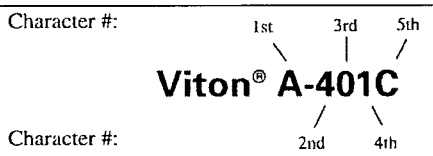

1st Character (Letter)

- Represents the Viton® fluoroelastomer family--A, B, F, or ETP.
- A "G" prefix, in addition to a family prefix, indicates that the polymer can be crosslinked with the peroxide cure system.
- An "L" designation indicates that the A, B, or F type polymer provides slightly improved low temperature flexibility characteristics versus other polymers within the same family. An "LT" designation indicates a more significant improvement in low temperature performance criteria.

2nd Character (Number)

Represents nominal Mooney Viscosity of the product—ML 1 + 10 at 121°C.

3rd Character (Number)

Represents the relative level of curative in a precompound on a scale of 10 ⟶ 1 (10 is represented by 0);

0 = High curative level (for optimum compression set)

9⟶2 = Intermediate, decreasing levels of curative (increased elongation at break, tear resistance)

1 = Low curative level (for optimum tear, flex resistance)

4th Character (Number)

Represents a slightly different version of a particular precompound.

5th Character (Letter)

- Absence of a letter suffix indicates that the product is a gum polymer only and contains no curatives (*may contain process aid*).
- "C" indicates that the product is a precompound, containing accelerator and curative.
- "S" indicates that the product incorporates Viton® made with Advanced Polymer Architecture technology

Choosing a Viton® Product for Use in a Particular Type of Manufacturing Process

The Viton® product line includes a wide variety of different types of fluoroelastomer products, which exhibit some inherent differences in their end-use capabilities (see Tables 3 and 4). In addition, a broad range of viscosities is offered for most types of Viton®, providing a wide degree of utility in various manufacturing processes.

Having selected a given class of Viton® products for an end use, the compounder must then choose which particular Viton® product is best suited for use in a specific manufacturing process.

The Viton® - Application Guide (Table 5) lists the Viton® products that are recommended for particular end-use applications, according to the various processes that are most commonly used in their manufacture.

The Viton® - Product Listing (Table 6) provides more specific information about the various individual Viton® products. Contact your DuPont Performance Elastomers sales or technical representative to obtain more detailed information or data on specific Viton® products.

How to Use the Viton® Application Guide

The Viton® - Application Guide (Table 5) has been designed to facilitate choice of the type of Viton® that is best suited for meeting both the property requirements of the intended end use and the needs of the production method used to manufacture the finished product.

The guide is divided into five general categories (columns) of end-use products, differentiated primarily by physical form:

- Sheet form goods, such as gaskets, diaphragms, etc.
- Simple shapes, such as O-rings, V-rings, etc., which do not typically require high levels of demolding tear resistance, but which generally require high states of cure to obtain the best compression set possible.
- Complicated molded shapes, such as shaft seals or valve stem seals, which require good hot tear upon demolding do to the undercuts in the molds used to form such parts and good adhesion to metal inserts (obtained during the vulcanization of the parts).
- Complicated molded shapes that do not involve adhesion to metal inserts during vulcanization, but which require good resistance to tear during demolding. Carburetor roll-over cages, boots, and reed valves are examples of such parts.
- Extruded shapes, such as rod, tubing, or hose constructions.

Each general end-use category listed is divided into four columns, each listing Viton® products within a specific family or type of Viton® fluoroelastomer—A, B, F, and specialty types.

The guide is further divided into the five major types of process (rows) by which these general end-use categories might be produced:

- Compression molding
- Transfer molding
- Injection molding
- Extrusion
- Calendering

Within the blocks formed by the "intersection" of a given end-use category (column) and the process type by which the end products will be manufactured (row), we have listed the types of Viton® that we believe are appropriate choices for meeting the physical property requirements of the finished product and that are best suited for the chosen manufacturing process.

The Viton® products we believe will provide the best combination of end-use physical properties, together with the best processing characteristics for given methods of manufacture, are listed in bold type.

Additional details for specific types of Viton® can be found in the Viton® Product Listing and in product-specific data sheets.

8

Table 5
Viton® Fluoroelastomer Application Guide

Manufacturing Process	Reinforced/Unreinforced Sheet Stock (Gaskets, Diaphragms, etc.)				Molded (Non-Bonded), Simple Shapes (O-Rings, V-Rings, etc.)			
	Viton® Types							
	A	B	F	Specialty	A	B	F	Specialty
Compression Molding	A-331C A-361C A-401C A-601C A-500 A-700 AL-600	B-435C B-601C B-651C GBL-600S B-600	F-605C GF-600S	GLT-600S GBLT-600S GFLT-600S ETP-600S	A-401C A-331C A-601C A-500 A-HV A-700 AL-600	B-601C B-651C GBL-600S B-600	F-605C GF-600S	GLT-600S GBLT-600S GFLT-600S ETP-600S
Transfer Molding	A-201C A-331C A-361C A-401C A-200 AL-300	B-435C GBL-200S B-202	F-605C GF-200S	GLT-200S GBLT-200S GFLT-200S ETP-600S	A-201C A-331C A-361C A-200 AL-300	B-651C GBL-200S B-202	F-605C GF-200S	GLT-200S GBLT-200S GFLT-200S ETP-600S
Injection Molding	A-201C A-331C A-361C A-200 AL-300	B-435C GBL-200S B-202	GF-200S	GLT-200S GBLT-200S GFLT-200S	A-201C A-331C A-361C A-100 A-200 A-500 AL-300	B-601C B-651C GBL-200S B-202	F-605C GF-200S	GLT-200S GBLT-200S GFLT-200S ETP-600S
Calendering	A-201C A-401C A-331C A-361C AL-300	B-435C B-601C B-651C GBL-200S GBL-600S B-202 B-600	F-605C GF-200S GF-600S	GLT-200S GLT-600S GBLT-200S GBLT-600S GFLT-200S GFLT-600S ETP-600S				
	Molded (Bonded), Complicated Shapes (Valve Stem, Shaft Seals, etc.)				Molded (Non-Bonded), Complicated Shapes (Boots, Valves, etc.)			
Compression Molding	A-361C A-500 A-700 AHV AL-600	B-435C B-651C GBL-600S B-600	F-605C/GF-200S GF-200S GF-600S	GLT-200S GLT-600S GBLT-200S GBLT-600S GFLT-200S GFLT-600S ETP-600S	A-331C A-401C/A-500 A-601C/A-200 A-361C A-700 AHV AL-600	B-435C B-651C GBL-600S B-600	F-605C/GF-600S GF-600S	GLT-600S GBLT-600S GFLT-600S ETP-600S
Transfer Molding	A-361C A-200 A-500 AL-300	B-435C GBL-200S B-202	GF-200S	GLT-200S GBLT-200S GFLT-200S ETP-600S	A-200 A-331C A-361C A-200 A-500 AL-300	B-435C B-651C GBL-200S B-600	F-605C/ GF-200S GF-300	GLT-200S GBLT-200S GFLT-200S ETP-600S
Injection Molding	A-361C A-100 A-200 A-500 AL-300	B-435C B-651C GBL-200S B-202	F-605C/ GF-200S GF-200S	GLT-200S GBLT-200S GFLT-200S	A-200 A-331C A-361C A-200 A-500 AL-300	B-435C B-651C GBL-200S B-202	F-605C/ GF-200S GF-200S	GLT-200S GBLT-200S GFLT-200S

9

Table 5
Viton® Fluoroelastomer Application Guide *(cont'd.)*

Manufacturing Process	Extruded Goods (Hose, Tubing, Extruded Profiles, etc.)			
	Viton® Types			
	A	B	F	Specialty
Extrusion	A-201C A-401C A-361C A-200 A-500 AL-300	B-435C B-651C GBL-200S B-202 B-600	F-605C GF-200S	GLT-200S GBLT-200S GFLT-200S ETP-600S

Table 6
Viton® Fluoroelastomer Product Listing

	Polymer Properties			Nominal Physical Properties*				
Viton® Product Type	Nominal Viscosity, ML1 + 10 at 121°C	Specific Gravity	Polymer Fluorine Content, %	Compression Set, % 70 hr/200°C	Temperature of Retraction (TR-10) °C	Volume Increase, After 7 days/ MeOH/23°C	Viton® Fluoroelastomer Product Description	Viton® Fluoroelastomer Product Suggested Uses/ Applications
A-Types: Curative-Containing Precompounds								
A-201C	20	1.81	66.0	15	-17	+75 to 105%	Fast cure rate, excellent injection molding rheology, mold release	FDA-compliant**; injection molding, O-rings, gaskets, extruded shapes
A-331C	30	1.81	66.0	20	-17	+75 to 105%	Excellent mold flow, high elongation/tear resistance	Compression—injection molding of complex shapes, requiring maximum hot tear
A-361C	30	1.81	66.0	20	-17	+75 to 105%	Excellent mold flow, tear resistance, bonding to metal inserts	Compression—injection molding of complex shapes, bonded metal inserts
A-401C	40	1.81	66.0	15	-17	+75 to 105%	Excellent rheology at high shear rates, excellent resistance to compression set	FDA-compliant**; compression, transfer, or injection molding of O-rings
A-601C	60	1.81	66.0	12	-17	+75 to 105%	High viscosity, high state of cure; optimum resistance to compression set	FDA-compliant**; compression molding of O-rings, simple shapes

*Nominal physical properties typical of those that can be expected of vulcanizates based on the specific type of Viton® noted, in a 70A hardness, MT carbon black-filled formulation. These are not intended to serve as specifications.
**Curative-containing precompounds, and polymers + VC-50 (at levels less than or equal to 2.50 phr rubber) have been determined to be in compliance with FDA 21 CFR-177.2600—Rubber Articles for Repeated Food Contact.

10

Table 6
Viton® Fluoroelastomer Product Listing *(cont'd.)*

	Polymer Properties			Nominal Physical Properties*				
Viton® Product Type	Nominal Viscosity, ML1 + 10 at 121°C	Specific Gravity	Polymer Fluorine Content, %	Compression Set, % 70 hr/200°C	Temperature of Retraction (TR-10) °C	Volume Increase, After 7 days/ MeOH/23°C	Viton® Fluoroelastomer Product Description	Viton® Fluoroelastomer Product Suggested Uses/ Applications
A-Types: Gum Polymers								
A-100	10	1.82	66.0	15	-17	+75 to 105%	Ultra-low viscosity: excellent polymer rheology	Coatings, viscosity modifier for higher viscosity types
A-200	20	1.82	66.0	15	-17	+75 to 105%	Low viscosity: excellent polymer rheology	FDA-compliant**, cured w. VC-50: injection molding applications
A-500	50	1.82	66.0	15	-17	+75 to 105%	Intermediate viscosity: excellent polymer rheology	FDA-compliant**, cured w. VC-50: compression, transfer, injection molding
A-700	70	1.82	66.0	15	-17	+75 to 105%	High viscosity: excellent physical properties	FDA-compliant**, cured w. VC-50: compression, transfer, injection molding
A-HV	160	1.82	66.0	15	-17	+75 to 105%	Ultra-high viscosity: excellent physical properties	FDA-compliant**, cured w. VC-50: compression molding, high strength vulcanizates
AL-300	30	1.77	66.0	25	-19	+75 to 105%	Slightly improved low temperature flexibility. Low viscosity	Transfer, or injection molded goods, where A-types are marginal in low-temperature flexibility
AL-600	60	1.77	66.0	20	-19	+75 to 105%	Slightly improved low temperature flexibility. Medium viscosity	General molded goods, where A-types are marginal in low-temperature flexibility

*Nominal physical properties typical of those that can be expected of vulcanizates based on the specific type of Viton® noted, in a 70A hardness, MT carbon black-filled formulation. These are not intended to serve as specifications.
**Various types of Viton® curative-containing precompounds have been determined to be in compliance with FDA 21 CFR-177.2600—Rubber Articles for Repeated Food Contact.

11

Table 6
Viton® Fluoroelastomer Product Listing *(cont'd.)*

	Polymer Properties			Nominal Physical Properties*				
Viton® Product Type	Nominal Viscosity, ML1 + 10 at 121°C	Specific Gravity	Polymer Fluorine Content, %	Compression Set, % 70 hr/200°C	Temperature of Retraction (TR-10) °C	Volume Increase, After 7 days/ MeOH/23°C	Viton® Fluoroelastomer Product Description	Viton® Fluoroelastomer Product Suggested Uses/ Applications
B-Types: Curative-Containing Precompounds								
B-435C	40	1.85	68.5	25	-14	+35 to 45%	Improved processing/mold release/bonding vs. B-641C, B-651C	Injection—compression molding of metal-bonded parts
B-601C	60	1.85	68.5	20	-14	+35 to 45%	Excellent balance of resistance to compression set/fluids	FDA-compliant**: compression – injection molding of O-rings, simple shapes
B-651C	60	1.85	68.5	30	-14	+35 to 45%	Excellent mold flow, very good tear resistance, bonding to metal inserts	Compression – injection molding of complex shapes, bonded metal inserts
B-Types: Gum Polymers								
GBL-200S	20-30	1.85	67.0	30	-16	+40 to 50%	Excellent resistance to automotive lubricating oils, aqueous fluids	FDA Compliant** Transfer – compression molding auto lubricating oil, coolant system seals
GBL-600S	65	1.85	67.0	30	-16	+40 to 50%	Excellent resistance to automotive lubricating oils, aqueous fluids	FDA Compliant** Compression molding automotive lubricating oil, coolant system seals
B-202	20	1.86	68.5	25	-14	+35 to 45%	Excellent extrudability; lower MeOH permeability than A-types	FDA-compliant**: high shear extrusion applications—fuel hose veneer, coatings
B-600	60	1.86	68.5	20	-14	+35 to 45%	Intermediate viscosity, excellent polymer rheology, superior fluids resistance	FDA-compliant**: compression, transfer, and injection molding

*Nominal physical properties typical of those that can be expected of vulcanizates based on the specific type of Viton® noted, in a 70A hardness, MT carbon black-filled formulation. These are not intended to serve as specifications.
**Various types of Viton® curative-containing precompounds have been determined to be in compliance with FDA 21 CFR-177.2600—Rubber Articles for Repeated Food Contact.

Table 6
Viton® Fluoroelastomer Product Listing *(cont'd.)*

	Polymer Properties			Nominal Physical Properties*				
Viton® Product Type	Nominal Viscosity, ML1 + 10 at 121°C	Specific Gravity	Polymer Fluorine Content, %	Compression Set, % 70 hr/200°C	Temperature of Retraction (TR-10) °C	Volume Increase, After 7 days/ MeOH/23°C	Viton® Fluoroelastomer Product Description	Viton® Fluoroelastomer Product Suggested Uses/ Applications
F-Types: Curative-Containing Precompounds								
F-605C	60	1.90	69.5	30	-8	+5 to 10%	Improved *polymer base* vs. F-601C—improved rheology, compression set	FDA-compliant**: compression molded goods requiring best fluids resistance
F-Types: Gum Polymers								
GF-200S	25-30	1.91	70.0	35	-6	+3 to 5%	Low viscosity version of GF-600S	FDA-compliant**: Injection transfer, or compression molded goods requiring best fluids resistance
GF-600S	65	1.91	70.0	35	-6	+3 to 5%	Superior resistance to broad range of fluids and chemicals, including MeOH	FDA-compliant**: Compression molded goods requiring best fluids resistance
Low-Temperature Types of Viton® Polymer								
GLT Types								
GLT-200S	25-30	1.78	64.0	30	-30	+75 to 105%	20-30 Mooney GLT: best FKM low-temperature flexibility	FDA Compliant** Injection – transfer molded automotive fuel, chemical, petroleum industry seals
GLT-600s	65	1.78	64.0	35	-30	+75 to 105%	Medium viscosity version of GLT	FDA Compliant** Transfer – compression molded automotive fuel, chemical, petroleum industry seals
GBLT Types								
GBLT-200S	25-30	1.80	65.0	40	-26	+65 to 90%	Low-temperature flexibility/fluid resistance intermediate between GLT/GFLT types	Fuel systems parts: resistance to low oxygenates, low-temperature flexibility
GBLT-600S	65	1.80	65.0	35	-26	+65 to 90%	Low-temperature flexibility/fluid resistance intermediate between GLT/GFLT types	Fuel systems parts: resistance to low oxygenates, low-temperature flexibility

*Nominal physical properties typical of those that can be expected of vulcanizates based on the specific type of Viton® noted, in a 70A hardness, MT carbon black-filled formulation. These are not intended to serve as specifications.

**Various types of Viton® curative-containing precompounds have been determined to be in compliance with FDA 21 CFR-177.2600—Rubber Articles for Repeated Food Contact.

13

Table 6
Viton® Fluoroelastomer Product Listing *(cont'd.)*

	Polymer Properties			Nominal Physical Properties*				
Viton® Product Type	Nominal Viscosity, ML1 + 10 at 121°C	Specific Gravity	Polymer Fluorine Content, %	Compression Set, % 70 hr/200°C	Temperature of Retraction (TR-10) °C	Volume Increase, After 7 days/ MeOH/23°C	Viton® Fluoroelastomer Product Description	Viton® Fluoroelastomer Product Suggested Uses/ Applications
GFLT Types								
GFLT-200S	25-30	1.86	66.5	35	-24	+5 to 10%	30 ML GFLT; best combination of low-temperature flexibility/fluids resistance	Bonded fuel systems parts: resistance to oxygenates, low-temperature flexibility
GFLT-600S	65	1.86	66.5	40	-24	+5 to 10%	65 ML GFLT; best combination of low-temperature flexibility/fluids resistance	Bonded fuel systems parts: resistance to oxygenates, low-temperature flexibility
Viton® Extreme™ Types								
ETP-600S	60	1.82	67.0	40	-12	+10 to 15%	Outstanding resistance to fluids/chemicals, including low molecular weight acids, aldehydes, ketones	FDA-compliant**: Transfer – compression molded seals, gaskets

*Nominal physical properties typical of those that can be expected of vulcanizates based on the specific type of Viton® noted, in a 70A hardness, MT carbon black-filled formulation. These are not intended to serve as specifications.

**Various types of Viton® curative-containing precompounds have been determined to be in compliance with FDA 21 CFR-177.2600—Rubber Articles for Repeated Food Contact.

14

Applications

Automotive

Parts produced from Viton® fluoroelastomer are widely used in the automotive industry because of their outstanding heat and fluid resistance. They are used in the following areas:

Powertrain Systems

- Crankshaft seals, Valve stem seals, Transmission seals
- Air Intake Manifold gaskets

Fuel Systems

- Veneered fuel hose
- In-tank fuel hose and tubing
- Pump seals, Diaphragms and Injector O-rings
- Accelerator pump cups
- Filter caps and filter seals
- Fuel sender seals, Carburetor needle tips

Appliances

The heat and fluid resistance of Viton® fluoroelastomer, coupled with its good mechanical strength, makes it a natural choice for many appliance parts. The use of seals and gaskets of Viton® has resulted in design of appliances in challenging environments. Here are some typical success stories:

- In one commercial automatic dry cleaning machine, no less than 107 components are made of Viton®: door seals, sleeve-type duct couplings, shaft seals, O-rings, and various static gaskets. They perform in an atmosphere of perchloroethylene fumes at temperatures up to 88°C, conditions that would quickly degrade other elastomers.
- A fluid-activated diaphragm-type thermostat for gas or electric ranges owes its success to the designer's choice of Viton® for the actuator element. Because Viton® adheres well to brass is virtually impermeable to and is not swelled or deteriorated by the fluids used, can withstand operating temperatures of 149 to 204°C, and has the mechanical strength to resist repeated flexing.

Chemical Industry

Viton® fluoroelastomer is essentially a universal seal for chemical process equipment. Its application in the chemical industry is illustrated by the following examples:

- In a pumping station that handles more than 80 different solvents, oils, and chemicals, seals of Viton® are used in the piping's swivel and telescoping joints. When these joints were inspected after two years' service, they were found to be as good as new.
- Valves lined with Viton® reduce heat and corrosion worries in many plants.
- Hose made of Viton® transfers solvents and reactive petrochemicals to and from processing and distribution facilities. There are installations on ocean tankers as well as on highway trailers.
- Processing rolls for hot or corrosive service are covered with Viton®.
- Flange gaskets for glass-bodied valves in a paper bleaching plant are of Viton®.
- Viton® replaced caulking on a process equipment enclosure, previously plagued with hot solvent leaks, and saved $4,000 per year in maintenance costs.
- Aerosol-propelled solvent solutions of Viton® are sprayed on chemical process equipment as multi-purpose maintenance coatings.

Industrial Use

The good mechanical properties of Viton® fluoroelastomer have permitted it to replace conventional elastomers in a range of applications that cut across industry lines. To cite a few:

- Stable-dimensioned O-rings in the meters of automatic gasoline blending pumps
- High vacuum seals for the world's most powerful proton accelerator
- Heat- and corrosion-resistant expansion joints for a utility company's stack gas exhaust ducts
- Tubing and seals for a variety of top-quality industrial instruments
- Compression pads for heavy-duty vibration mounts used for portable missile ground control apparatus
- Conveyor rolls for a solvent cleaning machine
- Packing rings for hydraulic activators on steel mill ladles
- Clamp cushions for parts dipped in 285°C solder
- Jacketing for steel mill signal cable
- Deflector rolls on high-speed tinplating lines
- Precision-molded balls for check valves in oil or chemical service
- O-ring seals for test equipment in an automotive manufacturer's experimental lab

Aerospace

Reliability of materials under extreme exposure conditions is a prime requisite in this field. Aircraft designers report that O-rings of Viton® fluoroelastomer have a useful thermal range of –54 to 316°C and that Viton® exhibits "long and consistent life," even at the upper end of this range. Higher temperatures can be tolerated for short periods. Viton® also resists the effects of thermal cycling, encountered in rapid ascent to and descent from the stratosphere. Other desirable characteristics of Viton® that are pertinent to aerospace applications are its excellent abrasion resistance and its ability to seal against "hard" vacuum, as low as 10^{-9} mm Hg (133 nPa), absolute.

The high-performance properties of Viton® have been demonstrated in these typical aircraft and missile components:

- O-rings and Manifold gaskets
- Coated fabric covers for jet engine exhausts between flights
- Firewall seals
- Abrasion-resistant solution coating over braid-sheathed ignition cable
- Clips for jet engine wiring harnesses
- Tire valve stem seals
- Siphon hose for hot engine lubricants

Fluid Power

Designers and engineers are discovering that seals of Viton® fluoroelastomer work better and last longer than any other rubber in most fluid power applications. Viton® seals effectively up to 204°C and is unaffected by most hydraulic fluids, including the fire-resistant types. Seals of Viton® can also cut maintenance costs under more moderate service conditions (below 121°C) by providing longer, uninterrupted seal reliability.

Some applications in which seals of Viton® can reduce fluid loss and minimize downtime include the following:

- Actuators are the hydraulic components most likely to develop small, steady leaks when rubber seals wear and lose resilience, which can be extremely expensive. In a working year, day-to-day leakage from the average hydraulic system wastes enough fluid to completely fill the system more than four times. Viton® prevents or reduces leakage by maintaining its toughness and resilience longer than other rubber seal materials under normal fluid power conditions.
- In pumps, poor sealing performance increases operating costs by wasting power. When internal seals lose resilience and allow more slippage than the pump design permits, power is wasted. When seals swell and drag, power is wasted. Seals of Viton® keep their resilience and don't swell, thus preventing power waste and helping hold down operating costs.

Test Procedures

Property Measured	Test Procedure
Compression Set	ASTM D3955, Method B (25% deflection)
Compression Set—Low Temperature	ASTM D1299, Method B (25% deflection)
Compression Set, O-Rings	ASTM D1414
Hardness	ASTM D2240, durometer A
Mooney Scorch	ASTM D1646, using the small rotor. Minimum viscosity and time to a 1-, 5-, or a 10-unit rise are reported.
Mooney Viscosity	ASTM D1646, ten pass 100°C and 121°C
ODR (vulcanization characteristics measured with an oscillating disk cure meter)	ASTM D2084
Property Change After Oven Heat-Aging	ASTM D573
Stress/Strain Properties 100% Modulus Tensile Strength Elongation at Break	ASTM D412, pulled at 8.5mm/s (20 in/min.)
Stiffness, Torsional, Clash-Berg	ASTM D1043
Temperature Retraction	ASTM D1329
Volume Change in Fluids	ASTM D471

*Note: Test temperature is 24°C. except where specified otherwise

For further information please contact one of the offices below, or visit our website at www.dupontelastomers.com/viton

Global Headquarters – Wilmington, DE USA
Tel. +1-800-853-5515
+1-302-792-4000
Fax +1-302-792-4450

European Headquarters - Geneva
Tel. +41-22-717-4000
Fax +41-22-717-4001

South & Central America Headquarters - Brazil
Tel. +55-11-4166-8978
Fax +55-11-4166-8989

Asia Pacific Headquarters - Singapore
Tel. +65-6275-9383
Fax +65-6275-9395

Japan Headquarters – Tokyo
Tel. +81-3-5521-2990
Fax +81-3-5521-2991

(11/05) Printed in U.S.A.
Reorder no: VTE-H68134-00-F1105

DuPont
Performance Elastomers

3.5.3 Eutectic Analysis of Ti-6Al-4V with Plutonium and Copper

LA-UR 08-07663

Plutonium Metal Compatibility with Materials of the Ti-6Al-4V Packaging System

Prepared by:
Richard E. Mason, PMT-1
and
Stephen P. Willson, PMT-1

2 December 2008

Los Alamos
NATIONAL LABORATORY
EST.1943

1

LA-UR-08-07663

Abstract

This technical basis report considers phase stability of plutonium metal encapsulated in a Ti-6Al-4V ampoule. The maximum temperature that these materials will be exposed to is 582°C. The plutonium metal may also be encapsulated in tantalum foil plus beryllium is potentially in contact with the plutonium. It is concluded by analysis of phase diagrams and composition of materials for all possible binary systems that no liquid phases are expected in this system at 582°C. Furthermore, it is anticipated that the lowest melting point phase that may form within this system is 595°C – the plutonium/beryllium eutectic temperature. This is 13°C higher than the highest temperature excursion considered for the system. This is not a large margin but the 595°C value is a conservative estimate, thus the system in a transient reaching 582°C is still considered safe. Review of the ternary phase diagrams available in the literature involving components of this system supports the conclusions drawn from the binary systems, however, the ternary systems are limited and this is a much more complex system than reviewed in the binary or ternary systems available in the literature.

LA-UR-08-07663

Table of Contents

LA-UR-08-07663

Introduction

The PAT-1 (Plutonium Air Transport) package was originally designed to transport plutonium oxide across the country and to other countries that process plutonium oxide. The TB-1 containment vessel was designed to contain this material. The TB-1 vessel is stainless steel. Because of the need to air transport alpha and delta-stabilized plutonium metal, the container or ampoule inside the TB-1 containment vessel is newly constructed of the Ti-6Al-4V alloy to protect the TB-1 vessel from attack by plutonium. This analysis focuses on binary eutectic compositions that could form in a hypothetical accident scenario in which the TB-1 vessel attains a maximum temperature of 582°C and is exposed to this temperature for up to four days. Within the liner is a copper foam support structure of ≥99.99% copper, and an alpha or delta-stabilized plutonium metal sample. Plutonium metal is loaded into the copper foam and the combined package is loaded into the Ti-6Al-4V liner in an inert atmosphere glove box. The interior void space of the liner is flushed with helium, then sealed and leak-checked.

The melting points of pure metals considered for this analysis are presented in Table 1.[Lide 1991] A summary of the lowest melting points for the possible binary systems has been taken from the binary phase diagrams, and assembled in Table 2.

Table 1. Melting points of pure metals considered in this system.

Element	Melt Temperature (°C)
Aluminum	660
Beryllium	1287
Copper	1085
Gallium	30
Plutonium	640
Tantalum	3017
Titanium	1668
Vanadium	1910

LA-UR-08-07663

Table 2. Lowest melting points and compositions derived from binary phase diagrams.

System	Lowest Melting Point (°C)
Ti6Al4V	1604°C
Aluminum – Beryllium	644°C eutectic
Aluminum – Copper	548°C at compositions between pure aluminum and about 45 atom percent aluminum, 660C for copper alloying with aluminum up to about 3 weight percent Al, greater than 600°C for aluminum alloying with copper up to 25 weight percent Cu
Aluminum – Gallium	26.3°C eutectic
Aluminum – Plutonium	640°C for pure Pu
Aluminum – Tantalum	660C for pure Al
Aluminum – Titanium	660°C for pure Al
Aluminum – Vanadium	660°C for pure Al
Aluminum – Beryllium	644°C eutectic
Beryllium – Copper	The congruent melt temperature of 858°C is the lowest melt temperature in the binary system
Beryllium – Gallium	30°C the gallium melt temperature. The gallium melts and there is minimal solution of the beryllium below 600°C
Beryllium – Plutonium	The additions of small amounts of beryllium may lower the plutonium rich metal to a melt temperature of 595°C
Beryllium – Tantalum	1287°C as there was no binary phase diagram found
Beryllium – Titanium	1287°C of pure Beryllium
Beryllium – Vanadium	1287°C of pure Beryllium
Copper – Gallium	625°C for phases containing greater than 55 atom percent gallium
Copper – Plutonium	626°C for 6 atom% Cu, 1.7 wt% Cu
Copper – Tantalum	1085°C of pure Cu
Copper – Titanium	880°C for 27 atom% Ti, 22 wt% Ti
Copper – Vanadium	1085°C for pure Cu
Titanium – Vanadium	>1600°C for 30 wt% V
Gallium – Aluminum	Compositions above 2 atom% (5 wt%) gallium are liquid at 625°C
Gallium – Copper	Compositions above 55 atom% gallium (57 wt%) are liquid at 625°C
Gallium – Plutonium	Compositions above 75 atom% gallium (47 wt%) are liquid at 625°C
Gallium – Titanium	Compositions above 99 atom% gallium (99 wt%) are liquid at 625°C
Gallium – Vanadium	Compositions above 97 atom% gallium (98 wt%) are liquid at 625°C
Plutonium – Tantalum	640°C of pure Pu
Plutonium – Titanium	640°C of pure Pu
Plutonium – Vanadium	625°C for < 2 wt% V
Tantalum – Titanium	1668°C for pure Ti
Tantalum – Vanadium	1910°C for pure V
Titanium – Vanadium	1668°C for pure Ti

LA-UR-08-07663

Interfacial Reaction Zones

Reactions between metals of the Ti-6Al-4V alloy with the contents it will hold are restricted to contact zones between different metal compositions. Because none of the major individual starting materials reach their melting points during a 582°C temperature excursion, formation of new phases must depend upon solid state transport of material from one of the original phases into another. The original starting materials are not pure materials. Gallium is never in the system as a metal but is dissolved in plutonium and the gallium-plutonium alloy has a melting point well above 582°C. Redistribution of the gallium into a pure metal will not be an issue. Gallium can only influence the performace of the materials in this system if it diffuses to another metal or alloy. Material transport will only occur between phases that are in mechanical contact. Transport will be substantially impeded by the presence of thin surface oxide layers, which will be present on the titanium alloy, the copper, the beryllium and the plutonium. Formation of any new phases in the container, eutectic or otherwise, is explicitly dependent upon sufficient solid state mass transport, which depends on solid state solubility of the components, intimacy of contact between the components, and the time the system is held at the elevated temperature. The kinetic data that would be required to quantitatively address solid state diffusion between the plutonium, the beryllium, the copper, and the titanium ampoule is not available. Qualitative conclusions are drawn based on the available phase diagrams, which capture the thermodynamically stable compositions of binary systems, at a given temperature.

When an alloy is in contact with another metal composition, solid state transport will be different for the different components of the alloy, resulting in preferential reaction with one component, and changing the resultant concentrations of both phases by enriching one and depleting the other with respect to the most mobile component. Contact reaction zones are discussed by reference to binary phase diagrams. At the low temperature of 582°C diffusion will be slow and the integrity of the ampoule alloy will only be compromised if a liquid was to form. As long as all component combinations do not form a liquid, the ampoule will remain intact and contain the material shipped.

Aluminum

Aluminum contact with components of the Ti-6Al-4V packaging system

Aluminum is initially present at only 10 atom percent in the titanium alloy. Although aluminum binaries with the elements of this system are considered, it is improbable that interactions with aluminum alone and the other components would ever occur. The aluminum is alloyed with titanium and vanadium and all three form high temperature alloys with all of the components expected in a shipment of plutonium metal.

Aluminum contact with beryllium

The aluminum-beryllium system forms a eutectic at 644°C, 16°C below the melt temperature of pure aluminum. There are no intermediate phases thus liquid aluminum

will exist above this temperature. This temperature is higher than the maximum temperature considered for safe operation of this system..[Landolt-Bornstein 1992]

Aluminum contact with copper

The aluminum-copper system is complex with a eutectic melt temperature of 548°C at 66.8 weight percent aluminum.[Landolt-Bornstein 1992] The 548°C solidus extends from about 5.6 weight percent aluminum to about 45 weight percent aluminum. The solidus temperatures between pure copper and 45 weight percent aluminum are much higher temperatures and with five intermediate phases in the system. Aluminum is an alloying element in copper is solid at 600C up to about 25 weight percent aluminum. This is not an issue because the aluminum is a minor alloy constituent and as titanium content increases the melt temperature of the copper-titanium-aluminum will likely increase. For alloy compositions with aluminum content greater than 45 weight percent aluminum, the melt temperature is much greater than 600°C and more than 5 weight percent aluminum would have to diffuse into the copper for the melt temperature to be lower than 600°C. Significant aluminum would have to diffuse out of the ampoule alloy into the copper or aluminum into the copper. Both are impractical at the maximum temperature that these materials could be exposed to.

Aluminum contact with gallium

Gallium metal melts at 29°C and the aluminum-gallium binary is a eutectic binary system. There are no intermediate phases in this system. This binary system is a simple eutectic system with eutectic temperature at 26.6°.[Landolt-Bornstein 1992] The liquidus is well known but the boundaries of the solid phases are not well known. The solubility of aluminum in gallium metal is very low. The maximum solubility of gallium in aluminum metal is approximately 9 atom percent and the aluminum is solid at 600C up to about 7 atom percent gallium. The formation of a separate gallium-aluminum phase is not credible because both gallium and aluminum are soluble in plutonium at the compositions present and at temperatures below the melting point of plutonium. It is impractical for an alloy composition to form that would be liquid because it would simultaneously require local concentration of the aluminum to 98 atom percent. This phase is highly unlikely.

Aluminum contact with plutonium

Aluminum forms five intermediate phases with plutonium with $PuAl_2$ being the dominant intermediate phase melting at 1540±50°C. The compound Pu_3Al of the plutonium rich compositions is formed by a very sluggish peritectoid reaction between the plutonium delta phase and PuAl. [Wick 1980] Aluminum goes into solid solution with plutonium up to 10 atom percent aluminum. As the content of aluminum increases the melt temperature increases up to the $PuAl_2$ solidus at 801°C.[Wick 1980] In this binary system the combination of the two elements increases the melt temperature.

Aluminum contact with tantalum

Aluminum and tantalum form four intermediate phases. With the addition of a small amount of tantalum to the aluminum the melt temperature of aluminum metal is raised about eight degrees and the solidus exists to 25 atom percent aluminum. At 25 atom percent aluminum Al_3Ta is the solid and it melts at about 1629°C. On the tantalum rich

LA-UR-08-07663

side of Al_3Ta the solidus temperature is a bit lower but remains close to 1629°C until the intermittent phase Al_3Ta_2 is reached where the solidus temperature is a few degrees lower. Thereafter, as the concentration of tantalum increased the solidus temperature increases.[Landolt-Bornstein 1992] Again the melting temperatures of the intermediate phases are much above the maximum temperature this system will be exposed to thus the combination of these two elements will not negatively affect the safe operation of this system but will more likely decrease the likelihood of liquid formation.

Aluminum contact with titanium
At aluminum concentrations between pure and 25 atom percent aluminum the solidus is 665°C. That is, with the addition of a small amount of titanium to the aluminum the melt temperature of aluminum metal is raised about five degrees and remains the solidus to 25 atom percent aluminum. The Al_3Ti melts at about 1387°C.[Landolt-Bornstein 1992] Again the melt temperatures of the intermediate phases are much above the maximum temperature this system will be exposed to thus the combination of these two elements will not affect the safe operation of this system.

Aluminum contact with Vanadium
Aluminum and Vanadium form five intermediate phases. With the addition of a small amount of tantalum to the aluminum the melt temperature of aluminum metal is raised about two degrees and remains the solidus to about 8 atom percent aluminum. As each intermediate phase is reached the solidus temperature is increased as the concentration of Vanadium increases.[Landolt-Bornstein 1992] Again the melting temperatures of the intermediate phases are much above the maximum temperature this system will be exposed to thus the combination of these two elements will not affect the safe operation of this system.

Beryllium

Beryllium and plutonium may contact the Ti-6Al-4V container if they are not wrapped with tantalum foil and either metal penetrates the copper foam. Tantalum may also be wrapped around the beryllium and/or plutonium pieces and in this case these materials would have to penetrate the tantalum wrapping material and then the copper foam before reaching the ampoule alloy.

Beryllium contact with copper
Beryllium and copper alloys are commonly used alloying elements. An alloy of beryllium and copper with 24 atom percent copper melts at 966°C.[Landolt-Bornstein 1992] This is the lowest melting alloy in this binary system with all other compositions and phases melting at higher temperatures. The combination of beryllium and copper will not compromise the safe use of this system.

LA-UR-08-07663

Beryllium contact with gallium
Beryllium and gallium do not form intermediate phases, consequently, at temperatures above gallium's melting point of 30°C and below 600°C there is minimal mixing of the two materials.[Landolt-Bornstein 1992] If the two materials were to interact, then above 30°C the gallium will be liquid at the grain boundaries causing a decrease in mechanical strength of the beryllium. Interaction of these two components of the system is an improbable scenario because the gallium in the plutonium is in solid solution and only at quantities less than 10 atom percent.

Beryllium contact with plutonium
The main feature of the beryllium-plutonium system is one intermediate compound $PuBe_{13}$ which has a higher melt temperature than either pure constituent at 1950±50°C. The eutectic at 96 atom percent plutonium probably lowers the melt temperature only 10°C. [Wick 1980] However, one experimenter reported the eutectic melt temperature lowered by as much as 45°C. Although, Wick et al. report that a melt temperature drop of 10°C is most accurate the worse case would be the 45°C decrease from 640C of plutonium metal or a melt temperature of 595°C. At 582°C the components are still solid but close to a potential melt temperature.[Wick 1980] This is the lowest melting material or alloy of the systems considered. It is a combination of material that could be present in an accident.

Beryllium contact with tantalum
The phase equilibria are not know.[Landolt-Bornstein 1992] In a sample containing 0.05 atom percent tantalum after solidification from the melt the solidified microstructure indicated a eutectic phase and several intermediate phases with one having a melting temperature of $Be_{12}Ta$ at 1850°C and for $Be_{17}Ta_2$ a melting temperature of 1980°C.

Beryllium contact with titanium
There are four or more intermediate compounds in this system with an eutectic at 70 atom percent titanium and at a temperature of 980°C. [Murray 1987 & Ohnuma 2004] Should the beryllium penetrate the copper, the beryllium could be mechanically mixed with the titanium at the surfaces of the pieces. Even mixed the eutectic temperature is not reached and the containment not affected.

Beryllium contact with vanadium
There are three or more intermediate compounds in this system. The solidus temperature is raised more than 230°C when the vanadium content exceeds about 7 atom percent.[Landolt-Bornstein 1992] Vanadium is only 4 atom percent in the ampoule alloy but its contribution to any alloy of these systems would be to increase the melt temperature. Should the beryllium penetrate the copper beryllium could be mechanically mixed with the titanium at the surfaces of the pieces. Even mixed the eutectic temperature is not reached and the containment not affected.

LA-UR-08-07663

Copper

It is not expected that a liquid phase will form at this interface at the highest temperature of any hypothetical accident (582°C). Because the copper surrounds the metal as the structural matrix to hold the plutonium metal in favored positions within the ampoule, it is the first to interact with the plutonium, beryllium or tantalum that the plutonium metal is wrapped in. At 582°C, both copper and the titanium alloy ampoule are solid and 582°C is well below their respective melting points. Aluminum-copper compositions with more than 64 atom percent (43 weight percent) aluminum will melt at 625°C, which is also the melting point of the plutonium-vanadium eutectic, considered later in this report. Aluminum is present in the titanium alloy at a concentration of 10 atom percent. In order to form a melting composition with copper at 625°C, it needs to attain a concentration within the copper of 64 atom percent or greater. Solid state transport on the scale required for formation of a low melting phase (below 625°C) at this boundary in four days is not expected.

Copper contact with gallium

Gallium is in solid solution in copper up to about 19 to 20 atomic percent gallium with the alloying of these two metals lowering the melt temperature to about 900°C at 20 percent gallium.[Landolt-Bornstein 1992] Solid state transport of gallium from a 10 atom percent gallium-plutonium alloy into pure copper sufficient to form a 20 atom percent gallium-copper alloy is improbable. Incorporation of enough gallium into the copper at 582°C to form a liquid phase requires passage through five successive solid state phases. Formation of each of these phases requires a microstructure rearrangement before more gallium atoms can be incorporated, thus reduction of melting temperatures due to the combination of these two metals is very unlikely.

Copper contact with Plutonium

The plutonium rich component of the binary phase has a eutectic at about 6 atom percent copper and a temperature of 625°C. [Wick 1980 & Copper 2000] It is not expected that a liquid phase will form at this interface at a temperature of 582°C. First consider possible reaction of copper with alpha plutonium. Due to the softening of plutonium metal near its melting point, 640°C, and the roughly 5% expansion of alpha plutonium upon conversion to epsilon plutonium it is possible that alpha plutonium samples will tightly contact the copper foam, and reaction will occur at the interface. The progression of the reaction will be limited by the temperature actually reached, and by the time held at that temperature. The plutonium-copper eutectic composition will not melt at 582°C.

Copper contact with Tantalum

The mutual solubility of copper and tantalum is negligibly small and intermediate phases do not exist.[Landolt-Bornstein 1992] Copper and tantalum are immiscible at temperatures lower than 1083°C. Even the solubility of tantalum in liquid copper above the melting point is small. The solubility of Ta in liquid copper amounts to 0.0088 atom percent tantalum at 1200°C. Combining these two materials in this storage system will not lower the melting temperatures of the materials and are of no consequence to the safety of the system but may enhance the safety margin.

LA-UR-08-07663

Copper contact with titanium
The copper-titanium system is also a complex binary system with five intermediate phases and a eutectic at 860°C and 27 atom percent titanium.[Landolt-Bornstein 1992] Combining these two materials in this storage system will not lower the melting temperatures of the materials and are of no consequence to the safety of the system but may enhance the safety margin.

Copper contact with vanadium
The copper vanadium system is a simple eutectic system. The eutectic is on the vanadium rich side at about 15 atom percent copper and a eutectic temperature of 1530°C.[Landolt-Bornstein 1992] Combining these two materials in this storage system will not lower the melting temperatures of the materials and are of no consequence to the safety of the system but may enhance the safety margin.

Gallium

Gallium has an extremely low melting temperature when compared to the other metals in the ampoule material and the material to be shipped. The gallium is soluble in the plutonium and is a component of the plutonium up to 10 atom percent. The only thermodynamic driver of this conversion is the leaching ability of other metals from the plutonium-gallium alloy. Gallium is soluble in the plutonium epsilon phase and will not segregate to the interface and is consequently not easily leachable from the plutonium should one of the other elements have a higher affinity to alloy gallium than plutonium.

Gallium contact with Plutonium
The gallium is soluble in the plutonium up to about 10 atom percent gallium in the plutonium. The delta phase of plutonium is stabilized at room temperature by the addition of less than 10 atom% gallium. [Wick 1980] Because delta plutonium contracts upon conversion to epsilon, it will not experience increased pressure at the interface upon heating. Up to 20 atom percent gallium is soluble in the plutonium epsilon phase, so there will be no segregation of gallium upon transition to epsilon plutonium. A liquid phase will not form in the plutonium rich material until the melt temperature of plutonium is reached. There is also no driver for the gallium to segregate since it is already in solid solution

Gallium in contact with tantalum
There are four intermediate phases in this binary system and with increasing tantalum the solidus increases with each intermediate phase. The liquidus remains at 29°C until the intermediate Ga_3Ta is reached.[Landolt-Bornstein 1992] The phase relations in this system are not sufficient to give additional detail. Given sufficient gallium in the system this combination could compromise the safety of the system but there is simply insufficient gallium in the entire mass of plutonium metal to compromise the container.

Gallium in contact with titanium

LA-UR-08-07663

The gallium-titanium system requires more than 99 atom percent gallium in order to form a phase that melts at 625°C.[Landolt-Bornstein 1992] Because the gallium is soluble and stable at lower concentrations, formation of a phase with such high gallium content, nearly pure gallium is not expected to occur. Formation of a molten phase of either gallium-titanium or gallium-vanadium is unlikely given the available quantity of gallium and the thermodynamic stability of lower concentration solid phases.

Gallium in contact with Vanadium
There are four intermediate phases in this binary system and with increasing vanadium the solidus increases with each intermediate phase. The solidus remains at 29°C until the intermediate Ga_4V_8 is reached where the solidus on the vanadium rich side of this intermediate compound is 500°C. The gallium-vanadium compositions require more than 84 atom percent of gallium in order to form a phase that melts at 625°C.[Landolt-Bornstein 1992] Given sufficient gallium in the system this combination could compromise the safety of the system but there is simply insufficient gallium in the entire mass of plutonium metal to compromise the container.

Plutonium

It is not expected that a liquid phase will form at this interface. In the event that plutonium is sheared from the bulk and contacts the Ti-6Al-4V liner, consideration must be given to the interfacial reaction zone. The possible binary compositions of interest for contact between the liner and alpha plutonium include plutonium-aluminum, plutonium-titanium, and plutonium-vanadium. In the case of both plutonium-aluminum and plutonium-titanium, the melting point is increased relative to that of pure plutonium for all concentrations.

Plutonium contact with tantalum
This combination of materials is very stable and will not negatively impact the safe operation of the system. Tantalum and plutonium form a eutectic very close to pure plutonium. The eutectic reduces the melt temperature by only a degree or two. At temperatures above the 640°C solid tantalum can contain increasing plutonium up to about 25% plutonium near 2550°C.[Boxi 1991] There is also significant solubility of plutonium in the tantalum metal at temperatures above the plutonium melt temperature but limited solubility of plutonium in tantalum at temperatures below 640°C. [Wick 1980] Consequently, pure plutonium stored in pure tantalum foil is compatible at temperatures below plutonium's melting temperature. Above plutonium's melt temperature there is little reaction except that as the temperature rises an increasing amount of plutonium will diffuse into the tantalum metal matrix.

Plutonium contact with titanium
There are no intermediate phases in the binary system. A peritectiod composition at 6.5 atom percent titanium increases the solubility of titanium in the plutonium metal to a maximum of 25 atom percent at 770°C. Above the melting temperature of plutonium the liquid plutonium will combine with the tantalum to form a solid mixture up to 770°C, the highest solidus temperature in the system.[Landolt-Bornstein 1992] This reaction would stabilize the system in a high temperature transient situation.

LA-UR-08-07663

Plutonium contact with vanadium
The plutonium-vanadium eutectic composition forms with less than 2 weight percent vanadium resulting in a solidus temperature of 625°C from 2 to 100 weight percent vanadium. At all concentrations of more than 2 wt% vanadium in plutonium, and at a temperature of 625°C or higher, the plutonium-vanadium system exhibits a liquid phase.[Landolt-Bornstein 1992] At all compositions, at temperatures less than 625°C, only solid phases are present. If mobility into the solid plutonium metal leaves the ampoule alloy depleted in one of its other constituents, the melting point of the liner in the depleted zone will be increased.

Tantalum, Titanium, and Vanadium

Vanadium and aluminum are the minor constituents of the alloy of the ampoule at 10 atom percent or less. Consequently, titanium will probably dominate the interactions of the container with the packaged material. When tantalum is used to wrap the plutonium metal it too will be a major contributor to the performance of the shipping container during the transient. Interaction between or alloying of these four components aluminum, tantalum, titanium and vanadium produce material that will probably not form lower melt temperature

Tantalum contact with titanium
The Ti-Ta binary phase diagram is characterized by an isomorphous body centered cubic phase field extending from pure titanium at elevated temperatures to pure tantalum with limited mutual solubilities.[Landolt-Bornstein 1992] Since there are no intermediate phases and the solidus is essentially linear between the melt temperature of titanium (1670°C) and tantalum (3017°C), a combination of these metals with other compound will probably increase the melt temperature of the system.

Tantalum contact with Vanadium
There are no intermediate phases and the solidus and liquidus increase from the 1910°C melt temperature to the 3017°C melt temperature of tantalum. Addition of any of these two metals will likely increase the melt temperature of the resulting mixture.

Titanium contact with Vanadium
There are three intermediate phases and the solidus and liquidus increase from the 1668°C titanium melt temperature to the 1910°C melt temperature of vanadium.[Landolt-Bornstein 1992] Addition of any of these two metals will likely increase the melt temperature of the resulting mixture of container and package materials.

Binary interaction summary

The lowest melt temperature is 595°C between the plutonium and beryllium with the next lowest between the plutonium-vanadium eutectic at 625°C. The 595°C temperature may be a low estimate because of impurities in the material tested with the melt temperature of the beryllium-plutonium probably closer to 630°C. However, for safety evaluations this is the worst case temperature.

LA-UR-08-07663

The lowest melting phase with plutonium/vanadium liner contact is 625°C, and is unlikely to form based on the absence of a clean contact surface under pressure between the plutonium and the liner. The melting temperature of this eutectic is 43°C higher than that of the proposed high temperature excursion.

Addition of the beryllium to the system brings the melt temperature close to the maximum temperature that the ampoule may be exposed to. If all the components internal to the titanium ampoule are combined and intimately mixed, that is, plutonium, beryllium, gallium, tantalum, and copper are completely alloyed, the melt temperature could be lower than 582°C. There is no data to show otherwise and 595°C is close to this temperature. However, it is unlikely and impractical to intimately mix these components together by mechanical impact and then expose them to temperatures above the binary melting points. Significant work on this complex metal alloy system would be required if a mechanism could be hypothesized to form such an alloy by impact of separate alloys and metals but it is not considered plausible.

Investigation of Ternary Systems

Published information was available for eleven of the possible ternary systems considered.[Petzow 1992 & Villars 1995] The Ti-6Al-4V alloy was designed to be solid to 1604°C. The tantalum-titanium-aluminum system is solid above 1100C.[Weaver 1995] It is generally true that for the ternary phase diagrams reviewed, there was little new information with respect to melting temperatures that was not captured by the binary diagrams. Expected compositions are those that do not require achieving large concentrations of a particular element in a phase against a strong concentration gradient. For example, given that aluminum begins at 10 atom percent in the titanium alloy used, it is considered unlikely that it would achieve concentrations of 20 atom percent or more in another phase. The same rule is applied with respect to the vanadium and gallium components, both of which begin at low concentrations in their respective thermodynamically stable alloys.

Reviewed binary and ternary systems that possess a liquid component at temperatures below 625°C are those with high concentrations of aluminum and gallium (greater than 50 atom percent combined aluminum and gallium content). It is considered improbable that with less than 9 atom percent gallium in the plutonium and 10 atom percent aluminum in the titanium alloy, any phases will form containing more than 50 atom percent combined gallium and aluminum.

In both titanium and plutonium, aluminum and gallium may substitute for each other, partially or completely, without altering the observed phase. Several of the ternary systems reviewed show no ternary phases, only mixtures of binary phases, all of which have already been captured by the preceding review of binary phase diagrams. The only ternary diagram available that contained plutonium was the aluminum-gallium-plutonium diagram.

Conclusions drawn by reference to the binary phase diagrams are consistent with the information present in the ten available ternary phase diagrams.

Additional Chemical Reaction

Finely divided metals tend to oxidize rapidly in air due to the high surface area relative to mass of metal present. The oxidation reaction for a metal is generally exothermic, and in the event of finely divided powders in air, can often result in pyrophoricity. During the proposed accident scenario for this analysis, the system containment is not mechanically breached, and an inert environment is maintained. The small amount of oxygen in the system will exist as oxide on the various system components, rather than as gaseous oxygen. In the event that small particles are generated within the titanium alloy ampoule, they will not ignite due to an absence of oxygen necessary for the reaction. The initial system components are bulk metal materials. These are not pyrophoric.

Conclusions

All of the expected phases formed from the original materials at a temperature of 582°C are solid. The lowest probable binary phase melting point is 595°C (plutonium-Beryllium). The second lowest probable binary phase melting point is 625°C (plutonium-vanadium) and the third lowest melting point is 626°C (plutonium-copper). The lowest is possible if other impurities not considered in this technical basis were present. It is anticipated that the second and third lowest compositions will not form due to the presence of surface oxide layers on the initial components of the system. A review of available ternary phase diagrams supports the conclusions drawn from the binary phase diagrams. However, the many combinations of the product materials and the container materials make it impossible to absolutely rule out a lowering of the melting point due to mechanical mixing that could occur in a severe impact and post impact fire until some testing verification on the materials are conducted.

References

Boxi, H.C., Massalski, T.B., and Rizzo, H.F., 1991, *The Pu-Ta (Plutonium-Tantalum) System*, Journal of Phase Equilibria, 12 No. 5 pp 593

Brandes, E. A., ed. 1983. Smithells Metals Reference Book, Sixth Edition. Ch. 11.

Kaufmann, A.R., Gordon, P., Lillie, D.W. 1950, ASM Trans. Q. **42** p 801.

Cooper, N. G., ed. 2000. *Challenges in Plutonium Science, Volume II.* Plutonium and Its Alloys. pp. 291-335.

Landolt-Bornstein – Group IV Physical Chemistry Volumes 5b and 5j (1992)

Lide, D. R., ed. 1991. *CRC Handbook of Chemistry and Physics*, pp. 4-122, 4-123.

LA-UR-08-07663

Murray, J.L., 1987, The Be-Ti (Beryllium-Titanium) System, *Phase Diagrams of Binary Titanium Alloys,* J.L. Murray, Ed., ASM International, p 40-43

Ohnuma, I.; Kainuma, R.; Uda, M.; Iwadachi, T.; Uchida, M., Kawamura, H., and Ishida, K., 2003 "Phase Equilibria in the Be-V and Be-Ti Binary Systems," *Proc. Sixth International Workshop on Beryllium Technology for Fusion, 2003*, Japan. Atom. Energy Res. Inst.,

Petzow, G., Effenberg, G., ed., 1992, *Ternary Alloys.* VCH Publishers, NY, NY: ASM International.

Villars, P.; Prince, A.; Okamoto, H., 1995. *Handbook of Ternary Alloy Phase Diagrams.* Materials Park, OH: ASM International.

Weaver, M.L. and Kaufman, M.J., 1995 "Phase Relationships and Transformations in the Ternary Aluminum-Titanium-Tantalum system," *Acta metall, mater.* Vol. 43, No. 7, pp. 2625-2640.

Wick, O. J., ed. 1980. *Plutonium Handbook.* Chaps. 7 and 12-3. La Grange Park, IL: American Nuclear Society

3.5.4 Determination of Most Damaging Package Orientation for HAC Analysis

This section of the Appendix contains a summary of the calculations used to determine which package orientation is the most thermally damaging configuration for the HAC analysis. The PAT-1 package was considered as a cylinder exposed to a fully-engulfing, uniform temperature, fire and to an open (cool) environment in both the vertical and the horizontal orientations. In both orientations, the maximum heat flux exchange between the package and the environment occurs soon after the fire starts or soon after the fire is extinguished. Assuming a fire environment temperature of 800°C (1472°F), an ambient temperature of 38°C (100°F), and equal view factor and emissivity for both orientations, the difference in absorbed or released heat flux between a vertically- and a horizontally-oriented package would be a function of the convective heat flux exchange only. Whether the package is heating or cooling, or in the vertical or horizontal positions, the model assumes the following dimensions, thermal conditions, and gas properties:

Parameters	Values
Hot temperature	$T_h := 1073K$
Cold temperature	$T_c := 311K$
Flow velocity during fire	$V = 5\frac{m}{s}$
Diameter of package	$D := 0.5715m$
Length of package	$L := 1.08585m$
Conductivity of the fluid (Air)	$k_f := 52 \cdot 10^{-3}\frac{W}{m \cdot K}$
Kinematic viscosity of fluid (Air)	$\nu := 68 \times 10^{-6}\frac{m^2}{s}$
Thermal diffusivity (Air)	$\alpha := 98 \times 10^{-6}\frac{m^2}{s}$
Prandtl Number	$Pr := \frac{\nu}{\alpha} = 0.694$
Area of cylindrical sides	$A_{cyl} := \pi \cdot D \cdot L = 1.95m^2$
Area of cylindrical ends	$A_{ends} := \frac{\pi \cdot D^2}{4} = 0.257m^2$

During the fire, convection is predominately considered to be forced convection as suggested by the ratio of Gr/Re^2 given in Table 3-9 of the Addendum. This ratio is much less than one; hence, only force convection is considered. On the other hand, during the cool-down process, convection is predominately free convection since the buoyancy forces are weak with no imposed flow. Therefore, there are four cases that need to be considered to determine which package orientation is the most thermally damaging configuration for the PAT-1:

1. Horizontal orientation with force convection during the fire
2. Vertical orientation with force convection during the fire
3. Horizontal orientation with free convection during the cool down period
4. Vertical orientation with free convection during the cool down period

In Case 1, the package is in the horizontal position and gas flows around the perimeter of the cylinder and across the vertical flat ends with an imposed velocity of 5 m/s (16.4 ft/s). In Case 2, the package is in the vertical position and gas "impinges" on the bottom (flat end) of the cylinder and flows across the vertical cylinder walls at an imposed velocity of 5 m/s (16 ft/s). In both cases, the maximum convection heat transfer will occur initially during the fire when the temperature of the fire is much greater than that of the package. For both of these cases, the following Nusselt (Nu_{avg}) number correlation is used to determine the effective convective heat transfer coefficient:

$$Nu_{avg}(C, m, Re, Pr) := C \cdot Re^{m} \cdot Pr^{\frac{1}{3}},$$

where C and m are experimentally determined coefficients; Re is the Reynolds number; and Pr is the Prandtl number. The coefficients C and m vary with the relative orientation between the flow and the object and with the geometry of the object. Values for C and m are given in Incropera and Dewitt (1996) and in Kobus and Shumway (2006).

The equations below show the calculations performed to obtain the effective convection heat transfer coefficient for Case 1. The effective convective heat transfer coefficient was obtained by assuming the same temperature difference for all surfaces (i.e., T_h-T_s).

$Re := \frac{V \cdot D}{\nu} = 4.202 \times 10^4$	
$Nu_{cyl} := Nu_{avg}(0.027, 0.805, Re, Pr) = 125.996$	$Nu_{ends} := Nu_{avg}(0.68, 0.5, Re, Pr) = 123.408$
$h_{cyl} := \frac{k_f \cdot Nu_{cyl}}{D} = 11.464 \frac{W}{m^2 \cdot K}$	$h_{ends} := \frac{k_f \cdot Nu_{ends}}{D} = 11.229 \cdot \frac{W}{m^2 \cdot K}$
$h_{hor\_eff} := \frac{h_{cyl} \cdot A_{cyl} + 2 \cdot h_{ends} \cdot A_{ends}}{A_{cyl} + 2 \cdot A_{ends}} = 11.415 \cdot \frac{W}{m^2 \cdot K}$	

The following equations show the calculations performed to obtain the effective convection heat transfer coefficient for Case 2. Note that the top (flat) end of the vertical cylinder is conservatively assumed to have the same convective heat transfer coefficient as the bottom ("impinged") flat end.

$Re_{cyl} := \frac{V \cdot L}{\nu} = 7.984 \times 10^4$	$Re_{end\_btm} := \frac{V \cdot D}{\nu} = 4.202 \times 10^4$
$Nu_{cyl} := Nu_{avg}(0.68, 0.5, Re_{cyl}, Pr) = 170.10$	$Nu_{end\_btm} := Nu_{avg}(0.966, 0.46, Re_{end\_btm}, Pr) = 114.5$
$h_{cyl} := \frac{k_f \cdot Nu_{cyl}}{L} = 8.146 \cdot \frac{W}{m^2 \cdot K}$	$h_{end\_btm} := \frac{k_f \cdot Nu_{end\_btm}}{D} = 10.42 \cdot \frac{W}{m^2 \cdot K}$
$h_{ver\_eff} := \frac{h_{cyl} \cdot A_{cyl} + 2 \cdot h_{end\_btm} \cdot A_{ends}}{A_{cyl} + 2A_{ends}} = 8.62 \cdot \frac{W}{m^2 \cdot K}$	

In Case 3 and Case 4, free convection dominates since the package is allowed to cool naturally. In both cases, the maximum free convection heat transfer will occur immediately after the fire which is when the temperature of the package is much higher than that of the environment. The following Nu_{avg} correlations are used to determine the effective convective heat transfer coefficient for both of these cases:

Nusselt number for free flow across a cylinder

$$Nu_{cyl}(Ra, Pr) := \left[0.60 + \frac{0.387 \cdot Ra^{\frac{1}{6}}}{\left[1 + \left(\frac{0.559}{Pr} \right)^{\frac{9}{16}} \right]^{\frac{8}{27}}} \right]^2$$

Nusselt number for free flow across a plate

$$Nu_{plate}(Ra, Pr) := \left[0.825 + \frac{0.387 \cdot Ra^{\frac{1}{6}}}{\left[1 + \left(\frac{0.492}{Pr} \right)^{\frac{9}{16}} \right]^{\frac{8}{27}}} \right]^2$$

Nusselt number for free flow perpendicular to a circular plate

$$Nu_{cyl\_ends}(C, m, Ra) := C \cdot Ra^m$$

where *Ra* is the Raleigh number, and *C* and *m* are empirical constants determined from experiments. The constants *C* and *m* vary with the relative orientation between the flow and the object. Values for *C* and *m* are given in Incropera and Dewitt (1996).

The equations below show the calculations performed to obtain the effective convection heat transfer coefficient for Case 3.

$Gr := \frac{g \cdot (T_h - T_c) \cdot D^3}{\frac{(T_c + T_h)}{2} \cdot \nu^2} = 4.4 \times 10^8$	$Ra := Gr \cdot Pr = 3 \times 10^8$
$Nu_{hcyl} := Nu_{cyl}(Ra, Pr) = 79.354$	$Nu_{ends} := Nu_{plate}(Ra, Pr) = 84.915$
$h_{hcyl} := \frac{Nu_{hcyl} \cdot k_f}{D} = 7.22 \cdot \frac{W}{m^2 \cdot K}$	$h_{ends} := \frac{Nu_{ends} \cdot k_f}{D} = 7.726 \cdot \frac{W}{m^2 \cdot K}$
$h_{hor\_eff} := \frac{h_{hcyl} \cdot A_{cyl} + 2 \cdot h_{ends} \cdot A_{ends}}{A_{cyl} + 2A_{ends}} = 7.326 \cdot \frac{W}{m^2 \cdot K}$	

The following equations show the calculations performed to obtain the effective convection heat transfer coefficient for Case 4. Note that the Nusselt number for flow over a plate was used for the cylindrical sides of the package. This assumption is valid as long as the ratio of D/L is greater or equal to the ratio of $35/Gr^{0.25}$.

$Gr_{vcyl} := \frac{g \cdot (T_h - T_c) \cdot L^3}{\frac{(T_h + T_c)}{2} \cdot \nu^2} = 3 \times 10^9$	$Gr_{ends} := \frac{g \cdot (T_h - T_c) \cdot D^3}{\frac{(T_h + T_c)}{2} \cdot \nu^2} = 4.4 \times 10^8$
$Ra_{vcyl} := Gr_{vcyl} \cdot Pr = 2.1 \times 10^9$	$Ra_{ends} := Gr_{ends} \cdot Pr = 3 \times 10^8$
$\frac{D}{L} \geq \frac{35}{Gr_{vcyl}^{\frac{1}{4}}}$	Since D/L is greater than the ratio of $35/Gr^{0.25}$, the vertical plate correlation can be used for the vertical walls of the cylinder.
$Nu_{vcyl} := Nu_{plate}(Ra_{vcyl}, Pr) = 153.5$	$h_{vcyl} := \frac{Nu_{vcyl} \cdot k_f}{L} = 7.4 \cdot \frac{W}{m^2 \cdot K}$
$Nu_{btm\_end} := Nu_{cyl\_ends}(0.27, 0.25, Ra_{ends}) = 35.6$	$h_{btm\_end} := \frac{Nu_{btm\_end} \cdot k_f}{D} = 3.2 \cdot \frac{W}{m^2 \cdot K}$
$Nu_{top\_end} := Nu_{cyl\_ends}(0.54, 0.25, Ra_{ends}) = 71.2$	$h_{top\_end} := \frac{Nu_{top\_end} \cdot k_f}{D} = 6.5 \frac{kg}{K \cdot s^3}$
$h_{ver\_eff} := \frac{h_{vcyl} \cdot A_{cyl} + h_{btm\_end} \cdot A_{ends} + h_{top\_end} \cdot A_{ends}}{A_{cyl} + 2 \cdot A_{ends}} = 6.8 \cdot \frac{W}{m^2 \cdot K}$	

In all cases, the difference between the vertical and the horizontal orientation was minimal, with the horizontal orientation being slightly more severe for the package. That is, the horizontal configuration provides the highest convection during the fire and the lowest convection during the cool-down.

For the HAC analysis in the Addendum, a value of 11.5 W/m^2-K (2.03 Btu/hr-ft^2-°F) was used during the regulatory fire analysis and a value of 3.5 W/m^2-K (0.62 Btu/hr-ft2-°F) was used during the cool-down period. The values used in the analyses described in the Addendum are conservative, as they bound all values that are presented in this section. That is, a higher convection heat transfer coefficient than those calculated in this section was used for the fire analysis and a lower convection heat transfer coefficient than those calculated in this section was used for the cool-down process.

References:

1. Incropera, F.P. and D.P. DeWitt. "Fundamentals of Heat and Mass Transfer, 4th ed.," New Jersey: Wiley & Sons, Inc., 1996.

2. Kobus, C.J. and G. Shumway. "An experimental investigation into impinging forced convection heat transfer from stationary isothermal circular disks,"International J. of Heat and Mass Transfer 49 (2006), pp. 411–414.

4. CONTAINMENT

The Plutonium Air Transportable Package, Model PAT-1, is certified under Title 10 Code of Federal Regulations, Part 71,[1] by the U.S. Nuclear Regulatory Commission (NRC) per Certificate of Compliance (CoC) USA/0361/B(U)F-96 (current Revision 9).[2] The current authorized contents are plutonium oxide (PuO_2) and its daughter products, or a mixture of PuO_2 and uranium oxide (UO_2) and its daughter products. The (-96) in the certificate of compliance number indicates that the NRC has evaluated the PAT-1 against the current regulations (including 10 CFR 71.63) and determined that the package satisfies the current regulations.

The purpose of this addendum is to incorporate plutonium metal as a new payload for the PAT-1 package and to demonstrate that the package with the new *T-Ampoule Assembly*[A] (Drawing 2A0261, designated the T-Ampoule) and packing within the TB-1 *Containment Vessel* (Drawing 1017, designated TB-1) meet the current containment requirements in 10 CFR 71.[3] The 71.63 requirement is satisfied for the PAT-1 with the T-Ampoule and its packing material configuration because the plutonium metal payload contents are solid, pure or alloyed plutonium metal contents or Pu/Be composite samples.

The CoC[2] describes the TB-1 as a stainless steel containment vessel surrounded by a stainless steel and redwood overpack (*Overpack, AQ*, Drawing 1002, designated AQ-1). The plutonium oxide contents are sealed within a stainless steel product can (designated PC-1). The CoC does not identify the PC-1 as a "containment vessel," but as a "sealed ... product can." For the plutonium metal content packaging configuration described in this addendum, the PC-1, aluminum honeycomb top spacer and packing material is replaced with a T-Ampoule, *Ring, Filler* (Drawing 2A0262, designated Ring Filler) and packing material which provides a eutectic prevention barrier between the TB-1 and the plutonium metal content. The T-Ampoule provides the following:

- A eutectic prevention barrier between the stainless steel TB-1 and the plutonium metal payload for NCT, HAC, and air transport accident conditions.
- A T-Ampoule seal area that is not significantly deformed (see Sections 2 and 3 of this addendum) nor a seal temperature that exceeds the allowable temperature of the gasket material during NCT or HAC. The T-Ampoule is expected to remain sealed during NCT and HAC, like the PC-1.
- A retained eutectic prevention barrier function following the air transport accident condition drops and fire. Although the O-ring in the T-Ampoule would be expected to fail in the 10 CFR 71.74 air transport of plutonium fire test, the T-Ampoule is shown in Sections 2 and 3 of this addendum to remain intact (no significant deformation in the seal area and no breaches). The T-Ampoule is more robust than the PC-1.

The documentation and analysis in this section and other sections of this addendum demonstrate that the replacing the PC-1 with oxide content and associated packing material with the T-Ampoule with plutonium metal content and associated packing material satisfies the

[A] The drawing titles are in italics and are used interchangeably with the designated names in this addendum. See Section 1.3.2 in this addendum and Chapter 9 in the SAR[4] for drawing number, title, and revision.

requirements specified in 10 CFR 71.19(d). That is, the modifications of the PAT-1 described in this addendum are not significant with respect to the design, operating characteristics, safe performance of the containment system, or prevention of criticality when the package is subjected to the tests specified in 10 CFR 71.71, 71.73, and 71.74.

4.1 Description of the Containment System

The CoC USA/0361/B(U)F-96[2] defines the TB-1 as the containment vessel for the PAT-1 for the current PuO_2 and its daughter products and UO_2 and its daughter products as authorized contents. The description of the TB-1 containment vessel is provided in Sections 1 and 9 of the SAR.[4] For this plutonium metals addendum, the TB-1 containment vessel (see Figure 4-1) provides the containment boundary for the proposed metal contents as it did for the oxide contents. The T-Ampoule replaces the PC-1. The TB-1 O-ring is not used for the plutonium metal shipments.

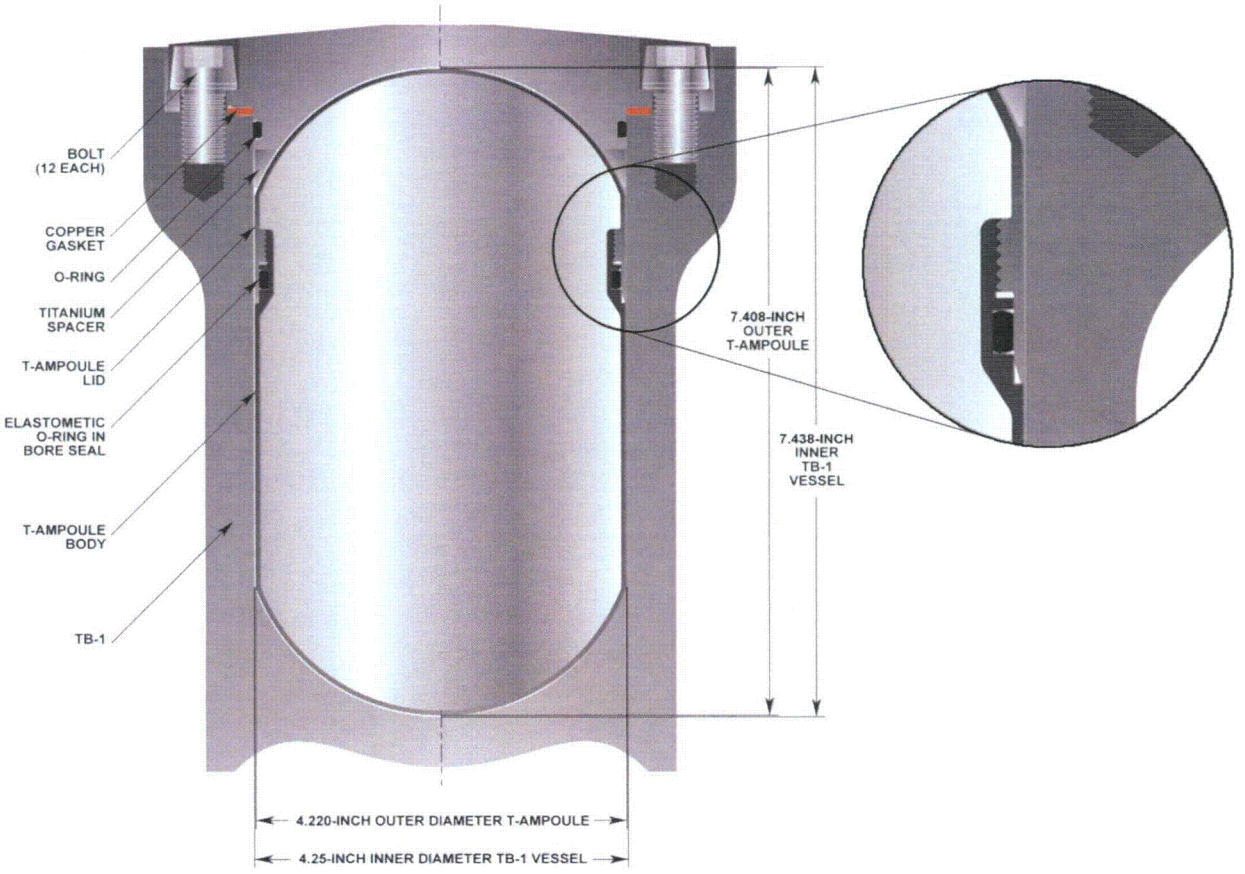

Figure 4-1. TB-1 Containment Vessel and T-Ampoule Contents Container

Table 4-1 of the SAR[4] summarizes the results of the post-test assessment of PAT-1 containment of its surrogate PuO_2 powder contents during the three transport tests (10 CFR 71.71, 10 CFR 71.73, and 10 CFR 71.74) and demonstrates that the containment criteria are met.

Table 4-1. PAT-1 Package Post-Test Containment

			Post Test Results	
Component	**Test Condition**	**Regulatory Acceptance Standard**	**Helium Leak-Rate (atm-cc/sec)**	**Maximum Mass of Powder Release[b] (mg)**
TB-1	NCT (71.71)	10^{-6} A_2/hr	Less than 1×10^{-10}	0
	HAC (71.73)	A_2/week	Less than 1×10^{-10}	0
	Plutonium Air Transport (71.74)	A_2/week[a]	Less than 4.5×10^{-5}	0.17

[a] For a typical mixture of plutonium oxide (PuO_2) powder, an A_2 quantity is approximately 2.55 mg.
[b] Depleted uranium oxide powder was used as the surrogate for plutonium oxide powder during PAT-1 testing. From the SAR, the bounding magnitude of potential PuO_2 powder leakage from the TB-1 vessel would be less than 0.17 mg in one week.

Section 4.5.5 provides a determination of A_2 for the PAT-1 package with plutonium metal in its most dispersible form as contents and Section 4.5.6 provides calculations of the PAT-1 containment vessel's regulatory reference air leakage rates.

The containment criteria for radioactive, fissile material packages are given in 10 CFR 71.51(a)(1) for NCT ($\leq 10^{-6}$ A_2/h), in 71.51(a)(2) for HAC ($\leq A_2$ in a week), and 71.64(a)(1)(i) for accident conditions for air transport of plutonium ($\leq A_2$ in a week). In Section 4.5.5, the A_2 value for the mixture of isotopes was determined to establish the content containment criteria and to determine the maximum release quantity that is allowed by the regulations. The A_2 values of the plutonium content to be shipped were evaluated based on the mass and weight percents of materials shown in Section 1.2.2. The analysis in Section 4.5.5 was conducted to establish an upper limit for the total activity and the maximum number of A_2s proposed for transport in the PAT-1 package. The values were determined using a maximum of 1300 g of plutonium as a bounding condition.

The PAT-1 leak-testing requirements of the containment boundary are based on the smallest maximum allowable leakage rate generated from the maximum plutonium content defined in Table 4.5.5.1 given the allowable leak rates defined in ANSI N14.5-1997, which defines the maximum allowable leakage rate based on the maximum allowable release rate. L_N, L_A, and L_{PA} are the maximum allowable seal leakage rates for NCT, HAC, and accident conditions for air transport of plutonium (ACATP). The worst case maximum allowable leakage rates are used to calculate an equivalent leakage hole diameter following ANSI N14.5-1997, Appendix B, for each condition of transport. This leakage hole diameter is used to calculate a reference air and helium leakage rate for leak testing. The bounding mass for the plutonium content of 1300 g was used in this calculation; note that a 831 g weight limit for the plutonium hollow cylinder was used in the structural analysis and is the maximum plutonium metal content for certification. The use of 1300 g was conservative; the maximum allowable leak rates are calculated using this maximum content mass in a much more dispersive form (oxide powder) for additional conservatism at the highest calculated pressures (assuming the maximum amount of material for disposition) and temperatures as analyzed in Section 2.12.8.

The regulatory leakage criteria for 1300 g plutonium (bounding case for containment analysis assuming oxide) are shown in Table 4-2 in this addendum.

In accordance with Table 4-1 of the SAR, the highest measured helium leakage rate following the accident conditions for air transport of plutonium was 4.5×10^{-5} cc/s. This leakage rate is considerably lower than the calculated maximum allowable regulatory leakage rate requirement of 1.4703×10^{-3} ref cc/s (see Table 4-2 in this addendum) for ACATP at 1110 psia, 1080°F. These results are from Table 4.5.6.1 (of Section 4.5.6 in this addendum). It can be concluded that the TB-1 containment vessel inside of the PAT-1 package maintains containment for NCT, HAC, and Accident conditions for air transport of plutonium.

The mass release during the Accident conditions for air transport of plutonium was calculated in Section 4.5.6. For the 1300 g bounding case, the allowable mass release for no decay of Pu-241 is 2.7634×10^{-1} g and for complete decay of Pu-241 to Am-241 is 2.3336×10^{-1} g. The maximum amount of powder released shown in Table 4-1 above after the Accident conditions for air transport of plutonium test was less than 0.17 mg.

Table 4-2. Regulatory Leakage Criteria for 1300 g Plutonium (Bounding Case)

Isotopic Distribution	Ancillary plastic composition	NCT [a]		HAC [a]		ACATP	
		$L_{R,N\text{-}air}$ (ref-cm^3/s)	$L_{R,N\text{-}He}$ (cm^3/s)	$L_{R,A\text{-}air}$ (ref-cm^3/s)	$L_{R,A\text{-}He}$ (cm^3/s)	$L_{R,PA\text{-}air}$ (ref-cm^3/s)	$L_{R,PA\text{-}He}$ (cm^3/s)
No Pu-241 decay	polyethylene terephthalate	5.1244 E-06	8.8373 E-06	9.4686 E-02	9.8072 E-02	1.7546E-03	2.0876E-03
	polyethylene	5.1244 E-06	8.8373 E-06	9.4686 E-02	9.8072 E-02	1.7339E-03	2.0642E-03
	polyvinyl chloride	5.1244 E-06	8.8373 E-06	9.4686 E-02	9.8072 E-02	1.7487E-03	2.0810E-03
	polytetrafluoroethylene	5.1244 E-06	8.8373 E-06	9.4686 E-02	9.8072 E-02	2.1844E-03	2.5725E-03
Complete Pu-241 decay to Am-241	polyethylene terephthalate	4.2787 E-06	7.4737 E-06	7.9817 E-02	8.3008 E-02	1.4703E-03	1.7873E-03
	polyethylene	4.2787 E-06	7.4737 E-06	7.9817 E-02	8.3008 E-02	1.4729E-03	1.7673E-03
	polyvinyl chloride	4.2787 E-06	7.4737 E-06	7.9817 E-02	8.3008 E-02	1.4854E-03	1.7816E-03
	polytetrafluoroethylene	4.2787 E-06	7.4737 E-06	7.9817 E-02	8.3008 E-02	1.8549E-03	2.2012E-03

[a] Since temperatures associated with pyrolysis of the ancillary plastics are not reached during NCT and HAC, the various plastics have no affect on the regulatory leakage criteria at those conditions.

4.1.1 Special Requirements for Plutonium

The proposed plutonium metal contents meet the current requirements set forth in 10 CFR 71.[3] In 10 CFR 71.63, "Shipments containing plutonium must be made with contents in solid form, if the contents contain greater than 0.74 TBq (20 Ci) of plutonium." This requirement is satisfied for the PAT-1 with the T-Ampoule and its packing because the proposed plutonium metal payload contents are solid, pure or alloyed plutonium metal or Pu/Be composite samples.

The PAT-1 Certificate of Compliance[2] (CoC) (USA/0361/B(U)F-96) (current Revision 9) in Item 5. (a) Packaging, (2) includes the description of the PAT-1,

"A stainless steel containment vessel (designated TB-1) surrounded by a stainless steel and redwood overpack (designated AQ-1). The contents are sealed within a stainless steel product can (designated PC-1) inside the containment vessel."

The "-96" in the certificate of compliance number indicates that the NRC has evaluated the PAT-1 against the current regulations (including 10 CFR 71.63) and determined that the package satisfies the current regulations. The CoC[2] identifies the TB-1 as the containment vessel.

For this addendum, the PAT-1 is unchanged from the inside surface of the TB-1 containment vessel to the outside surface of the AQ-1 overpack. The only change to the PAT-1 package is replacement of the PC-1 and its contents, top spacer and packing material with the T-Ampoule and its contents, Ring Filler and packing material. The T-Ampoule, a titanium container, provides eutectic prevention for the metal payload.

The proposed contents include plutonium metal in the form of hollow cylinders, disks, plates, solid cylinders and test samples. The plutonium metal contents are typically loaded into the T-Ampoule in a glove box containing a limited quantity of oxygen and moisture ($\leq$ 100 ppm). Prior to loading, the contents are brushed clean to remove any oxide present on the surface. The quantity of oxide that could form in the T-Ampoule during transport is limited by less than 100 ppm concentration of oxygen and moisture in the glove box atmosphere. The estimate of oxide formation due to this atmosphere is provided in Section 4.5.2.1 and is approximately 1.64 mg (3.62 E-6 lb). If the atmosphere is assumed to be air and because this is an oxygen-limited system, the estimated quantity of oxide formed on the metal contents is 3.46 g, the activity of PuO_2 formed is 3.74 Ci if no decay is assumed (100% Pu-241), and 0.397 Ci if 100% decay is assumed (100% Am-241). If the metal contents are not cleaned sufficiently, conservative estimates that double the quantity of oxide could be present on the metal, 6.92 g, which is less than 8 Ci.

The function of the T-Ampoule is to provide a safety barrier that prevents the formation of a eutectic between the plutonium metal contents and the iron in the TB-1 containment vessel. The structural analyses in Section 2 of this addendum demonstrate that the bore seal area (see Figure 4-1) of the T-Ampoule is not significantly deformed and is expected to remain intact for all accident conditions analyzed. It can be concluded from these analyses that the T-Ampoule is more robust than the PC-1.

The PC-1 Product Can used for the oxide shipment must not be used for the metal shipment since the iron in the can could possibly form a eutectic with the plutonium metal contents. The titanium material for the T-Ampoule was selected to provide a eutectic prevention barrier between the metallic Pu contents and the TB-1 containment vessel. The *Body, T-Ampoule* (Drawing 2A0259, designated T-Ampoule Body) and *Lid, T-Ampoule* (Drawing 2A0260, designated T-Ampoule Lid) are fabricated from a solid block of Ti-6Al-4V Grade 5 alloy. There are no welds, penetrations, valves, or pressure relief devices in the T-Ampoule. Once placed within the TB-1, the T-Ampoule cannot be opened unintentionally. The clearance between the T-Ampoule and the TB-1 is 0.038 cm (0.015 in.) all around; thus, both walls have immediate contact to resist the impact forces created by the deceleration of the internal Pu contents during the impact accident environment. The sample containers (*Sample Container-1 [SC-1] Assembly*, Drawing 2A0268, designated SC-1, and *Sample Container-2 [SC-2] Assembly*, Drawing 2A0265, designated SC-2) and structure (*Inner Cradle*, Drawing 2A0385, designated Inner Cradle) are also constructed of Ti-6Al-4V Grade 5 alloy that is resistant to the formation of eutectics with the plutonium metal content. Tantalum foil, which may be used to wrap and protect the samples from contamination, was selected for its resistance to eutectic formation.

The shielding evaluation in Section 5 of this addendum demonstrates that the package with plutonium metal contents complies with the dose rate limits of 10 CFR 71.47(a) (non-exclusive use) for the normal conditions of transport (NCT) and 10 CFR 71.51(a)(2) for hypothetical accident conditions (HAC). The criticality evaluation in Section 6 of this addendum demonstrates that the package with plutonium metal contents remains subcritical under NCT and HAC and has a CSI value of 0.1 per 10 CFR 71.59.

The modifications to the PAT-1 package are not significant with respect to design, operating characteristics, or safe operation of the PAT-1 package when subjected to the tests specified in 10 CFR 71.71 and 10 CFR 71.73:

- The PAT-1 package is unchanged from the inside surface of the TB-1 containment vessel to the outside surface of the AQ-1 overpack.
- The T-Ampoule and its contents, Ring Filler and packing material replace the PC-1 and its contents, top spacer and packing material and provide protection for its metal contents.
- The T-Ampoule is a eutectic prevention barrier between the plutonium metal contents and the stainless steel TB-1 containment vessel. The structural analysis in Section 2 of this addendum demonstrates that the T-Ampoule does not breach during the 10 CFR 71.71, 10 CFR 71.73, and 10 CFR 71.74 structural evaluations, thus maintaining its eutectic function.
- The structural analyses in Section 2 demonstrated that the TB-1 met containment requirements. The TB-1's containment capability will be unaffected by the addition of metals contents through the plutonium air transport tests.
- The packing materials within the T-Ampoule are also not susceptible to eutectic formation with plutonium metal.
- The structural analysis in Section 2, the thermal analysis in Section 3, the shielding analysis in Section 5, and the criticality analysis in Section 6 of this addendum show that the requirements of 10 CFR 71.19(d) are met because the modifications to PAT-1

package are not significant with respect to the design, operating characteristics, or safe performance of the package design when subjected to the tests specified in 10 CFR 71.71 and 10 CFR 71.73.

4.1.2 Plutonium Metal Contents

The proposed plutonium metal contents include:

- Electro-Refined (ER) Pu (Purity ≥ 99.8% Pu 239).
- Pu of various ages containing stabilization alloys such as gallium (Ga).
- Composite samples consisting of Pu and beryllium (Be) separated by an alpha barrier (Ti) to preclude neutron generation.
- The forms of the metal include hollow cylinders, cylinders, discs, strips, etc.
- The container configurations within the TB-1 containment vessel are:
- T-Ampoule for bulk metal hollow cylinders and sample containers; and
- Sample containers (SC-1 and SC-2) carried within the Inner Cradle of the T-Ampoule for smaller metal samples.

The isotopic compositions, masses, A_2 values, decay heat, activities, and impurities for ER plutonium metal, alloyed plutonium metal, and bonded plutonium metal are presented below.

4.1.2.1 ER Plutonium Metal[5]

The maximum ER content is 831 g (1.83 lb) for an isotopic composition that assumes no Pu-241 decay (see Table 4-3). The ER metal mass estimates for 3000 A_2 range from 831 g (1.83 lb) assuming no Pu-241 decay (Table 4-3), and 707 g (1.56 lb) assuming 100% Pu-241 decay (see Table 4-4). Table 4-4 assumes that all of the Pu-241 has decayed to Am-241 which results in the 707 g quantity for 3000 A_2. Note that Table 4-4 is used for comparative purposes only to determine the effect of assuming 100% Pu-241 decay to Am-241. The ER metal will be manufactured and shipped prior to significant Pu-241 decay. The minimum ER cylinder weight as documented in Table 1-1 of Section 1 is 731 g.

Table 4-3. 831 g (1.83 lb): 3,000 A_2 Quantity of ER Plutonium Metal Assuming No Pu-241 Decay to Am-241

831 grams: 3,000 A_2 quantity of ER Pu metal assuming 0% Pu241 decay to Am241									
Metal Mass (g) (max)	Mass % (max)	Grams (max)	LANL Specification 55Y-638728	Isotope	Pu Isotopic % (max)	Pu Isotopic mass (g)	Decay Heat (W)	Activity (Ci)	A_2
831.00	Plutonium 99.84%	Plutonium 829.67		Pu238	0.05%	0.41	2.35E-01	7.05E+00	2.61E+02
				Pu239*	92.35%	766.20	1.46E+00	4.75E+01	1.76E+03
				Pu240	6.50%	53.93	3.83E-01	1.24E+01	4.59E+02
				Pu241	1.00%	8.30	1.04E-01	8.30E+02	5.19E+02
				Pu242	0.10%	0.83	8.30E-05	3.24E-03	1.20E-01
				Am241	0.00%	0.00	0.00E+00	0.00E+00	0.00E+00
	Impurities 0.16%	Impurities 1.33		Impurities: N/A					
* stated as % balance						Total:	2.18E+00	8.97E+02	3.00E+03

Table 4-4. 707 g (1.56 lb): 3,000 A_2 Quantity of ER Plutonium Metal Assuming 100% Pu-241 Decay to Am-241

707 grams: 3,000 A_2 quantity of ER Pu metal assuming 100% Pu241 decay to Am241									
Metal Mass (g) (max)	Mass % (max)	Grams (max)	LANL Specification 55Y-638728	Isotope	Pu Isotopic % (max)	Pu Isotopic mass (g)	Decay Heat (W)	Activity (Ci)	A_2
707.00	Plutonium 99.84%	Plutonium 705.87		Pu238	0.05%	0.35	2.00E-01	6.00E+00	2.22E+02
				Pu239*	92.35%	651.87	1.24E+00	4.04E+01	1.50E+03
				Pu240	6.50%	45.88	3.26E-01	1.06E+01	3.91E+02
				Pu241	0.00%	0.00	0.00E+00	0.00E+00	0.00E+00
				Pu242	0.10%	0.71	7.06E-05	2.75E-03	1.02E-01
				Am241	1.00%	7.06	8.10E-01	2.40E+01	8.89E+02
	Impurities 0.16%	Impurities 1.13		Impurities: N/A					
* stated as % balance						Total:	2.57E+00	8.10E+01	3.00E+03
Note: Table shown for comparative purposes only. ER metal will be manufactured and shipped prior to significant Pu241 decay									

4.1.2.2 Alloyed Plutonium Metal[5]

The maximum contents in two SC-2 sample containers within the T-Ampoule are 676 g (1.49 lb). A_2 calculations were performed assuming 100% Pu-241 decay to Am-241 (2840 A_2) (see Table 4-5) and No Pu-241 decay (2410 A_2) (see Table 4-6). Alloyed plutonium metal may be shipped in a hollow log form in the T-Ampoule if the requirements in Table 1-1 of this addendum and the shipper are met.

Table 4-5. 676 g (1.49 lb): Alloyed Plutonium Metal Assuming 100% Pu-241 Decay to Am-241

676 grams: Alloyed Pu metal assuming 100% Pu241 decay to Am241									
Metal Mass (g) (max)	Mass % (max)	Grams (max)	LANL Specification 55Y-638728	Isotope	Pu Isotopic % (max)	Pu Isotopic mass (g)	Decay Heat (W)	Activity (Ci)	A_2
676.00	Plutonium 98.84%	Plutonium 668.16		Pu238	0.05%	0.33	1.89E-01	5.68E+00	2.10E+02
				Pu239*	92.35%	617.04	1.17E+00	3.83E+01	1.42E+03
				Pu240	6.50%	43.43	3.08E-01	9.99E+00	3.70E+02
				Pu241	0.00%	0.00	0.00E+00	0.00E+00	0.00E+00
				Pu242	0.10%	0.67	6.68E-05	2.61E-03	9.65E-02
				Am241	1.00%	6.68	7.67E-01	2.27E+01	8.41E+02
	Impurities 0.16%	Impurities 1.08		Impurities: N/A					
	Gallium 1.00%	Gallium 6.76		Gallium: N/A					
* stated as % balance						Total:	2.44E+00	7.66E+01	2.84E+03

Table 4-6. 676 g (1.49 lb): Alloyed Plutonium Metal Assuming No Pu-241 Decay to Am-241

676 grams: Alloyed Pu metal assuming 0% Pu241 decay to Am241									
Metal Mass (g) (max)	Mass % (max)	Grams (max)	LANL Specification 55Y-638728	Isotope	Pu Isotopic % (max)	Pu Isotopic mass (g)	Decay Heat (W)	Activity (Ci)	A_2
676.00	Plutonium 98.84%	Plutonium 668.16		Pu238	0.05%	0.33	1.89E-01	5.68E+00	2.10E+02
				Pu239*	92.35%	617.04	1.17E+00	3.83E+01	1.42E+03
				Pu240	6.50%	43.43	3.08E-01	9.99E+00	3.70E+02
				Pu241	1.00%	6.68	8.35E-02	6.68E+02	4.18E+02
				Pu242	0.10%	0.67	6.68E-05	2.61E-03	9.65E-02
				Am241	0.00%	0.00	0.00E+00	0.00E+00	0.00E+00
	Impurities 0.16%	Impurities 1.08		Impurities: N/A					
	Gallium 1.00%	Gallium 6.76		Gallium: N/A					
* stated as % balance						Total:	1.75E+00	7.22E+02	2.41E+03

4.1.2.3 Bonded Plutonium Metal[5]

A 60 g (0.13 lb) bonded 16.85 mm diameter × 16.85 mm height Pu/Be metal cylinder (or a number of smaller cylinders [up to 25 5.1 mm diameter × 5.1 mm height cylinders] as described in Table 1.1, Section 1 of this addendum) may each be shipped in the SC-1 sample container for a total payload weight of 180 g (0.39 lb) (657 A_2) or in the SC-2 sample container for a total payload weight of 120 g (0.26 lb) within the T-Ampoule. The composite payload weight is limited to 60 grams or less in each sample container. See Table 4-7 for estimate of curies, number of A_2, decay heat, weight, and isotopic composition of the Pu/Be material based upon a disk configuration.

Table 4-7. 60 g (0.13 lb): Bonded Pu/Be Metal Disk Assuming 100% Pu-241 Decay to Am-241

60 grams: Bonded Pu/Be metal disc assuming 100% Pu241 decay to Am241										
Composite %	Metal Mass (g) (max)	Mass % (max)	Grams (max)	LANL Specification 55Y-638728	Isotope	Pu Isotopic % (max)	Pu Isotopic mass (g)	Decay Heat (W)	Activity (Ci)	A_2
Pu metal 87.00%	52.20	MT52 Plutonium 98.84%	MT52 Plutonium 51.59		Pu238	0.05%	0.03	1.46E-02	4.39E-01	1.62E+01
					Pu239*	92.35%	47.65	9.05E-02	2.95E+00	1.09E+02
					Pu240	6.50%	3.35	2.38E-02	7.71E-01	2.86E+01
					Pu241	0.00%	0.00	0.00E+00	0.00E+00	0.00E+00
					Pu242	0.10%	0.05	5.16E-06	2.01E-04	7.45E-03
					Am241	1.00%	0.52	5.92E-02	1.75E+00	6.50E+01
		Impurities 0.16%	Impurities 0.08		Impurities: N/A					
		Gallium 1.00%	Gallium 0.52		Gallium: N/A					
Beryllium 13.00%	7.80	Beryllium 13.00%	Beryllium 7.80		Beryllium: N/A					
Alpha Barrier 0.00%	0.00	Alpha Barrier 0.00%	Alpha Barrier 0.00		Assumes no alpha barrier to yield maximum dose					
100.00%	60.00	◄◄◄ Totals ►►►						1.88E-01	5.92E+00	2.19E+02
*stated as % balance										

4.2 Containment under Normal Conditions of Transport (NCT)

The TB-1 containment vessel meets the regulatory acceptance standard for NCT of 10^{-6} A_2/hr as demonstrated in Table 4-1. The T-Ampoule is not a containment vessel under NCT.

The thermal analysis in Section 3.3 of this addendum, which analyzed a localized 25-watt (85.3 Btu/hr) thermal source against the O-ring seal of the T-Ampoule, indicated an average temperature of 103.3°C (218°F).

The internal pressure within the TB-1 during NCT with an internal heat generation of 25 watts (85.3 Btu/hr) from the plutonium metal contents indicated a maximum pressure of 18.8 psia, due to the temperature difference. The calculation assumes an initial room temperature of 20°C (70°F), then:

$$P2 = 1atm*(678/530R) = 1.28 \text{ atm or } \sim 18.8 \text{ psia}$$

To determine the pressure generated from the alpha decay of plutonium, the TB-1 was assumed to be filled at ambient temperature and to reach the NCT temperature quickly (see Section 4.5.3). The helium pressure, shown below, is thus:

$$P_{He} = n_{He}*(RT/V)$$

where $n_{He} = gm_{He}/4$

T = the NCT average temperature in Kelvin (absolute)
V = 1.252 liters

R = 0.082 l-atm/mole-K, the gas constant
Pressure in psi = 14.7*Pressure in atmospheres
The pressure from helium (He) generation for 1300 g Pu (for conservatism) at NCT temperature via alpha decay is 0.067 psia.

The total pressure as the result of internal heat generation and alpha decay is 18.9 psia, or 4.2 psig, which defines the maximum normal operating pressure (MNOP) for the TB-1.

The MNOP of 4.2 psig (18.9 psia) calculated above is slightly less than that calculated for the PuO_2 contents in the SAR (34.3 psia) since a small quantity of moisture was assumed to be present in the PuO_2 within the TB-1.

4.3 Containment under Hypothetical Accident Conditions (HAC)

The TB-1 meets the regulatory acceptance standard for HAC of A_2 in a week as documented in Table 4-1. The T-Ampoule is not a containment vessel under HAC.

The thermal analysis in Section 3.4 of this addendum includes localized heating produced by the plutonium metal contents, and the HAC evaluation indicated that the average temperature is 136°C (276°F) in the T-Ampoule. The temperature of the T-Ampoule seal does not exceed the manufacturer's specification for the operating range of the seal material (204°C [400°F]).

The pressure calculated within the TB-1 as the result of internal heat generation of 25 watts from the plutonium metal contents and the HAC indicated that the maximum pressure is 20.4 psi. The calculation assumes an initial room temperature of 21°C (70°F), then:

$$P2 = 1atm*(736R/530R) = 1.39 \text{ atm or } \sim 20.4 \text{ psia}$$

Pressure from He generation for 1300 g of Pu metal (for conservatism) via alpha decay is 0.073 psia from Section 4.5.3 of this addendum.

The total pressure as a result of internal heat generation and alpha decay is 20.5 psia. The pressure of 20.5 psia is less than the HAC pressure reported in the SAR[4] (38.7 psia [Section 3.5.4 of the SAR[4]]).

4.3.1 Containment under Plutonium Air Transport Fire Test

The TB-1 meets the regulatory acceptance standard for the plutonium air transport tests of A_2 in a week as documented in Table 4-1. The T-Ampoule is not a containment vessel under the plutonium air transport conditions.

In Section 2.12.8, an initial calculation was performed using an air-filled TB-1 as a realistic starting assumption to examine the rise in pressure from decomposition of the elastomeric O-rings within the T-Ampoule and two SC-2 or three SC-1 sample containers and a range of weights for ancillary plastics. The three SC-1 configurations and the selected 70 gram quantity of HDPE yielded the highest pressure rise of 572 psia. Including the rise in pressure from ambient temperature to 582°C (1080°F) of 42.7 psia and the helium pressure generation from 1300 g of plutonium (for conservatism) from alpha decay of 0.11 psia, the total pressure within

the TB-1 is 615 psia. The PAT-1 SAR,[4] Section 4.4.2 stipulates that the maximum allowable TB-1 pressure during the post-fire plutonium air transport accident condition was 1,110 psia.

A subsequent calculation was performed in Section 2.12.8 which assumed the no-char assumption for O-ring decomposition in LA-UR-10-05846 in Section 4.5.4. The no-char assumption was also used for decomposition of the ancillary plastic. The pressures from the original atmosphere, helium generation from alpha decay, O-ring decomposition and the pressure from ancillary plastics were set equal to 1110 psia, the pressure of the TB-1 from the post-fire plutonium air transport accident condition. The resulting ancillary plastic pressure was then used to determine the masses of the plastics that could be used within the TB-1. The various pressures from the components are reported in Table 11 in Section 2.12.8.

The results of the highly conservative calculation of the thermal degradation of *Viton A® O-rings* and ancillary plastic in Section 2.12.8 used the maximum internal pressure of 1110 psia. Therefore, this will be the pressure for plutonium air transport fire test for plutonium metals.

In summary, the TB-1 structure is unaffected by the impact and thermal environments and maintains its containment integrity for NCT, HAC, and the accident conditions for air transport of plutonium.

4.4 Leakage Rate Tests for Type B Packages

The leakage rate tests for the TB-1, which is the primary containment vessel, is described in Sections 7 and 8.

4.5 Appendix

4.5.1 References

1. United States. Nuclear Regulatory Commission. Code of Federal Regulations. 10 CFR 71. "Packaging and Transportation of Radioactive Material." January 1, 2009.

2. United States. Nuclear Regulatory Commission. "Certificate of Compliance for Radioactive Material Packages." Certificate Number 0361, Revision Number 9, Docket Number 71-0361, Package Identification Number USA/0361/B(U)F-96. March 4, 2009.

3. United States. Nuclear Regulatory Commission. Code of Federal Regulations. 10 CFR 71.63. "Special requirements for plutonium shipments," as published in 69 FR 3795. January 26, 2004.

4. United States. Nuclear Regulatory Commission. NUREG-0361, "Safety Analysis Report for the Plutonium Air Transportable Package, Model PAT-1." Washington, D.C. 1978.

5. Caviness, M. L., and J.B. Rubin. "Authorized Contents Proposed for the Plutonium Air Transporter (PAT-1) Packaging (U)," LA-UR-08-05154. Los Alamos National Laboratory. Los Alamos, NM: August 7, 2008.

6. Rubin, J. B. "Thermal Decomposition of Viton® O-rings for the PAT-1 Packaging Accident Scenario," LA-UR-10-05846. Los Alamos National Laboratory. Los Alamos, NM: August 31, 2010.

4.5.2 PAT-1 Contents

LA-UR-08-05154

Approved for public release; distribution is unlimited.

Title:	Authorized Contents Proposed for the Plutonium Air Transporter (PAT-1) Packaging (U)
Author(s):	Michael L. Caviness, PMT-3 Jim B. Rubin, PMT-2
Intended for:	Development of an application to the US Nuclear Regulatory Commission for the transport of plutonium metal by air in the Plutonium Air Transporter (PAT-1) packaging

Los Alamos
NATIONAL LABORATORY
EST.1943

Form 836 (7/06)

Authorized Contents Proposed for the Plutonium Air Transporter (PAT-1) Packaging

Authors: Michael Caviness, PMT-3, Nuclear Materials Management

Jim Rubin, PMT-2, Actinide Process Chemistry

PAT-1 Packaging Assembly

Page 1 of 5

ELECTRO-REFINED PLUTONUM METAL

1,300 grams: Maximum quantity of Electro-refined (ER) Pu metal excluding Pu241 decay

Metal Mass (g) (max)	Mass % (max)	Grams (max)	LANL Specification 55Y-638728	Isotope	Pu Isotopic % (max)	Pu Isotopic mass (g)	Decay Heat (W)	Activity (Ci)	A_2
1,300.00	Plutonium 99.84%	Plutonium 1297.92		Pu238	0.05%	0.65	3.68E-01	1.10 E+01	4.09 E+02
				Pu239*	92.35%	1198.63	2.28E+00	7.43 E+01	2.75 E+03
				Pu240	6.50%	84.36	5.99E-01	1.94 E+01	7.19 E+02
				Pu241	1.00%	12.98	1.62E-01	1.30 E+03	8.11 E+02
				Pu242	0.10%	1.30	1.30E-04	5.06 E-03	1.87 E-01
				Am241	0.00%	0.00	0.00E+00	0.00 E+00	0.00E +00
	Impurities 0.16%	Impurities 2.08		Impurities: N/A					
* stated as % balance						Total:	3.41E+00	1.40E+ 03	4.69E +03

Reference Values	
Decay Heat	
Isotope	Watts/ gram
Pu238	5.67E-01
Pu239	1.90E-03
Pu240	7.10E-03
Pu241	1.25E-02
Pu242	1.00E-04
Am241	1.15E-01
DOE-STD-3013-00, Table B-5	

831 grams: **3,000 A_2** quantity of ER Pu metal assuming 0% Pu241 decay to Am241

Metal Mass (g) (max)	Mass % (max)	Grams (max)	LANL Specification 55Y-638728	Isotope	Pu Isotopic % (max)	Pu Isotopic mass (g)	Decay Heat (W)	Activity (Ci)	A_2
831.00	Plutonium 99.84%	Plutonium 829.67		Pu238	0.05%	0.41	2.35E-01	7.05 E+00	2.61 E+02
				Pu239*	92.35%	766.20	1.46E+00	4.75 E+01	1.76 E+03
				Pu240	6.50%	53.93	3.83E-01	1.24 E+01	4.59 E+02
				Pu241	1.00%	8.30	1.04E-01	8.30 E+02	5.19 E+02
				Pu242	0.10%	0.83	8.30E-05	3.24 E-03	1.20 E-01
				Am241	0.00%	0.00	0.00E+00	0.00 E+00	0.00 E+00
	Impurities 0.16%	Impurities 1.33		Impurities: N/A					
* stated as % balance						Total:	2.18E+00	8.97 E+02	3.00 E+03

Reference Values		
A_2 values of radionuclides		
Isotope	A_2 (Ci)	Ci/g
Pu238	2.70E-02	1.70 E+01
Pu239	2.70E-02	6.20 E-02
Pu240	2.70E-02	2.30 E-01
Pu241	1.60E+00	1.00 E+02
Pu242	2.70E-02	3.90 E-03
Am241	2.70E-02	3.40 E+00
49 CFR 173.435, Table of A1 and A2 Values for Radionuclides		

707 grams: **3,000 A_2** quantity of ER Pu metal assuming 100% Pu241 decay to Am241

Metal Mass (g) (max)	Mass % (max)	Grams (max)	LANL Specification 55Y-638728	Isotope	Pu Isotopic % (max)	Pu Isotopic mass (g)	Decay Heat (W)	Activity (Ci)	A_2
707.00	Plutonium 99.84%	Plutonium 705.87		Pu238	0.05%	0.35	2.00E-01	6.00 E+00	2.22 E+02
				Pu239*	92.35%	651.87	1.24E+00	4.04 E+01	1.50 E+03
				Pu240	6.50%	45.88	3.26E-01	1.06 E+01	3.91 E+02
				Pu241	0.00%	0.00	0.00E+00	0.00 E+00	0.00 E+00
				Pu242	0.10%	0.71	7.06E-05	2.75 E-03	1.02 E-01
				Am241	1.00%	7.06	8.10E-01	2.40 E+01	8.89 E+02
	Impurities 0.16%	Impurities 1.13		Impurities: N/A					
* stated as % balance						Total:	2.57E+00	8.10 E+01	3.00 E+03

Note: Table shown for comparative purposes only. ER metal will be manufactured and shipped prior to significant Pu241 decay

Impurity Limits (max)		
Values in parts per million (ppm)		
Al: 100	Fe: 200	Ta: 100
Am: 200	Ga: 300	Th: 100
B: 50	Mg: 500	Ti: 100
Be: 3	Mn: 100	U: 100
C: 200	Ni: 100	W: 200
Ca: 500	Np: 100	Zn: 100
Cd: 10	Pb: 100	
Cr: 100	Si: 100	
Cu: 100	Sn: 100	
LANL Specification 55Y-638728		

ALLOYED PLUTONUM METAL

676 grams: Alloyed Pu metal assuming 0% Pu241 decay to Am241

Metal Mass (g) (max)	Mass % (max)	Grams (max)	LANL Specification 55Y-638728	Isotope	Pu Isotopic % (max)	Pu Isotopic mass (g)	Decay Heat (W)	Activity (Ci)	A_2
676.00	Plutonium 98.84%	Plutonium 668.16		Pu238	0.05%	0.33	1.89E-01	5.68 E+00	2.10 E+02
				Pu239*	92.35%	617.04	1.17E+00	3.83 E+01	1.42 E+03
				Pu240	6.50%	43.43	3.08E-01	9.99 E+00	3.70 E+02
				Pu241	1.00%	6.68	8.35E-02	6.68 E+02	4.18 E+02
				Pu242	0.10%	0.67	6.68E-05	2.61 E-03	9.65 E-02
				Am241	0.00%	0.00	0.00E+00	0.00 E+00	0.00 E+00
	Impurities 0.16%	Impurities 1.08		Impurities: N/A					
	Gallium 1.00%	Gallium 6.76		Gallium: N/A					
* stated as % balance						Total:	1.75E+00	7.22 E+02	2.41 E+03

Reference Values	
Decay Heat	
Isotope	Watts/ gram
Pu238	5.67E-01
Pu239	1.90E-03
Pu240	7.10E-03
Pu241	1.25E-02
Pu242	1.00E-04
Am241	1.15E-01
DOE-STD-3013-00, Table B-5	

676 grams: Alloyed Pu metal assuming 100% Pu241 decay to Am241

Metal Mass (g) (max)	Mass % (max)	Grams (max)	LANL Specification 55Y-638728	Isotope	Pu Isotopic % (max)	Pu Isotopic mass (g)	Decay Heat (W)	Activity (Ci)	A_2
676.00	Plutonium 98.84%	Plutonium 668.16		Pu238	0.05%	0.33	1.89E-01	5.68 E+00	2.10 E+02
				Pu239*	92.35%	617.04	1.17E+0 0	3.83 E+01	1.42 E+03
				Pu240	6.50%	43.43	3.08E-01	9.99 E+00	3.70 E+02
				Pu241	0.00%	0.00	0.00E+0 0	0.00 E+00	0.00 E+00
				Pu242	0.10%	0.67	6.68E-05	2.61 E-03	9.65 E-02
				Am241	1.00%	6.68	7.67E-01	2.27 E+01	8.41 E+02
	Impurities 0.16%	Impurities 1.08		Impurities: N/A					
	Gallium 1.00%	Gallium 6.76		Gallium: N/A					
* stated as % balance						Total:	2.44E+0 0	7.66 E+01	2.84 E+03

Reference Values		
A_2 values of radionuclides		
Isotope	A_2 (Ci)	Ci/g
Pu238	2.70 E-02	1.70 E+01
Pu239	2.70 E-02	6.20 E-02
Pu240	2.70 E-02	2.30 E-01
Pu241	1.60 E+00	1.00 E+02
Pu242	2.70 E-02	3.90 E-03
Am241	2.70 E-02	3.40 E+00
49 CFR 173.435, Table of A1 and A2 Values for Radionuclides		

Impurity Limits (max) Values in parts per million (ppm)		
Al: 100	Fe: 200	Ta: 100
Am: 200	Ga: N/A	Th: 100
B: 50	Mg: 500	Ti: N/A
Be: N/A	Mn: 100	U: 100
C: 200	Ni: 100	W: 200
Ca: 500	Np: 100	Zn: 100
Cd: 10	Pb: 100	
Cr: 100	Si: 100	
Cu: 100	Sn: 100	
LANL Specification 55Y-638728		

BONDED PLUTONUM METAL

60 grams: Bonded Pu/Be metal disc assuming 100% Pu241 decay to Am241

Com-posite %	Metal Mass (g) (max)	Mass % (max)	Grams (max)	LANL Specification 55Y-638728
Pu metal 87.00%	52.20	MT52 Plutonium 98.84%	MT52 Plutonium 51.59	
		Impurities 0.16%	Impurities 0.08	
		Gallium 1.00%	Gallium 0.52	
Beryllium 13.00%	7.80	Beryllium 13.00%	Beryllium 7.80	
Alpha Barrier 0.00%	0.00	Alpha Barrier 0.00%	Alpha Barrier 0.00	
100.00%	60.00	◄◄◄ Totals ►►►		
*stated as % balance				

Isotope	Pu Isotopic % (max)	Pu Isotopic mass (g)	Decay Heat (W)	Activity (Ci)	A_2
Pu238	0.05%	0.03	1.46E-02	4.39 E-01	1.62 E+01
Pu239*	92.35%	47.65	9.05E-02	2.95 E+00	1.09 E+02
Pu240	6.50%	3.35	2.38E-02	7.71 E-01	2.86 E+01
Pu241	0.00%	0.00	0.00E+00	0.00 E+00	0.00 E+00
Pu242	0.10%	0.05	5.16E-06	2.01 E-04	7.45 E-03
Am241	1.00%	0.52	5.92E-02	1.75 E+00	6.50 E+01
Impurities: N/A					
Gallium: N/A					
Beryllium: N/A					
Assumes no alpha barrier to yield maximum dose					
			1.88E-01	5.92 E+00	2.19 E+02

Dose rate calculations:

Total (max) dose (5X)	Surface	0.3m (1ft)	1.0m (3.3 ft)
	9.72E+03	2.65E-01	2.45E-02

The maximum dose rates stated above assumes the following: 1) three bonded Pu/Be disks are assumed to preferentially stack during HAC conditions (see layout at right), 2) the alpha barrier between the 3 bonded Pu/Be disks are conservatively ignored, 3) the 3 bonded Pu/Be disks without alpha barriers yield 5 instances of Pu/Be contact surfaces, and 4) the dose rate is calculated for 5X a given Pu/Be surface area of an undefined disk diameter (max)***.

*** The bonded Pu/Be disk diameter is not stated due to a security classification determination. The information (disk diameter) is available through classified communication.

Unit dose (mrem/h/cm2) provided in LANL Memorandum, RP-3-08-32, Crawford to Caviness, Subject: MT52-Be Interface Disc Dose Calculations

Configuration Layout

The following configuration shows 3 bonded Pu/Be disks preferentially stacked with the alpha barriers conservatively removed to yield 5 instances of Pu/Be contact surfaces.

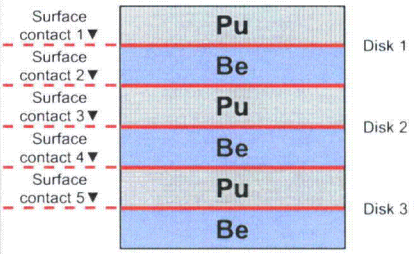

Reference Values	
Decay Heat	
Isotope	Watts/ gram
Pu238	5.67E-01
Pu239	1.90E-03
Pu240	7.10E-03
Pu241	1.25E-02
Pu242	1.00E-04
Am241	1.15E-01
DOE-STD-3013-00, Table B-5	

Reference Values		
A_2 values of radionuclides		
Isotope	A_2 (Ci)	Ci/g
Pu238	2.70 E-02	1.70 E+01
Pu239	2.70 E-02	6.20E -02
Pu240	2.70 E-02	2.30 E-01
Pu241	1.60 E+00	1.00 E+02
Pu242	2.70 E-02	3.90 E-03
Am241	2.70 E-02	3.40 E+00
49 CFR 173.435, Table of A1 and A2 Values for Radionuclides		

Impurity Limits (max)		
Values in parts per million (ppm)		
Al: 100	Fe: 200	Ta: 100
Am: 200	Ga: N/A	Th: 100
B: 50	Mg: 500	Ti: N/A
Be: N/A	Mn: 100	U: 100
C: 200	Ni: 100	W: 200
Ca: 500	Np: 100	Zn: 100
Cd: 10	Pb: 100	
Cr: 100	Si: 100	
Cu: 100	Sn: 100	
LANL Specification 55Y-638728		

Maximum PU Oxide and Curies (CI) formed in the TB-1 with a 21% Oxygen

Oxide and Curie Values					
No Pu-241decay (100% Pu-241)			100% Pu-241decay (100% Am-241)		
Isotope	Oxide (g)	Curies	Isotope	Oxide (g)	Curies
Pu-238	1.73E-03	2.94E-02	Pu-238	1.73E-03	2.94E-02
Pu-239	3.20E+00	1.98E-01	Pu-239	3.20E+00	1.98E-01
Pu-240	2.25E-01	5.17E-02	Pu-240	2.25E-01	5.17E-02
Pu-241	3.46E-02	3.46E+00	Pu-241	0.00E+00	0.00E+00
Pu-242	3.46E-03	1.35E-05	Pu-242	3.50E-03	1.37E-05
Am-241	0.00E+00	0.00E+00	Am-241	3.46E-02	1.18E-01
Total:	3.46E+00	3.74E+00	Total:	3.46E+00	3.97E-01

Isotopic % (max)	
Pu-238	0.05%
Pu-239	92.35%
Pu-240	6.50%
Pu-241	1.00%
Pu-242	0.10%
Am-241	0.00%
LANL Specification 55Y-638728	

Reference Values		
radionuclides		
Isotope	A_2(Ci)	Ci/g
Pu-238	2.70E-02	17.0E+01
Pu-239	2.70E-02	6.20E-02
Pu-240	2.70E-02	2.30E-01
Pu-241	1.60E+00	1.00E+02
Pu-242	2.70E-02	3.90E-03
Am-241	2.70E-02	3.40E+00
49 CFR 173.435, Table of A_1 and A_2 Values for Radionuclides		

Basis of Calculated Values			
Variable:	Variable Unit:	Value	Definition of value
pressure inside of TB-1 P	atmosphere (atm)	0.21	1atmosphere pressure at 21% O_2 in TB-1
Internal volume of TB-1 V	cubic centimeters (cm^3)	1460.00	internal volume of TB-1without contents as stated in the PAT-1SAR
universal gas constant, R	constant	82.06	gas constant values based on pressure and volume units
temperature, T	kelvin (K)	298.00	assumes room temperature of 25°C
O_2 in TB-1internal volume, n	moles	0.013	n = PV/RT (ideal gas law is suitable since the compressibility factor (Z) for air at 1.01bar and 15°C(59°F) is 0.9992)
PuO_2 formed from O_2 in the TB-1 m	moles	0.013	$Pu(s) + O_2(g) \rightarrow PuO_2(s)$
Molar mass PuO_2, M	constant	276	grams per mole (assuming molar mass of Pu = 244)
PuO_2 formed, g	grams (g)	3.46	grams of PuO_2 formed when all O_2 reacts completely in the sealed TB-1

Basis of Calculated Values			
Variable:	Variable Unit:	Value	Definition of value
pressure inside of TB-1 P	atmosphere (atm)	0.00010	1atmosphere pressure at 100ppm O_2 in TB-1
Internal volume of TB-1 V	cubic centimeters (cm^3)	1460.00	internal volume of TB-1without contents as stated in the PAT-1SAR
universal gas constant, R	constant	82.06	gas constant values based on pressure and volume units
temperature, T	kelvin (K)	298.00	assumes room temperature of 25°C
O_2 in TB-1internal volume, n	moles	5.97E-06	n = PV/RT (ideal gas law is suitable since the compressibility factor (Z) for air at 1.01bar and 15°C (59°F) is 0.9992)
PuO_2 formed from O_2 in the TB-1 m	moles	5.97E-06	$Pu(s) + O_2(g) \rightarrow PuO_2(s)$
Molar mass PuO_2, M	constant	276.06	grams per mole (assuming molar mass of Pu = 244)
PuO_2 formed, g	grams (g)	1.65E-03	grams of PuO_2 formed when all O_2 reacts completely in the sealed TB-1

4.5.2.1 Summary of Maximum Pu Oxide and Curies (Ci) Formed in the TB-1 with 21% and 100 ppm Oxygen:

An analysis[1] was performed to determine the maximum quantity of PuO_2 that would form on the plutonium metal content contained within the TB-1 containment vessel. The table on Page 5 of 5 in LA-UR-08-05154 in this appendix presents the analysis methodology for calculating the quantities of oxides formed. The TB-1, which is normally filled with glove box atmosphere, was assumed to contain 1 atmosphere of air at 21% O_2. Using a TB-1 conservative internal empty volume of 1460 cm^3 (89.19 in^3) and the Ideal Gas Law, there are 0.013 moles of O_2 in the internal volume and 0.013 moles of PuO_2 in the TB-1. The molar mass of PuO_2 is 276 g/mole assuming a molar mass of Pu = 244. The quantity of PuO_2 formed is 3.46 g when all of the O_2 reacts completely inside of a sealed TB-1. Because this is an oxygen-limited system, no more than 3.46 g (0.0076 lb) of PuO_2 are formed when all of the O_2 completely reacts inside of a sealed TB-1 containment vessel.

If a glove box atmosphere (assume all 100 ppm oxygen in an inert atmosphere) is assumed within the TB-1, the quantity of PuO_2 formed on the surface of the plutonium metal content is 1.64 mg (3.62 E-6 lb).

To determine the isotopic composition of the PuO_2 that was formed, Los Alamos National Laboratory (LANL) Specification 55Y-638728[4] on Page 5 of 5 in LA-UR-08-0514 in this appendix presents the maximum isotopic composition for the Pu contents. Included in the table are oxide and curie values assuming no decay (100% Pu-241) and 100% Pu-241 decay to Am-241.

The above calculations provide estimates of the amount of oxides formed due to the oxygen present in the T-Ampoule from the glovebox atmosphere and assumption of air. The oxide formation does not affect the safety of the package since the containment analysis assumed that all of the plutonium material was in its most dispersible form.

4.5.2.2 Reference

1. Caviness, M. L., and J.B. Rubin. "Authorized Contents Proposed for the Plutonium Air Transporter (PAT-1) Packaging (U)," LA-UR-08-05154. Los Alamos National Laboratory. Los Alamos, NM: August 7, 2008.

4.5.3 Helium Generation

PAT-1 Analyses for Helium Generation

Ruth F. Weiner

Sandia National Laboratories

Calculation of Helium Production

A helium is produced when an alpha particle, which is a helium nucleus, picks up an electron. The production rate of helium is thus directly proportional to the production rate of alpha particles. The production rate of alpha particles is equal to the rate of decay of alpha emitters: each decay results in an alpha particle. The basic equation for radioactive decay is

$$N = N_0 \exp(-\lambda t) \qquad (1)$$

Where N = the number of atoms of the radionuclide at time t
N_0= the number of atoms of the radionuclide at time t=0
$\lambda = \ln 2/t_{1/2}$; $t_{1/2}$ is the half life of the radionuclide

When a radionuclide emits an alpha particle, the atomic number decreases by 2 and the mass number decreases by 4, because an alpha particle is a helium nucleus: $_2He^4$. The radionuclides in delta plutonium emit alpha particles by the following equations:

$_{94}Pu^{238} = \alpha + {}_{92}U^{234}$
$_{94}Pu^{239} = \alpha + {}_{92}U^{235}$
$_{94}Pu^{240} = \alpha + {}_{92}U^{236}$
$_{94}Pu^{242} = \alpha + {}_{92}U^{238}$

However, $_{94}Pu^{241}$ is a beta emitter and decays by the equation $_{94}Pu^{241} = \beta^- + {}_{95}Am^{241}$ since a beta particle is the same as an electron. $_{95}Am^{241}$ decays by emitting an alpha particle by the equation

$_{95}Am^{241} = \alpha + {}_{93}Np^{237}$

Table1 gives the radioactive composition of delta plutonium and the half-lives of each radioactive component:

Table 1. Radioactive Composition of Delta and Half-Lives of Each Radioactive Component

Element	Atomic mass	gm/gm delta[1]	$t_{1/2}$ (yr)	$t_{1/2}$ sec	λ	Bq/gm delta	Ci/gm delta
Pu	238	0.0001	87.7	2.77E+09	2.51E-10	6.34E+07	1.71E-03
Pu	239	0.9378	24100	7.60E+11	9.12E-13	2.15E+09	5.82E-02
Pu	240	0.06	6560	2.07E+11	3.35E-12	5.04E+08	1.36E-02
Pu	241	0.002	14.4	4.54E+08	1.53E-09	7.62E+09	2.06E-01
Pu	242	0.0002	3.75E+05	1.18E+13	5.86E-14	2.92E+04	7.88E-07
Am	241	0	432	1.36E+10	5.09E-11	0	0
U	234	0	2.46E+05	7.76E+12	8.93E-14	0	0

One Becquerel (Bq) is = sec^{-1}. The numbers in the last column were obtained by the equation that converts mass to radioactivity:

$$Bq = \frac{(ln2)(6.02 \times 10^{23})\left(\frac{gm}{gm\ atomic\ wt}\right)}{t_{1/2}} \qquad (2)$$

Where Bq = the radioactivity in sec^{-1}; one curie (Ci) = 3.7×10^{10} Bq.

6.02×10^{23} is Avogadro's number, the number of atoms in one gram atomic weight
$t_{1/2}$ = half life of the radionuclide in seconds.
$\ln(2)/t_{1/2} = \lambda$

So that, e.g.,

$6.34 \times 10^{7} = \lambda\ (6.02 \times 10^{23})(0.0001/238) = (2.51 \times 10^{-10})\ (6.02 \times 10^{23})(0.0001/238)$

The last column in Table 1 thus gives the initial activity—the N_0—of each radionuclide.

$_{95}Am^{241}$ builds up as $_{94}Pu^{241}$ decays, by the first Bateman equation

$$N_{Am}(t) = N_{Pu}(t) * \left(\frac{\lambda_{Pu}}{\lambda_{Am} - \lambda_{Pu}}\right) * \{exp(-\lambda_{Pu}t) - exp(-\lambda_{Am}t)\}$$

Where $N_{Am}(t)$ = the number of $_{95}Am^{241}$ atoms at time t

$N_{Pu}(t)$ = the number of $_{94}Pu^{241}$ atoms at time t

Am refers to $^{95}Am^{241}$

Pu refers to $_{94}Pu^{241}$

$_{92}U^{234}$ builds up by a similar equation. Because of its long half-life, however, its alpha decay does not contribute significantly to helium production.

Conversion from radioactivity to weight can be done in two ways—by using Equation (2) or by calculating Bq/gm delta or Ci/gm delta from Table 1 (which is based on Equation (2)). The latter was used, resulting in Table 2. The values for $_{95}Am^{241}$ and $_{92}U^{234}$ were calculated using Equation (2).

Table 2. Weight Conversions

Element	gm/gm delta	Ci/gm delta	Ci/gm
Pu-238	0.0001	1.71E-03	1.71E-03
Pu-239	0.9378	5.82E-02	6.21E-02
Pu-240	0.06	1.36E-02	2.27E-01
Pu-241	0.002	2.06E-01	1.03E+02
Pu-242	0.0002	7.88E-07	3.94E-03
Am-241	0	0	3.43
U-234	0	0	6.21E-03

Every decay produces an alpha particle and every alpha particle becomes a helium atom. Equation (1) allows calculation of decay of each radionuclide, and Equation (2) relates that decay to loss of mass of that radionuclide. Because of conservation of mass, the mass of He produced is equal to the total loss of mass of the decaying radionuclides, or

$$gm(He_t) = gm(delta_{t=0})-\{gm(Pu\text{-}238_t)+gm(Pu\text{-}239_t)+gm(Pu\text{-}240_t)+gm(Pu\text{-}241_t)+ gm(Pu\text{-}242_t)+ gm(Am\text{-}241_t)+ gm(U\text{-}234_t)\} \quad (3)$$

where the subscript t is time.

Calculation of Gas Pressure

The basic equation is the Ideal Gas Law:

$$pV = nRT$$
$$p = nRT/V \quad (4)$$

where p = total pressure in the volume V
V = void volume
T = absolute temperature (K)
N = number of moles of gas
R = the gas constant, 0.082 liter-atm/mole-K

Calculations were done using liters, atmospheres, etc., and converted to psia at the end. Conversions used were:

1 mole He = 4 grams
$n(He_t) = gm(He_t)/4$
$gm(He_t)$: from Equation (3).
K = °C + 273
1 atm = 14.7 psia

Since the container was initially filled at atmospheric pressure, the total pressure in atmospheres at any time t, at a particular volume and temperature, is

$$p_t = 1 + p(He_t) = 1 + n(He_t)*RT/V \quad (5)$$

The TB-1 and the TB-1 internal configurations were considered. From Table 3, the SC-1 and SC-2 quantities were less the 831 g Electro-Refined (ER) Pu hollow cylinder. The 1300 gram Pu metal hollow cylinder represents an upper limit of the quantity of Pu metal considered for the PAT-1 and is presented for reference. Consequently, pressure calculations for alpha decay were only performed for the 831 and 1300 gram amounts. The temperatures considered were the "normal" extremes, -40°C (-40°F) NCT temperature (104°C), 136°C (276°F) HAC fire temperature, and 582°C (1080°F) in the accident conditions of plutonium air transport fire. A calculation at room temperature (21°C) was provided for reference.

Containments were assumed to be loaded at 1 atmosphere pressure (14.7 psi). Table 3 presents RT/V at these temperatures and volumes.

A 1300 g evaluation is provided for reference in Tables 3, 5, and 7; 831 g is the maximum plutonium content for this addendum. Helium generation was calculated from the mass loss of

the Pu isotopic mixture. Table 4 shows the helium generation, per g of plutonium isotopic mixture, for the first year.

Table 3. RT/V for TB-1 Containment

	Maximum Plutonium Mass (g)	676.00	523.00	831.00	1300.00
		Void Volume TB-1 Containment Boundary (liters)			
		1.1103	1.1112	1.2749	1.2519
Deg C	Deg K	P=RT/V(atm/mole)[a]			
104	377	27.84	27.82	24.25	24.69
-40	233	17.21	17.19	14.99	15.26
136	409	30.21	30.18	26.31	26.79
20	293	21.64	21.62	18.85	19.19
582	855	63.15	63.09	54.99	56.00

[a]R=0.082 liter-atm/mole-deg

Table 4. Helium Generation Per Gram of Pu Isotopic Mixture for One Year

Time (weeks)	gm Pu	gm He	moles He	Time (weeks)	gm Pu	gm He	moles He
0	1.00E+00	0.00E+00	0.00E+00	28	1.00E+00	3.06E-07	7.65E-08
2	1.00E+00	2.19E-08	5.46E-09	30	1.00E+00	3.28E-07	8.20E-08
4	1.00E+00	4.37E-08	1.09E-08	32	1.00E+00	3.50E-07	8.74E-08
6	1.00E+00	6.56E-08	1.64E-08	34	1.00E+00	3.72E-07	9.29E-08
8	1.00E+00	8.74E-08	2.19E-08	36	1.00E+00	3.93E-07	9.83E-08
10	1.00E+00	1.09E-07	2.73E-08	38	1.00E+00	4.15E-07	1.04E-07
12	1.00E+00	1.31E-07	3.28E-08	40	1.00E+00	4.37E-07	1.09E-07
14	1.00E+00	1.53E-07	3.82E-08	42	1.00E+00	4.59E-07	1.15E-07
16	1.00E+00	1.75E-07	4.37E-08	44	1.00E+00	4.81E-07	1.20E-07
18	1.00E+00	1.97E-07	4.92E-08	46	1.00E+00	5.03E-07	1.26E-07
20	1.00E+00	2.19E-07	5.46E-08	48	1.00E+00	5.24E-07	1.31E-07
22	1.00E+00	2.40E-07	6.01E-08	50	1.00E+00	5.46E-07	1.37E-07
24	1.00E+00	2.62E-07	6.56E-08	52	1.00E+00	5.68E-07	1.42E-07
26	1.00E+00	2.84E-07	7.10E-08				

The partial pressure of helium and the total pressure in the containment depend on the containment volume and on the temperature. The total pressure is the sum of the partial pressure of helium and the pressure at which the containment was loaded; the latter is assumed to be one atmosphere (14.7 psi).

The container was assumed to be filled at ambient temperature (294 K or 21 deg. C) and to reach the indicated temperature quickly. At two weeks the indicated temperature would have been reached. The helium pressure, shown in Table 3, is thus:

$$P_{He} = n_{He}*(RT/V)$$

where $n_{He} = gm_{He}/4$

T= the final average temperature in Kelvin (absolute)
V = 1.252 liters
R = 0.082 l-atm/mole K, the gas constant.
Pressure in psi= 14.7*Pressure in atmospheres

Table 5 shows helium pressure increase in atm and psi in the TB-1 in weeks up to one year assuming 1300 g Pu content.

Table 5. Helium Pressure Increase in TB-1, Void Volume 1.252 Liters, for 1300 g Pu

	deg C	104	-40	136	582	104	-40	136	582
	Kelvin	377	233	409	855	377	233	409	855
	RT/V	24.69	15.26	26.79	56.18	24.69	15.26	26.79	56.18
	gm Pu	1300.0	1300.0	1300.0	1300.0	1300.0	1300.0	1300.0	1300.0
Weeks	mole He/gm	Atmospheres				PSI			
0	0.000	0.000	0.000	0.000	0.000	0.000	0.000	0.000	0.000
2	5.46E-09	1.75E-04	1.08E-04	1.90E-04	3.98E-04	2.58E-03	1.59E-03	2.80E-03	5.85E-03
4	1.09E-08	3.51E-04	2.17E-04	3.81E-04	7.96E-04	5.16E-03	3.19E-03	5.59E-03	1.17E-02
6	1.64E-08	5.26E-04	3.25E-04	5.71E-04	1.19E-03	7.74E-03	4.78E-03	8.39E-03	1.75E-02
8	2.19E-08	7.02E-04	4.34E-04	7.61E-04	1.59E-03	1.03E-02	6.37E-03	1.12E-02	2.34E-02
10	2.73E-08	8.77E-04	5.42E-04	9.51E-04	1.99E-03	1.29E-02	7.97E-03	1.40E-02	2.92E-02
12	3.28E-08	1.05E-03	6.50E-04	1.14E-03	2.39E-03	1.55E-02	9.56E-03	1.68E-02	3.51E-02
14	3.82E-08	1.23E-03	7.59E-04	1.33E-03	2.78E-03	1.80E-02	1.12E-02	1.96E-02	4.09E-02
16	4.37E-08	1.40E-03	8.67E-04	1.52E-03	3.18E-03	2.06E-02	1.27E-02	2.24E-02	4.68E-02
18	4.92E-08	1.58E-03	9.76E-04	1.71E-03	3.58E-03	2.32E-02	1.43E-02	2.52E-02	5.26E-02
20	5.46E-08	1.75E-03	1.08E-03	1.90E-03	3.98E-03	2.58E-02	1.59E-02	2.80E-02	5.85E-02
22	6.01E-08	1.93E-03	1.19E-03	2.09E-03	4.38E-03	2.84E-02	1.75E-02	3.08E-02	6.43E-02
24	6.56E-08	2.10E-03	1.30E-03	2.28E-03	4.77E-03	3.09E-02	1.91E-02	3.36E-02	7.02E-02
26	7.10E-08	2.28E-03	1.41E-03	2.47E-03	5.17E-03	3.35E-02	2.07E-02	3.64E-02	7.60E-02
28	7.65E-08	2.46E-03	1.52E-03	2.66E-03	5.57E-03	3.61E-02	2.23E-02	3.92E-02	8.19E-02
30	8.20E-08	2.63E-03	1.63E-03	2.85E-03	5.97E-03	3.87E-02	2.39E-02	4.20E-02	8.77E-02
32	8.74E-08	2.81E-03	1.73E-03	3.04E-03	6.36E-03	4.13E-02	2.55E-02	4.48E-02	9.36E-02
34	9.29E-08	2.98E-03	1.84E-03	3.23E-03	6.76E-03	4.38E-02	2.71E-02	4.76E-02	9.94E-02
36	9.83E-08	3.16E-03	1.95E-03	3.43E-03	7.16E-03	4.64E-02	2.87E-02	5.03E-02	1.05E-01
38	1.04E-07	3.33E-03	2.06E-03	3.62E-03	7.56E-03	4.90E-02	3.03E-02	5.31E-02	1.11E-01
40	1.09E-07	3.51E-03	2.17E-03	3.81E-03	7.96E-03	5.16E-02	3.19E-02	5.59E-02	1.17E-01
42	1.15E-07	3.68E-03	2.28E-03	4.00E-03	8.35E-03	5.41E-02	3.35E-02	5.87E-02	1.23E-01
44	1.20E-07	3.86E-03	2.38E-03	4.19E-03	8.75E-03	5.67E-02	3.51E-02	6.15E-02	1.29E-01
46	1.26E-07	4.03E-03	2.49E-03	4.38E-03	9.15E-03	5.93E-02	3.66E-02	6.43E-02	1.34E-01
48	1.31E-07	4.21E-03	2.60E-03	4.57E-03	9.55E-03	6.19E-02	3.82E-02	6.71E-02	1.40E-01
50	1.37E-07	4.38E-03	2.71E-03	4.76E-03	9.94E-03	6.45E-02	3.98E-02	6.99E-02	1.46E-01
52	1.42E-07	4.56E-03	2.82E-03	4.95E-03	1.03E-02	6.70E-02	4.14E-02	7.27E-02	1.52E-01

Table 6 shows the helium pressure increase in atm and psi in the TB-1, in weeks up to one year assuming an 831 g Pu content.

Table 6. Helium Pressure in TB-1, Void Volume 1.275 Liters, for 831 g Pu

	deg C	104	-40	136	582	104	-40	136	582
	deg K	377	233	409	855	377	233	409	855
	RT/V	24.25	14.99	26.31	54.99	24.25	14.99	26.31	54.99
	gm Pu	831	831	831	831	831	831	831	831
Weeks	mole He/gm	Atmospheres				PSI			
0	0.00	0.00	0.00	0.00	0.00	0.0000	0.0000	0.0000	0.000
2	5.46E-09	1.10E-04	6.80E-05	1.19E-04	2.50E-04	0.0016	0.0010	0.0018	0.004
4	1.09E-08	2.20E-04	1.36E-04	2.39E-04	4.99E-04	0.0032	0.0020	0.0035	0.007
6	1.64E-08	3.30E-04	2.04E-04	3.58E-04	7.49E-04	0.0049	0.0030	0.0053	0.011
8	2.19E-08	4.40E-04	2.72E-04	4.78E-04	9.99E-04	0.0065	0.0040	0.0070	0.015
10	2.73E-08	5.50E-04	3.40E-04	5.97E-04	1.25E-03	0.0081	0.0050	0.0088	0.018
12	3.28E-08	6.61E-04	4.08E-04	7.17E-04	1.50E-03	0.0097	0.0060	0.0105	0.022
14	3.82E-08	7.71E-04	4.76E-04	8.36E-04	1.75E-03	0.0113	0.0070	0.0123	0.026
16	4.37E-08	8.81E-04	5.44E-04	9.56E-04	2.00E-03	0.0129	0.0080	0.0140	0.029
18	4.92E-08	9.91E-04	6.12E-04	1.07E-03	2.25E-03	0.0146	0.0090	0.0158	0.033
20	5.46E-08	1.10E-03	6.80E-04	1.19E-03	2.50E-03	0.0162	0.0100	0.0176	0.037
22	6.01E-08	1.21E-03	7.48E-04	1.31E-03	2.75E-03	0.0178	0.0110	0.0193	0.040
24	6.56E-08	1.32E-03	8.17E-04	1.43E-03	3.00E-03	0.0194	0.0120	0.0211	0.044
26	7.10E-08	1.43E-03	8.85E-04	1.55E-03	3.25E-03	0.0210	0.0130	0.0228	0.048
28	7.65E-08	1.54E-03	9.53E-04	1.67E-03	3.50E-03	0.0227	0.0140	0.0246	0.051
30	8.20E-08	1.65E-03	1.02E-03	1.79E-03	3.75E-03	0.0243	0.0150	0.0263	0.055
32	8.74E-08	1.76E-03	1.09E-03	1.91E-03	3.99E-03	0.0259	0.0160	0.0281	0.059
34	9.29E-08	1.87E-03	1.16E-03	2.03E-03	4.24E-03	0.0275	0.0170	0.0298	0.062
36	9.83E-08	1.98E-03	1.22E-03	2.15E-03	4.49E-03	0.0291	0.0180	0.0316	0.066
38	1.04E-07	2.09E-03	1.29E-03	2.27E-03	4.74E-03	0.0307	0.0190	0.0334	0.070
40	1.09E-07	2.20E-03	1.36E-03	2.39E-03	4.99E-03	0.0324	0.0200	0.0351	0.073
42	1.15E-07	2.31E-03	1.43E-03	2.51E-03	5.24E-03	0.0340	0.0210	0.0369	0.077
44	1.20E-07	2.42E-03	1.50E-03	2.63E-03	5.49E-03	0.0356	0.0220	0.0386	0.081
46	1.26E-07	2.53E-03	1.56E-03	2.75E-03	5.74E-03	0.0372	0.0230	0.0404	0.084
48	1.31E-07	2.64E-03	1.63E-03	2.87E-03	5.99E-03	0.0388	0.0240	0.0421	0.088
50	1.37E-07	2.75E-03	1.70E-03	2.99E-03	6.24E-03	0.0405	0.0250	0.0439	0.092
52	1.42E-07	2.86E-03	1.77E-03	3.11E-03	6.49E-03	0.0421	0.0260	0.0456	0.095

Table 7 presents helium pressure increase for all four masses of Pu at ambient temperature (21°C; 294 K) with their respective void volumes.

Table 7. Helium Pressure Increase in TB-1, Void Volume at 21 degrees C (294 K)

	V (liters	1.1103	1.1112	1.2749	1.2519	1.1103	1.1112	1.2749	1.2519
	RT/V	21.71	21.70	18.91	19.26	21.71	21.70	18.91	19.26
	gm Pu	676.00	523.00	831.00	1300.00	676.00	523.00	831.00	1300.0
Week	mole He/gm	Atmospheres				PSI			
0	0.00	0.00	0.00	0.00	0.00	0.00	0.00	0.00	0.00
2	5.46E-09	8.02E-05	6.20E-05	8.59E-05	1.37E-04	1.18E-03	9.11E-04	1.26E-03	2.01E-03
4	1.09E-08	1.60E-04	1.24E-04	1.72E-04	2.74E-04	2.36E-03	1.82E-03	2.52E-03	4.02E-03
6	1.64E-08	2.41E-04	1.86E-04	2.58E-04	4.10E-04	3.54E-03	2.73E-03	3.79E-03	6.03E-03
8	2.19E-08	3.21E-04	2.48E-04	3.43E-04	5.47E-04	4.72E-03	3.65E-03	5.05E-03	8.04E-03
10	2.73E-08	4.01E-04	3.10E-04	4.29E-04	6.84E-04	5.89E-03	4.56E-03	6.31E-03	1.01E-02
12	3.28E-08	4.81E-04	3.72E-04	5.15E-04	8.21E-04	7.07E-03	5.47E-03	7.57E-03	1.21E-02
14	3.82E-08	5.61E-04	4.34E-04	6.01E-04	9.57E-04	8.25E-03	6.38E-03	8.83E-03	1.41E-02
16	4.37E-08	6.42E-04	4.96E-04	6.87E-04	1.09E-03	9.43E-03	7.29E-03	1.01E-02	1.61E-02
18	4.92E-08	7.22E-04	5.58E-04	7.73E-04	1.23E-03	1.06E-02	8.20E-03	1.14E-02	1.81E-02
20	5.46E-08	8.02E-04	6.20E-04	8.59E-04	1.37E-03	1.18E-02	9.11E-03	1.26E-02	2.01E-02
22	6.01E-08	8.82E-04	6.82E-04	9.44E-04	1.50E-03	1.30E-02	1.00E-02	1.39E-02	2.21E-02
24	6.56E-08	9.62E-04	7.44E-04	1.03E-03	1.64E-03	1.41E-02	1.09E-02	1.51E-02	2.41E-02
26	7.10E-08	1.04E-03	8.06E-04	1.12E-03	1.78E-03	1.53E-02	1.18E-02	1.64E-02	2.61E-02
28	7.65E-08	1.12E-03	8.68E-04	1.20E-03	1.91E-03	1.65E-02	1.28E-02	1.77E-02	2.81E-02
30	8.20E-08	1.20E-03	9.30E-04	1.29E-03	2.05E-03	1.77E-02	1.37E-02	1.89E-02	3.02E-02
32	8.74E-08	1.28E-03	9.92E-04	1.37E-03	2.19E-03	1.89E-02	1.46E-02	2.02E-02	3.22E-02
34	9.29E-08	1.36E-03	1.05E-03	1.46E-03	2.33E-03	2.00E-02	1.55E-02	2.15E-02	3.42E-02
36	9.83E-08	1.44E-03	1.12E-03	1.55E-03	2.46E-03	2.12E-02	1.64E-02	2.27E-02	3.62E-02
38	1.04E-07	1.52E-03	1.18E-03	1.63E-03	2.60E-03	2.24E-02	1.73E-02	2.40E-02	3.82E-02
40	1.09E-07	1.60E-03	1.24E-03	1.72E-03	2.74E-03	2.36E-02	1.82E-02	2.52E-02	4.02E-02
42	1.15E-07	1.68E-03	1.30E-03	1.80E-03	2.87E-03	2.48E-02	1.91E-02	2.65E-02	4.22E-02
44	1.20E-07	1.76E-03	1.36E-03	1.89E-03	3.01E-03	2.59E-02	2.00E-02	2.78E-02	4.42E-02
46	1.26E-07	1.84E-03	1.43E-03	1.97E-03	3.15E-03	2.71E-02	2.10E-02	2.90E-02	4.62E-02
48	1.31E-07	1.92E-03	1.49E-03	2.06E-03	3.28E-03	2.83E-02	2.19E-02	3.03E-02	4.83E-02
50	1.37E-07	2.00E-03	1.55E-03	2.15E-03	3.42E-03	2.95E-02	2.28E-02	3.16E-02	5.03E-02
52	1.42E-07	2.08E-03	1.61E-03	2.23E-03	3.56E-03	3.06E-02	2.37E-02	3.28E-02	5.23E-02

4.5.3.1 Reference

1. Caviness, M., LANL Content Description for PAT-1 PACKAGING, Updated August 9, 2007.

4.5.4 O-Ring Decomposition

LA-UR-10-05846

Approved for public release; distribution is unlimited.

Title:	Thermal Decomposition of Viton® O-rings for the PAT-1 Packaging Accident Scenario
Author(s):	J.B. Rubin
Intended for:	Support an amendment application to the US Nuclear Regulatory Commission for the PAT-1 packaging

Los Alamos
NATIONAL LABORATORY
EST. 1943

Form 836 (7/06)

Abstract

As part of the submission package to the NRC to amend the approved contents for the PAT-1 container, a calculation was necessary to determine the theoretical pressure rise in the PAT-1 containment vessel (TB-1) due to the thermal decomposition of O-rings within the container. These o-rings are composed of Viton®A, whose number and mass are determined by the internal packing configuration. This report contains a conservative calculation of the decomposition of these O-rings, in the theoretical accident conditions defined by the PAT-1 SARP. The calculation assumes a scenario whereby the O-ring material is completely volatized, using a reaction scheme which generates the maximum number of gaseous reaction products, and the maximum pressure rise within the TB-1. The results show that even for the case of complete thermal decomposition to gaseous products, the total pressure rise inside of the TB-1 containment vessel is less than the maximum allowable, as defined in the PAT-1 SARP.

The o-rings are treated as tori, with a volume given by

$$V = (2\pi R)(\pi r^2) \quad (1)$$

where r is the radius of the cross-sectional area of the torus and R is the distance from the center of the torus to the center of the cross sectional area, Figure 1 :

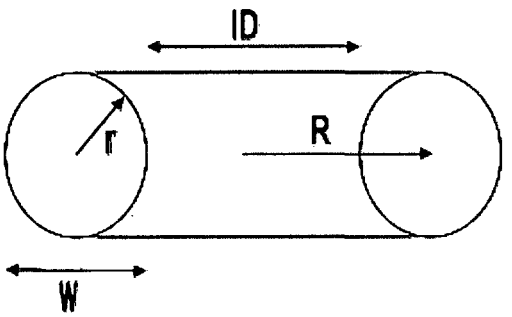

Figure 1. Cross section of a torus, showing the dimensional relations to Eq. (1).

Table 1. Dimensions and volumes of Viton A® O-rings contained within the TB-1 for the Packing Configurations described in Table 3 and shown schematically in Figure 2.

O-ring location	O-ring Size Standard[i]	w (in)	r (in)	ID (in)	R (in)	Volume (in^3)	Volume (cm^3)
T-Ampoule[ii]	241	0.139	0.070	3.859	2.000	0.1906	3.1233
SC-1/2	147	0.103	0.052	2.675	1.389	0.0727	1.1916
Packing Configuration #1							
T-Ampoule	241	0.139	0.070	3.859	2.000	0.1906	3.1233
					Total	**0.1906**	**3.1233**
Packing Configuration #2							
T-Ampoule	241	0.139	0.070	3.859	2.000	0.1906	3.1233
SC-2	147	0.103	0.052	2.675	1.389	0.0727	1.1916
SC-2	147	0.103	0.052	2.675	1.389	0.0727	1.1916
					Total	**0.3360**	**5.5065**
Packing Configuration #3							
T-Ampoule	241	0.139	0.070	3.859	2.000	0.1906	3.1233
SC-1	147	0.103	0.052	2.675	1.389	0.0727	1.1916
SC-1	147	0.103	0.052	2.675	1.389	0.0727	1.1916
SC-1	147	0.103	0.052	2.675	1.389	0.0727	1.1916
					Total	**0.4087**	**6.6981**

Table 1 gives the relevant dimensions (w, r and R as defined in Figure 1) of the O-rings, while the ID and w are provided from SAE AS568C "Aerospace Size Standard for O-rings". From these dimensions, the volume of each O-ring is calculated using Eq. (1) and compared to the values given in the SAE AS568C standard (as verification that the volume of each O-ring is accurate). From these individual O-ring volumes, the total O-ring (volume) inventory in the TB-1, for each of the three packing configurations, is obtained. ***Note that the TB-1 O-ring is not used for the plutonium metal shipments and is not included in the volume calculation.***

Based on literature review, the reaction products produced by pyrolysis of Viton A® in air is similar to that of pyrolysis of PTFE in air, namely, CO, CO_2, COF_2, HF, CF_4, C_2F_4, C_3F_6, C_3F_6, C_4F_8. This is to be expected since the atomic species present in the two fluoropolymers are nominally similar, both composed largely of carbon and fluorine. Once volatilized, these atomic species will re-form into other molecular species having stoichiometries determined by the prevailing thermodynamic conditions in the gas phase.

Viton A® is a vinylidene fluoride/hexafluoropropylene copolymer, manufactured by DuPont Corporation, with a nominal composition of 78 wt% CF_2CH_2 and 22 wt% C_3F_6 [iii]. (By comparison, PTFE has a nominal composition of 100 wt% C_2F_4. In the case of PTFE, the hydrogenous compounds observed on pyrolysis would obtain the necessary hydrogen from water vapor, which is invariably present during air oxidation.[iv]) It is noted that air oxidation of

PTFE can result in significant fractions of higher molecular weight products, such as COF_2,[v] relative to the oxidative pyrolysis of Viton A® (which produces larger fractions of HF and CF_4). In order to be ***conservative***, we will assume that the pyrolysis products of Viton A® are composed of lower molecular weight products, resulting in the greatest number of moles of gaseous reaction product, and therefore the largest pressure increase. Consequently, for gas generation calculations, we will assume that the maximum amount of HF(g) is formed, since this specie would form the greatest amount of product, on a molar basis, from the degradation products, and therefore represents the maximum pressure contribution of any (single) pyrolysis product. It is further assumed that any fluorine in excess of that taken up in the formation of HF(g) will react with carbon to form the maximum amount of CF_4(g).

It is known that Viton A® contains inorganic fillers, such as metal oxides and diatomaceous earth, to aid in processing.[vi,vii] Again, to be ***conservative***, no credit is given for any non-volatile components within the elastomer.

In the following section, a calculation will be given of the pressure rise due to O-ring degradation for Packing Configuration #3, which includes four O-rings, as shown in Table 1. Table 2 gives the results of this calculation, as well as the results for Packing Configurations 1 & 2.

The basis of the calculation assumes the sequential formation of

(1) HF, to completely account for the hydrogen present in the original O-ring material, then

(2) saturated fluorocarbon (CF_4), to account for the excess amount of fluorine over that taken up by HF formation, followed lastly by

(3) either CO(g) or CO_2(g), to account for the excess amount of carbon remaining after accounting for the hydrogen and fluorine present in the original O-ring(s).

This reaction scheme results in the maximum number of moles of gaseous reaction products, thereby generating the highest amount of internal pressure in the TB-1 unoccupied volume. This is the most conservative case.

For Packing Configuration #3, the total elastomer volume is 6.698 cm^3 (Table 1). Assuming an elastomer specific gravity of 1.8 g/cm^3,[viii] we have 12.057 g of elastomer material, or 9.404 g (0.147 moles) CF_2CH_2 and 2.652 g (0.018 moles) C_3F_6. The overall decomposition reaction, based on the assumed decomposition products is therefore

$$0.147\ CF_2CH_2(s) + 0.018\ C_3F_6(s) \rightarrow 0.320\ C(s) + 0.294\ HF(g) + 0.027\ CF_4(g) \quad (2a)$$

$$0.320\ C(s) + 0.160\ O_2(g) \rightarrow 0.320\ CO_2(g) \text{ or } 0.320\ CO(g) \quad (2b)$$

For the elastomer inventory in Packing Configuration #3, we have

$$9.404\ g\ CF_2CH_2\left(\frac{37.996\ g\ F}{64.034\ g\ CF_2CH_2}\right) = 5.580\ g\ F \quad (3)$$

$$9.404\ g\ CF_2CH_2\left(\frac{2.016\ g\ H}{64.034\ g\ CF_2CH_2}\right) = 0.296\ g\ H \quad (4)$$

$$9.404\ g\ CF_2CH_2\left(\frac{24.022\ g\ C}{64.034\ g\ CF_2CH_2}\right) = 3.528\ g\ C \quad (5)$$

plus

$$2.652\ g\ C_3F_6\left(\frac{113.988\ g\ F}{150.021\ g\ C_3F_6}\right) = 2.015\ g\ F \quad (6)$$

$$2.652\ g\ C_3F_6\left(\frac{36.033\ g\ C}{150.021\ g\ C_3F_6}\right) = 0.637\ g\ C \quad (7)$$

or

$$7.596\ g\ F \quad (8)$$

$$4.165\ g\ C \quad (9)$$

$$0.296\ g\ H \quad (10)$$

If we assume that all available hydrogen and fluorine are liberated and form the maximum *moles* of gaseous products, we would have

$\left(\frac{0.296\ g\ H}{1.008\ g/mole\ H}\right) = 0.294$ moles hydrogen available for HF generation, and

$\left(\frac{7.595\ g\ F}{18.998\ g/mole\ F}\right) = 0.400$ moles total fluorine minus the 0.294 moles of fluorine in HF, leaving 0.106 moles of fluorine available for $CF_4(g)$ generation, or 0.027 moles $CF_4(g)$. If these reaction products add incrementally, and ideally, then we would have 0.294 moles HF(g) + 0.027 mole $CF_4(g)$, or a total of 0.320 moles of gaseous [HF(g) + $CF_4(g)$] reaction products. For an unoccupied internal TB-1 volume of 1103.01 cm^3 (see Packing Configuration #3 in Table 3), and T = 1080°F (582.2°C, 855.4 K) for the PAT-1 hypothetical accident condition, there would be a pressure increase of[x]

$$P = \frac{(0.320\ \text{mole})\left(82.056\ {}^{\text{atm cm}^3}/_{\text{mole K}}\right)(855.4\ \text{K})}{1103.01\ \text{cm}^3} = 20.38\ \text{atm} \qquad (11)$$

or 299.49 psi due to the assumed o-ring degradation products. Once the hydrogen and fluorine are consumed in the formation of HF(g) and CF_4(g), there is a theoretical excess of

$\left(\frac{4.165\ \text{g C}}{12.011\ {}^{\text{g}}/_{\text{mole}}}\right) = 0.347$ moles of carbon in the virgin elastomer minus 0.027 moles carbon in CF_4, or 0.320 moles.

At this point we could assume that (1) the theoretical excess of carbon will remain as solid, unreactive char, or that (2) the excess carbon can be further reacted with oxygen to form CO(g) or CO_2(g) (the formation of either CO(g) or CO_2(g) would produce the same number of moles of gaseous reaction products and therefore, in the ideal gas case, an equal pressure contribution).

The formation of residual carbon char, as opposed to the formation of CO(g) or CO_2(g), would be supported based on (a) any oxygen present at the time of initial packaging is scavenged completely by the formation of plutonium oxide, and (b) the TB-1 remains intact at the theoretical accident conditions. Solid char is experimentally observed, even in the oxidative thermal decomposition of fluoroelastomers.[v1,x1] Further, for studies of the thermal degradation of Viton®A in non-oxidizing environments, an incomplete volatilization of the polymer is evidenced by a low yield of fluorine with respect to the theoretical quantity.[t1] However, for the purposes of a ***conservative*** estimate, we assume the case where additional oxygen were to be made available in the TB-1 and sample containers, in a quantity sufficient to react completely with the excess carbon from the elastomer, to produce CO(g) or CO_2(g). Such a reaction would increase the overall moles of gaseous reaction products to 0.320 moles [HF(g) + CF_4(g)] + 0.320 moles [CO(g) or CO_2(g)], thereby (approximately) doubling the overall pressure rise from 20.38 atm to 40.76 atm, or 598.98 psi.

Table 2 summarizes the calculation given above, which, again, represents the elastomer inventory in Packaging Configuration #3, along with a similar calculation of the remaining two Packing Configurations, which have a reduced elastomer loading.

Table 2. Calculation of elastomer degradation products for the three Packing Configurations described in Table 1 and shown schematically in Figure 2. The summation in the right-hand column of each row is the total number of moles assuming that the excess carbon reacts completely to form gaseous product, either CO(g) or CO_2(g).

Packing Configuration #1 (3.1233 cm^3 of Viton®A)	4.385 g (0.068 moles) CF_2CH_2 1.237 g (0.008 moles) C_3F_6	0.138 g (0.137 moles) H 3.542 g (0.186 moles) F 1.942 g (0.162 moles) C	0.137 moles HF(g) 0.012 moles CF_4(g) 0.149 moles CO(g) ***Σ = 0.299 moles***
Packing Configuration #2 (5.5065 cm^3 of Viton®A)	7.731 g (0.121 moles) CF_2CH_2 2.181 g (0.015 moles) C_3F_6	0.243 g (0.241 moles) H 6.244 g (0.329 moles) F 3.424 g (0.285 moles) C	0.241 moles HF(g) 0.022 moles CF_4(g) 0.263 moles CO(g) ***Σ = 0.527 moles***
Packing Configuration #3 (6.6981 cm^3 of Viton®A)	9.404 g (0.147 moles) CF_2CH_2 2.652 g (0.018 moles) C_3F_6	0.296 g (0.294 moles) H 7.596 g (0.400 moles) F 4.165 g (0.347 moles) C	0.294 moles HF(g) 0.027 moles CF_4(g) 0.320 moles CO(g) ***Σ = 0.640 moles***

Table 3 gives the overall pressure rise calculation for the three Packing Configurations, using the appropriate O-ring inventory (Table 1) and unoccupied TB-1 volume (Table 3) for each Configuration.

Table 3. Internal volume of the TB-1 container (top line), and solid volumes of T-ampoule, filler ring, sample containers (SC-1 or SC-2) and Pu metal payloads for each Packing Configuration (volume of O-ring lubricant and optional tantalum foil are not included). The amount of lubricant on the O-ring would be minimal to permit joining the lid to the body of the T-Ampoule or sample containers. Column 4 gives the pressure rise for the case of complete volatilization of all contained o-ring materials. Column 5 is a summation of the pressure rise from Column 4 plus an additional 2.9 atmospheres, due to an initial 1 atm of pressure assumed to be present in the TB-1 at the time of packaging, and then heated from ambient to 582.2 K during the accident scenario.

components	Volume (in^3)	Volume (cm^3)	Pressure rise (psi)	Pressure rise (psia)
Empty TB-1	89.10	1460.09		
Packing Configuration #1				
T-ampoule	7.63	128.31		
Filler ring	0.90	14.75		
Pu cylinder 831 g.	2.57	42.11		
Unoccupied TB-1 volume	**77.80**	**1274.91**	**241.63**	**284.25**
Packing Configuration #2				
T-ampoule	7.83	128.31		
Filler ring	0.90	14.75		
SC-2	2.75	45.06		
SC-2	2.75	45.06		
SC-2 Cradle Assembly	4.90	80.30		
Pu cylinder 1.1" Ø x 1.1" h	1.05	17.21		
Pu cylinder 1.1" Ø x 1.1" h	1.05	17.21		
Unoccupied TB-1 volume	**67.87**	**1112.19**	**488.33**	**530.94**
Packing Configuration #3				
T-ampoule	7.83	128.31		
Filler ring	0.90	14.75		
SC-1	2.15	35.23		
SC-1	2.15	35.23		
SC-1	2.15	35.23		
SC-1 Cradle Assembly	5.02	82.26		
Pu cylinder 0.88"Ø x 0.88" h	0.53	8.69		
Pu cylinder 0.88"Ø x 0.88" h	0.53	8.69		
Pu cylinder 0.88"Ø x 0.88" h	0.53	8.69		
Unoccupied TB-1 volume	**67.31**	**1103.01**	**598.94**	**641.56**

The PAT-1 SARP (section 4.4.2) stipulates that the maximum allowable internal TB-1 pressure, in the theoretical accident conditions, must remain less than 1,110 psia. The results of this highly conservative calculation of the thermal degradation of Viton® A in the theoretical accident conditions show that this maximum internal pressure is not exceeded for any of the three Packing Configurations.

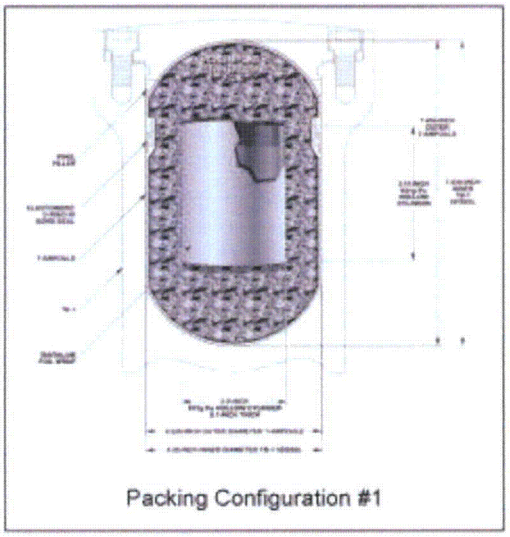

Packing Configuration #1

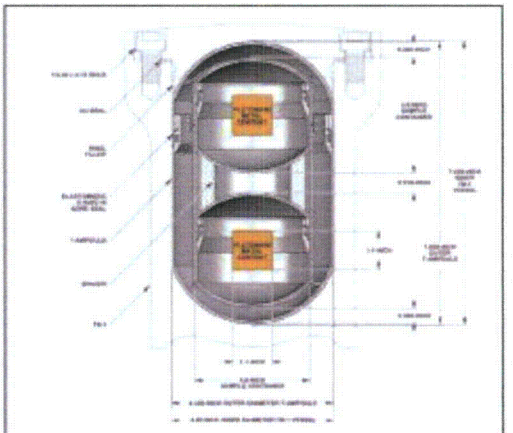

Packing Configuration #2

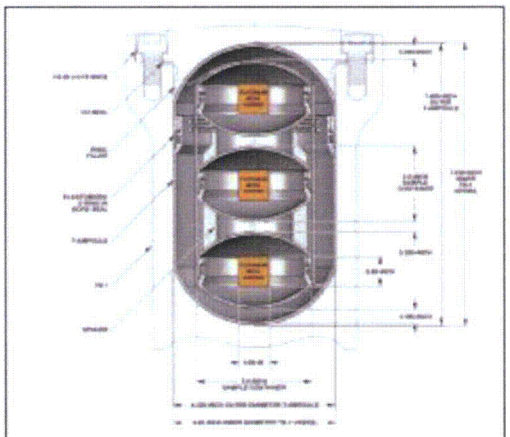

Packing Configuration #3

Figure 2. Schematic illustration of the Packing Configurations of the TB-1.

[i]. From SAE AS568C, "Aerospace Size Standard for O-rings". ID, w, and Volume are provided from Table 1, r and R are derived.

[ii]. The TB-1 O-ring is not used for plutonium metal shipments.

[iii]. A.K. Burnham and R.K. Weese, "Kinetics of thermal degradation of explosive binders Viton A, Estane, and Kel-F", Thermochimica Acta 426 (2005) pp. 85–92.

[iv]. H. Arito and R. Soda "Pyrolysis Products of Polytetrafluoroethylene and Polytetrafluoroethylenepropylene with Reference to Inhalation Toxicology", Korean J. Chem. Eng. 12 (1995) pp. 247-255.

[v]. L.D. Scheel, W.C. Lane and W.E. Colemen, "The Toxicity of Polytetraethylene Pyrolysis Products- Including Carbonyl Fluoride and a Reaction Product, Silicon Tetrafluoride", Amer. Ind. Hygiene Ass. 29 (1968) pp. 41-48.

[vi]. J. F. Smith and G. T. Perkins, "The Mechanism of Post Cure of Viton A® Fluorocarbon Elastomer", J. Appl. Polym. Sci. 16 (1961) pp. 460-467.

[vii]. Technical Information - Viton® fluoroelastomer Fluid Resistance Guide (DuPont Dow Elastomers, 1998).

[viii]. Technical Information - Viton® A-100 (DuPont Dow Elastomers, 2003).

[ix]. The ideal gas law gives relates pressure, as a function of temperature and volume, as $P = nRT/V$. If temperature (T) is expressed in Kelvin, volume (V) is expressed in cm^3, and mass (n) in moles, then the pressure can be expressed in units of atmospheres (atm) using a conversion factor of $\left(82.056\ {}^{atm\,cm^3}/_{mole\,K}\right)$.

[x]. Analytical Pyrolysis of Synthetic Organic Polymers, ed. by Şerban Moldoveanu (2005) p.289.

[xi]. I. Lee, R.R. Reed, V.L. Brady, and S.A. Finnegan, "Energy release in the reaction of metal powders with fluorine containing polymers", J. Thermal Anal. 49 (1997) pp. 1699-1705.

[xii]. A.E. Venger, et al., "Thermogravimetric Study of the Thermal Decomposition of poly(tetrafluoroethylene) under Nonisothermal Conditions", Vestsi Akademii Navuk BSSR, Seryya Fizika-Energetychnykh Navuk 2 (1976) pp. 65.

[xiii]. G. J. Knight and W. W. Wright, "The Thermal Degradation of Hydrofluoro Polymers", J. Appl. Polym. Sci. 16 (1972) pp. 683-693.

4.5.5 Determination of A_2 for the PAT 1 Package with Plutonium Contents

Prepared by Monty L. Goins and reviewed by Drew Winder, both of B&W Y-12 Technical Services, L.L.C., on November 23, 2010.

Introduction

The containment criteria for radioactive, fissile material packages are given in 10 CFR 71.51(a)(1) for Normal Conditions of Transport (NCT) ($\leq 10^{-6}$ A_2/h), in 71.51(a)(2) for Hypothetical Accident Conditions (HAC) ($\leq A_2$ in a week), and 71.64(a)(1)(i) for Accident conditions for air transport of plutonium ($\leq A_2$ in a week). The A_2 value for this mixture of radioisotopes must be determined to establish the content containment criteria and to determine the maximum release quantity that is allowed by the regulations. These values for a mixture of isotopes are determined by the methodology given in 10 CFR 71, Appendix A, "Determination of A_1 and A_2," Section IV. The results of these analyses are used to demonstrate compliance of the PAT-1 package with the containment requirements of 10 CFR 71.

Scope

The A_2 value of the plutonium content to be shipped is evaluated based on the mass and weight percents of materials shown in Tables 4.5.5.1 and 4.5.5.2 defined in Section 1.2.2 of the addendum. The analysis documented in this section was conducted to establish the upper limit for the total activity and the maximum number of A_2s proposed for transport in the PAT-1 package. The maximum activity [53.281 TBq (1440.02 Ci)] occurs at initial fabrication. However, the maximum activity-to-A_2 value (5.5708 H 10^3) of the contents occurs when the Pu-241 fully decays to Am-241. These values have been determined using a maximum of 1300 gram of plutonium. By applying the weight percents of isotopes shown in Tables 4.5.5.1 and 4.5.5.2, the maximum activity, minimum A_2 value, and the minimum leakage requirements were determined for the proposed contents and are summarized in Tables 4.5.5.3, 4.5.5.4, and 4.5.5.5. The mass and isotopic concentrations used for the proposed content do not take into consideration limits based on shielding, criticality or structural.

According to 10 CFR 71, Appendix A, parent and daughter nuclides are considered to be a mixture of different nuclides than those of the parent nuclide. The radioactive decay of uranium (refer to the decay chains presented by Dr. David C. Kocher, *Radioactive Decay Data Tables* [Kocher 1981]) creates isotopes that will accumulate enough activity to exceed their respective criteria for limited quantities (*Shippers*C*General Requirements for Shipments and Packagings* [49 CFR 173.425], Table 4, AActivity Limits for Limited Quantities, Instruments, and Articles@) and for Type A quantities of radionuclides (10 CFR 71, Table A-1, "A_1 and A_2 Values for Radionuclides"). Furthermore, the A_2 value for the mixture will change over time as a result of radioactive decay. The analysis below shows that the A_2 value for this mixture reaches a minimum when the Pu-241 is fully decayed to Am-241.

Analysis

Mass Tables. The mass and weight fractions for the isotopes used in the containment calculations are presented in Tables 4.5.5.1 and 4.5.5.2.

Table 4.5.5.1. Isotopic mass and weight percent for the Plutonium contents [a]

Nuclide	Weight percent	Mass (g)
Pu-238	0.050000	0.650000
Pu-239	92.350000	1200.550000
Pu-240	6.500000	84.500000
Pu-241	1.000000	13.000000
Pu-242	0.100000	1.300000
Am-241	0.000000	0.000000
Total	100.000000	1300.000000

[a] Entire weight of contents is assumed to be plutonium. Maximum content mass is assumed to be 1300 grams.

Table 4.5.5.2. Isotopic mass and weight percent for the Plutonium contents with full Pu-241 decay to Am-241[a]

Nuclide	Weight percent	Mass (g)
Pu-238	0.050000	0.650000
Pu-239	92.350000	1200.550000
Pu-240	6.500000	84.500000
Pu-241	0.000000	0.000000
Pu-242	0.100000	1.300000
Am-241	1.000000	13.000000
Total	100.000000	1300.000000

[a] Entire weight of contents is assumed to be plutonium. Maximum content mass is assumed to be 1300 grams.

Table 4.5.5.3. A_2 value and activity calculation for 1300 g of radioactive material at 0 years

Isotope	Mass (g)	Specific activity (TBq/g)	Activity (TBq)	A_2 (TBq)	f(i) (TBq/TBq)	f(i) / A_2 (1/TBq)
Pb-210	0.00000	2.8000E+00	0.0000E+00	5.0000E-02	0.0000E+00	0.0000E+00
Pb-212	0.00000	5.1000E+04	0.0000E+00	2.0000E-01	0.0000E+00	0.0000E+00
Bi-210	0.00000	4.6000E+03	0.0000E+00	6.0000E-01	0.0000E+00	0.0000E+00
Bi-212	0.00000	5.4000E+05	0.0000E+00	6.0000E-01	0.0000E+00	0.0000E+00
Po-210	0.00000	1.7000E+02	0.0000E+00	2.0000E-02	0.0000E+00	0.0000E+00
Rn-222	0.00000	5.7000E+03	0.0000E+00	4.0000E-03	0.0000E+00	0.0000E+00
Ra-223	0.00000	1.9000E+03	0.0000E+00	7.0000E-03	0.0000E+00	0.0000E+00
Ra-224	0.00000	5.9000E+03	0.0000E+00	2.0000E-02	0.0000E+00	0.0000E+00
Ra-225	0.00000	1.5000E+03	0.0000E+00	4.0000E-03	0.0000E+00	0.0000E+00
Ra-226	0.00000	3.7000E-02	0.0000E+00	3.0000E-03	0.0000E+00	0.0000E+00
Ra-228	0.00000	1.0000E+01	0.0000E+00	2.0000E-02	0.0000E+00	0.0000E+00
Ac-225	0.00000	2.1000E+03	0.0000E+00	6.0000E-03	0.0000E+00	0.0000E+00
Ac-227	0.00000	2.7000E+00	0.0000E+00	9.0000E-05	0.0000E+00	0.0000E+00
Ac-228	0.00000	8.4000E+04	0.0000E+00	5.0000E-01	0.0000E+00	0.0000E+00
Th-227	0.00000	1.1000E+03	0.0000E+00	5.0000E-03	0.0000E+00	0.0000E+00
Th-228	0.00000	3.0000E+01	0.0000E+00	1.0000E-03	0.0000E+00	0.0000E+00
Th-229	0.00000	7.9000E-03	0.0000E+00	5.0000E-04	0.0000E+00	0.0000E+00
Th-230	0.00000	7.6000E-04	0.0000E+00	1.0000E-03	0.0000E+00	0.0000E+00
Th-231	0.00000	2.0000E+04	0.0000E+00	2.0000E-02	0.0000E+00	0.0000E+00
Th-232	0.00000	4.0000E-09	0.0000E+00	1.0000E+75	0.0000E+00	0.0000E+00
Pa-231	0.00000	1.7000E-03	0.0000E+00	4.0000E-04	0.0000E+00	0.0000E+00
Pa-233	0.00000	7.7000E+02	0.0000E+00	7.0000E-01	0.0000E+00	0.0000E+00
U-232	0.00000	8.3000E-01	0.0000E+00	1.0000E-03	0.0000E+00	0.0000E+00
U-233	0.00000	3.6000E-04	0.0000E+00	6.0000E-03	0.0000E+00	0.0000E+00
U-234	0.00000	2.3000E-04	0.0000E+00	6.0000E-03	0.0000E+00	0.0000E+00
U-235	0.00000	8.0000E-08	0.0000E+00	1.0000E+75	0.0000E+00	0.0000E+00
U-236	0.00000	2.4000E-06	0.0000E+00	6.0000E-03	0.0000E+00	0.0000E+00
Np-237	0.00000	2.6000E-05	0.0000E+00	2.0000E-03	0.0000E+00	0.0000E+00
Pu-236	0.00000	2.0000E+01	0.0000E+00	3.0000E-03	0.0000E+00	0.0000E+00
Pu-238	0.65000	6.3000E-01	4.0950E-01	1.0000E-03	7.6857E-03	7.6857E+00
Pu-239	1200.5500	2.3000E-03	2.7613E+00	1.0000E-03	5.1825E-02	5.1825E+01
Pu-240	84.50000	8.4000E-03	7.0980E-01	1.0000E-03	1.3322E-02	1.3322E+01
Pu-241	13.0000	3.8000E+00	4.9400E+01	6.0000E-02	9.2716E-01	1.5453E+01
Pu-242	1.30000	1.5000E-04	1.9500E-04	1.0000E-03	3.6599E-06	3.6599E-03
Mass =	**1300.0000**	**ACTIVITY SUM =**	**5.3281E+01**		**SUM OF F_i/A_2 =**	**8.8289E+01**

$$(\text{mixture}) = \frac{1}{3f(i)/A_2} = \frac{1}{8.8289 \text{ H } 10^{1} \text{ (1/TBq)}} = 1.1326 \text{ H } 10^{-2} \text{ TBq}$$

Table 4.5.5.4. A_2 value and activity calculation for 1300 g of radioactive material with full Pu-241 decay to Am-241

Isotope	Mass (g)	Specific activity (TBq/g)	Activity (TBq)	A_2 (TBq)	f(i) (TBq/TBq)	f(i) / A_2 (1/TBq)
Pb-210	0.00000	2.8000E+00	0.0000E+00	5.0000E-02	0.0000E+00	0.0000E+00
Pb-212	0.00000	5.1000E+04	0.0000E+00	2.0000E-01	0.0000E+00	0.0000E+00
Bi-210	0.00000	4.6000E+03	0.0000E+00	6.0000E-01	0.0000E+00	0.0000E+00
Bi-212	0.00000	5.4000E+05	0.0000E+00	6.0000E-01	0.0000E+00	0.0000E+00
Po-210	0.00000	1.7000E+02	0.0000E+00	2.0000E-02	0.0000E+00	0.0000E+00
Rn-222	0.00000	5.7000E+03	0.0000E+00	4.0000E-03	0.0000E+00	0.0000E+00
Ra-223	0.00000	1.9000E+03	0.0000E+00	7.0000E-03	0.0000E+00	0.0000E+00
Ra-224	0.00000	5.9000E+03	0.0000E+00	2.0000E-02	0.0000E+00	0.0000E+00
Ra-225	0.00000	1.5000E+03	0.0000E+00	4.0000E-03	0.0000E+00	0.0000E+00
Ra-226	0.00000	3.7000E-02	0.0000E+00	3.0000E-03	0.0000E+00	0.0000E+00
Ra-228	0.00000	1.0000E+01	0.0000E+00	2.0000E-02	0.0000E+00	0.0000E+00
Ac-225	0.00000	2.1000E+03	0.0000E+00	6.0000E-03	0.0000E+00	0.0000E+00
Ac-227	0.00000	2.7000E+00	0.0000E+00	9.0000E-05	0.0000E+00	0.0000E+00
Ac-228	0.00000	8.4000E+04	0.0000E+00	5.0000E-01	0.0000E+00	0.0000E+00
Th-227	0.00000	1.1000E+03	0.0000E+00	5.0000E-03	0.0000E+00	0.0000E+00
Th-228	0.00000	3.0000E+01	0.0000E+00	1.0000E-03	0.0000E+00	0.0000E+00
Th-229	0.00000	7.9000E-03	0.0000E+00	5.0000E-04	0.0000E+00	0.0000E+00
Th-230	0.00000	7.6000E-04	0.0000E+00	1.0000E-03	0.0000E+00	0.0000E+00
Th-231	0.00000	2.0000E+04	0.0000E+00	2.0000E-02	0.0000E+00	0.0000E+00
Th-232	0.00000	4.0000E-09	0.0000E+00	1.0000E+75	0.0000E+00	0.0000E+00
Pa-231	0.00000	1.7000E-03	0.0000E+00	4.0000E-04	0.0000E+00	0.0000E+00
Pa-233	0.00000	7.7000E+02	0.0000E+00	7.0000E-01	0.0000E+00	0.0000E+00
U-232	0.00000	8.3000E-01	0.0000E+00	1.0000E-03	0.0000E+00	0.0000E+00
U-233	0.00000	3.6000E-04	0.0000E+00	6.0000E-03	0.0000E+00	0.0000E+00
U-234	0.00000	2.3000E-04	0.0000E+00	6.0000E-03	0.0000E+00	0.0000E+00
U-235	0.00000	8.0000E-08	0.0000E+00	1.0000E+75	0.0000E+00	0.0000E+00
U-236	0.00000	2.4000E-06	0.0000E+00	6.0000E-03	0.0000E+00	0.0000E+00
Np-237	0.00000	2.6000E-05	0.0000E+00	2.0000E-03	0.0000E+00	0.0000E+00
Pu-236	0.00000	2.0000E+01	0.0000E+00	3.0000E-03	0.0000E+00	0.0000E+00
Pu-238	0.65000	6.3000E-01	4.0950E-01	1.0000E-03	7.3509E-02	7.3509E+01
Pu-239	1200.5500	2.3000E-03	2.7613E+00	1.0000E-03	4.9567E-01	4.9567E+02
Pu-240	84.50000	8.4000E-03	7.0980E-01	1.0000E-03	1.2742E-01	1.2742E+02
Pu-241	0.0000	3.8000E+00	0.0000E+00	6.0000E-02	0.0000E+00	0.0000E+00
Pu-242	1.30000	1.5000E-04	1.9500E-04	1.0000E-03	3.5004E-05	3.5004E-02
Am-241	13.0000	1.3000E-01	1.6900E+00	1.0000E-03	3.0337E-01	3.0337E+02
Mass =	**1300.0000**	**Activity sum =**	**5.5708E+00**		**Sum of f_i/A_2 =**	**1.0000E+03**

$$A_2(\text{mixture}) = \frac{1}{3f(i) / A_2} = \frac{1}{1.0000 \text{ H } 10^3 \text{ (1/TBq)}} = 1.0000 \text{ H } 10^{-3} \text{ TBq}$$

The total number of A_2 proposed for shipment is equal to the ratio of total activity divided by the A_2 of this particular mixture as shown in Table 4.5.5.5.

Table 4.5.5.5. Activity, A_2 value, and number of A_2 proposed for transport

Isotopic distribution	Activity (TBq)	A_2 (TBq)	Act / A_2
Full Pu-241 (see Table 4.5.5.1)	5.3281E+01	1.1326E-02	4.7042E+03
Full Am-241 (see Table 4.5.5.2)	5.5708E+00	1.0000E-03	5.5708E+03

4.5.6 Calculation of the PAT-1 Containment Vessel's Regulatory Reference Air Leakage Rates

Prepared by Monty L. Goins and reviewed by Drew Winder, both of B & W Y-12 Technical Services, L.L.C., on November 23, 2010.

Introduction

The PAT-1 leak-testing requirements of the containment boundary are based on the smallest maximum allowable leakage rate generated from the maximum plutonium content defined in Tables 4.5.5.1 and 4.5.5.2. Section 5 of ANSI N14.5-1997 defines the maximum allowable leakage rate based on the maximum allowable release rate. These leakage rates, L_N , L_A , and L_{PA} , are the maximum allowable seal leakage rates for Normal Conditions of Transport (NCT), Hypothetical Accident Conditions (HAC), and Accident condition for air transport of plutonium (ACATP). The worst-case maximum allowable leakage rates are used to calculate an equivalent leakage hole diameter following ANSI N14.5-1997, Appendix B, for each condition of transport. This leakage hole diameter is used to calculate a reference air and a helium leakage rate for leak testing. A bounding mass for the plutonium content of 1300 gram is used in this calculation to certify the PAT-1 package for shipment. The maximum allowable leakage rates are calculated using this maximum content mass in a much more dispersive form (oxide powder) at the highest calculated pressures and temperatures. This section shows the following procedure used to calculate the leak criteria for the plutonium constituents at initial fabrication. Table 4.5.6.1 shows the results of using this procedure for both set of isotopic distributions.

Plutonium Content with no Pu-241 decay

Calculate R_N , R_A, and R_{PA}:

where

R_N = allowable release rate for normal conditions of transport;
R_A = allowable release rate for hypothetical accident condition, and
R_{PA} = allowable release rate for accident condition for air transport of plutonium.

The maximum allowable release rate is based on using A_2.

A_2 = 1.1326×10^{-2} TBq, (3.0611×10^{-1} Ci). Table 4.5.5.5

The containment requirements for NCT, HAC, and ACATP are:

R_N = $A_2 \times 10^{-6}$ TBq/h = $A_2 \times 2.78 \times 10^{-10}$ TBq/s, ANSI N14.5-1997 (Eq. 1)
= $1.1326 \times 10^{-2} \times 2.78 \times 10^{-10}$ TBq/s,
= 3.1488×10^{-12} TBq/s, (8.5102 H 10^{-11} Ci/s).

R_A = A_2 (TBq/week),
= $A_2 \times 1.65 \times 10^{-6}$ (TBq/s), ANSI N14.5-1997 (Eq. 2)
= $1.1326 \times 10^{-2} \times 1.65 \times 10^{-6}$ TBq/s,
= 1.8689×10^{-8} TBq/s, (5.0510×10^{-7} Ci/s). or limited to 10 A2 /week of 85Kr

R_{PA} = A_2 (TBq/week),
= $A_2 \times 1.65 \times 10^{-6}$ (TBq/s), ANSI N14.5-1997 (Eq. 2)
= $1.1326 \times 10^{-2} \times 1.65 \times 10^{-6}$ TBq/s,

= 1.8689×10^{-8} TBq/s, (5.0510×10^{-7} Ci/s).

Following ANSI N14.5-1997, the medium aerosol activity must be calculated to determine the leakage rates.

m = total nuclide mass in the package available for release (g),
TotA = total activity in the package available for release (TBq),
TSA = total specific activity in the package available for release (TBq/g).

For the plutonium content:

TSA = TotA / m,
TSA = 5.3281×10^{1} (TBq) / 1300 (g), Table 4.5.5.5
TSA = 4.0985×10^{-2} TBq/g.

ρ_P = 9×10^{-6} g/cm^3. The maximum density of powder aerosols in the fill gas Curren, W.D. and R.D. Bond, 1980, *Leakage of Radioactive Powders from Containers.*

For the packaging arrangement:

C_N = activity per unit volume of medium that could escape from the containment system (TBq/cm^3).
C_N = TSA $\times$ ρ_P,
= 4.0985×10^{-2} (TBq/g) $\times$ 9×10^{-6} (g/cm^3),
C_N = 3.6887×10^{-7} TBq/cm^3. NCT

Using Curren's maximum aerosol density, $C_A = C_N = C_{PA}$:

C_A = activity per unit volume of exiting gas (TBq/cm^3), HAC
C_A = 3.6887×10^{-7} TBq/cm^3.

C_{PA} = activity per unit volume of exiting gas (TBq/cm^3), ACATP
C_{PA} = 3.6887×10^{-7} TBq/cm^3.

Section 6.1 of ANSI N14.5-1997 calculates L_N with (Eq. 3) and L_A, and L_{PA} with (Eq. 4). L_N, L_A, and L_{PA} are the maximum allowable leakage rates for the containment vessel fill gas aerosol during NCT, HAC, and ACATP, respectively.

L_N = maximum allowable leakage rate for the medium for NCT (TBq/cm^3),
L_N = R_N / C_N, ANSI N14.5-1997 (Eq. 3)
L_N = 3.1488×10^{-12} (TBq/s) / 3.6887×10^{-7} (TBq/cm^3),
L_N = 8.5363×10^{-6} cm^3/s.

L_A = maximum allowable leakage rate for the medium for HAC (TBq/cm^3),
L_A = R_A / C_A,
L_A = 1.8689×10^{-8} (TBq/s) / 3.6887×10^{-7} (TBq/cm^3),
L_A = 5.0665×10^{-2} cm^3/s.

L_{PA} = maximum allowable leakage rate for the medium for ACATP (TBq/cm^3),

L_{PA} = R_{PA} / C_{PA},
L_{PA} = 1.8689×10^{-8} (TBq/s) / 3.6887×10^{-7} (TBq/cm^3),
L_{PA} = 5.0665×10^{-2} cm^3/s.

L_N , L_A, and L_{PA} correspond to the upstream volumetric leakage rate (L_u) at the upstream pressure (P_u) in the ANSI N14.5-1997 formulas for use later in this section. The reference air leakage rates $L_{R,N}$. $L_{R,A}$, and $L_{R,PA}$ for NCT, HAC, and ACATP based on the L_N, L_A, and L_{PA} are then calculated using the maximum temperatures and pressure combinations from Sections 4.2, 4.3, and 4.3.1.

Determination of the Leakage Test Procedure Requirements for the Plutonium Content

This calculation will examine the most conservative effects of a fully loaded containment vessel with a plutonium mass of 1300 gram. The smallest allowable leakage values are shown in Table 4.5.6.1. The A_2 value and the maximum content activity-to-A_2 value ratio for this mixture were calculated in Section 4.5.5 and summarized in Table 4.5.5.5. As calculated in Section 4.5.5, the A_2 value and the maximum content activity-to-A_2 ratio used in the following calculations occur at initial fabrication and are 1.1326×10^{-2} TBq (3.0611×10^{-1} Ci) and 4.7042×10^{3} respectively. These values are used to determine the leakage test procedural requirements when packaging the TB-1 containment vessel.

The following analysis determines the maximum allowable seal air reference leakage rate for NCT, HAC, and ACATP. The ANSI N14.5-1997 recommended method using a straight circular tube to model the leakage path is applied. Using this Astandard@ leakage hole model permits the calculation of equivalent reference leakage rates from which leak-test requirements can be established. Viscosity data for air and helium used in the following analyses were obtained from curve fitting routines at specific temperatures based on viscosity data for air (Handbook of Chemistry and Physics, 55th ed.) and helium (NBS Technical Note 631).

L_N and L_A correspond to the upstream volumetric leakage rate (L_u) at the upstream pressure (P_u).

L_N = 8.5363×10^{-6} cm^3/s,
L_A = 5.0665×10^{-2} cm^3/s,
L_{PA} = 5.0665×10^{-2} cm^3/s.

Find the maximum pressure and temperature in the containment vessel:
Converting the temperature to degrees Kelvin:

T = 273.15 + T(°C),
T = 273.15 + 5 / 9 (°F - 32) (K).

T_N = 273.15 + 5 / 9 (218.00°F - 32) (K), (T = 218.00°F)
T_N = 376.48 K. NCT (Section 4.2)

T_A = 273.15 + 5 / 9 (276.00°F - 32) (K), (T = 276.00°F)
T_A = 408.71 K. HAC (Section 4.3)

T_{PA} = 273.15 + 5 / 9 (1080.00°F - 32) (K), (T = 1080°F)
T_{PA} = 855.37 K. ACATP (Section 4.3.1)

Converting the pressures from psia to atmospheres:

P_N	=	P (psia) / 14.696 (psia/atm),	where P is the pressure in Section 4.2
P_N	=	18.872 (psia) / 14.696 (psia/atm),	for NCT
P_N	=	1.2842 atm.	

P_A	=	P (psia) / 14.696 (psia/atm),	where P is the pressure in Section 4.3
P_A	=	20.486 (psia) / 14.696 (psia/atm),	for HAC
P_A	=	1.3940 atm.	

For ACATP conditions, a pressure of 1110 psia will be analyzed:

P_{PA}	=	P (psia) / 14.696 (psia/atm),	where P is the pressure in Section 4.3.1
P_{PA}	=	1110 (psia) / 14.696 (psia/atm),	for ACATP
P_{PA}	=	75.5308 atm.	

The molar gas percentages, determined later in this section for ACATP at 1110 psia, will be used for the P_{PA} analysis during ACATP.

NCT Leakage Hole Diameter for the Plutonium Content

The following calculations determine the leakage hole diameter that generates the maximum allowable leakage rate during NCT. To keep these calculations conservative, the maximum values for temperature and pressure were used as steady-state conditions for NCT. According to Section 4.1.1, the gas inside the containment vessel may consist of nitrogen/helium/argon with a maximum 100 parts per million of oxygen. Based on sample calculations, the lowest regulatory leakage rate was predicted with 100 percent helium in the void volumes of the TB-1 containment vessel and T-Ampoule. The leak path length was assumed to be 0.022 inches (0.056 cm) based on the length of the copper gasket seal compression.

Input data for NCT with 100% helium gas:

L_N	=	8.5363×10^{-6} cm^3/s,	Maximum upstream leakage
P_u	=	1.2842 atm,	Upstream pressure = 18.872 psia
P_d	=	0.2382 atm,	Downstream pressure = 3.5 psia, per 10 CFR 71.71(3)
a	=	0.056 cm,	Leak path length (copper gasket seal compression)
T	=	376.48 K,	Fill gas temperature = 218.00EF
μ	=	0.02310 cP,	Viscosity at temperature
M	=	4.0 g/g-mole.	Molecular weight of fill gas

The average pressure is:

P_a	=	$(P_u + P_d)/2$,	
	=	(1.2842 + 0.2382) / 2,	
P_a	=	0.7612 atm.	Average pressure during NCT

According to ANSI N14.5-1997, the flow leakage hole diameter is unknown. Therefore, the mass-like leakage flow rate must be calculated to calculate the average leakage flow rate.

Q is the mass-like leakage for flow using the upstream leakage, L_u, and pressure, P_u:

$Q = P_u L_u$, (Eq. B1)
$L_u = L_N$. NCT leakage

$Q = (1.2842)(atm)\ (8.5363 \times 10^{-6})(cm^3/s)$,
$Q = 1.0962 \times 10^{-5}$ atm-cm^3/s. NCT mass-like leakage rate

$Q = P_a L_a$, (Eq. B1)
$L_a = Q / P_a = 1.0692 \times 10^{-5}$ (atm-cm^3/s) / (0.7612)(atm),
$L_a = 1.4403 \times 10^{-5}\ 10^{-5}\ cm^3/s$. NCT average leakage rate

Solve equations B2BB4 from ANSI N14.5-1997:

$L_a = (F_c + F_m)\ (P_u - P_d)\ cm^3/s$, (Eq. B2)
$L_a = (F_c + F_m)\ (1.2842 - 0.2382)$,
$L_a = (1.0460)\ (F_c + F_m)\ cm^3/s$.

$F_c = (2.49 \times 10^6)\ D^4 / (a\ \mu)\ (cm^3/atm\text{-}s)$, (Eq. B3)
$F_c = (2.49 \times 10^6)\ D^4 / (\ (0.056)\ (0.02310)\ )$,
$F_c = (1.9245 \times 10^9)\ D^4\ cm^3/atm\text{-}s$.

$F_m = (3.81 \times 10^3)\ D^3\ (T / M)^{.5} / (a\ P_a)\ (cm^3/atm\text{-}s)$, (Eq. B4)
$F_m = (3.81 \times 10^3)\ D^3\ (376.48 / 4.0)^{.5} / (\ (0.056)\ (0.7612)\ )$,
$F_m = (8.6717 \times 10^5)\ D^3\ cm^3/atm\text{-}s$.

From the mass-like leakage calculation:

$L_a = 1.4403 \times 10^{-5}\ cm^3/s$. NCT average leakage rate

Find the leakage hole diameter that sets:

$L_2 = L_a$.

Using the equations:

$L_2 = (1.0460)\ (F_c + F_m)\ cm^3/s$,
$F_c = (1.9245 \times 10^9)\ D^4\ cm^3/atm\text{-}s$,
$F_m = (8.6717 \times 10^5)\ D^3\ cm^3/atm\text{-}s$.

To get a better guess on a new D use:

$D = D_2\ (L_a / L_2)^{0.252}$.

Now a guess must be made for D_2 to solve Eq. B2 for NCT:

D_2 = 0.001 cm, and solve for $L_a = 1.4403 \times 10\text{-}^5\ cm^3/s$. NCT average leakage rate

Diameter	F_c	F_m	L_2	L_a / L_2
1.0000E-03	1.9245E-03	8.6717E-04	2.9201E-03	0.0049
2.6221E-04	9.0966E-06	1.5632E-05	2.5867E-05	0.5568
2.2623E-04	5.0410E-06	1.0041E-05	1.5775E-05	0.9129
2.2110E-04	4.5987E-06	9.3723E-06	1.4614E-05	0.9855
2.2028E-04	4.5315E-06	9.2693E-06	1.4436E-05	0.9976
2.2015E-04	4.5207E-06	9.2528E-06	1.4407E-05	0.9996
2.2013E-04	4.5190E-06	9.2502E-06	1.4403E-05	0.9999
2.2013E-04	4.5187E-06	9.2498E-06	1.4402E-05	1.0000

The NCT leakage hole diameter for the plutonium content:

$D = 2.2013 \times 10^{-4}$ cm. NCT diameter

NCT Reference Air Leakage Rate for the Plutonium Content

The leakage hole diameter found for the maximum allowable leakage rate for NCT will be used to determine the reference air leakage rate. O-ring seal leakage testing must ensure that no leakage is greater than the leakage generated by the hole diameter $D = 2.2013 \times 10^{-4}$ cm. Therefore, the NCT reference leakage flow rate ($L_{R,N}$) must be calculated to determine the allowable test leakage rate.

Input data for NCT reference air leakage rate:

$D = 2.2013 \times 10^{-4}$ cm, From NCT
$a = 0.056$ cm, Leak path length (copper gasket seal compression),
$P_u = 1.0$ atm, Upstream pressure
$P_d = 0.01$ atm, Downstream pressure
$T = 298$ K, Fill gas temperature, 77°F
$M = 29$ g/g-mole, Molecular weight of air
$\mu = 0.0185$ cP, Viscosity of air at reference temperature

Calculate P_a:

$P_a = (P_u + P_d) / 2,$
$= (1.0 + 0.01) /2,$
$P_a = 0.505$ atm. NCT average pressure

$F_c = (2.49 \times 10^6) D^4 / (a \mu)$ (cm^3/atm-s), (Eq. B3)
$F_c = (2.49 \times 10^6) (2.2013 \times 10^{-4})^4 / ((0.056) (0.0185)),$
$F_c = (2.4035 \times 10^9) (2.2013 \times 10^{-4})^4,$
$F_c = 5.6433 \times 10^{-6}$ cm^3/atm-s.

$F_m = (3.81 \times 10^3) D^3 (T / M)^5 / (a P_a)$ (cm^3/atm-s), (Eq. B4)

$F_m = (3.81 \times 10^3) (2.2013 \times 10^{-4})^3 (298 / 29)^5 / ((0.056) (0.505)),$
$F_m = (4.3187 \times 10^5) (2.2013 \times 10^{-4})^3,$
$F_m = 4.6066 \times 10^{-6}$ cm^3/atm-s.

$L_u = (F_c + F_m) (P_u - P_d) (P_a / P_u)$ (cm^3/s), (Eq. B5)
$L_u = (5.6433 \times 10^{-6} + 4.6066$ H $10^{!6})$(cm^3/atm-s) (1.0 - 0.01)(atm) (0.505 / 1.0),
$L_u = (1.0250 \times 10^{-6})$(cm^3/atm-s) (0.49995)(atm),
$L_u = 5.1244 \times 10^{-6}$ cm^3/s.

The reference air leakage rate as defined in ANSI N14.5-1997, Section B.3, is the upstream leakage in air.

$L_{R,N\text{-}Air} = 5.1244 \times 10^{-6}$ ref-cm^3/s. plutonium content

The same equations can be used to calculate an allowable leakage rate using helium for leak testing.

M = 4 g/g-mole, Molecular weight of helium
μ = 0.0198 cP. Viscosity of helium at temperature

$F_c = (2.49 \times 10^6) D^4 / (a \mu)$ (cm^3/atm-s), (Eq. B3)
$F_c = (2.49 \times 10^6) (2.2013 \times 10^{-4})^4 / ((0.056) (0.0198)),$
$F_c = (2.2457 \times 10^9) (2.2013$ H$\times 10^{-4})^4,$
$F_c = 5.2728 \times 10^{-6}$ cm^3/atm-s.

$F_m = (3.81 \times 10^3) D^3 (T / M)^5 / (a P_a)$ (cm^3/atm-s), (Eq. B4)
$F_m = (3.81 \times 10^3) (2.2013 \times 10^{-4})^3 (298 / 4.0)^5 / ((0.056) (0.505)),$
$F_m = (1.1629 \times 10^6) (2.2013 \times 10^{-4})^3,$
$F_m = 1.2404 \times 10^{-5}$ cm^3/atm-s.

$L_u = (F_c + F_m) (P_u - P_d) (P_a / P_u)$ (cm^3/s), (Eq. B5)
$L_u = (5.2728 \times 10^{-6} + 1.2404 \times 10^{-5})$(cm^3/atm-s) (1.0 - 0.01)(atm) (0.505 / 1.0),
$L_u = (1.7676 \times 10^{-5})$(cm^3/atm-s) (0.49995)(atm),
$L_u = 8.8373 \times 10^{-6}$ cm^3/s.

The allowable leakage rate using helium for leak testing is:

$L_{R,N\text{-}He} = 8.8373 \times 10^{-6}$ cm^3/s. NCT helium test value

HAC Leakage Hole Diameter for the Plutonium Content

The calculation of a maximum allowable leakage rate hole diameter is based on the temperature and pressure of the fill gas aerosol for HAC, assuming the content is in an oxide powder form. Keeping this calculation conservative, the maximum values for temperature and pressure were used as steady-state conditions for a week. The maximum values were generated during the 30-min burn test for HAC.

Input data for HAC:

L_A = 5.0665 H 10^{-2} cm^3/s, Maximum exit leakage
P_u = 1.3940 atm, Upstream pressure = 20.486 psia
P_d = 1.0 atm, Downstream pressure

T	=	408.71 K,	Fill gas temperature = 276°F
μ	=	0.02442 cP,	Viscosity of gas mixture at temperature
M	=	29 g/g-mole,	Molecular weight of gas mixture
a	=	0.056 cm.	Leak path length (copper gasket seal compression)
P_a	=	$(P_u + P_d) / 2$	
	=	(1.3940 + 1.0) / 2,	HAC average pressure
P_a	=	1.1970 atm.	

Q is the mass-like leakage for flow using the upstream leakage, L_u, and pressure, P_u:

Q	=	$P_u L_u$,	(Eq. B1)
L_u	=	L_A.	HAC leakage
Q	=	$(1.3940)(atm)\ (5.0665 \times 10^{-2})(cm^3/s)$,	
Q	=	7.0626×10^{-2} atm-cm^3/s.	HAC mass-like leakage rate
Q	=	$P_a L_a$,	(Eq. B1)
L_a	=	Q / P_a	
L_a	=	7.0626×10^{-2} (atm-cm^3/s) / (1.1970)(atm),	
L_a	=	5.9003×10^{-2} cm^3/s.	HAC average leakage rate

Solve equations B2BB4 from ANSI N14.5-1997:

L_a	=	$(F_c + F_m)\ (P_u - P_d)\ (cm^3/s)$,	(Eq. B2)
L_a	=	$(F_c + F_m)$ (1.3940 - 1.0),	
L_a	=	$0.3940\ (F_c + F_m)\ cm^3/s$.	
F_c	=	$(2.49 \times 10^6)\ D^4 / (a\ \mu)\ (cm^3/atm\text{-}s)$,	(Eq. B3)
F_c	=	$(2.49 \times 10^6)\ D^4 / ((0.056)\ (0.02442))$,	
F_c	=	$(1.8211 \times 10^9)\ D^4\ cm^3/atm\text{-}s$.	
F_m	=	$(3.81 \times 10^3)\ D^3\ (T / M)^{.5} / (a\ P_a)\ (cm^3/atm\text{-}s)$,	(Eq. B4)
F_m	=	$(3.81 \times 10^3)\ D^3\ (408.71 / 4.0)^{.5} / ((0.056)\ (1.1970))$,	
F_m	=	$(5.7454 \times 10^5)\ D^3\ cm^3/atm\text{-}s$.	

From the mass-like leakage calculation:

L_a	=	$5.9003\ H\ 10^{-2}$ cm^3/s.	HAC average leakage rate

Find the leakage hole diameter that sets:

$$L_2 = L_a.$$

Using the equations:

L_2	=	$0.3940(F_c + F_m)\ cm^3/s$,	
F_c	=	$(1.8211 \times 10^9)\ D^4\ cm^3/atm\text{-}s$,	
F_m	=	$(5.7454 \times 10^5)\ D^3\ cm^3/atm\text{-}s$.	

To get a better guess on a new D use:

$$D = D_2 (L_a / L_2)^{0.252}.$$

Now a guess must be made for D_2 to solve Eq. B2 for HAC:

D_2 = 0.001 (cm), and solve for $L_a = 5.9003 \text{ H } 10^{-2}$ (cm^3/s). HAC average leakage rate

Diameter	F_c	F_m	L_2	L_a / L_2
1.0000E-02	1.8211E+01	5.7454E-01	7.4014E+01	0.00797
2.9593E-03	1.3967E-02	1.4890E-02	6.0896E-02	0.96891
2.9359E-03	1.3530E-02	1.4539E-03	5.9034E-02	0.99948
2.9355E-03	1.3523E-02	1.4533E-03	5.9004E-02	0.99999
2.9355E-03	1.3523E-02	1.4533E-03	5.9003E-02	1.00000

The HAC leakage hole diameter for the Plutonium content is:

$D = 2.9355 \text{ H } 10^{-3}$ cm. HAC diameter

HAC Reference Air Leakage Rate for Plutonium Content

The leakage hole diameter found for the maximum allowable leakage rate for HAC will be used to determine the reference air leakage rate. O-ring seal leakage testing must assure that no leakage is greater than the leakage generated by the hole diameter $D = 2.9355 \times 10^{-3}$ cm. Therefore, the HAC reference air leakage rate ($L_{R,A}$) must be calculated to determine the acceptable test leakage rate for post-HAC leakage testing.

Input data for HAC reference air leakage rate:

D	=	2.9355×10^{-3} cm,	From the HAC of transport
a	=	0.056 cm,	Leak path length (copper gasket seal compression)
P_u	=	1.0 atm,	Upstream pressure
P_d	=	0.01 atm,	Downstream pressure
T	=	298 K,	Fill gas temperature, 77EF
M	=	29 g/g-mole,	Molecular weight of air
μ	=	0.0185 cP.	Viscosity at temperature

Calculate P_a:

$P_a = (P_u + P_d) / 2$

$= 0.505$ atm. HAC average pressure

$F_c = (2.49 \times 10^6) D^4 / (a \mu) (cm^3/atm\text{-}s)$, (Eq. B3)

$F_c = (2.49 \times 10^6) (2.9355 \times 10^{-3})^4 / ((0.056) (0.0185))$,

$F_c = (2.4035 \times 10^9) (2.9355 \times 10^{-3})^4$,

$F_c = 1.7847 \times 10^{-1}$ cm^3/atm-s.

$F_m = (3.81 \times 10^3) D^3 (T / M)^{-5} / (a P_a)$ (cm^3/atm-s), (Eq. B4)
$F_m = (3.81 \times 10^3) (2.9355 \times 10^{-3})^3 (298 / 29)^{-5} / ((0.056) (0.505))$,
$F_m = (4.3187 \times 10^5) (2.9355 \times 10^{-3})^3$,
$F_m = 1.0924 \times 10^{-2}$ cm^3/atm-s.

$L_u = (F_c + F_m) (P_u - P_d) (P_a / P_u)$ (cm^3/s), (Eq. B5)
$L_u = (1.7847 \times 10^{-1} + 1.0924 \times 10^{-2})$(cm^3/atm-s) (1.0 - 0.01)(atm) (0.505 / 1.0),
$L_u = (1.8939 \times 10^{-1})$(cm^3/atm-s) (0.49995)(atm),
$L_u = 9.4686 \times 10^{-2}$ cm^3/s.

The HAC reference air leakage rate as defined in ANSI N14.5-1997, Section B.3, is the upstream leakage in air.

$L_{R,A\text{-}Air} = 9.4686 \times 10^{-2}$ ref-cm^3/s. for plutonium content

The same equations can be used to calculate an allowable leakage rate using helium for leak testing.

M = 4 g/g-mole, Molecular weight of helium
μ = 0.0198 cP. Viscosity of helium at temperature

$F_c = (2.49 \times 10^6) D^4 / (a \mu)$ (cm^3/atm-s), (Eq. B3)
$F_c = (2.49 \times 10^6) (2.9355 \text{ H } 10^{-3} \text{ cm})^4 / ((0.056) (0.0198))$,
$F_c = (2.2457 \times 10^9) (2.9355 \text{ H } 10^{-3} \text{ cm})^4$,
$F_c = 1.6675 \times 10^{-1}$ cm^3/atm-s.

$F_m = (3.81 \times 10^3) D^3 (T / M)^{0.5} / (a P_a)$ (cm^3/atm-s), (Eq. B4)
$F_m = (3.81 \times 10^3) (2.9355 \times 10^{-3} \text{ cm})^3 (298 / 4)^{-5} / ((0.056) (0.505))$,
$F_m = (1.1629 \times 10^6) (2.9355 \times 10^{-3} \text{ cm})^3$,
$F_m = 2.9415 \times 10^{-2}$ cm^3/atm-s.

$L_u = (F_c + F_m) (P_u - P_d) (P_a / P_u)$ (cm^3/s), (Eq. B5)
$L_u = (1.6675 \times 10^{-1} + 2.9415 \times 10^{-2})$(cm^3/atm-s) (1.0 - 0.01)(atm) (0.505 / 1.0),
$L_u = (1.9617 \times 10^{-1})$(cm^3/atm-s) (0.49995)(atm),
$L_u = 9.8072 \times 10^{-2}$ cm^3/s.

The allowable leakage rate using helium for leak testing for HAC is:

$L_{R,A\text{-}He} = 9.8072 \times 10^{-2}$ cm^3/s. HAC helium test value

Accident Condition for Air Transport of Plutonium (ACATP)

The calculation of a maximum allowable leakage rate hole diameter is based on the temperature and pressure of the fill gas aerosol for ACATP, assuming the content is in an oxide powder form. Keeping this calculation conservative, the maximum values for temperature and pressure were used as steady-state conditions for a week. The maximum values were generated during the 60-min burn test for ACATP [10 CFR 71.74(a)(5)]. In accordance with 4.5.3, 1.42 H 10^{-7} moles of He gas are generated per gram of plutonium in one year. Therefore, using 1300 grams of plutonium, 1.846 H 10^{-4} moles of helium is generated in one year. The basic assumption for the packaging assumed that the contents are

assembled inside a glove box filled with an inert gas. Using helium as the inert gases will lower the regulatory leakage criteria. Therefore, the 1103.01 cm^3 of void volume would contain 0.0452 moles of helium. According to the O-ring decomposition and pyrolysis of ancillary plastic analysis shown in Section 2.12.8, the following molar quantity of gases (shown in the table below) are created during ACATP for each proposed ancillary plastic type.

Common Name	Units	**Metalized PET**	**Polyethylene**	**PVC**	**Teflon (PTFE)**
Chemical name of monomer		Polyethylene terephthalate	Polyethylene	Polyvinyl chloride	polytetrafluoro-ethylene
Monomer formula		$C_{10}H_8O_4$	CH_2	C_2H_4Cl	C_2F_4
Allowable mass (plastic only)	**g**	**6.9**	**3.5**	**12.2**	**12.5**
Molar Contribution (mol)					
Original Atmosphere	mol	0.0452	0.0452	0.0452	0.0452
O-ring Thermal Decomposition					
HF	mol	0.2940	0.2940	0.2940	0.2940
CF_4	mol	0.0270	0.0270	0.0270	0.0270
CO_2	mol	0.3200	0.3200	0.3200	0.3200
Helium generated from alpha decay	mol	0.0002	0.0002	0.0002	0.0002
Subtotal of all above sources	mol	**0.6864**	**0.6864**	**0.6864**	**0.6864**
Ancillary Plastic -- thermal decomposition and oxidation					
CO_2	mol	0.3577	0.2504	0.2504	0.2504
H_2O	mol	0.1431	0.2504	0.1878	
Cl_2	mol			0.0626	
F_2	mol				0.2504
Total	mol	**1.1872**	**1.1872**	**1.1872**	**1.1872**

This table represents four different packaging scenarios. The gases in each scenario are assumed perfectly mixed generating the following gas percentages:

	Shipping arrangement ancillary plastic material (percent of total gas mixture)			
Gas constituents	Polyethylene terephthalate	Polyethylene	Polyvinyl chloride	Polytetrafluoroethylene
He	3.8241	3.8241	3.8241	3.8241
HF	24.7642	24.7642	24.7642	24.7642
CF_4	2.2743	2.2743	2.2743	2.2743
CO_2	57.0838	48.0458	48.0458	48.0458
H_2O	12.0536	21.0916	15.8187	0.0000
Cl_2	0.0000	0.0000	5.2729	0.0000
F_2	0.0000	0.0000	0.0000	21.0916
Total	100.0000	100.0000	100.0000	100.0000

Normally, the leakage hole length, a, is assumed to be the basic diameter of the O-ring seal. In this case where the seal is created by deformation into a copper gasket, the value for "a", is the indentation depth into the copper gasket of 0.022 inches (0.056 cm.). Varying this value by a factor of 10 will increase the leakage rates by approximately the same factor. The following calculations are shown for the case where the Pu-241 has not decayed to Am-241 and the ancillary plastic is metalized PET. Table 4.5.6.1 summarizes the results for both decay conditions with the various gas mixtures.

Input data for ACATP:

L_{PA}	=	5.0665×10^{-2} cm^3/s,	Maximum exit leakage
P_u	=	75.5308 atm,	Upstream pressure = 1110 psia (P_{PA})
P_d	=	1.0 atm,	Downstream pressure
T	=	855.37 K,	Fill gas temperature = 1080°F
μ	=	0.04168 cP,	Viscosity of gas mixture at temperature
M	=	34.40 g/g-mole,	Molecular weight of gas mixture
a	=	0.056 cm.	Leak path length (copper gasket seal compression)

$P_a = (P_u + P_d) / 2$

$= (75.5308 + 1.0) / 2,$ ACATP average pressure

$P_a = 38.2654$ atm.

Q is the mass-like leakage for flow using the upstream leakage, L_u, and pressure, P_u:

$Q = P_u L_u,$ (Eq. B1)

$L_u = L_A.$ ACATP leakage

$Q = (75.5308)(\text{atm})\ (5.0665 \text{ H } 10^{-2})(\text{cm}^3/\text{s}),$

$Q = 3.8268$ atm-cm^3/s. ACATP mass-like leakage rate

$Q = P_a L_a,$ (Eq. B1)

$L_a = Q / P_a$

$L_a = 3.8268$ (atm-cm^3/s) / (38.2654)(atm),

$L_a = 1.0001 \text{ H } 10^{-1}$ cm^3/s. ACATP average leakage rate

Solve equations B2BB4 from ANSI N14.5-1997:

$L_a = (F_c + F_m)(P_u - P_d)$ (cm^3/s), (Eq. B2)

$L_a = (F_c + F_m)(75.5308 - 1.0),$

$L_a = 74.5308 (F_c + F_m)$ cm^3/s.

$F_c = (2.49 \times 10^6) D^4 / (a \mu)$ (cm^3/atm-s), (Eq. B3)

$F_c = (2.49 \times 10^6) D^4 / ((0.056)(0.04168)),$

$F_c = (1.0668 \times 10^9) D^4$ cm^3/atm-s.

$F_m = (3.81 \times 10^3) D^3 (T / M)^{.5} / (a P_a)$ (cm^3/atm-s), (Eq. B4)

$F_m = (3.81 \times 10^3) D^3 (855.37 / 34.40)^{.5} / ((0.056)(38.2654)),$

$F_m = (8.8665 \times 10^3) D^3$ cm^3/atm-s.

From the mass-like leakage calculation:

$L_a = 1.0001 \text{ H } 10^{-1}$ cm^3/s. ACATP average leakage rate

Find the leakage hole diameter that sets:

$L_2 = L_a.$

Using the equations:

$L_2 = 74.5308 (F_c + F_m)$ cm^3/s,
$F_c = (1.0668 \times 10^9) D^4$ cm^3/atm-s,
$F_m = (8.8665 \times 10^3) D^3$ cm^3/atm-s.

To get a better guess on a new D use:

$D = D_2 (L_a / L_2)^{0.252}$.

Now a guess must be made for D_2 to solve Eq. B2 for ACATP:

D_2 = 0.01 (cm), and solve for $L_a = 1.0001$ H 10^{-1} (cm^3/s). ACATP average leakage rate

Diameter	F_c	F_m	L_2	L_a / L_2
1.0000E-02	1.0668E+01	8.8665E-03	7.9574E+02	0.00013
1.0400E-03	1.2477E-03	9.9722E-06	9.3738E-02	1.06687
1.0571E-03	1.3319E-03	1.0472E-05	1.0005E-01	0.99961
1.0569E-03	1.3313E-03	1.0469E-05	1.0001E-01	1.00000

The ACATP leakage hole diameter for the Plutonium content is:

$D = 1.0569$ H 10^{-3} cm. ACATP diameter

ACATP Reference Air Leakage Rate for Plutonium Content

The leakage hole diameter found for the maximum allowable leakage rate for ACATP will be used to determine the reference air leakage rate. O-ring seal leakage testing must assure that no leakage is greater than the leakage generated by the hole diameter $D = 1.0569 \times 10^{-3}$ cm. Therefore, the ACATP reference air leakage rate ($L_{R, PA-AIR}$) must be calculated to determine the acceptable test leakage rate for post-ACATP leakage testing.

Input data for ACATP reference air leakage rate:

D	=	1.0569×10^{-3} cm,	From the ACATP of transport
a	=	0.056 cm,	Leak path length (copper gasket seal compression)
P_u	=	1.0 atm,	Upstream pressure
P_d	=	0.01 atm,	Downstream pressure
T	=	298 K,	Fill gas temperature, 77°F
M	=	29 g/g-mole,	Molecular weight of air
μ	=	0.0185 cP.	Viscosity at temperature

Calculate P_a:

$P_a = (P_u + P_d) / 2$
$= 0.505$ atm. ACATP average pressure

$F_c = (2.49 \times 10^6) D^4 / (a \mu) (cm^3/atm\text{-}s),$ (Eq. B3)
$F_c = (2.49 \times 10^6) (1.0569 \times 10^{-3})^4 / ((0.056) (0.0185)),$
$F_c = (2.4035 \times 10^9) (1.0569 \times 10^{-3})^4,$
$F_c = 2.9995 H\times 10^{-3}$ $cm^3/atm\text{-}s.$

$F_m = (3.81 \times 10^3) D^3 (T / M)^{.5} / (a P_a) (cm^3/atm\text{-}s),$ (Eq. B4)
$F_m = (3.81 \times 10^3) (1.0569 \times 10^{-3})^3 (298 / 29)^{.5} / ((0.056) (0.505)),$
$F_m = (4.3187 \times 10^5) (1.0569 \times 10^{-3})^3,$
$F_m = 5.0994 \times 10^{-4}$ $cm^3/atm\text{-}s.$

$L_u = (F_c + F_m) (P_u - P_d) (P_a / P_u) (cm^3/s),$ (Eq. B5)
$L_u = (2.9995 \times 10^{-3} + 5.0994 \times 10^{-4})(cm^3/atm\text{-}s) (1.0 - 0.01)(atm) (0.505 / 1.0),$
$L_u = (3.5095 \times 10^{-3})(cm^3/atm\text{-}s) (0.49995)(atm),$
$L_u = 1.7546 \times 10^{-3}$ $cm^3/s.$

The ACATP reference air leakage rate as defined in ANSI N14.5-1997, Section B.3, is the upstream leakage in air.

$L_{R,PA\text{-}AIR} = 1.7546 \times 10^{-3}$ ref-$cm^3/s.$ for plutonium content

The same equations can be used to calculate an allowable leakage rate using helium for leak testing.

$M = 4$ g/g-mole, Molecular weight of helium

$\mu = 0.0198$ cP. Viscosity of helium at temperature

$F_c = (2.49 \times 10^6) D^4 / (a \mu) (cm^3/atm\text{-}s),$ (Eq. B3)
$F_c = (2.49 \times 10^6) (1.0569 H\ 10^{-3} cm)^4 / ((0.056) (0.0198)),$
$F_c = (2.2457 \times 10^9) (1.0569 \times 10^{-3} cm)^4,$
$F_c = 2.8026 \times 10^{-3}$ $cm^3/atm\text{-}s.$

$F_m = (3.81 \times 10^3) D^3 (T / M)^{0.5} / (a P_a) (cm^3/atm\text{-}s),$ (Eq. B4)
$F_m = (3.81 \times H\ 10^3) (1.0569 \times 10^{-3} cm)^3 (298 / 4)^{.5} / ((0.056) (0.505)),$
$F_m = (1.1629 \times 10^6) (1.0569 H\ 10^{-3} cm)^3,$
$F_m = 1.3730 \times 10^{-3}$ $cm^3/atm\text{-}s.$

$L_u = (F_c + F_m) (P_u - P_d) (P_a / P_u) (cm^3/s),$ (Eq. B5)
$L_u = (2.8026 \times 10^{-3} + 1.3730 \times 10^{-3})(cm^3/atm\text{-}s) (1.0 - 0.01)(atm) (0.505 / 1.0),$
$L_u = (4.1757 \times 10^{-3})(cm^3/atm\text{-}s) (0.49995)(atm),$
$L_u = 2.0876 \times 10^{-3}$ $cm^3/s.$

The allowable leakage rate using helium for leak testing for ACATP is:

$L_{R,PA\text{-}He} = 2.0876 \times 10^{-3}$ $cm^3/s.$ ACATP helium test value

In accordance with Table 4.2 of the SAR, the highest measured air leakage rate following the ACATP conditions was 4.5 H 10^{-5} cc/sec at atmosphere conditions (atm cc/s). This leakage rate is considerably lower than the calculated maximum allowable regulatory leakage rate requirement of 1.4703×10^{-3} ref cc/s shown in Table 4.5.6.1. Therefore, the TB-1 containment vessel inside the PAT-1 shipping package maintains containment for NCT, HAC, and ACATP conditions.

Mass Release During ACATP

To determine the amount of material that leaks out of the containment boundary in one week under ACATP conditions, the measured volumetric leakage rate shown in Table 4.2 (4.5×10^{-5} cm^3/s) is multiplied by the aerosol mass density (9.0×10^{-6} g/cm^3) and by time (6.048×10^5 sec/week). You obtain a mass release of approximately 2.45×10^{-4} grams in one week. This release amount disregards orifice size and particle size limits.

The regulatory release mass limit for the material in the containment vessel is calculated by using the regulatory activity limit of an A_2 in one week divided by the specific activity of the mixture. Assuming a homogenous mixture, the material leaving the containment vessel has a specific activity determined by dividing the total activity (TBq) by the total mass (grams) or TBq/gram. Therefore, the allowable mass release is then the A_2 in a week (TBq/week) divided by the specific activity of the mixture (TBq/gram) or grams/week. Using this approach for the material that has no Pu-241 decay and Table 4.5.5.3, you obtain an activity release rate of 1.1326×10^{-2} TBq/week; total activity of 53.2808 TBq; total mass of 1300 grams; a specific activity of 4.0985×10^{-2} TBq/g; and finally an allowable mass release of 2.7634×10^{-1} grams. Again using this approach for the material with total Pu-241 decay to Am-241 and Table 4.5.5.4, you obtain an allowable mass release of 2.3336×10^{-1} grams. Since both of these material conditions release much less than the regulatory allowable mass release, the TB-1 containment vessel inside the PAT-1 shipping package maintains containment during ACATP conditions.

Table 4.5.6.1 Regulatory Leakage Criteria for 1300 g plutonium

Isotopic Distribution	Ancillary plastic composition	NCT [a]		HAC [a]		ACATP	
		$L_{R,N\text{-}air}$ (ref-cm^3/s)	$L_{R,N\text{-}He}$ (cm^3/s)	$L_{R,A\text{-}air}$ (ref-cm^3/s)	$L_{R,A\text{-}He}$ (cm^3/s)	$L_{R,PA\text{-}air}$ (ref-cm^3/s)	$L_{R,PA\text{-}He}$ (cm^3/s)
No Pu-241 decay	polyethylene terephthalate	5.1244 E-06	8.8373 E-06	9.4686 E-02	9.8072 E-02	1.7546E-03	2.0876E-03
	polyethylene	5.1244 E-06	8.8373 E-06	9.4686 E-02	9.8072 E-02	1.7339E-03	2.0642E-03
	polyvinyl chloride	5.1244 E-06	8.8373 E-06	9.4686 E-02	9.8072 E-02	1.7487E-03	2.0810E-03
	polytetrafluoroethylene	5.1244 E-06	8.8373 E-06	9.4686 E-02	9.8072 E-02	2.1844E-03	2.5725E-03
Complete Pu-241 decay to Am-241	polyethylene terephthalate	4.2787 E-06	7.4737 E-06	7.9817 E-02	8.3008 E-02	1.4703E-03	1.7873E-03
	polyethylene	4.2787 E-06	7.4737 E-06	7.9817 E-02	8.3008 E-02	1.4729E-03	1.7673E-03
	polyvinyl chloride	4.2787 E-06	7.4737 E-06	7.9817 E-02	8.3008 E-02	1.4854E-03	1.7816E-03
	polytetrafluoroethylene	4.2787 E-06	7.4737 E-06	7.9817 E-02	8.3008 E-02	1.8549E-03	2.2012E-03

[a] Since temperatures associated with pyrolysis of the ancillary plastics are not reached during NCT and HAC, the various plastics have no affect on the regulatory leakage criteria at those conditions.

4.5.7 References for Sections 4.5.5 and 4.5.6

10 CFR 71, *Packaging and Transportation of Radioactive Material,* Jan. 1, 2010.

49 CFR 173, *Shippers—General Requirements for Shipments and Packagings,* Oct. 1, 2010.

ANSI N14.5-1997, *Radioactive Materials—Leakage Tests on Packages for Shipment*, American Natl. Standards Institute, Feb. 5, 1998.

Curren, W. D. and R. D. Bond, *Leakage of Radioactive Powders from Containers*, Proceedings of the Sixth International Symposium on Packaging and Transportation of Radioactive Material: PATRAM '80, West Berlin, F.R.G., November 10–14, 1980, pp. 463–471.

Kocher, D. C., *Radioactive Decay Data Tables, A Handbook of Decay Data for Application to Radiation Dosimetry and Radiological Assessments*, DOE/TIC-11026, U.S. DOE, Office of Scientific and Technical Information, 1981.

R.H. Perry, D.W. Green, and J.O. Maloney, *Perry's Chemical Engineers' Handbook*, 7th edition, 1997, p. 2-363)

R.D. McCarty Cryogenics Division, *National Bureau of Standards Technical Note 631*, "Thermophysical Properties of Helium-43 from 2 to 1500 K with Pressures to 100 Atmospheres," pg 49, Nov. 1972.

Robert C. Weast, Ph. D., *Handbook of Chemistry and Physics*, 55th ed., pg. F-13, 1974.

This page intentionally left blank